ASPHALT PERMEABILITY
AND
MOISTURE DAMAGE

by
Cindy Venter

Thesis presented in fulfilment of the requirements for the degree of Master of Engineering in Civil Engineering in the Faculty of Engineering at Stellenbosch University

Supervisor: Prof. Kim Jonathan Jenkins

April 2019

DECLARATION

By submitting this thesis electronically, I declare that the entirety of the work contained therein is my own, original work, that I am the sole author thereof (save to the extent explicitly otherwise stated), that reproduction and publication thereof by Stellenbosch University will not infringe any third party rights and that I have not previously in its entirety or in part submitted it for obtaining any qualification.

Date: April 2019

ABSTRACT

For several years the design methods for a pavement surface have evolved. Starting with the very first bituminous road surface which was laid in Paris, France, in the eighteen-fifties. The main purpose of a surfacing layer is to protect the underlying layers from moisture ingress. These supporting layers can absorb the forces imposed by repeated traffic if the layers are kept moisture-free. Thus, the only layer preserving the supporting layers is the bituminous surface mixture.

The research covered in this study analyses the permeability of asphalt surfacing specimens. The permeability of an asphalt surface is a measure of the amount of air, water and water vapour that penetrates the layer. Layers with adequately low permeability will promote long term durability of the surface and protect the underlying pavement layers from the ingress of water.

This research study is focused on investigating 'Asphalt Permeability and Moisture Damage'. As part of this research study, extensive laboratory experiments and testing were required to investigate the permeability of asphalt cores and how moisture ingress influences the inter-connected voids. To determine if the inter-connected voids increased after MIST (Moisture Inducing Simulating Test) conditioning, CT-scanning (Computed Tomography) images were used for further analysis.

After initiating an extensive literature review and identifying factors which can influence the permeability of asphalt, an experimental research methodology was developed to achieve the primary and secondary objectives.

Several asphalt cores were acquired from different sources all over South Africa, which was used for laboratory testing. This research methodology was executed at Stellenbosch University where all the results and conclusions related to this study were reported.

The primary objective of this research study is to analyse the permeability of asphalt cores by means of the laboratory Marvil and High Pressure Permeability (HPP) tests; and through this to determine the influence of pressure and moisture on the permeability of asphalt cores.

The secondary objectives of this research study are focused on the determination of the volumetric properties of various asphalt cores, and determining if a correlation exists between the:

- Marvil and HPP;
- Marvil and air void content; and
- HPP and air void content.

It was also necessary to develop asphalt permeability classification ranges for the Marvil and HPP under laboratory conditions.

The primary choice for testing permeability of asphalt surfacing in South Africa is the Marvil permeability test. This test uses no external pressure and is only reliable on the water pressure inside the apparatus at atmospheric pressure, which is minimal. The Marvil apparatus was re-designed for laboratory use, and then used to test the permeability of various asphalt cores for this research study.

A second permeability test was used in order to gain more insight into how pressure could affect the asphalt surfacing behaviour. The High Pressure Permeability (HPP) test was designed by Ockert Grobbelaar in 2016 in order to simulate the effect of normal speed traffic and its hydrostatic effect on surfacing layers (Grobbelaar, 2016). The asphalt cores were tested at three realistic pressure intervals based on previous research, namely 100, 150 and 200 *kPa* (Jenkins & Twagira, 2009). The HPP test was conducted before and after moisture damage was induced by the use of the Moisture Inducing Simulating Test (MIST), to analyse what the effect on the permeability of the asphalt cores would be.

After completing the permeability and moisture damage testing, the Indirect Tensile Strength (ITS) test was performed on the cores to determine if MIST conditioning influences the tensile strength of an asphalt core. For these cores, it was concluded that MIST conditioning causes a decrease in tensile strength for an asphalt core. Further results from the CT-scans also indicated that MIST conditioning increases the inter-connected voids in an asphalt core.

Results of the secondary objectives indicated that a correlation exists between the permeability results of the Marvil and the HPP for several of the asphalt cores. However, correlation only exists for the HPP at 100 and 150 *kPa* testing pressure, but at 200 *kPa* inconsistencies exist - leading to high variability in the results. It is postulated that testing pressures of 200 *kPa* and above lead to a great risk of leakage and other secondary effects during testing.

Finally, asphalt permeability classification ranges were developed for the Marvil and HPP under laboratory conditions which can be used for future research.

UITTREKSEL

Gedurende die afgelope dekades het die ontwerpmetodes van padoppervlaktes heelwat verander. Dit het begin met die heel eerste bitumen oppervlak wat in die agtien-vyftigs op ‘n pad in Parys, Frankryk, neergelê is. Die hoofdoelwit van ‘n oppervlaklaag is om te verseker dat vog nie die kroon- en stutlaag binnedring nie. Hierdie lae kan net die kragte wat deur die verkeersdruk uitgeoefen word absorbeer indien dit vog-vry is. Die oppervlaklaag is die enigste laag wat die stutlae kan beskerm.

Hierdie navorsingsprojek handel oor die ontleding van verskillende asfaltkerns en die deurlaatbaarheid daarvan. Die deurlaatbaarheid van so ‘n kern word beskryf as die hoeveelheid vog, water en lug wat deur ‘n asfaltkern dring. Oppervlaklae wat lae deurlaatbaarheid eienskappe besit, sal verseker dat die stutlae langer beskerm sal word teen die indringing van vog.

Hierdie navorsingsprojek ondersoek hoofsaaklik ‘Asfalt deurlaatbaarheid en vog skade’. Uitgebreide laboratoruimeksperimente en toetse was uitgevoer om ondersoek in te stel van presies hoe die vog ‘n asfaltkern binnedring, asook die hoeveelheid lugruimtes in ‘n kern. Deur middel van rekenaar tomografie skandering (CT-skandering) was daar ondersoek ingestel om vas te stel of verbinde lugruimtes vermeerder het na die ‘MIST’ kondisionering.

Verskeie asfaltkerns was ingesamel van regoor Suid-Afrika en na die laboratorium gebring by Stellenbosch Universiteit. Dit is ook by hierdie instansie waar al die toetse afgelê is en die resultate verkry was. Nadat ‘n uitgebreide literatuurstudie saamgestel was, kon daar vasgestel word dat sekere faktore wel ‘n invloed sal hê op die deurlaatbaarheid van die asfaltkern. ‘n Eksperimentnavorsingsprosedure was saamgestel om te verseker dat die primêre- en sekondêre doelwitte bereik kan word.

Die primêre doelwit van hierdie navorsingsprojek is om die deurlaatbaarheid van asfaltkerns te toets deur middel van die Marvil en hoëdrukdeurlaatbaarheidstoets (HPP), en ondersoek in te stel oor wat die invloed van druk en vog op die deurlaatbaarheid van ‘n asfaltkern is. Die sekondêre doelwitte was om die volumetriese eienskappe te ondersoek en vas te stel of daar enige verwantskap bestaan tussen die:

- Marvil en die hoëdrukdeurlaatbaarheids (HPP) toets;
- Marvil en die lugruimte inhoud; en
- Hoëdrukdeurlaatbaarheidstoets (HPP) en die lugruimte inhoud.

Dit was ook noodsaaklik om graderings te ontwikkel vir die Marvil en HPP toetse onder laboratoriumtoestande.

Die primêre keuse vir die deurlaatbaarheidstoetse van asfalt oppervlaklae is die Marvil toets. Hierdie toets gebruik geen bygevoegde druk op die kern nie en maak slegs staat op die druk wat die water uitoefen tesame met atmosferiesedruk – wat weglaatbaar klein is. Die Marvil apparaat was aangepas om in die laboratorium gebruik te word en sodoende verskillende asfaltkerns te kan toets.

'n Tweede deurlaatbaarheidstoets was gebruik om te ondersoek hoe die byvoeging van druk die asfaltkerns sou beïnvloed. Die hoëdrukdeurlaatbaarheidstoets (HPP) was ontwerp deur Ockert Grobbelaar in 2016 (Grobbelaar, 2016). Hierdie apparaat was gebruik om die hidrostatiese kragte te ondersoek wat veroorsaak word deur normale verkeerssnelheid op 'n asfaltoppervlak. Die verskeie asfaltkerns was onder 100, 150 en 200 *kPa* druk geplaas (Jenkins & Twagira, 2009). Die hoëdrukdeurlaatbaarheidstoets was voor en na 'MIST' kondisionering afgelê om sodoende die invloed van die hidrostatiese kragte op die lugruimtes te kon ondersoek.

Na die afloop van die deurlaatbaarheids- en vog skade toetse was elke kern se indirektetrekspanning (ITS) getoets. Dit sou meer duidelikheid bied oor die invloed wat die bogenoemde toetse op die monster se sterkte het. Dit het te lig gekom dat die kerns wat onderwerp was aan 'MIST' kondisionering wel swakker trekspanningskragte ervaar het. Deur middel van rekenaar tomografie skandering (CT-skandering) was daar ook gesien dat 'MIST' kondisionering die lugruimtes binne die kerns vergroot en ook 'n groter verbinding gevorm het as voor die toetse.

Die resultate vir die sekondêre doelwitte het genoegsame bewyse opgelewer om te toon dat daar wel 'n verwantskap bestaan tussen die deurlaatbaarheidsresultate van die Marvil en die HPP. Hierdie verwantskap bestaan wel net tussen die twee toetse indien die HPP by 100 en 150 *kPa* getoets word. Sodra die druk verhoog word na 200 *kPa* verdwyn hierdie verwantskap. Die oorhoofse rede vir hierdie gevolgtrekking is hoofsaaklik dat die apparaat nie akkuraat kan toets teen 'n hoë druk van 200 *kPa* nie. Daar was uitdagings ondervind om die apparaat waterdig te hou en te verseker dat die seël nie lek nie.

Laastens was daar deurlaatbaarheidsgraderings ontwikkel vir die Marvil asook die HPP onder laboratoriumtoestande wat gebruik kan word vir toekomstige deurlaatbaarheidsstudies.

ACKNOWLEDGEMENTS

I would like to express my heartfelt gratitude to the following people who have guided me, inspired me and helped me every step of the way. I am forever grateful for:

Prof Kim Jenkins, for giving me this opportunity to develop my knowledge and interest in Pavement Engineering. Thank you for always finding time to guide and support me on my research journey. You inspire me daily to work harder, learn more and think outside the box. I have learned so much from you, and I will be forever grateful for the opportunity you have given me to be a part of your research team. It has been an honour to work with you.

Mrs Chantal Rudman for her guidance with my studies and for always making time to help. I am truly inspired by your passion for Pavement Engineering.

Gavin Williams, Collin Isaac, Eric Nojewu and **Riaan Briedenhann** for always finding time to help me in the laboratory. Thank you for always having a smile on your face and helping in every way you can.

The **supporting staff** of the **Civil Engineering department**, for always making time to ask about my well-being, for laughing with me (and at me), and for supporting me during my time at Stellenbosch University.

My fellow **Pavement Specials**, for all the late-night assignment sessions, good coffee and support when I needed it.

My family, for supporting me every day and loving me unconditionally. I shall strive to make you proud every day.

Dirk Kotzé, for believing in me and supporting me throughout this entire process. Thank you for your patience, kindness and love. You inspire me every day to work even harder to achieve my dreams and goals.

Lastly and earnestly, my biggest thanks go to **God**. My rock, my saviour and protector. I am blessed abundantly by your grace.

TABLE OF CONTENTS

LIST OF FIGURES

Page

LIST OF TABLES

Page

LIST OF ABBREVIATIONS

AIP	-	Air-Induced Permeameter
ASA	-	Agrément South Africa
BRD	-	Bulk Relative Density
BSM	-	Bitumen Stabilised Material
BWP	-	Between Wheel Paths
COLTO	-	Committee of Land Transport Officials
CT	-	Computed Tomography
EAPA	-	European Asphalt Pavement Association
HMA	-	Hot Mix Asphalt
HPP	-	High Pressure Permeability
ITS	-	Indirect Tensile Strength
MIST	-	Moisture Inducing Simulating Test
MMLS	-	Model Mobile Load Simulator
OWP	-	Outer Wheel Path
PVC	-	Polymerizing Vinyl Chloride
RA	-	Reclaimed Asphalt
RICE	-	Maximum Theoretical Relative Density
SABITA	-	Southern Africa Bitumen Association
SANRAL	-	South African National Roads Agency
SANS	-	South African National Standards
SABS	-	South African Bureau of Standards
SAPEM	-	South African Pavement Engineering Manual
SMA	-	Stone Matrix Asphalt

TMH	-	Technical Methods for Highways
TRH	-	Technical Recommendations for Highways
UTFC	-	Ultra-Thin Friction Course
UTM	-	Universal Testing Machine
VIM	-	Voids in Mix
WHU	-	Water Heating Unit

CHAPTER 1 - INTRODUCTION

1.1 BACKGROUND

All around the world Hot Mix Asphalt (HMA) has been used for several years by the asphalt industry to provide surfaces and base layers for pavements. Over the years, the asphalt industry has established that working with HMA mixtures satisfy the essential performance criteria for roads.

Hot Mix Asphalt (HMA) can be defined as a combination of aggregate and asphalt binder (bitumen) which is mixed together at very high temperatures. This warm mixture then forms a hard and strong construction material once it is cooled to the appropriate temperature. The mixture is produced at a high temperature of up to 190°C, it is then compacted onto the base layers of a pavement structure. By volume, a typical HMA mixture is about (NCHRP, 2011):

- 85 % aggregate;
- 10 % bitumen; and
- 5 % air voids.

The bitumen in the asphalt mixture holds the aggregate together. Without bitumen, the HMA would merely be crushed gravel or stone. Bitumen is a thick, heavy residue remaining after gasoline, kerosene, diesel oil, and other fuels are refined from crude oil (NCHRP, 2011). Bitumen consists mainly of carbon and hydrogen and its physical properties vary vastly with temperature. At room temperature, bitumen has the consistency of putty or soft rubber. At very high temperatures, bitumen is in fluid form and has the consistency of motor oil. At sub-zero temperatures, bitumen becomes very brittle and can shatter like glass if dropped on a hard surface.

By designing an HMA mixture with smaller aggregate sizes and a higher bitumen content, it can improve both the fatigue resistance and resistance to moisture damage. Since increased bitumen content typically improves the fatigue resistance, it also reduces the permeability to water for an HMA mixture (NCHRP, 2011).

Every HMA mixture contains a certain amount of air voids. When an HMA mixture is designed in a laboratory, it is designed to contain an air void content of about 4 % (with a range of about 3 to 5 %), which is dependent on the design procedure being followed and the type of asphalt mixture

being designed (NCHRP, 2011). A properly design and constructed HMA pavement will typically have about 6 to 8 % of air voids immediately after placement and compaction. Once the construction is completed and traffic passes over the pavement, the HMA in the wheel paths will be compacted further to an air void percentage close to the design value of 3 to 5 % (NCHRP, 2011). However, if adequate compaction is not ensured during the construction phase, the additional compaction under traffic conditions will fail to reduce the air void content of the HMA to the design value and, as an end result, it will lead to a pavement which is more permeable to air and water.

Poor field compaction causes surface cracking by decreasing the strength of the pavement surface (NCHRP, 2011). An asphalt mixture with a high air void content will lead to a higher pavement permeability, which will then allow air and water into the pavement, both of which can increase the rate of fatigue cracking and lead to rutting and moisture damage.

If an HMA is properly constructed, water will not flow easily through the pavement. However, even in a well-compacted HMA pavement, water will still flow through very slowly. The water will slowly work its way between the aggregate surfaces and bitumen in a mixture, which will eventually weaken or even destroy the bitumen-aggregate bond. This type of moisture damage is commonly referred to as stripping (NCHRP, 2011).

Moisture damage easily occurs when water exists in a pavement. This is also the case when pavements are built over poorly drained areas and has a poor design which does not include drainage of water from the pavement structure. Even if an HMA pavement is only occasionally exposed to water, it can cause moisture damage because of poor material selection, faulty design or inadequate compaction.

By ensuring proper construction, especially adequate compaction, the permeability of HMA pavements can be reduced significantly, which will also lead to a reduction in the possibility of moisture damage. Anti-stripping additives can also be added to the HMA mixture to improve the moisture resistance of the pavement (NCHRP, 2011).

By using different combinations of aggregate and bitumen in an asphalt mixture, it will exhibit a very broad degree of resistance to moisture damage. It is impossible to predict what the moisture resistance of a specific combination of aggregate and bitumen will be. Notwithstanding this, an HMA mixture with aggregates that have large amounts of silica, such as sandstone and quartzite, and some granites, tend to be more prone to moisture damage (NCHRP, 2011).

One of the main factors affecting pavement performance is the ability of the HMA to prevent water from entering the pavement system. Low durability in pavements are caused by high permeability asphalt layers. A permeable asphalt layer can cause excess water to develop underneath the asphalt layer and endanger the base layer. This can lead to cracking, rutting, deflection and a reduction in the carrying capacity of the pavement (Redivo, 2012).

In South Africa, simple permeability testing apparatus, such as the Marvil permeameter, is used to determine the permeability of an asphalt layer on-site. Due to the great variability of these tests, the repeatability thereof is mostly unreliable. Generally, it is assumed that the permeability of an asphalt mixture is related to the air void content once compacted. There are various factors that can influence the permeability of asphalt, but the most common factors are (Redivo, 2012):

- Aggregate shape;
- Aggregate size;
- Aggregate gradation;
- Air void content; and
- Inter-connected voids.

The permeability of an asphalt layer is an indication of the severity of the inter-connected voids within the layer. This can be detrimental to the pavement due to the ingress of water to the underlying layers.

1.2 GOAL AND OBJECTIVES

The overall project goal as well as the various objectives for this research project are discussed in the following sections.

1.2.1 OVERALL PROJECT GOAL

The primary goal of this research project is to investigate various methods of realistically assessing the permeability of asphalt in a more accurate and reliable way, in order to check the moisture resistance of the asphalt. There is damage seen in some of the asphalt, but current methods (such

as the Marvil permeameter) only evaluate permeability at low pressures. A new method of evaluating permeability at high pressures are needed, such as the new developed apparatus by Ockert Grobbelaar - the High Pressure Permeameter (HPP) (Grobbelaar, 2016).

1.2.2 OBJECTIVES OF RESEARCH

The primary objective of this research is to analyse the permeability of asphalt cores by means of the laboratory Marvil and High Pressure Permeability (HPP) tests; and through this to determine the influence of pressure on the permeability of asphalt. By evaluating the permeability of asphalt at low and high pressures, a more realistic conclusion can be made with regards to moisture damage in asphalt.

To accomplish this primary objective, it is necessary to investigate specific secondary tasks and objectives. These secondary tasks and objectives include:

i. Determining the volumetric properties of various asphalt cores from different sources;

ii. Determining if correlation exists between the permeability of the Marvil and HPP (at its various pressures of 100, 150 and 200 *kPa*);

iii. Determining if correlation exists between the Marvil permeability results and the air void percentage of an asphalt core;

iv. Determining if correlation exists between the HPP results (at 100, 150 and 200 *kPa*) and the air void percentage of an asphalt core; and

v. Developing asphalt permeability classification ranges for the Marvil and HPP under laboratory conditions.

1.3 LIMITATIONS OF STUDY

The limitations of this study include the following:

i. The availability of asphalt cores to be used for testing, which led to a limited number of asphalt cores being tested;

ii. Since the asphalt cores are provided from external sources, not all mixture properties are known;

iii. The road drainage conditions on-site will not be taken into account;

iv. The availability of clean water to be used for permeability testing in a drought-stricken area;

v. All the tests will be performed under room temperature conditions and no tests will be conducted at different temperatures, thus the effect of temperature on the asphalt permeability will not be assessed. MIST conditioning will be done at 60°C;

vi. No previous permeability classification ranges have been developed for asphalt permeability in laboratory conditions for the Marvil as well as the High Pressure Permeability (HPP) tests;

vii. The Marvil permeability test has only been used in laboratory testing for seals. Thus, it will be necessary to develop appropriate equipment for testing asphalt cores in laboratory conditions. The accuracy of this experiment will have to be assessed by means of doing several in-field and laboratory testing on the same asphalt mixture, which will not be possible in this research project;

viii. The Marvil test will be stopped after two hours due to time constraints;

ix. The availability of reliable equipment, as the HPP had to be rebuilt a number of times;

x. On the road, the traffic loading results in a dynamic force, but for the HPP only a static pressure will be applied.

1.4 THESIS LAYOUT

This thesis will consist of seven chapters. The content of each chapter is briefly discussed below:

Chapter 1 includes a brief background of asphalt and permeability. This chapter also provides the overall project goal, objectives of this research study as well as limitations to the study.

Chapter 2 is a literature review on asphalt, permeability and moisture damage. It includes the history and failure mechanisms of asphalt, asphalt mix types as well as permeability of an asphalt surface. More information with regards to the types of asphalt permeability testing methods is also presented.

Chapter 3 gives an outline of the experimental research methodology that was followed to acquire the relevant results. The testing matrix, sample acquisition, sample preparation and different apparatus setups are also outlined.

Chapter 4 presents the results obtained from the execution of the experimental research methodology. Marvil permeability, High Pressure Permeability (HPP), MIST conditioning and ITS testing form the basis of this chapter.

Chapter 5 discusses the interpretations made with regards to the Marvil, HPP and air void test results from the asphalt cores. Interpretations are made with regards to the permeability of the Marvil versus HPP; as well as interpretations with regards to the Marvil and HPP versus the respective air void content.

Chapter 6 introduces the development of asphalt permeability classification ranges for the Marvil and HPP.

Chapter 7 concludes the research and discusses the outcomes of the project, providing recommendations for further studies.

CHAPTER 2 - LITERATURE REVIEW

2.1 INTRODUCTION

This literature review focuses on the aspects relevant to the specific research topic. The aim of this literature review is to gain knowledge about asphalt permeability and moisture damage. This chapter provides a brief overview of the applications of Hot Mix Asphalt (HMA) in South Africa, as well as the surfacing failure mechanisms that are related to asphalt pavements.

In addition, the following concepts related to asphalt mixtures are covered: asphalt production in South Africa, the purpose of asphalt surfacing, moisture susceptibility, adhesion and cohesion theories, disbonding mechanisms related to moisture damage, factors that influence the bitumen-aggregate bond and also the permeability, asphalt mix and grading types, and permeability testing methods.

Finally, the knowledge gained from this literature review is used to develop an experimental research methodology to test asphalt permeability and investigate moisture damage.

2.2 HISTORY OF ASPHALT AND ITS DEVELOPMENT OVER TIME

The word *asphalt* is derived from the ancient Akkadian term *asphaltic*. The Homeric Greeks used the term as a*sphaltos*, which meant “to make firm or stable” (Asphalt Institute, 2007). The Akkadian *asphaltic* evolved over time to *asphaltum*, *asphalte* and ultimately to the English *asphalt*, as it is known today.

The very first bituminous road surface was laid in Paris, France, in the 1850s. This road surface consisted of natural rock, filled with asphalt, which was then crushed to form a powder and consolidated with hot compacting irons.

Since the ancient past up until the present day, asphalt has been used as a bonding, coating and waterproofing mechanism for several objects. In the earlier years, asphalt occurred naturally and was found in geological strata as soft “mortars” (Asphalt Institute, 2007). Asphalt was also found naturally in a lake in Trinidad. These natural asphalts were used comprehensively around the world until the early years of the twentieth century.

In the early 1900s the asphalt industry expanded, as a new method of refining bitumen from crude oil was discovered. Since then, asphalt has been seen as a cheap resource for the construction of smooth, modern roads and other uses in terms of bonding, coating and waterproofing. As this asphalt industry flourished, it was necessary to determine the required physical properties for asphalt to ensure that these asphalt roads were durable and reliable.

2.3 PAVEMENT TYPES

Road pavement types can be categorized according to the material that is used to construct the surfacing of a road. There are two main types of surfaced pavements, namely a flexible pavement and a rigid pavement (SAPEM Chapter 2, 2014).

The types of materials, whether asphalt or concrete, determines the performance of a pavement in a certain climate with a given level of traffic. The material also gives an indication of the distress mechanisms that develop in the pavement over a period of time.

2.3.1 FLEXIBLE PAVEMENTS

A flexible pavement would typically have an asphalt or seal surfacing, which means that they can deflect vertically on the support. It is composed of properly graded aggregates with bitumen as binder. The strength of a flexible pavements' surface depends on the interlocking of the aggregates, friction and cohesion of the underlying layers. A flexible pavement is typically constructed in a number of layers, which can be seen in Figure 2.1.

A flexible pavement is laid continuously, which means that there are no joints. The initial cost of constructing a flexible pavement is lower with regards to a rigid pavement, but this leads to high maintenance costs. The loads created by the traffic are distributed to the underlying layers by grain to grain distribution. An advantage of a flexible pavement is the fact that it can be opened to traffic within 24 hours of construction. Flexible pavements are designed to have, on average, a 30-year life span.

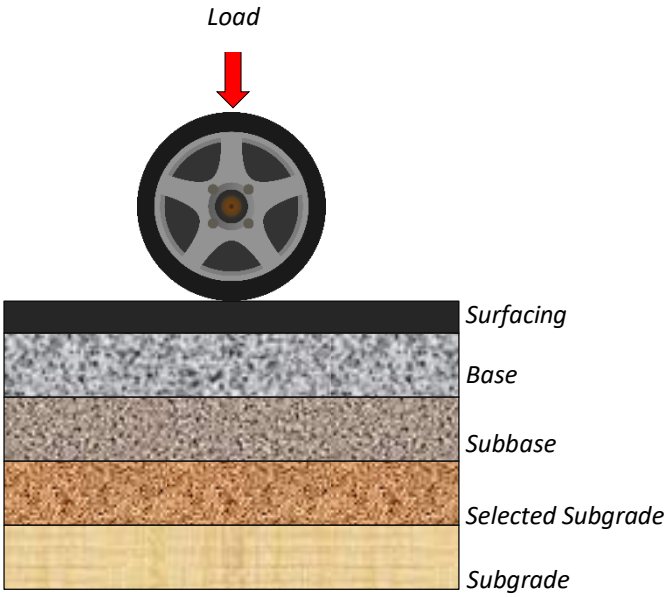

Figure 2.1: Flexible pavement

2.3.2 RIGID PAVEMENTS

A rigid pavement would typically be a concrete surface, which means that the concrete layer acts rigid and cannot deflect vertically. It is typically constructed by using cement, aggregate, water and reinforcement bars (for the joints). The strength of a rigid pavement depends on the flexural strength of the placed concrete. A rigid pavement surface and base is casted as a single concrete slab with reinforcements. This indicates that rigid pavements are typically constructed in bays, forming several joints.

The initial cost of constructing a rigid pavement is relatively high, which in its turn, leads to lower maintenance costs. The loads created by traffic are distributed over a wider area of the subbase due to its rigidity and high elastic modulus, thus leading a rigid pavement to take more load than a flexible pavement.

A disadvantage of a rigid pavement is the fact that it cannot be open to traffic within 24 hours, a minimum of 14 days is required. A rigid pavement is typically designed to have, on average, a life span of 30 years.

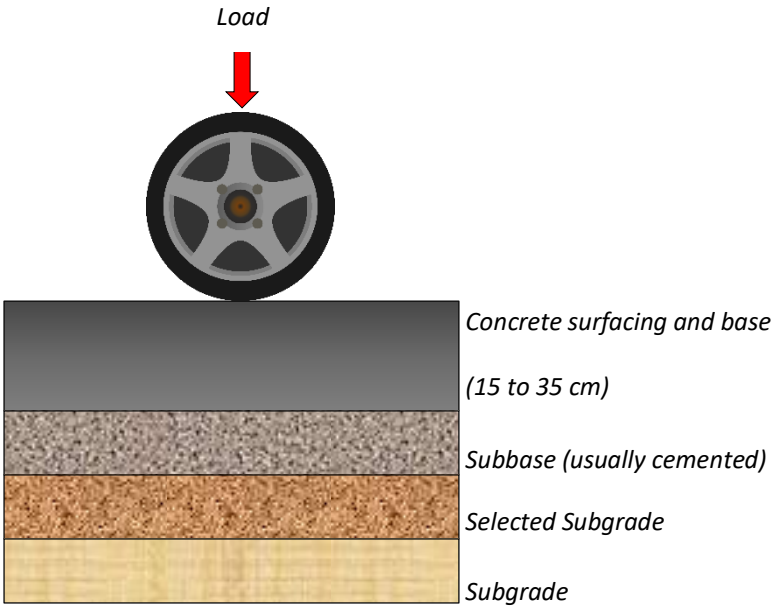

Figure 2.2: Rigid pavement

2.4 ASPHALT SURFACING IN SOUTH AFRICA

Approximately 80 % of surfaced roads in South Africa are surfaced with seals, which means that only a small fraction of roads are surfaced with either asphalt or concrete (SAPEM Chapter 2, 2014).

In South Africa, an asphalt surface can be mainly found in areas that are prone to heavy traffic loads since a surfacing seal would be insufficient in this regard. Typical asphalt surfacing in South Africa is between 30 and 50 *mm* thick (SAPEM Chapter 2, 2014). This thin asphalt surface layer is a pavement design that is unique to southern Africa and specifically South Africa.

The guiding principles for the design of an asphalt surfacing in South Africa are stipulated in the *Technical Recommendations for Highways 8 (TRH8)* (1987) and the *Interim Guidelines for the Design of Hot-Mix Asphalt in South Africa* (2001). Although these manuals have been widely used for asphalt design, SABITA compiled a new Hot-Mix Asphalt (HMA) design manual in February 2016; *SABITA Manual 35/TRH 8: Design and Use of Asphalt in Road Pavements* (2016).

All three these manuals establish design methods that are used for conventional asphalt surfacing, ultra-thin asphalt surfacing and asphalt bases. These South African design manuals include the methods used to evaluate fatigue and rutting, the selection of the different asphalt components, traffic considerations and the volumetric design of asphalt. All these methods are used to produce sufficient asphalt mixes for South African road pavements.

2.5 ASPHALT PRODUCTION IN SOUTH AFRICA

Asphalt mixes that are used in the surfacing of roads in South Africa generally composes of aggregate, bituminous binder, filler and sometimes Reclaimed Asphalt (RA). All of these components are mixed together in pre-determined quantities to ensure that the asphalt mix performs under the anticipated service conditions (Asphalt Institute, 2007).

Asphalt manufacturers make use of both fixed and mobile asphalt plants, where a mobile plant is relatively popular since it has the ability to quickly disassemble and move to another project location. The mobile plant is widely used in South Africa since several projects only work on a contract basis and the regions where it is required differs. Fixed plants are very expensive to establish and requires a large area for setup. These types of plants are usually established in regions where large road networks are situated that needs constant maintenance and upgrading. Most of these plants are completely computerised and thus reduces human error and improves the overall quality of the asphalt mix (Asphalt Institute, 2007).

South Africa is starting to incorporate more advanced technologies into the manufacturing processes of asphalt production. Hot Mix Asphalt (HMA) can be manufactured in either a drum-mix plant or a batch plant. Both of these plants produce high quality mixes, but the choice of which is to be used is solely based on the business' commercial decisions, since additive procedures are slightly different in each process.

2.5.1 BATCH PLANT

The very first hot mix asphalt plants that were invented, were batch mix plants (Asphalt Institute, 2007). The batch plant is suitable for a commercial environment and can produce a wide variety of different mixes. The asphalt is mixed inside the pugmill mixers. A disadvantage of the batch plant is that it is relatively expensive to repair and maintain. The layout of a batch plant can be seen in Figure 2.3.

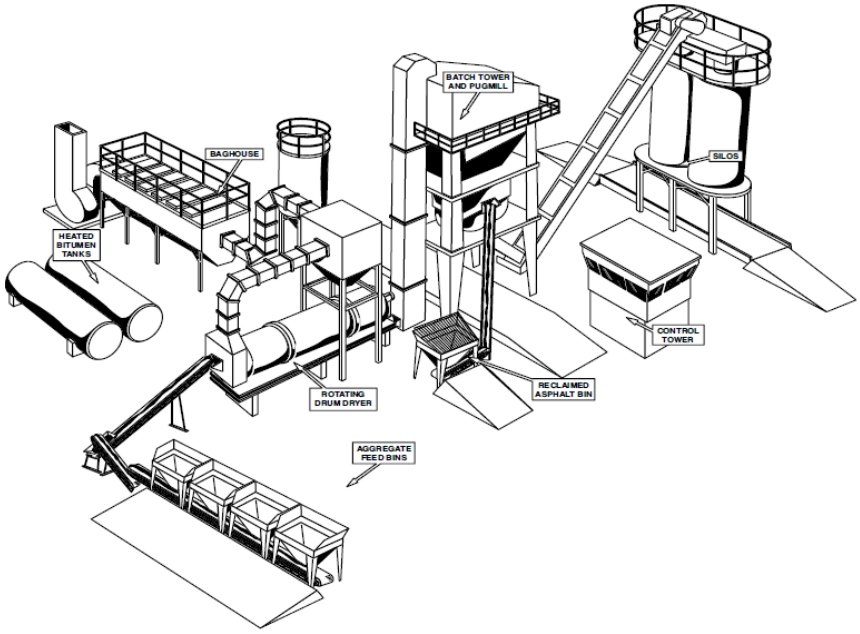

Figure 2.3: Batch plant layout (European Asphalt Pavement Association, 2011)

2.5.2 DRUM-MIX PLANT

A drum-mix plant is used where a single-mix is required, since the asphalt is mixed in the drying drum. To frequently change the mix type can be costly and cumbersome. The drum-mix plant is very cost effective to repair and maintain, and thus usually more favourable than the batch plant due to cost differences. The layout of a drum-mix plant can be seen in Figure 2.4.

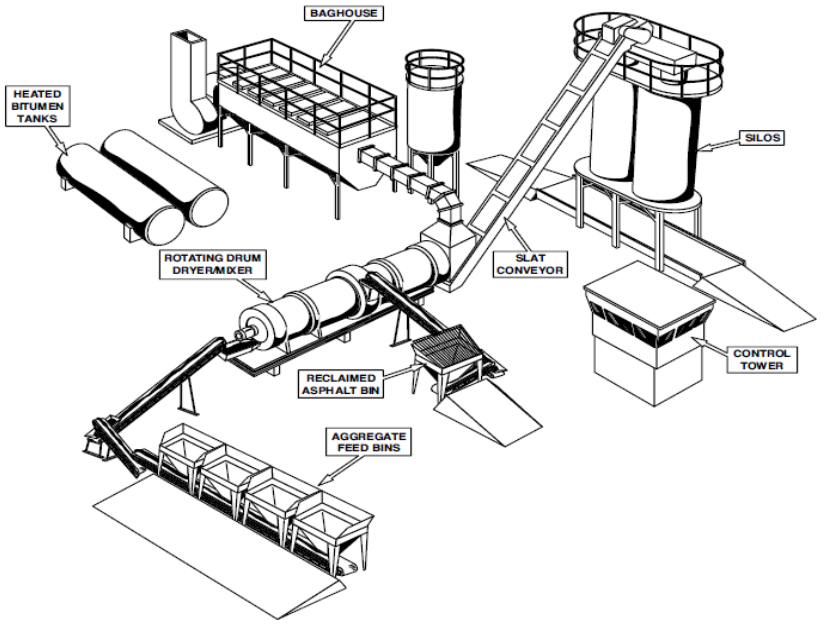

Figure 2.4: Drum-mix plant layout (European Asphalt Pavement Association, 2011)

The similarities between the batch plant and drum-mix plant include the aggregate feeding bins, Reclaimed Asphalt (RA) bins, heated bitumen tanks, storage silos and the dust removal components (baghouse).

The main difference between the batch plant and the drum-mix plant occurs when the aggregate needs to be mixed with the bitumen. In the batch plant, the heated aggregate exits the drum dryer and is elevated to the batch tower where the aggregate is divided into different batches. The aggregates are then only mixed with the RA and specified bitumen. In the drum-mix plant, the heated aggregate is mixed with the RA and bitumen inside the drum itself.

2.5.3 SUMMARY

A summary of the advantages (highlighted in green) and disadvantages (highlighted in red) regarding the factors influencing the asphalt production of the batch plant and drum-mix plant can be seen in Table 2.1.

Table 2.1: Advantages and disadvantages of asphalt production plants

BATCH PLANT	FACTOR	DRUM-MIX PLANT
Rescreen in batch tower	MAINTAIN ACCURATE GRADINGS	No rescreen
More cold feed bins		Typically, less cold feed bins
Separate dryer and weigh dry aggregate	SENSITIVE MIX PRODUCTION	Dryer and mixer are the same and weigh wet aggregate
Can re-add filler from primary/secondary collector		Less control over dust
Easy to change	SMALL MIX QUANTITY PRODUCTION	Need high tons to adjust
Mixing in batches in pugmill (discontinuous)	MIXING PROCESS AND CONTINUITY	Mixing continuous in drum
Weight of aggregate and bitumen is accurate		Flow of aggregate and bitumen is important
Expensive and time consuming to move and set-up	PLANT MOBILITY	Less expensive and time consuming to move and set-up
RAP easily added (high %)	RAP INCLUSION	RAP must be added further along the drum (lower %)

2.6 PURPOSE OF ASPHALT SURFACING

The purpose of an asphalt layer is to provide durability against elements such as noise-damping, skid resistance, surface drainage and visibility (SAPEM Chapter 9, 2014). The asphalt layer should also protect the underlying layers against water ingress and provide sufficient riding quality for road users.

Hot Mix Asphalt (HMA) is designed to meet specific necessary engineering properties which is critical for the acceptable performance of an asphalt surface. It is essential to design an asphalt mix that is durable and will exhibit minimal cracking and deformation during its design life. These properties can be seen in Figure 2.5 (SAPEM Chapter 9, 2014).

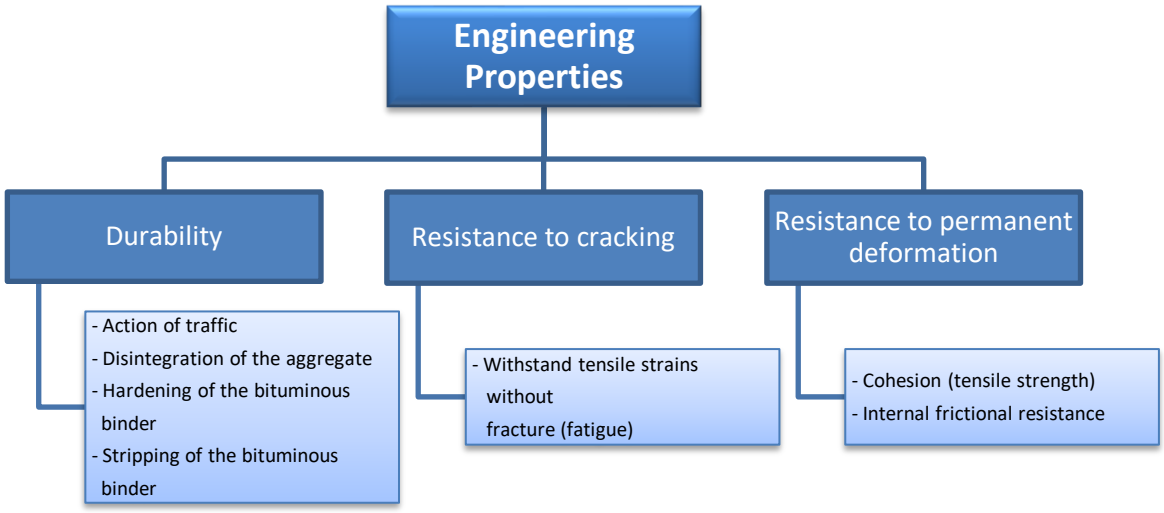

Figure 2.5: Hot Mix Asphalt (HMA) Engineering Properties

Secondary engineering properties that should be taken into account during the design of HMA include flexibility, permeability, resistance to shrinkage, skid resistance, stiffness (elastic modulus) as well as workability (SAPEM Chapter 9, 2014). These properties are briefly discussed below. In practice it is necessary to achieve a balance between these properties to produce the best mix design for a particular application.

2.6.1 DURABILITY

The durability of an HMA can be described as its ability to resist adverse changes to the binder, disintegration of the aggregate as well as stripping of the bitumen from the aggregate over time. The main factors affecting the durability of an asphalt layer are the action of water, sunlight and traffic. An asphalt layer with poor durability will result in ravelling of the surface, brittleness, early cracking, loss of binder film and potholes.

The durability of an asphalt layer can be improved by using dense aggregate packing (ensuring low voids), durable aggregate which can resist stripping and also relatively thick bituminous binder films (TRH 8, 1987).

2.6.2 RESISTANCE TO CRACKING

The resistance to cracking of an HMA can be described as its ability to withstand a tensile stress and associated strains without cracking. Thus, the resistance to cracking is dependent on the tensile strength. The tensile strength of an asphalt layer is gradually reduced by repeated stressing, which then leads to added strain and is commonly known as fatigue.

Traffic and other non-traffic factors are the forces that contribute to the cracking of an asphalt layer. The repeated forces of several heavy vehicle wheel loads can gradually lead to the fatigue of an asphalt layer and essentially cause failure. However, heavy vehicle wheel loads are not the only factor stressing an asphalt layer, other factors that also cause stresses in the layer include thermal and shrinkage forces in the layer itself as well as heave of underlying layers (TRH 8, 1987).

2.6.3 RESISTANCE TO PERMANENT DEFORMATION

Permanent deformation can be described as the change in the surface profile of the road. The ability of an HMA to resist permanent deformation depends on factors such as frictional resistance, tensile strength (cohesion) as well as inertia (TRH 8, 1987). Frictional resistance is the main contributing factor in the resistance to permanent deformation.

Permanent deformation is most likely to occur when the road surface has a high surface temperature as well as high traffic loading. An indication of poor resistance to permanent deformation is forms of rutting, undulations and shoving.

The resistance to permanent deformation can be improved by ensuring a dense aggregate packing and a low binder content which has a high viscosity. It is necessary to ensure that there is proper bonding to the underlying layers by implementing sufficient compaction during the construction process.

2.6.4 RESISTANCE TO SHRINKAGE

Shrinkage is commonly caused by the absorption of the binder by the aggregate, the ageing of the binder, temperature-related volume changes, or by the combination of these factors (TRH 8, 1987). Shrinkage cracking usually occurs in dry areas where the temperature changes are relatively extreme.

The resistance to shrinkage cracking can be improved by the same factor that promotes durability – dense aggregate packing. Shrinkage is directly proportional to the tensile strength of the asphalt mix and indirectly proportional to the voids in the aggregate (VMA). To assess the shrinkage potential of an asphalt mix at its design stage, it is necessary to consider these properties.

2.6.5 SKID RESISTANCE

Skid resistance can be described as the property where traction between tyres and a specific surface is maintained. This is one of the most important properties to consider for road safety, especially in wet weather conditions. Skid resistance is the product of:

- Macro-texture: measured by texture depth; and
- Micro-texture: measured by the Pendulum Test.

Adequate skid resistance can be achieved by using aggregates that consist of a rough surface texture, as well as ensuring sufficient air voids to avoid bleeding. The aggregate type that is most suitable for adequate skid resistance is an aggregate that is resistant to the polishing action of traffic and one that also contains minerals with diverse wear characteristics (TRH 8, 1987). An aggregate

that has diverse wear characteristics will have its rough surface texture continually renewed under the action of traffic. This will provide the sharp-coarse-grained macro-texture that is required to achieve traction between the tyre and the surface.

Examples of good and poor skid resistance can be seen in Figure 2.6 and Figure 2.7.

Figure 2.6: Asphalt with good skid resistance (SAPEM Chapter 9, 2014)

Figure 2.7: Asphalt with poor skid resistance (SAPEM Chapter 9, 2014)

2.6.6 PERMEABILITY

Permeability can be described as the penetration of an asphalt mix by air, water and water vapour. If an asphalt layer has low permeability, it leads to a long-term durability and also protects the underlying layers from water ingress. It also lowers the rate at which oxygen, micro-organisms and volatile constituents transfer through to asphalt layer, and thus prevents damage to the layer itself as well as the underlying layers.

Impermeability of the asphalt layer can be achieved by the same factors which promote durability – dense aggregate packing, dispersion of air voids within the mix, high binder content with adequate film thickness, and a well-compacted mixture (TRH 8, 1987). However, taking all the engineering properties (which was already discussed above) into account, a rough texture (permeable) asphalt surface can sometimes be required in order to provide adequate skid resistance. An asphalt surface like this should always be laid over an impermeable supporting layer to avoid moisture ingress to the underlying layers.

2.6.7 STIFFNESS (ELASTIC MODULUS)

The stiffness of an HMA layer can be described as the layers' ability to carry and spread traffic loads. The stiffness of a material can also be referred to as its elastic modulus. The elastic modulus of an HMA usually has an average of 2 500 *MPa*, and can range from 600 to 6 000 *MPa* depending on temperature, loading frequency and mix constituents (TRH 8, 1987).

The ratio of the stiffness of the asphalt layers, to that of the underlying layers is very important, and is known as the modular ratio. A thin asphalt layer with a high stiffness which is supported by a weak base layer should be avoided.

The stiffness of an asphalt layer can be increased by ensuring a dense aggregate packing, optimum binder content with a high viscosity and good compaction. Stiffness is mainly controlled by the selection of the mix type and also the type of binder being used.

2.6.8 WORKABILITY

Workability can be described as the property that simplifies the compaction, handling and spreading of an HMA. It is important that an HMA will compact sufficiently and be easy to handle and spread, even under adverse conditions, to obtain a durable layer. The workability of an asphalt mix can be influenced by: aggregate grading, binder content, viscosity, setting properties, shape and type, as well as the temperature of the mix at the time of handling (TRH 8, 1987).

Workability can be improved by increasing the binder content, decreasing the binder viscosity, limiting the maximum aggregate size and to also use less angular aggregates. When the coarse aggregate fraction of the mix is very high, tearing may occur, especially when laying thin asphalt layers.

2.7 ASPHALT FAILURE MECHANISMS

The main failure mechanisms of an asphalt surfacing are fatigue and permanent deformation. Guidelines for visually assessing flexible pavements in South Africa are set out in the *Technical Methods for Highways 9* (TMH 9) manual. According to the TMH 9, a poor asphalt mix can initiate distresses such as aggregate loss, bleeding, cracking, potholing, pumping and rutting (TMH 9, 1992).

Fatigue and permanent deformation should not be seen as the only main failure mechanisms. Moisture susceptibility of an asphalt surfacing should also be considered and deemed important (Nel, 2017).

Permanent deformation, fatigue and moisture susceptibility of an asphalt surfacing will be discussed in the sections that follow.

2.7.1 PERMANENT DEFORMATION

Permanent deformation can be described as the change in the surface profile of the road. This is shown as an area of the pavement where the surface is either above or below the original level. Permanent deformation typically occurs due to shear deformation which is caused by repetitive traffic loads and is limited to the road's wheel path. Permanent deformation can also be described as rutting or undulation.

When rutting occurs, it is important to investigate the shape of the deformation, as this will give an indication of where in the pavement structure the problem is located. When the rutting is wide and even-shaped, it is an indication that the problem is located in the lower pavement layers. When the rutting is narrow and more sharply defined, it is an indication that the problem is located in the upper pavement layers, which is an indication of a poor asphalt mix design (TMH 9, 1992). An illustration of severe rutting can be seen in Figure 2.8.

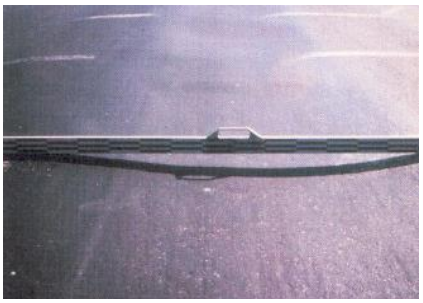

Figure 2.8: Severe form of rutting (TMH 9, 1992)

Testing for permanent deformation of an asphalt surface can be a challenging task, as none of the developed tests have proven to deliver a consistent evaluation of rutting performance for different mix types. One of the tests that have the best correlation with rutting in the industry, is the wheel tracking test. However, this test is relatively expensive to perform and requires a large number of

asphalt slabs to be prepared and compacted before testing can commence. In South Africa the Model Mobile Load Simulator (MMLS) and the Transportek Wheel Tracking Device is used as wheel tracking tests (Taute et al., 2001).

Rutting is one of the most frequent and serious observed distresses on HMA layers (Taute et al., 2001). It can lead to ponding of water in the road's wheel path and pose a serious threat to road users in wet weather conditions. It can also lead to poor riding quality and thus cause an increase in vehicle operating costs.

The occurrence of rutting on flexible pavement structures in South Africa has increased significantly. This can be due to high rainfall, an increase in axle loads and tyre pressure, as well as the significant increase in traffic volumes (Taute et al., 2001).

The ability of an asphalt layer to resist permanent deformation depends on the environmental and mixture aspects. The environmental aspects include the stress state (for a particular loading and pavement situation), the temperature as well as the vehicle speed (loading rate). The mixture aspects include the aggregate characteristics, packing characteristics of the mix, viscosity of the mastic and the volumetric aspects (Taute et al., 2001).

2.7.2 FATIGUE

Fatigue can be described as the occurrence of fracture or cracking under repeated traffic loading. Fatigue consists of two phases, namely: the initiation of cracking and crack propagation (caused by the tensile strains from traffic loading), construction practices and temperature variation (Jenkins, 2016).

Testing for the fatigue characteristics of an asphalt surface can be a challenging task, as very few laboratory tests provide a reliable evaluation. One of the laboratory tests that can be used is the four-point bending beam fatigue test. This test is relatively expensive to perform and is therefore mostly used for high trafficked roads (Taute et al., 2001). For low trafficked roads, the Indirect Tensile Strength (ITS) test can be performed to determine whether premature fatigue failure is a risk, although this is only an indicator and does not have a high correlation.

When subjected to traffic loading, the asphalt layer acts as a flexible beam and this induces strain at the bottom of the asphalt layer. Once this strain is larger than what the asphalt layer was designed

to endure, forms of cracking will develop in this layer. This cracking usually occurs at the bottom of the asphalt layer and is limited to the road's wheel path. These cracks can range from hair line cracks to macroscopic cracks. Macroscopic cracks usually form when the hair line cracks are left unattended and could lead to complete loss of structural reliability in the asphalt layer (Nel, 2017).

Fatigue failure of an asphalt surface normally occurs in the form of crocodile cracks. This is related to the inability of the asphalt layer to carry the traffic loads. An illustration of severe crocodile cracking can be seen in Figure 2.9.

Figure 2.9: Crocodile cracking due to fatigue (TMH 9, 1992)

In addition, crocodile cracks can also occur as a result of traffic fatigue due to the surfacing layer being brittle or dry. This could lead to the ingress of moisture into the underlying layers and usually shows no sign of rutting.

Crocodile cracks usually occur in isolated patches where failure is caused by poor drainage and sealed-in moisture (TMH 9, 1992). Therefore, it is important to also investigate the moisture susceptibility of an asphalt layer.

2.7.3 MOISTURE SUSCEPTIBILITY

Moisture susceptibility can be defined as an asphalt surfacing's tendency towards stripping. Stripping is known as the disbonding of aggregate from the bitumen in the asphalt surface. If sufficient drainage is not provided, the air voids in the HMA can become saturated with moisture and lead to disbonding. When disbonding occurs, it causes a loss of strength in the HMA layer. Stripping usually starts at the bottom of the HMA layer and then travels to the top of the surface (Hunter & Ksaibati, 2002). Even though there are several causes for stripping, such as traffic loading due to stresses induced; inadequate surface drainage can be seen as the main contributor.

To ensure that stripping does not occur, a proper mix design is crucial. Most asphalt mix designs stipulate an air void content of 3 to 5 %. When the air voids are below 5 % the HMA is almost impermeable to water (Hunter & Ksaibati, 2002). However, even if a proper mix is designed but it is not compacted correctly, it can still lead to high air void percentages and cause the surface to be susceptible to moisture and lead to reduced pavement life. Thus, it is necessary to do certain tests for scenarios where moisture infiltrates the air voids of a mixture to evaluate the influence it has on the pavement.

To improve the moisture susceptibility of asphalt it is necessary to investigate the adhesion properties. The adhesion of asphalt can be mainly determined by factors such as the aggregate and bitumen properties. Furthermore, improvements can also be provided by investigating the volumetric properties of a mix as it is related to the permeability of asphalt. It has become standard protocol to evaluate the moisture susceptibility of an asphalt mix as various types of tests have been developed to measure stripping (Nel, 2017).

2.8 LIMITING MOISTURE SUSCEPTIBILITY

If a water-sensitive asphalt layer is exposed to moisture, it can cause damage to the pavement layers and lead to a reduced pavement life and performance, but also lead to increased maintenance costs. To solve this problem several liquid or solid anti-stripping additives have been developed to increase the adhesion between the aggregate and the bitumen bond (Nel, 2017). Another method used to improve the bitumen-aggregate bond is by applying aggregate pre-treatment. Both these methods for increasing the bitumen-aggregate bond will be briefly discussed.

2.8.1 ANTI-STRIPPING AGENTS

An anti-stripping agent is used to minimise stripping of the binder from the aggregate. An anti-stripping additive usually softens the bitumen to ensure a reduction in moisture susceptibility, but this can cause the rut resistance of the mix to be compromised. The effect of an anti-stripping additive is also bitumen specific (Hunter & Ksaibati, 2002). However, if an additive is used incorrectly, the opposite effects may occur, which includes early maintenance and rehabilitation leading to increased economic cost.

If an asphalt mix design exhibits moisture-induced damage, it may be necessary to use an anti-stripping agent to prevent any further moisture susceptibility. Liquid and lime anti-stripping additives are among the most commonly used types.

2.8.1.1 Liquid anti-stripping additives

A liquid anti-stripping agent is a chemical compound that contains polyamines (Hunter & Ksaibati, 2002). An amine is defined as "an organic compound derived from ammonia by replacement of one or more hydrogen atoms by organic groups" (Dictionary.com, 2015). The function of a liquid anti-stripping agent is to reduce the surface tension that occurs between the aggregate and bitumen in a given mix. Once the surface tension is reduced, it leads to an increase in the adhesion of the bitumen-aggregate bond.

According to Hunter and Ksaibati (2002), the most economical and commonly used method to mix the anti-stripping agent into the asphalt mixture, is by heating the bitumen until it reaches a liquid state, and then to add the anti-stripping agent before the aggregates are placed into the mix. However, a more successful method has been discovered where the anti-stripping agent is applied directly to the aggregate before it gets mixed with the binder.

2.8.1.2 Lime anti-stripping additives

Lime additives are a very effective method for reducing the moisture susceptibility of asphalt mixes. When the aggregates in an asphalt mix has poor bitumen adhesion properties, and active filler, usually hydrated lime, can be used as an anti-stripping agent (SAPEM Chapter 4, 2014).

Hydrated lime has a low bulk density and high surface area which improves the adhesion of the bitumen-aggregate bond as well as the mix durability by retarding oxidative hardening of the binder. The general practice is to add 1 to 1.5 percent lime by dry weight of aggregate to the mix (SAPEM Chapter 9, 2014). If an excess quantity of lime is added to the mix it tends to produce dry and brittle asphalt.

2.8.2 AGGREGATE PRE-TREATMENT

Several methods of aggregate pre-treatment have been successful in improving the adhesion of the bitumen-aggregate bond. These methods include: crushing of the aggregates, preheating aggregates to evaporate water vapour, washing aggregates to remove surface coatings and also weathering (Hunter & Ksaibati, 2002). Another method that improves the resistance to moisture damage is by pre-coating the aggregates with bitumen or recycled materials.

2.9 ADHESION AND COHESION

To obtain a better understanding about moisture susceptibility and how to improve it, an in-depth understanding of the adhesive and cohesive properties of an asphalt mixture is needed. The damage in an asphalt layer can be caused by either adhesive or cohesive failure. It is necessary to define these two concepts to understand the disbonding mechanisms associated with the moisture susceptibility of asphalt.

2.9.1 ADHESION

The adhesion of an asphalt mixture is determined by the bitumen-aggregate bond, thus adhesive failure can be described as the fracturing of the bitumen-aggregate bond (Little & Jones IV, 2003). An illustration of adhesion loss can be seen in Figure 2.10.

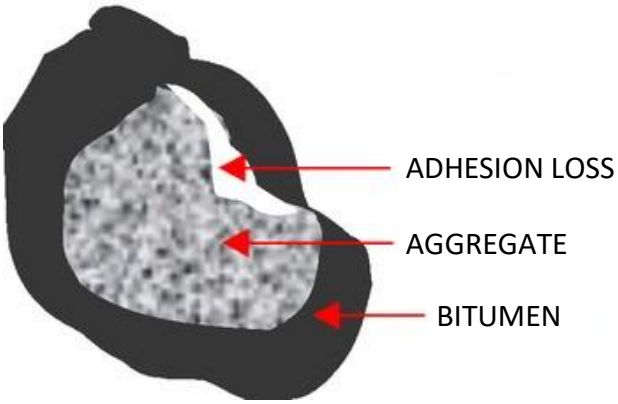

Figure 2.10: Adhesive failure (Tarefder & Zaman, 2010)

According to Terrel and Shute (1989), there are four theories that can describe the adhesion between the aggregate and bitumen in an asphalt mixture. These theories include chemical reaction, mechanical adhesion, molecular orientation and surface energy. Terrel and Shute (1989) concluded that the adhesion of an asphalt mixture can be the result of more than one of the theories combined. As a result, no single theory exists to describe the adhesion of an asphalt mixture. They also identified that the adhesion theories can be affected by the following factors:

- Aggregate and bitumen chemical composition;
- Aggregate and bitumen surface tension;
- Aggregate porosity, cleanliness, moisture content and temperature during mixing; and
- Bitumen viscosity.

From these factors it can be concluded that the properties of the bitumen and aggregate have a significant influence on the adhesion of an asphalt mixture.

2.9.2 COHESION

Cohesion describes the shear strength of a material when it is unconfined, while cohesive failure can be described as the fracturing of the bitumen mastic (Little & Jones IV, 2003). An illustration of cohesion loss can be seen in Figure 2.11.

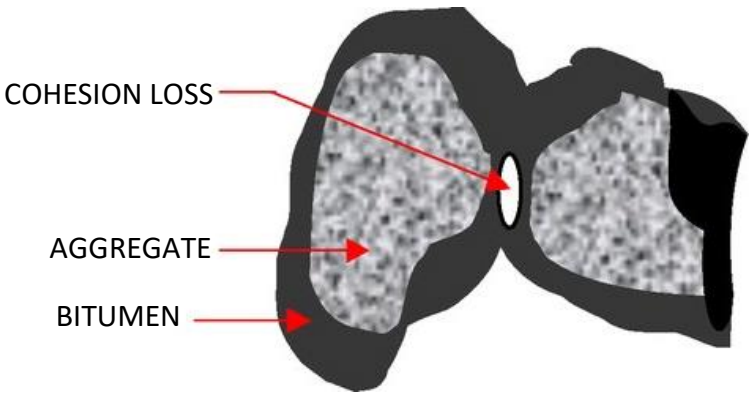

Figure 2.11: Cohesive failure (Tarefder & Zaman, 2010)

To determine the shear strength of a material, an equation was developed by Coulomb. This equation takes the cohesion of the material into account to determine the relationship between the shear strength and the cohesion. Equation 2.1 represents the equation developed by Coulomb.

$$\tau = c + \sigma \cdot tan\emptyset \qquad \text{Equation 2.1}$$

Where: τ = Shear strength

c = Cohesion

σ = Normal pressure

$\emptyset$ = Angle of internal friction

According to De Sombre et al. (1998), an asphalt mixture exhibits cohesive behaviour somewhere between a cohesive and non-cohesive soil. During compaction, the aggregates in the asphalt mixture gets distorted and reorientation occurs as for a cohesive material. As the binder in an asphalt mixture increases, the cohesiveness decreases. During compaction, the friction between the aggregates provide a resistance to the reorientation of particles, thus exhibiting cohesive behaviour similar to a non-cohesive soil (Nel, 2017). This behaviour supports the adequacy of using Coulomb's equation to determine the shear stress of an asphalt mixture.

The bitumen mastic provides cohesion within an asphalt mixture. According to Terrel and Al-Swailmi (1994), the presence of water inside an asphalt mixture causes the bitumen mastic to saturate and lead to swelling of the voids. This leads to a weakened bitumen mastic resulting in a loss of cohesion. By adding filler materials such as cement and lime to the asphalt mixture, an improvement in the cohesion and shear resistance can be made.

The cohesion of an asphalt mixture is also reliant on the temperature at which compaction takes place. There exists an indirect relationship between the cohesion and temperature of an asphalt mixture. By increasing the temperature, it will lead to a decrease in the cohesion of the mix and vice versa (De Sombre, et al., 1998).

According to research done by Schmidt and Graf (1972), asphalt can lose up to 50 % of its stiffness when it is saturated with water. On the other hand, they also concluded that the loss in stiffness can be regained upon drying. According to Cheng et al. (2002), the saturation and rate of moisture damage in asphalt mixtures are related to the distribution of water into the asphalt mixture and the movement of water through the bitumen-aggregate interface. They also concluded that asphalt mixtures which have the ability to hold great quantities of water, accumulate moisture damage at a faster rate.

2.10 DISBONDING MECHANISMS

Moisture damage is described as the loss of strength and durability of an asphalt layer due to the ingress of water. Moisture damage can cause either adhesive failure or cohesive failure. For cohesive failure to occur, the moisture must penetrate the bitumen mastic and weaken it. For adhesive failure to occur, the bitumen needs to be stripped from the aggregate surface.

Once moisture penetrates the asphalt layer, the constant traffic loads can increase the rate at which damage occurs and will lead to an asphalt layer that is more susceptible to moisture.

Moisture damage is the result of combined disbonding mechanisms. Five primary disbonding mechanisms have been identified by Little and Jones (2003), which relates to moisture damage. These five mechanisms can be seen in Figure 2.12 and will be explained in further detail.

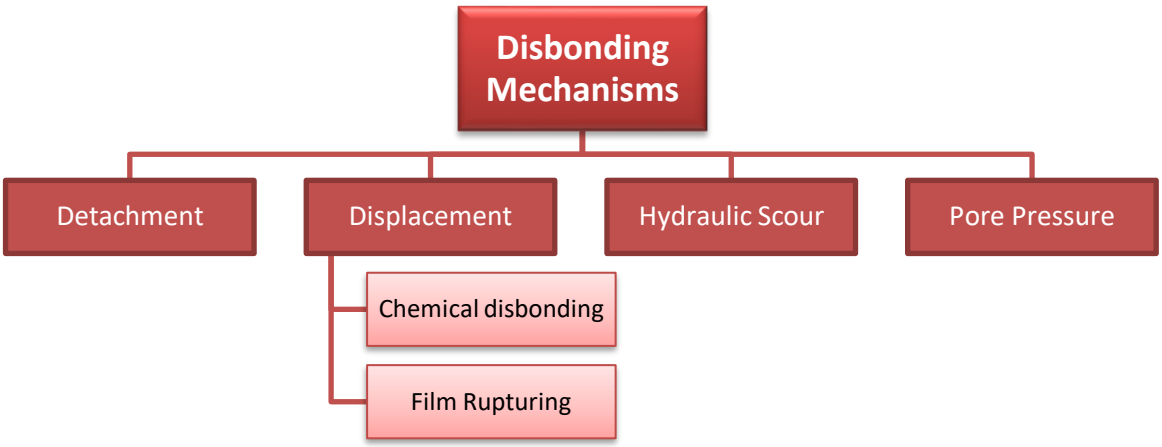

Figure 2.12: Disbonding mechanisms related to moisture damage

2.10.1 DETACHMENT

Detachment can be described as a case where the bitumen film is separated from the aggregate particles while the bitumen coating still remains intact. This means that the aggregate particles are coated with bitumen, but no adhesive bond exists between the binder and the aggregate (Brovold & Majidzadeh, 1968). Detachment is usually caused by a thermodynamic replacement of the bitumen with a thin film of water without an obvious break in the film. The water may come from either within the aggregate or outside the binder. Detachment is not only caused by water but can also be caused by aggregate particles that are contaminated by dust.

Detachment can also be explained by means of the surface energy adhesive theory. According to the surface energy adhesive theory, the adhesive bond strength between the aggregate and

bitumen is related to the ability of the bitumen to wet the aggregate. According to Brovold and Majidzadeh (1968), the wettability of aggregate increases as the surface energy of adhesion decreases. However, water has a considerably greater wetting ability as it meets the surface energy demands of aggregate better than bitumen.

According to Brovold and Majidzadeh (1968), if a three-phase interface system consisting of aggregate, bitumen and water exists, the water would reduce the surface energy of the aggregates more than bitumen, thus generating a much more thermodynamically stable condition of minimum surface energy.

This theory was validated at the Texas A&M University with surface energy measurements. With the conclusion being made that energy is being released at the bitumen-aggregate interface when the asphalt mixture is subject to water (Little & Jones IV, 2003). This means that the aggregate surface has a strong preference for water over bitumen to yield a thermodynamically stable condition. Thus, in conclusion, the more negative the surface energy in the presence of water, the greater the chance is of detachment of the bitumen to occur.

According to the Road Research Laboratory (United Kingdom), bitumen has a relatively low polarity which can cause weak dispersion forces to form the bond between aggregates and bitumen. Due to the intermolecular attraction between molecules, dispersion forces occur. However, water molecules have a high polarity which can disturb the bitumen-aggregate interface by replacing the bitumen in the mix. Cheng et al. (2002) established this theory and therefore developed a method to measure the surface energies and to calculate the adhesive bond strengths of asphalt mixtures. Figure 2.13 illustrates the detachment theory as suggested by the Road Research Laboratory.

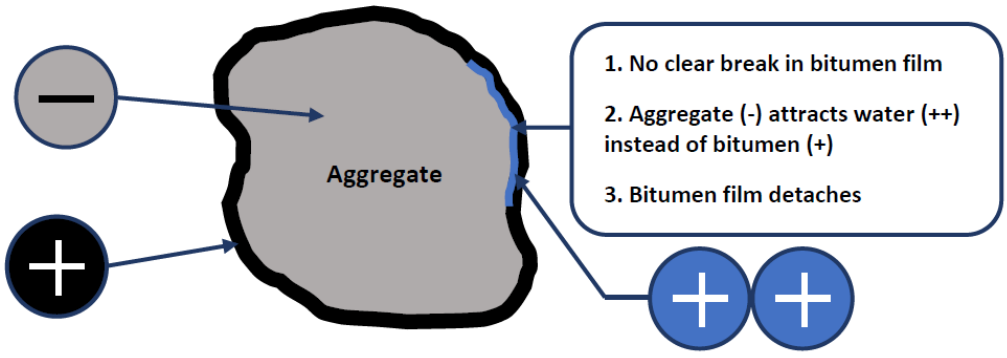

Figure 2.13: Low polarity of bitumen compared to polarity of water (Nel, 2017)

According to Read and Whiteoak (2003), the detachment process cannot be reversed. Due to traffic loading the process is accelerated as a result of continuous compression and tension cycles in the surface voids. Read and Whiteoak (2003) added that: "Suspended dust and silt in the water can act as an abrasive and can accelerate detachment."

2.10.2 DISPLACEMENT

According to Tarrer and Wagh (1991) displacement differs from detachment in the manner that it involves displacement of bitumen at the aggregate surface through a disruption in the bitumen film. The cause of the disruption may be due to inadequate coating of the aggregate surface with bitumen, or a rupture in the bitumen film at sharp edges and corners of the aggregate. Once moisture penetrates these disruptions, it displaces the bitumen from the aggregate surface.

The process of displacement can also occur due to changes in the pH-level of the water at the aggregate surface that enters through the point of disruption (Little & Jones IV, 2003). This process is known as chemical disbonding. A change in the pH-level of the water can cause a build-up of negative polarity on the opposing aggregate and bitumen surfaces. By attracting more water to the aggregate's surface (causing displacement of the bitumen there from), equilibrium is achieved. This theory is supported by Hughes et al. (1960) and Scott (1978) by stating that adhesion losses occur between the aggregate and bitumen when the pH of water is increased from 7.0 up to 9.0.

The pH sensitivity at the bitumen-aggregate interface was investigated by Kiggundu and Roberts (1998). They concluded that the bond strength increased, and stripping decreased by stabilising the pH-level at this interface. Little and Jones (2003) acknowledged that between a pH-level of 9.0 and 10.0, no dislodging of amines from the surface of acidic-aggregates will occur. Even though hydrated lime can be used to control the pH-level, a pH-level less than 4.0 will dissolve the hydrated lime and cause amines to dislodge from the aggregate's surface (Little & Jones IV, 2003).

Displacement of the bitumen film can also be caused by the rupturing thereof. Rupturing occurs at the sharp edges of the aggregate which then creates pathways for moisture to ingress, leading to displacement of the bitumen film. The combined action of traffic and the environmental effects can also lead to rupturing of the bitumen film. Once rupturing takes place, the rate of displacement is dependent on the following factors (Greyling, et al., 2015):

- Bitumen film thickness;
- Bitumen rheology (viscosity);
- Nature of aggregate surface; and
- Presence of binder modifying agents and filler material.

2.10.3 HYDRAULIC SCOUR

Hydraulic scour can be defined as the stripping of the pavement surface as a result from the action of vehicle tyres on a saturated surface (Little & Jones IV, 2003). Due to the action of the tyres, the water on the asphalt surface gets sucked under the tyre and forced into the pavement.

According to Little and Jones (2003), osmosis can be seen as a possible mechanism of hydraulic scour. Osmosis is a term used to describe the tendency of water to pass through a semi-permeable membrane into a solution where the solvent concentration is higher. Osmosis occurs in the presence of salts (or salt solutions) in the aggregate pores which then creates an osmotic pressure gradient that sucks the water through the bitumen film. Figure 2.14 illustrates the hydraulic scour process.

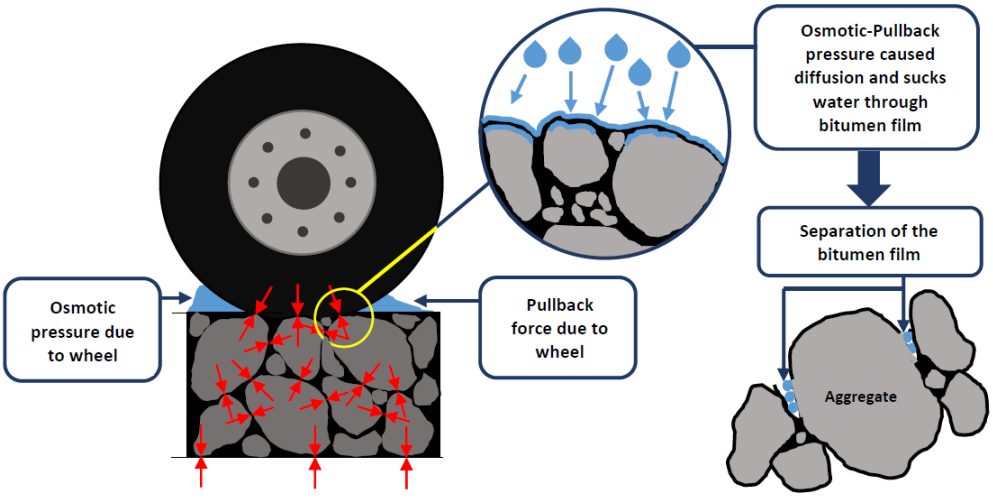

Figure 2.14: Flow of water through bitumen film due to osmosis (Nel, 2017)

Even though several researchers do not support this process, Cheng et al. (2002) went on to investigate the diffusion of water vapour through the bitumen film. They concluded that the bitumen film is permeable and can store a considerable large amount of water. This conclusion supported the theory that water can penetrate the bitumen film by means of the osmotic process.

Thus, due to the permeability of the bitumen film and the presence of salts in the aggregate pores, hydraulic scour can be seen as a plausible disbonding mechanism.

2.10.4 PORE PRESSURE

When the water that is trapped inside the air voids of an asphalt mixture is stressed, pore pressure damage can occur. Due to repeated traffic loading, the pore pressure cumulatively accumulates in the asphalt layer. The continued accumulation of pore pressure causes damage to the bitumen film on the aggregate surface which then leads to the development of micro-cracks in the bitumen mastic. These micro-cracks provide additional channels for moisture ingress into the asphalt layer and can lead to extensive moisture damage. The rate of crack growth will increase once the bitumen-aggregate bond is disrupted. Figure 2.15 illustrates the distribution of stresses through the pavement surface and the water induced stresses due to pore pressure in the air voids.

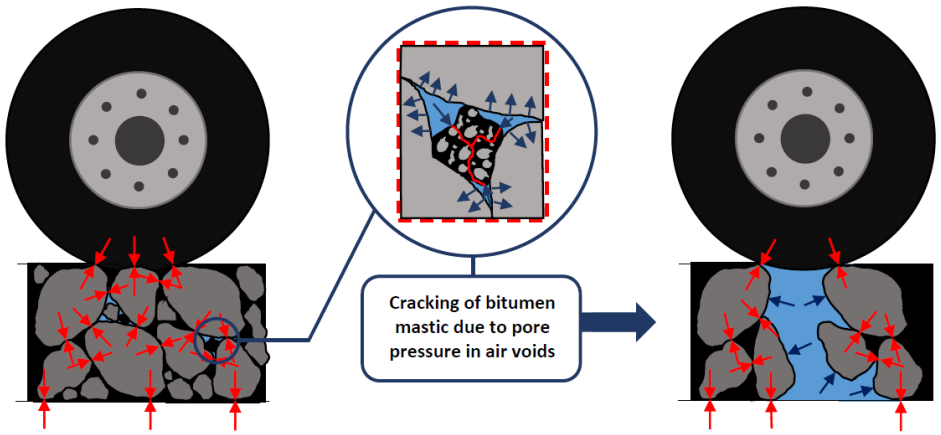

Figure 2.15: Distribution of traffic and water induced stresses throughout the asphalt layer (Nel, 2017)

When designing for the moisture susceptibility of an asphalt mixture, it is important to consider the pore pressure damage. In surfacing layers, values of 150 *kPa* pore pressure are not uncommon (Twagira, 2009). Cracks that are formed by pore pressure damage can lead to moisture ingress in the underlying layers of the pavement and cause erosion. This can have a significant influence on the asphalt layer's resistance to fatigue and permanent deformation.

Terrel and Al-Swailmi (1994) defined the concept of pessimum air void range. This describes the specification range of air void content, between 8 % and 10 %, within which most asphalt mixtures are typically compacted to. Terrel and Al-Swailmi (1994) also advised that if the air void content is

within this specification, it can cause the air voids to become saturated with moisture. The moisture can enter these non-interconnected voids and create the ideal situation for pore pressure accumulation which can then cause moisture damage.

An air void content greater than 10 % results in the air voids becoming inter-connected, causing channels for the moisture to flow out under the stress created by traffic loading. An air void content lower than 4 % leads to an asphalt mixture that is relatively impermeable and has no inter-connected air voids.

2.11 FACTORS AFFECTING THE BITUMEN-AGGREGATE BOND

The Shell Bitumen Handbook, written by Read and Whiteoak (2003), established that there are several factors that affect the bitumen-aggregate bond. The main factors affecting the bitumen-aggregate bond can be divided into four groups, namely: aggregate properties, bitumen properties, external factors and mixing properties. Each group has various factors that affect the bitumen-aggregate bond. According to Read and Whiteoak (2003), 80 % of these factors can be controlled during the production and construction phase. These factors, divided into their four groups, can be seen in Figure 2.16 and will be discussed in more detail.

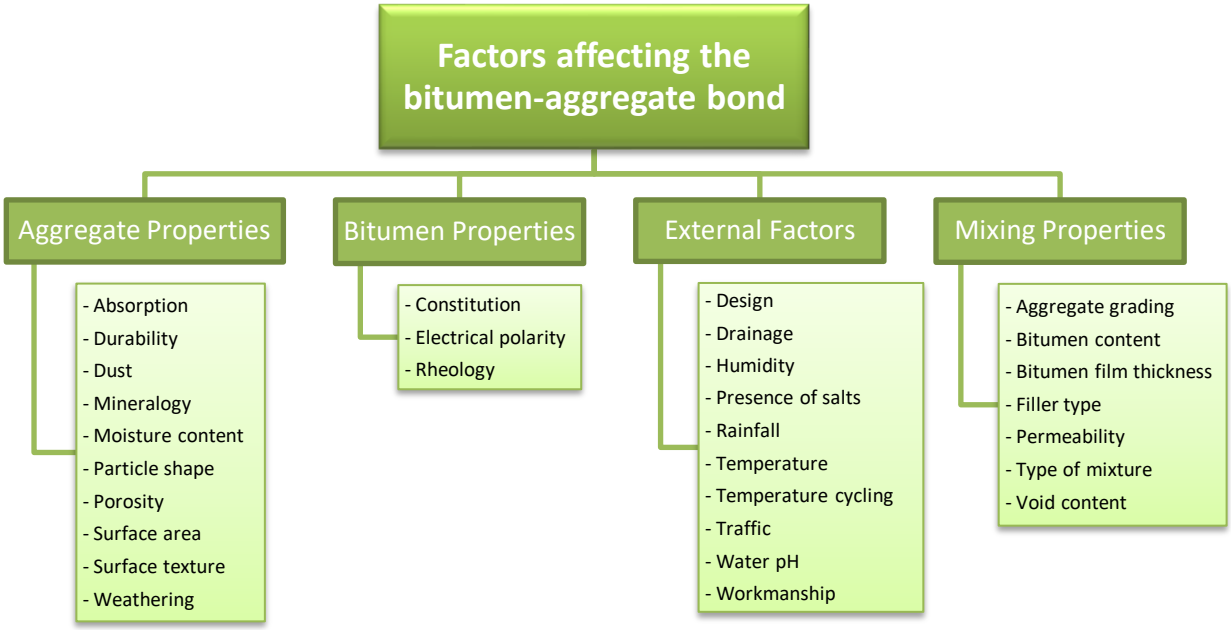

Figure 2.16: Factors affecting the bitumen-aggregate bond

One of the main factors influencing the bitumen-aggregate bond is the type of aggregate being used. Aggregate properties have a significant influence on the moisture susceptibility of an asphalt mixture.

The volumetric properties of an asphalt mixture depend on the grading of the aggregate as well as the mixture's compactibility. The permeability of an asphalt mixture is determined by the volumetric properties and thus the moisture susceptibility is controlled by these volumetric properties. An illustration of the interaction between the aggregates, bitumen and air voids of an asphalt mixture can be seen in Figure 2.17.

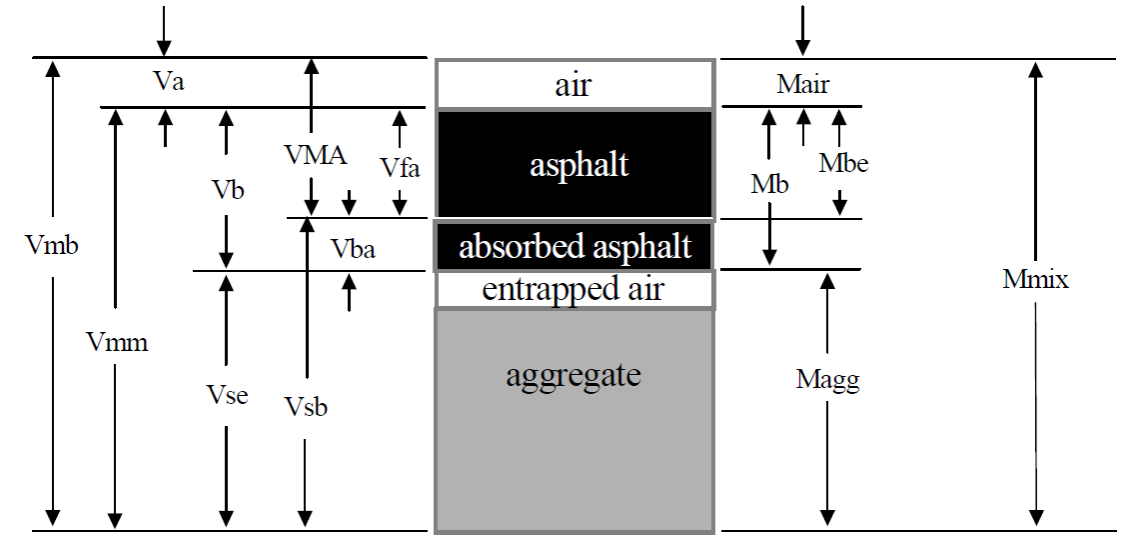

VMA = Volume of voids in mineral aggregate
V_{mb} = Bulk volume of compacted mix
V_{mm} = Voidless volume of paving mix
V_{fa} = Volume of voids filled with asphalt
V_a = Volume of air voids
V_b = Volume of asphalt binder
V_{ba} = Volume of absorbed asphalt binder
V_{sb} = Volume of mineral aggregate (by bulk specific gravity)
V_{se} = Volume of mineral aggregate (by effective specific gravity)

M_{mix} = Total mass of asphalt mixture
M_b = Mass of asphalt binder
M_{be} = Mass of effective aggregate binder
M_{agg} = Mass of aggregate
M_{air} = Mass of air = 0

Figure 2.17: Components of a compacted hot mix asphalt (Huner & Brown, 2001)

The volumetric properties that are required in an asphalt mixture include the voids in the mineral aggregate (VMA), the voids filled with binder (VFM) and the voids in the mixture (VIM). These properties can be defined as follows (Huner & Brown, 2001):

- **Voids in the mineral aggregate (VMA):** The VMA is a measure of the volume intergranular void spaces located between the aggregate particles of an asphalt mixture. The VMA percentage is calculated by dividing the sum of the volume of air voids and binder not absorbed by aggregates, with the total volume of the compacted asphalt mixture.
- **Voids filled with binder (VFB):** The VFB is the percentage VMA volume that is filled with binder, divided by the total volume VMA of the compacted asphalt mixture.
- **Voids in the mixture (VIM):** The VIM is the total volume of air pockets which is located between the coated aggregate particles of a compacted asphalt mixture. It is expressed as a percentage of the total volume of the compacted asphalt mixture.

The VIM is directly related to the VMA and indirectly related to the VFB. This indicates that an increase in the VIM of an asphalt mixture will also increase the VMA, while the VFB of the mixture will decrease. As previously stated, the moisture susceptibility of an asphalt mixture is determined by the volumetric properties. Thus, by decreasing the air void content in an asphalt mixture it also decreases the permeability. The air void content can be decreased by means of increasing the extent to which the mixture is compacted, or by increasing the binder content. However, the extent of compaction is dependent on the grading of the aggregate in the asphalt mixture (Douries, 2004).

2.12 ASPHALT MIX TYPES AND PROPERTIES

Asphalt mix types can be categorised in terms of their grading parameters. However, this cannot be the only factor taken into account, the volumetric concepts should also be considered (SAPEM Chapter 9, 2014). By taking the abovementioned into account a better understanding of how the components in the mix are packed together, as well as how this packing influences the performance of the mix, is developed. This packing can be divided into two types that are generally in use, namely a sand-skeleton mix and a stone-skeleton mix.

2.12.1 MIX CATEGORIES

A sand-skeleton mix is normally a thin layer where its main purpose is to provide a water-tight seal on flexible, untreated pavements on a low speed road (SAPEM Chapter 9, 2014). Sand-skeleton mixes are mostly used for residential streets. In a sand-skeleton mix the loads acting on the layer are primarily carried by the finer aggregate fraction. The larger aggregate fractions provide bulk and replaces a proportion of the finer fractions. There is no significant contact between the individual larger aggregate fractions. An illustration of a sand-skeleton mix can be seen in Figure 2.18.

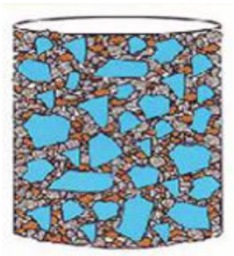

Figure 2.18: Sand-skeleton mix (SAPEM Chapter 9, 2014)

A stone-skeleton mix is usually used on high volume roads where resistance to permanent deformation (rutting) under elevated temperature conditions as well as anti-skid properties are required (SAPEM Chapter 9, 2014). In a stone-skeleton mix the spaces between the larger aggregate fractions are filled by finer aggregate fractions, but do not push the larger aggregate fractions apart. Thus, contact between the larger aggregate fractions are guaranteed, and therefore the larger aggregate fractions create a "skeleton" that carry the loads acting on the layer. An illustration of a stone-skeleton mix can be seen in Figure 2.19.

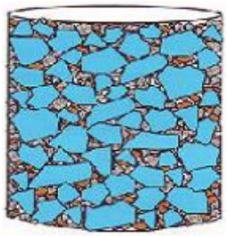

Figure 2.19: Stone-skeleton mix (SAPEM Chapter 9, 2014)

Ternary diagrams can also be useful in classifying a mix according to its relative proportions of sand, stones and filler. An example of such a ternary diagram can be seen in Figure 2.20.

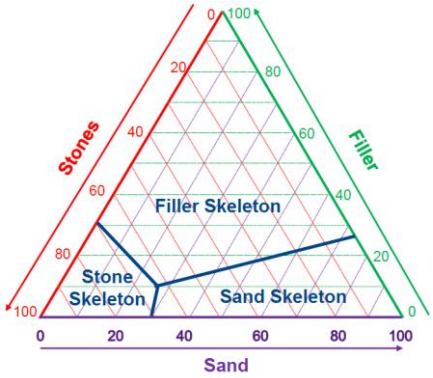

Figure 2.20: Ternary diagram for classifying asphalt mixes according to skeleton type (SAPEM Chapter 9, 2014)

Asphalt mixes can be classified in terms of their particle size distribution (grading) once the packing characteristics for a specific source of aggregate has been decided upon. These gradings are then used in quality control tests to ensure that the required design parameters are being met.

2.12.2 CHOICE OF MIX TYPE

Asphalt surfacing can be divided into two general categories by means of their main purpose. These two categories are functional and structural (SAPEM Chapter 2, 2014).

2.12.2.1 Functional

An asphalt surface can be labelled as a functional layer when it has a thickness of less than 30 *mm*. A functional layer is also defined as a layer that does not contribute to the strength of the pavement. It should conform to the functional criteria which includes a suitable surface texture for surface drainage, noise reduction and adequate skid resistance against environmental elements for the prevailing traffic. It should also conform to the sealing of the underlying layers to prevent any moisture ingress.

Functional layers can be used for thin asphalt layers in residential areas where the traffic and speed are relatively low. It can also be used as an Ultra-Thin Friction Course (UTFC) on major highways where the traffic volume and speed are substantially higher.

2.12.2.2 Structural

An asphalt surface can be labelled as a structural layer when it has a thickness of more than 30 *mm*. A structural layer is also defined as a layer that is designed to contribute to the strength of the pavement. It should provide adequate skid resistance against environmental elements for the prevailing traffic. A structural asphalt layer should be designed with low permeability to protect the underlying layers against moisture ingress.

In South Africa, an asphalt surfacing is typically between 30 and 50 *mm* thick, which means that it is mostly used as a structural layer (SAPEM Chapter 2, 2014).

A summary of the key properties and quality assurance for functional and structural asphalt layers can be seen in Table 2.2.

Table 2.2: Functional and structural asphalt layers summary

	STRUCTURAL ≥ 30 *mm*	FUNCTIONAL < 30 *mm*
KEY PROPERTIES	• Adequate skid resistance; • Low permeability to protect underlying layers; • Structural reliability.	• Surface texture for low speed (< 80 km/h) skid resistance; • Low permeability to protect underlying layers; • Compactibility, since thin layers cool quickly.
QUALITY ASSURANCE	Performance related testing.	Examination of: • Permeability; • Skid resistance; • Uniformity of surface texture.

2.13 ASPHALT GRADING TYPES

The particle size distribution (grading) of asphalt mixes can be categorized into 5 classes for use in South Africa. These classes are:

- Continuously graded;
- Gap-graded;
- Semi-gap graded;
- Open-graded; and
- Semi-open graded.

Continuously graded can be either continuous-coarse or continuous-fine. Special cases of gap-graded asphalt include Stone Matrix Asphalt (SMA) and UTFC. Open-graded mixes are coarser than semi-open graded mixes. This means that semi-open graded mixes' voids are mostly filled with binder, which is typically a modified binder such as bitumen-rubber (SAPEM Chapter 9, 2014). The general relationship between the packing characteristics and the various particle size distribution types is illustrated in Figure 2.21.

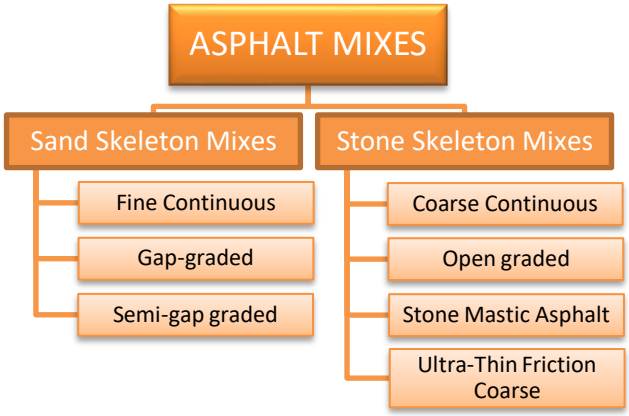

Figure 2.21: Packing characteristics and particle size distribution relationship

Asphalt mixes are designed and produced from different aggregate types, different aggregate size combinations and also different binder types. Each asphalt mix has its own engineering properties to comply with, which is required for a specific design condition. These engineering properties differ for each asphalt mix and Table 2.3 (TRH 8, 1987) gives an indication of which asphalt mix complies with the specified engineering properties. The comparison between the mixes is made on an escalating performance scale from 1 to 5, where 5 indicates a good performance and 1 indicates a poor performance for the specified engineering property.

Table 2.3: Rating of asphalt mixes in terms of engineering properties

	Continuously graded	Gap-graded	Semi-gap graded	Open-graded
Durability	4 – 5	3 – 4	4	1
Fatigue resistance	3	4 – 5	4	4
Impermeability to water	3 – 4	5	4	1
Resistance to deformation	4 – 5	2 – 3	3 – 4	3
Shrinkage	5	3	4	4
Skid resistance	3	4	5	5
Stiffness	4 – 5	3	4	1
Tensile Strength	5	3	4	1
Workability	4	4	4	5

It is important to note that the fatigue resistance in Table 2.3 was tested in constant strain mode, but in reality, actual fatigue life is dependent on the layer thickness, layer stiffness as well as the stiffness of the underlying layers (support condition). Also, even though a low rating was given for several engineering properties in Table 2.3, it does not imply that the asphalt mix type cannot be designed to accommodate this inadequacy.

2.13.1 CONTINUOUSLY GRADED ASPHALT

Maximum density gradings are mostly used for continuously graded asphalt mixes. This mix type is able to resist plastic deformation due to its interlocking stone-skeleton, which is obtained by carefully selecting the aggregate fractions which should be used in the asphalt mix. A continuously graded asphalt mix has a very high stiffness and thus it is suitable to use as a structural layer. It has a high durability and resistance to shrinkage due to relatively few voids in the mix. Even though the air void percentage is relatively low, the voids can still be inter-connected, which means that water is allowed to seep through the layer. This is usually the case with coarse mixes.

2.13.2 GAP-GRADED AND SEMI-GAP GRADED ASPHALT

Gap-graded and semi-gap graded asphalt mixes have a specific range of particle sizes omitted from the overall aggregate grading. A gap-graded asphalt mix consists of a uniform size coarse aggregate which is blended with fine aggregate and filler. While a semi-gap graded asphalt mix consists of a more varied size coarse aggregate blended with fine aggregate and filler. These two mix types have been used with great success as surfacing, bases and overlays in South Africa.

2.13.3 OPEN-GRADED AND SEMI-OPEN GRADED ASPHALT

Open-graded asphalt mixes have a very coarse and open surface finish, which is the result of an aggregate structure designed to have a high air void content. This mix is normally used for a very thin asphalt layer, more or less 25 *mm* thick, for the purpose of improving skid resistance, reducing spray and splash from vehicles and also to reduce surface noise (TRH 8, 1987). These requirements can be achieved if the open-graded mixture is well designed.

However, having a high air void content, as to meet the requirements, can lead to several complications. A complication such as the voids being filled with dust which will essentially lead to a reduction in the effectiveness of this mix.

Since this mix type requires a high air void content, it leads to a high surface permeability which can cause moisture ingress to the underlying layers. It is thus imperative that an open-graded asphalt mix is laid over an impermeable asphalt layer or seal to ensure that no moisture damage occurs in the underlying layers.

An open-graded asphalt mix should not be used as a structural layer as it does not distribute traffic stresses as effective as a dense mix would, thus it should only be used as a surfacing layer.

This mix is commonly produced by using a higher binder content, where the binder is usually modified. To accommodate for this additional binder, without affecting the mechanical stability of the mix, the grading of the aggregate needs to be adjusted (TRH 8, 1987). This type of mix is referred to as a semi-open graded asphalt mix.

2.13.4 ULTRA-THIN FRICTION COURSE (UTFC)

A UTFC is a hard-wearing surface system which has to ensure that an impermeable membrane at the base of the layer is achieved. This can be done by using an open-graded stone-skeleton mix which has a sprayed layer of binder applied with self-priming pavers (SAPEM Chapter 9, 2014). These binders are usually modified.

Agrément South Africa (ASA) has to authorise UTFC's as being fit for purpose in agreement with the criteria which is set out in their guidelines. Some of the criteria that they assess include the aggregate polishing resistance, aggregate strength, durability, permanent deformation, resistance to moisture induced stripping, skid resistance, texture depth and torque bond value (SAPEM Chapter 9, 2014).

2.14 COMPACTION AND COMPACTIBILITY

To ensure sufficient performance of an asphalt layer it is critical to achieve adequate compaction. By adequately compacting a layer, it improves the strength and stability of the layer by ensuring an

aggregate lock-up. It should also accomplish partial closing of air and water channels. Table 2.4 gives an indication of the effects that good and poor compaction have on an asphalt layer (Asphalt Institute, 2007).

Table 2.4: Effects of good and poor compaction

GOOD COMPACTION	POOR COMPACTION
• Acceptable functional and structural performance; • Durability; • Prevents oxidative hardening of binder; • Protects underlying layers against water ingress.	• Excessive oxidative hardening; • Insufficient long-term traffic compaction; • Permeability and moisture damage to underlying layers; • Rutting in wheel paths.

2.14.1 IMPORTANCE OF COMPACTION

During the compaction process of an HMA, there are three factors that affect the performance of the pavement. Firstly, the bitumen-coated aggregate particles are pressed together, the air voids are reduced, and the mix density increases. Higher mix stability and pavement strength is achieved when the aggregates are pressed together, since it causes their surface-to-surface contact and inter-particle friction to increase (Asphalt Institute, 2007).

A nearly impermeable pavement can be produced if the air voids in the mix are reduced to their optimum level. If a mix is under-compacted, the voids inside the mix tend to be inter-connected, which then leads to a pavement that is more susceptible to air and water ingress. This can ultimately lead to premature pavement distress. The air that infiltrates the pavement oxidizes the asphalt binder, causing it to become more brittle and causing the mix to crack under repeated traffic loads (Asphalt Institute, 2007). If water permeates through the pavement it can lead to stripping of the bitumen binder from the aggregate as well as a weakened base and subbase.

If an optimal level of compaction is not achieved during the construction phase, the repeated traffic will further densify the mix. This will mainly occur in the wheel paths, causing rutting on the road which can be a safety hazard for road users during wet weather conditions.

2.14.2 MECHANICS OF COMPACTION

The main purpose of compacting HMA is to achieve the optimum air void content. The HMA typically has an in-place air void percentage of 15 to 20 % behind the paver. For dense-graded HMA mixes, adequate rollers are needed to reduce this air void content to 8 % or less. A stone-matrix asphalt (SMA) mix should typically be compacted to contain an air void content of 6 % or less. With air void percentages at these levels, it ensures that the air voids are not inter-connected and avoids the detrimental effects of air and water, which is mainly ravelling and stripping. If a mix is compacted to a level where the air voids are 2 % or less, it gives an indication that a problem exists with the mix design or the mix production process, such as excessive bitumen binder or dust (Asphalt Institute, 2007).

Adequate compaction of an HMA can only be achieved if two conditions exist, namely: mix confinement and the correct mix temperature. If the temperature is too high, the bitumen binder becomes less viscous, which then allows the aggregate particles to readily move past one another and rearrange itself into a tight mass (Asphalt Institute, 2007). As this mix then cools down, the bitumen binder stiffens and resists further mix densification. Thus, it is preferable that the asphalt mix be compacted while the mix is still hot and workable. Further, there are no specific temperature ranges that apply to all asphalt mixes. For example, an asphalt mix that uses a polymer-modified bitumen binder stiffens at a higher temperature, which means that there is less time for compaction to take place than with mixes using an unmodified bitumen binder.

Even if the mix has the correct temperature for compaction, the target density can only be achieved when the mix is also adequately confined. The confinement is controlled by the compressive force of the roller, the cohesion of the mix, as well as the support provided by the underlying layers. The compressive force of the rollers comes from their weight as well as the dynamic energy due to vibration (Asphalt Institute, 2007). The cohesion of the mix is a result of the inter-particle friction of the aggregates and the bitumen binder's viscosity. The supporting force of the underlying layers is a result of its firmness and stability.

2.15 THEORETICAL BACKGROUND OF ASPHALT PERMEABILITY

Permeability, also known as hydraulic conductivity, can be defined as the property that described the flow of water through a specific porous medium.

Typically, permeability is represented by the coefficient of permeability (*K*), which is the constant of proportionality of the relationship between the hydraulic gradient and the flow velocity between two points in a porous medium (Garber & Hoel, 2009).

The permeability of a porous medium can be explained due to the work done by the French engineer, Henry Darcy, in 1856. Darcy's Law explains permeability by means of an experimental framework shown in Figure 2.22.

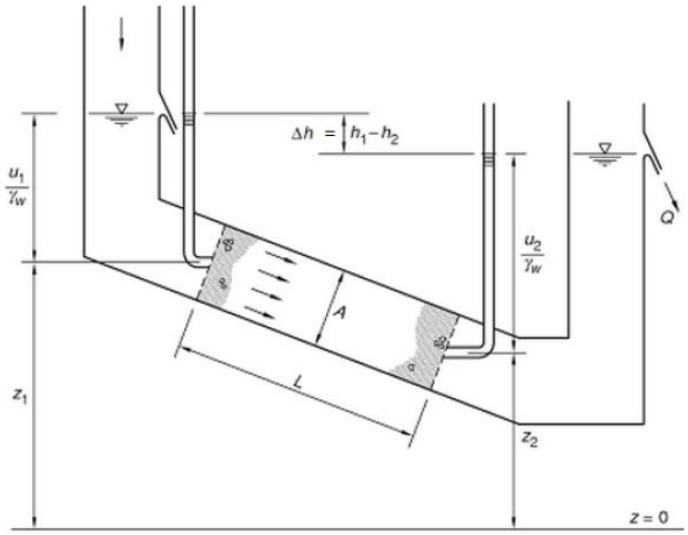

Figure 2.22: Schematic framework of Darcy's Law (Lancellotta, 2008)

Darcy attempted to develop a water purification system by using sand as a medium. Darcy's Law states that the discharge velocity of the fluid is directly proportional to the hydraulic gradient. Equation 2.2 represents Darcy's Law (Awadalla, 2015):

$$Q = \mathrm{K} \cdot \left(\frac{\Delta h}{L}\right) \cdot A \qquad \text{Equation 2.2}$$

Where: Q = Rate of flow

K = Permeability coefficient

Δh = Change in hydraulic head

L = Length of flow

A = Cross-sectional area perpendicular to the flow direction

By using Darcy's Law, the permeability coefficient can be determined by using two different testing techniques, namely: the constant head and the falling head permeability tests.

2.16 FACTORS AFFECTING ASPHALT PERMEABILITY

During the construction of HMA, it is vital that the mix be effectively compacted in-place to ensure that the initial permeability is low. If the in-place density is low, it will allow water and air to penetrate into the HMA pavement. This condition can then lead to an increased potential for damage of the pavement such as cracking, ravelling, stripping and excessive oxidation of the bitumen binder. The type of compaction equipment and practices being used during construction can affect the final in-place air voids – also, using a coarse-graded mixture can increase the potential of creating a more permeable pavement (Weston, 2005).

According to research, the most common factors that affect the permeability of HMA include inter-connected voids, Nominal Maximum Aggregate Size (NMAS), and compaction. These factors can be seen in Figure 2.23.

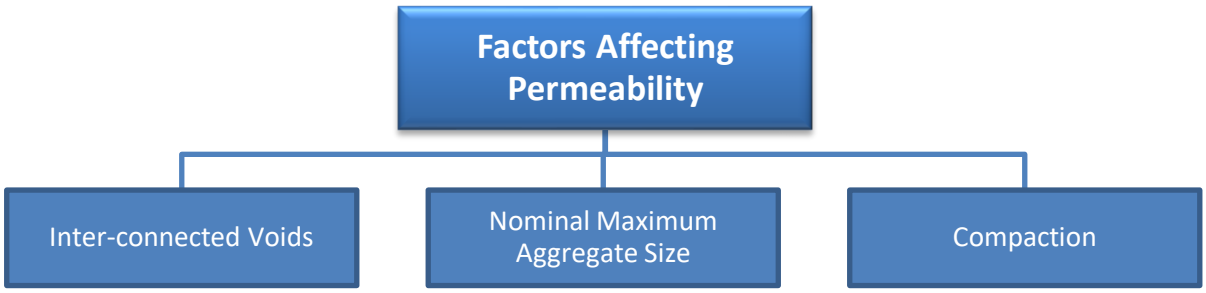

Figure 2.23: Factors that influence the permeability of an asphalt mixture

According to previous studies, it has been found that the factor which has the greatest influence on permeability is the content of inter-connected voids (Brown et al., 2004).

According to Weston (2005), research has shown that coarse-graded mixes are more permeable than fine-graded mixes. It has also shown that when comparing two fine-graded mixes, the mix with the higher NMAS will naturally be more permeable.

Typically, as the NMAS in an asphalt mixture increases, the size of the individual air voids also increases, which then leads to the pavement having an increased permeability.

In Figure 2.24, the fine-graded mix, on the left side of the image, has an air void space which is filled with smaller aggregate particles. The coarse-graded mix, on the right side of the image, has more air void space created by the lack of fine aggregate particles.

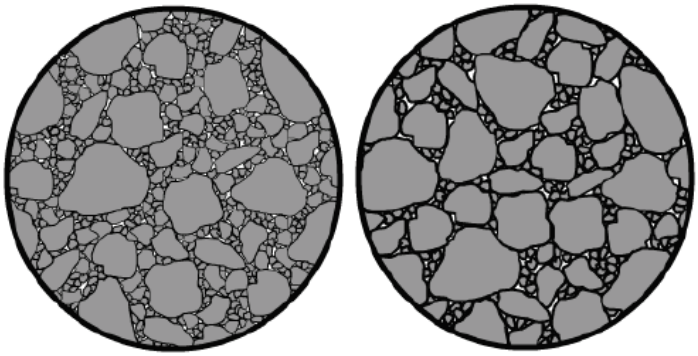

Figure 2.24: Fine-graded mix (left) and coarse-graded mix (right) (Weston, 2005)

According to a study done by the National Centre for Asphalt Technology (NCAT), the higher the NMAS, the larger the individual air voids and greater volume of inter-connected air voids (Weston, 2005). This statement is supported by the best-fit curves for in-place air voids versus permeability for different NMAS mixes, shown in Figure 2.25.

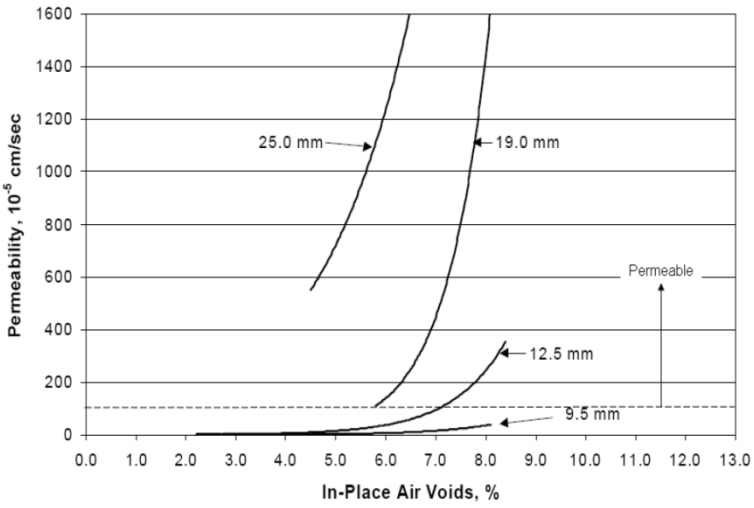

Figure 2.25: In-place air voids versus permeability (Weston, 2005)

It is important to avoid excessive permeability to ensure pavement longevity. An asphalt mixture needs to be designed and constructed in such a way that permeability will not become a

performance issue. To achieve this, it is necessary to ensure that the inter-connected voids, NMAS and compaction be taken into account when designing an asphalt mixture.

2.17 PERMEABILITY TESTING

There are a number of devices and mechanisms available for researchers to determine the permeability of a pavement. This literature study involves the investigation of various types of permeameters which are available commercially, both for in-field and laboratory scenarios. There are several types of permeameters available and a summary of these can be seen in Figure 2.26. Some of these permeameters utilize water as the fluid that will seep through the pavement structure, while others use air as a penetrating fluid. The techniques which the devices are based on can also differ; some are based on the constant head concept, while others are based on the falling head concept. These permeameters will be discussed in more detail in the following chapter.

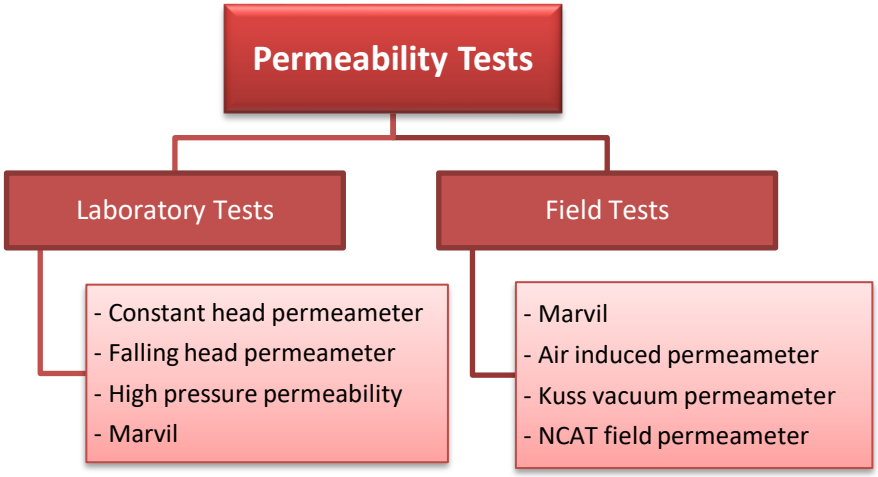

Figure 2.26: Types of laboratory and field permeability tests

2.17.1 CONSTANT HEAD PERMEAMETER

The calculation of the permeability coefficient with the use of a constant head permeameter is based on Darcy's Law of fluid filtration through a porous material (Redivo, 2012). For several years the constant head technique has been used in laboratories to determine the permeability coefficient of HMA pavement cores.

The constant head soil testing system (see Figure 2.27), used to measure the permeability of soil, can be used for asphalt core testing as well. A 152 *mm* diameter asphalt core can be placed inside the testing cell where it is enclosed with a rubber membrane along with porous stones placed at its top and bottom faces (Awadalla, 2015). In this testing configuration, water is used to apply a confining pressure on the core by using an inlet pressure and outlet pressures. The difference in the applied pressures should not be high in order to ensure that the water flow is laminar (not turbulent).

Figure 2.27: Constant head permeameter (Maupin, 2000)

It has been found that the constant head test is more applicable to high permeable materials such as sand, while the falling head test is more applicable to low permeable materials such as an asphalt layer (Awadalla, 2015).

2.17.2 FALLING HEAD PERMEAMETER

The falling head permeameter is based on measuring the change in head and quantity of flow over time. Figure 2.28 illustrates the schematic setup to conduct one variation of the falling head permeability test.

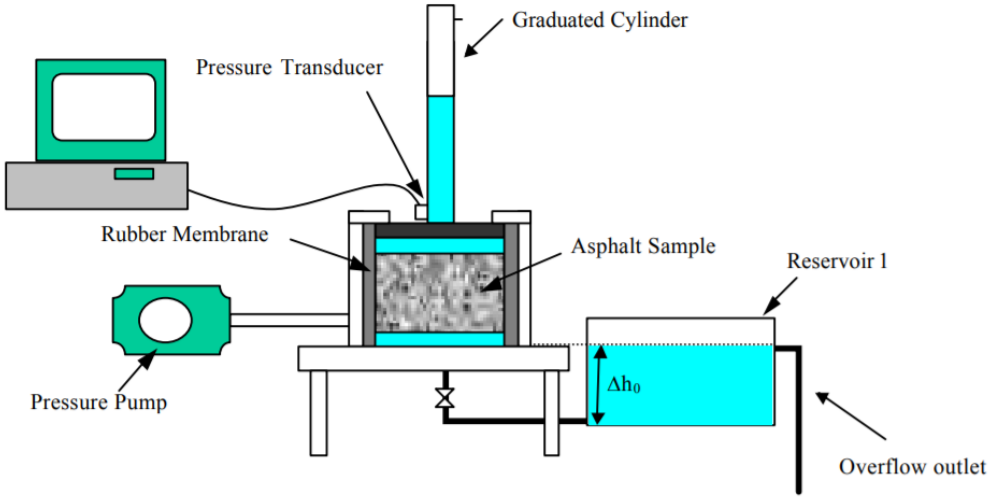

Figure 2.28: Schematic setup of falling head permeameter (Faghri & Sadd, 2002)

The falling head apparatus consists of a metal cylinder which has a flexible membrane on the inside of the cylinder where air pressure can be applied. An asphalt core is placed between plastic plates on the top and bottom. Clamps are used to ensure that the assembly is compressed and sealed together.

The plastic plate at the top has a hole that attaches to the graduated cylinder for water to be introduced into the system. The hole on the bottom plastic plate is fitted with an outlet pipe and valve for water to flow out of the system. The outflow of water from the system is directed to a reservoir which has an overflow slot to keep the reference head constant.

By using a hand pump, pressurised air is induced into the space between the membrane and the cylinder. The pressure that is applied on the rubber membrane seals the flow paths along the sides of the asphalt core.

2.17.2.1 Procedure

To start the testing procedure, the graduated cylinder is filled with water and the permeameter is slightly tilted and gently tapped to remove all the air bubbles inside the system. The water is then allowed to flow through the asphalt core by opening the bottom valve of the permeameter.

A high precision pressure transducer, at the base of the graduated cylinder, is used to make measurements of the falling head time history through the asphalt core. This data is then directly transmitted to a computer which is equipped with the correct data analysis software.

2.17.3 HIGH PRESSURE PERMEABILITY TEST

The High Pressure Permeability (HPP) test was designed and developed by Ockert Renaldo Grobbelaar in 2016 at the University of Stellenbosch (Grobbelaar, 2016). It was originally developed to test the permeability of chip seals under pressure but can also be used to determine the in-situ water permeability of an asphalt (or bituminous) surface.

2.17.3.1 Apparatus

The HPP apparatus consists of two sections (see Figure 2.29). The top section of the apparatus contains a quick coupling nozzle to apply pressure to the system by means of a compressor. The pressure valve (Valve 1), is fitted with a funnel to help fill the apparatus with water without any spillage. The top section of the apparatus also contains a water flow gauge and level indicator to measure the water drop during testing.

The bottom section of the apparatus contains two sockets, one below and one above the test specimen. The socket above the test specimen, contains a pressure gauge and a high pressure valve (Valve 2). The gauge is used to monitor the pressure inside the apparatus, since it is a constant head test. The high pressure valve (Valve 2) is used to drain the apparatus once testing is complete. The socket below the test specimen also contains a high pressure valve (Valve 3), which is opened during testing to allow the water to drain free from the apparatus.

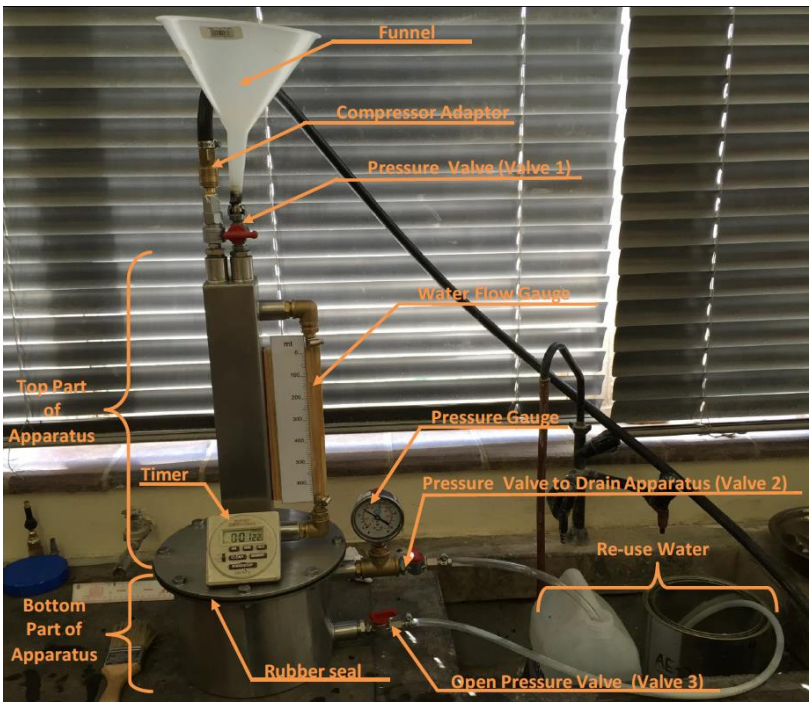

Figure 2.29: HPP test apparatus (Grobbelaar, 2016)

The top and bottom sections of the apparatus are bolted together and has a rubber seal between them to prevent leakage. These two sections enable the apparatus to be opened and used to insert and remove a test specimen.

2.17.3.2 Procedure

To test the permeability of a seal, the seal is placed inside the apparatus with the top and bottom sections being bolted together. The apparatus gets filled with water until the level indicator reaches the zero-millilitre mark. The apparatus is slightly tilted to the side to remove all air bubbles from the system.

Set the pressure and attach the compressor to the quick coupling nozzle. The pressure which is applied to the testing specimen can range from 100 *kPa* to 200 *kPa*. Once testing has started, the water level should be recorded constantly as it drops. If the water level drops rapidly, it indicates that the specimen has a high permeability coefficient and vice versa.

2.17.4 MARVIL PERMEABILITY TEST

The Marvil permeability test can be described as the procedure used to determine the in-situ water permeability of an asphalt (or bituminous) surface based on the falling head permeameter principle. By determining the permeability of a layer, it provides a better understanding of the material's susceptibility to the ingress of water as well as the inter-connectivity of the air voids. Ultimately, the permeability of an asphalt layer can also give an indication of the relative compaction, especially in thin layers where core densities are not valid (SANS 3001-BT12, 2012).

The Marvil permeability test is usually performed on-site at the bituminous surface where the permeability is required. However, this procedure cannot be used on a surface that is too rough or irregular where an adequate seal between the surface and the base of the permeameter cannot be achieved.

2.17.4.1 Apparatus

The standard Marvil permeameter consists of an acrylic tube that has a 70 *mm* diameter. The tube is inscribed with volume markings ranging from 0 *mℓ* at the top to 650 *mℓ* at the bottom, in 50 *mℓ* increments. At the bottom of the acrylic tube is a conical base of steel plate.

The Marvil permeameter also consists of a circular base weight made out of corrosion resistant steel. It has a thickness of 40 *mm*, external diameter of 270 *mm* and an internal diameter of 235 *mm*.

An illustration of the Marvil permeameter can be seen in Figure 2.30.

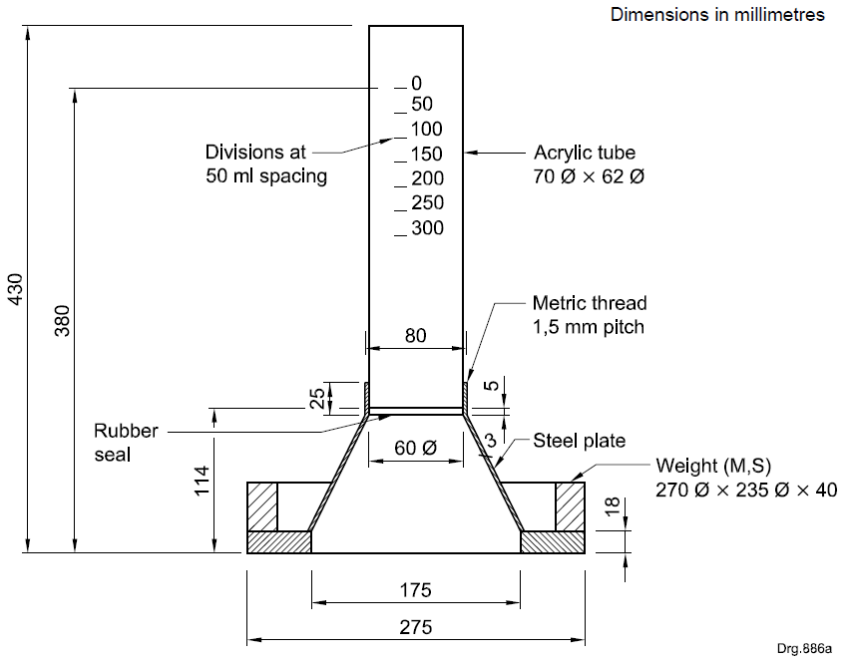

Figure 2.30: Marvil permeameter and circular base weight (SANS 3001-BT12, 2012)

2.17.4.2 Procedure

It is necessary to select an appropriate test area that is randomly located along the road and does not have any contaminated areas such as grease, oil or animal droppings. Since the condition of a bituminous road surface is not uniform all over, it is recommended that at least five Marvil permeability tests be performed at different locations on the road. If a single result varies quite significantly from the other test results, it is necessary to perform more tests on the specific area on the road. Once the area of testing is selected (larger than the base of the Marvil permeameter), it should be cleaned with a brush to remove all loose material.

This method is dependent on achieving an adequate seal between the surface of the road and the base of the Marvil permeameter. To achieve an effective seal, sealants such as grease, silicone or fresh putty can be used. If this sealant is not effective enough, it can cause leaking between the surface of the road and the base of the Marvil permeameter and lead to inadequate permeability results. It is very difficult to obtain an effective seal on an irregular or rough surface and should thus be avoided to achieve successful tests.

Once a successful seal is acquired, the testing procedure can commence by filling the apparatus with drinking water from the top until the 0 *mℓ* mark is reached - maintain this level for five minutes.

This is done to ensure that the surface being tested has a uniform saturated condition before the test is started (SANS 3001-BT12, 2012). Start the stopwatch with the water level at 0 *mℓ* and do not add any additional water to the apparatus. Record the time it takes the water level within the permeameter to drop to the 50 *mℓ*, 100 *mℓ* and 150 *mℓ* volume markings, taking into account the following conditions (SANS 3001-BT12, 2012):

a) LOW PERMEABILITY:

If the water level does not reach the 50 *mℓ* volume marking within 3 minutes, stop the test and state in the results that the test failed to reach 50 *mℓ* within 3 minutes. No calculations are required for this scenario, but it should be reported that the Marvil permeability is less than 1 litre per hour.

b) MODERATE PERMEABILITY:

If the water level is between the 50 *mℓ* and 150 *mℓ* volume markings at the end of 3 minutes, stop the test and refill the apparatus and repeat the test once. Calculations should be done for each test to determine the Marvil permeability at the 50 *mℓ* and 100 *mℓ* volume marking using the following equation:

$$P_M = 3{,}6 \cdot \frac{V_w}{t} \qquad \text{Equation 2.3}$$

Where: P_M = Marvil permeability (ℓ/h)

V_w = Volume of water (*mℓ*)

t = Time taken to reach millilitre mark (s)

The 50 *mℓ* Marvil permeability (P_M) from the second test should be reported as the overall Marvil permeability. If the first and second test results for the 50 *mℓ* reading differ by more than 30 %, the result should be reported as questionable.

c) HIGH PERMEABILITY:

If the water level reaches the 150 *mℓ* volume marking before the end of 3 minutes, stop the test and refill the apparatus and repeat the test twice. Calculations should be done for each test to determine the Marvil permeability using Equation 2.3. Report the Marvil permeability (P_M) from the third test at the smallest volume marking recorded, as the overall Marvil permeability. If this reading differs by more than 30 % from the corresponding readings in the first or second test, the results should be reported as questionable.

2.17.4.3 Laboratory Marvil permeability test

The procedure discussed above is used for on-site Marvil permeability testing. However, there was a need to complete Marvil permeability testing in a laboratory which was implemented by an undergraduate student at Stellenbosch University in 2012. This student, Willem Annandale, conducted a thesis in which he tested the Marvil permeability of surfacing seals under laboratory conditions (Annandale, 2012). According to available resources, this was the first time in South Africa that this test was performed under these conditions.

The aim of Annandale's study was to determine if the method of testing the Marvil permeability of surfacing seals under laboratory conditions was practical and accurate (Annandale, 2012). The method that was used to test these specimens in the laboratory were very similar to the Marvil permeability on-site testing procedure discussed above. Only a few adjustments were made to the procedure process as to make it more appropriate for laboratory testing conditions. By conducting the Marvil permeability test inside the laboratory, it allowed for a longer testing time as well as more accurate measurements in terms of the flow direction of water.

Once a seal sample was acquired, the laboratory testing procedure could commence by ensuring that an adequate seal is achieved between the surface of the seal slab and the base of the Marvil permeameter. This was done by using bentonite as a sealing material since other sealants failed to provide a waterproof seal. The seal and apparatus are then placed on a PVC container which is inside a larger container, to adequately determine the horizontal and vertical flow of the water inside the seal slab. Figure 2.31 illustrates this test setup.

Figure 2.31: Laboratory Marvil permeability test setup (Annandale, 2012)

The Marvil permeameter is filled with potable water from the top until the 0 *mℓ* mark is reached. This level is maintained for five minutes to allow the slab to fully saturate the vicinity of the test area. Start the stopwatch with the water level at 0 *mℓ* and do not add any additional water to the apparatus. Record the time it takes the water level within the permeameter to drop to the 50 *mℓ*, 100 *mℓ*, 150 *mℓ*, 200 *mℓ*, 250 *mℓ* and 300 *mℓ* volume markings.

If a seal slab is not very permeable, the testing time is limited to two hours after which the test will be stopped. If after two hours the water level inside the permeameter drops past the 50 *mℓ* volume marking, the testing time is extended by an additional hour (Annandale, 2012). The longer testing times were chosen by Annandale to ensure that more accurate and complete results are recorded for each seal slab.

Once the Marvil permeability test is complete, either due to the 300 *mℓ* volume marking flow completion or due to the end of the two or three-hour testing period, the apparatus together with the sample are removed from the containers. The water inside the PVC container as well as the water inside the larger container are measured and recorded and allows one to effectively determine the horizontal and vertical permeation of the seal slab. This leads to a more accurate and complete representation of the permeability inside a seal slab. An illustration of the horizontal and vertical flow in a seal slab can be seen in Figure 2.32 and Figure 2.33 respectively.

Figure 2.32: Horizontal permeability (Annandale, 2012)

Figure 2.33: Vertical permeability (Annandale, 2012)

Once Annandale finished conducting several tests, he created a classification for the Marvil permeability of surfacing seals according to their permeability results. This classification was developed with regards to guidelines set out in SANS 3001-BT12 and can be seen in Table 2.5.

Table 2.5: Marvil permeability classification for laboratory testing

PERMEABILITY CLASSIFICATION	WATER LEVEL REACHED
High	150 *mℓ* or more after 3 minutes.
Moderate	Between 50 and 150 *mℓ* after 3 minutes.
Low	Less than 50 *mℓ* after 3 minutes, 150 *mℓ* mark reached during testing procedure.
Very low	Less than 50 *mℓ* after 3 minutes; but lies between 50 and 150 *mℓ* when test is stopped.
Impermeable	Between 0 and 50 *mℓ* when test is stopped.

2.17.5 AIR-INDUCED PERMEAMETER (AIP)

The Air-Induced Permeameter (AIP) was developed by the Kentucky Transportation Centre Their objective was to develop a field test for measuring the permeability of asphalt mixtures and aggregate bases that was rapid and repeatable (Allen et al., 2001). Figure 2.34 illustrates the AIP device.

Figure 2.34: The air-induced permeameter (Allen, et al., 2001)

For the development of the AIP, it was decided that a vacuum would be used instead of pressurised air or water, which would then enable the permeameter to be self-sealing. The use of a vacuum instead of water also increased the portability and user-friendly aspect of the AIP device. By producing a device made out of heavy-duty LEXAN®, it contributed to the advantage of being able to see through the device during testing.

The AIP works on the principle that it forces pressurised air at a constant pressure through a multi-port venture. This condition then creates a vacuum within the chamber that draws air through the pavement voids which then registers a vacuum reading on the gauge (Allen et al., 2001).

The AIP gauge is based on the principle that the more difficult it is to draw air through the pavement, the smaller the voids in the underlying layers. The smaller the size and percentage of the air voids in the pavement, the less permeable it is. When conducting tests with the AIP, it is important to remember that a low reading on the AIP gauge means a high permeability is present, while a high reading on the AIP gauge indicates a low permeability – an inverse relationship.

2.17.6 KUSS VACUUM PERMEAMETER

The Kuss Vacuum permeameter uses a different approach of measuring the permeability of a pavement surface. This permeameter utilizes the air vacuum to indicate the locations of the air voids across the specified testing area (Awadalla, 2015).

The apparatus consists of two main components, namely: the encasement and the vacuum machine. An illustration of this apparatus and setup can be seen in Figure 2.35.

Figure 2.35: Kuss Vacuum permeameter (Awadalla, 2015)

2.17.6.1 Procedure

The selected testing area needs to be cleaned in order to ensure a surface without debris. Once the testing area is cleaned, it should be saturated with water. For testing to start, the encasement should be placed in the center over the testing area. Apply the vacuum and record a video tape of the testing area. When the testing is complete, study and analyse the recorded video tape with regards to the location and size of the air voids. A judgement can then be made about the percentage of air voids in the pavement surface.

This testing method does not provide the permeability results in common forms, but rather reports it as a percentage (for example: 24 % air permeability) (Awadalla, 2015).

2.17.7 NCAT IN-PLACE FIELD PERMEAMETER

In the late 1990s, The National Centre for Asphalt Technology (NCAT) developed a three-tier device to measure the permeability of the pavement. This device is based on the falling head principle and measures the falling head of water over a given period of time. This principle is applied through the three tiers of the permeameter, where the difference in head loss and the time period can be used to determine the coefficient of permeability. According to Allen et al. (2001), this type of permeability test is more suitable for less permeable materials.

2.17.7.1 Apparatus

Theoretically, this method follows Darcy's Law to measure the rate at which water seeps through the pavement structure. The NCAT device consists of four standpipes, all with a different inner diameter, which is designed in such a way that the smallest is at the top and the largest is at the bottom. An illustration of this can be seen in Figure 2.36. The intention of the hierarchical sandpipe arrangement is to provide the operator with different levels of measuring the permeability. In general, a pavement with a low permeability would be determined through the top tier and vice versa (Awadalla, 2015).

Figure 2.36: NCAT field permeameter (Awadalla, 2015)

2.17.7.2 Procedure

The testing area needs to be cleaned in order to ensure a surface without debris and dust particles. This will improve the sealing between the pavement surface and the bottom of the testing device. Once the testing apparatus is placed on the pavement surface, equal weights (see Figure 2.36) are added on the square base to prevent water from escaping.

The standpipes are filled with water until it reaches the top. Depending on the permeability of the pavement layer, the water inside the standpipes gradually starts to drop down. If the water drops very fast, it indicates that the asphalt layer has a relatively high permeability coefficient and vice versa (Awadalla, 2015). The time it takes for the water to drop between two marked graduations within an individual tier should be recorded. From these recordings the permeability coefficient of the pavement surface can be calculated.

2.17.8 SUMMARY

A tabular summary of the various permeability tests and its properties can be seen in Table 2.6. This summary provides an overview of the pressure type that is used for each test, what type of mix porosity the test is used for, the pressure applied to the test (if any), if the test can be performed in the laboratory or in-field, and the duration of each individual test. A few comments regarding the various permeability tests are also provided.

Table 2.6: Summary of permeability tests

TEST PROPERTIES	PRESSURE TYPE	MIX POROSITY	PRESSURE (KPA)	LOCATION	DURATION	COMMENTS
CONSTANT HEAD	Constant head	High	0	Lab	Dependent on porosity of specimen	Commercial product; Based on Darcy's Law
FALLING HEAD	Falling head	Low	0	Lab	Dependent on porosity of specimen	Commercial product; Not sensitive to changes in porosity;
HPP	Pressurised water	Low	100 - 200	Lab	20 minutes	Self-made apparatus; Susceptible to leakages
MARVIL	Falling head	Low	0	Lab & Field	Lab: 2 hours Field: 3 minutes	Commercial product; Susceptible to leakages
AIP	Pressurised air	Moderate Low	± 470	Lab & Field	1 minute	Self-made apparatus; Can self-seal; No water required
KUSS VACUUM	Air vacuum	Low	-	Field	1 minute	Self-made apparatus; Video-tape analysis
NCAT	Falling head	Low	0	Field	10 - 15 minutes	Self-made apparatus; 3-tier standpipe; Susceptible to leakages

2.17.9 SYNTHESIS

From the literature study it is evident that more research and laboratory testing with regards to asphalt permeability is needed. No research with regards to the High Pressure Permeability of asphalt has been done, only the testing of seals. Thus, to determine the influence that pressure has on asphalt permeability it is necessary to do an in-depth study and investigation.

CHAPTER 3 - EXPERIMENTAL RESEARCH METHODOLOGY

3.1 INTRODUCTION

In the Literature Review, factors were established for consideration when evaluating asphalt permeability and moisture damage. The purpose of this research project is to investigate various methods of realistically assessing the permeability of asphalt in a more accurate and reliable way, in order to check the moisture damage in the asphalt. To reach all the objectives stated in Chapter 1, it was necessary to develop a research methodology.

In this chapter, a research methodology is developed to investigate asphalt permeability and moisture damage. The research focuses on applying methods learned in the Literature Review and South African asphalt design practises. In this research methodology, a complete breakdown of the volumetric properties to consider during asphalt permeability testing, the preparation of samples as well as laboratory testing procedures are presented. Thereafter the permeability testing and moisture damage procedures are presented and discussed in detail.

Finally, the validation of all the data obtained from the test results is discussed. All the results from the laboratory testing are discussed in Chapter 4.

3.2 EXPERIMENTAL DESIGN

The determination of asphalt permeability and its link to moisture damage requires the development of a primary research methodology. This is known as the experimental research methodology and its structure can be seen in Figure 3.1.

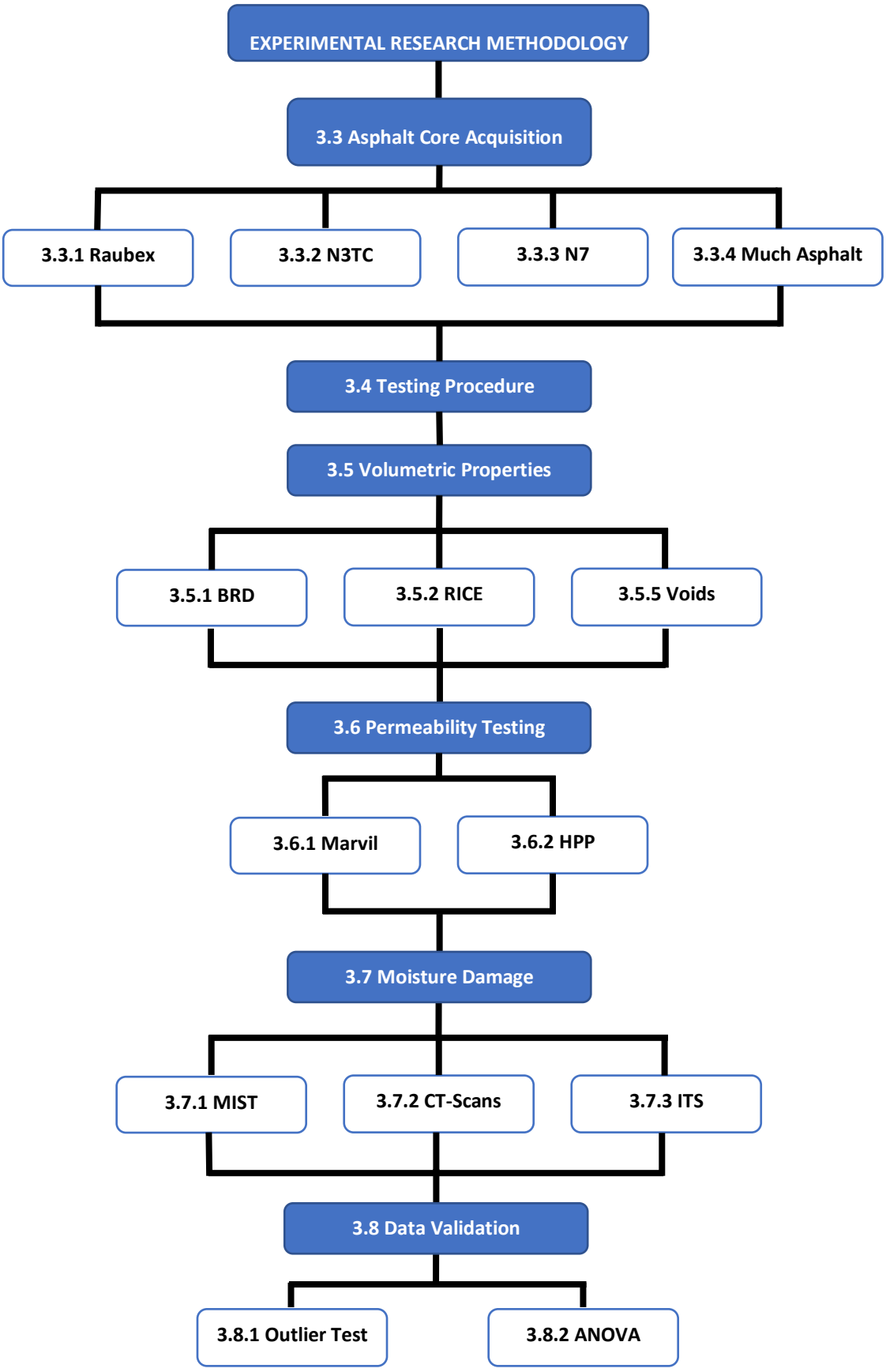

Figure 3.1: Experimental research methodology outline

3.3 ASPHALT CORE ACQUISITION

To reach the objectives for this research project, it was necessary to obtain asphalt cores that could be used for laboratory testing. These cores were acquired from different sources such as Raubex, N3 Toll Concession (N3TC), the N7 highway as well as Much Asphalt.

3.3.1 RAUBEX

Raubex Group Ltd sent Stellenbosch University a total of 19 asphalt cores to be used for laboratory testing. These 19 cores were obtained from the N3 highway near Harrismith in the Free State at three different locations on the road. All the cores had a diameter of 150 *mm* and were ready for testing without any adjustment to the cores. An example of the cores sent from Raubex can be seen in Figure 3.2.

Figure 3.2: Raubex asphalt core

3.3.2 N3 TOLL CONCESSION (N3TC)

The N3 Toll Concession (N3TC) sent Stellenbosch University a total of 17 asphalt cores to be used for laboratory testing. 12 of the 17 cores were double asphalt layered cores (see Figure 3.3). These double layered cores had to be separated by means of saw cutting. Once the layers were separated, both the asphalt layers could be used for further laboratory testing. The remaining 5 asphalt cores sent from the N3TC were 100 *mm* diameter cores.

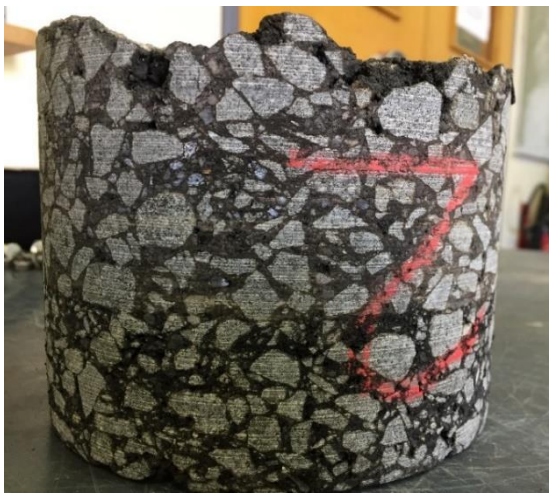

Figure 3.3: Double asphalt layered core

3.3.3 N7 HIGHWAY

To obtain more asphalt cores to use for laboratory testing, it was necessary to drill cores from the N7 highway, dated between July 2017 and August 2017. Several cores broke during the drilling procedure which was not usable for testing, but the cores that did not break during drilling were prepared for further testing at Stellenbosch University's Pavement Engineering laboratory.

Only a limited number of the abovementioned asphalt cores could be obtained due to the high cost of traffic accommodation and the specialised equipment needed for core drilling. The asphalt cores were drilled between the wheel paths (BWP) as well as from the outer wheel path (OWP). All the cores had a diameter of 146 *mm.*

3.3.3.1 Core Drilling

Core samples were drilled on the road at different locations to acquire sufficient asphalt samples for testing. These cores were acquired using the Eibenstock EVM 182/3 drill which was mounted on the Eibenstock BST 182V drill stand. The cores were drilled by using the 152 x 450 mm diamond core barrel. The entire setup for the drill, drill stand and barrel can be seen in Figure 3.4.

Figure 3.4: Core drill setup

The core drill setup is fastened to the pavement surface with the use of anchor sleeves that are drilled into the asphalt layer of the pavement. These sleeves are then put in place with the use of an eight-millimetre pin. An anchor bolt is screwed into the sleeve and the drill stand is kept in place by the use of a washer and anchor nut. During the drilling operation, only a moderate amount of water is used as coolant. While each core is being drilled, the drill operator has to stand on the base plate to ensure that the drill-bit does not move. This operation can be seen in Figure 3.5.

Figure 3.5: Core drill operation

Once the drilling is complete, the core is extracted from the road to use for further laboratory testing. The cores that were obtained consisted of an asphalt layer as well as a Bitumen Stabilised Material (BSM) layer, which had to be separated by means of saw cutting to acquire only the asphalt core. An example of the cores that were drilled from the N7 highway can be seen in Figure 3.6.

Figure 3.6: Asphalt and BSM layer

3.3.4 MUCH ASPHALT

Only four asphalt cores were obtained from Much Asphalt to be used for further laboratory testing. These cores were not drilled from the road, but were mixed, compacted and prepared in their laboratory. Two of these cores are a semi-gap graded mix, while the other two are a COLTO medium mix.

These cores are used for testing in the research project to see how laboratory prepared asphalt cores differ from on-site asphalt cores in the industry. A photo of the four laboratory prepared asphalt cores received from Much Asphalt can be seen in Figure 3.7.

Figure 3.7: Much Asphalt laboratory prepared cores

3.4 TESTING PROCEDURE

The laboratory tests that are required to reach the stated objectives include: performing the relevant procedures to determine the air void percentage and Bulk Relative Density (BRD) of each asphalt core; permeability tests such as the Marvil permeability and High Pressure Permeability (HPP) tests; the Moisture Inducing Simulating Test (MIST) and also determining the moisture damage induced by means of CT-scanning and performing Indirect Tensile Strength (ITS) tests. The following test matrix (Figure 3.8) is used to ensure that all the objectives for this project are reached.

Figure 3.8: Testing matrix with number of respective tests

3.5 VOLUMETRIC PROPERTIES

To determine the air void content (VIM) of an asphalt core, it is necessary to acquire the maximum theoretical relative density (RICE) along with the bulk relative density (BRD) for each core. These three volumetric properties are important factors to take into account during permeability testing and moisture damage of asphalt cores.

3.5.1 BULK RELATIVE DENSITY (BRD)

The BRD can be determined as the ratio of the specimen mass to the mass of an equal volume of water. This can be done by determining the dry mass of the asphalt core, as well as the mass of the core in water. The BRD for each asphalt core obtained from the road authorities are determined by means of the procedure discussed below.

3.5.1.1 Sample Preparation

To ensure that the BRD determination for each asphalt core is done effectively, it is necessary to isolate the asphalt core and ensure that there are no other materials that could influence the results. It is thus necessary to perform some saw cutting and plastic bag vacuuming to adequately perform the BRD test. This is discussed in more detail below.

3.5.1.1.1 Saw Cutting

Several of the cores that were acquired for laboratory testing consisted of asphalt, Bitumen Stabilised Material (BSM) as well as granular materials (see Figure 3.9). To accurately test the permeability and properties of the asphalt, the materials had to be isolated before any testing could commence. The BSMs and surfacing layers were sawed off with the use of a diamond blade saw which is shown in Figure 3.10. The saw cutting was dry and no water was used in order to prevent any moisture damage (erosion) to the material before testing.

Figure 3.9: Cores before preparation

Figure 3.10: Sawing of asphalt core

3.5.1.1.2 Vacuum

To determine the BRD of an asphalt core, it is necessary to submerge the core in water to determine the water mass. But, since the cores were acquired for permeability testing, it was not possible to submerge these cores in water before testing is started, as this could have an influence on the permeability results. Thus, it was necessary to find an alternative method for BRD testing, which led to the idea of vacuuming the asphalt cores.

To vacuum-seal these cores, all loose particles have to be brushed off carefully. These cores are then taken to the nearest local butchery for vacuuming. The vacuumed cores consisted of two plastic bags used for vacuuming, as one plastic bag was not sufficient enough because some of these cores had rough edges and it led to punctures in the plastic bag. Some of the edges on the cores were extremely sharp and not even three plastic bags could be used without a puncture occurring. Thus, for these extremely sharp-edged cores, cling wrap was used instead as no other solution was viable. Figure 3.11 illustrates the vacuumed asphalt cores.

Figure 3.11: Vacuum-sealed asphalt cores

3.5.1.2 Apparatus Setup

For BRD testing it is necessary to setup a five-kilogram scale with an accuracy of 0,1 gram. It is also necessary to set the temperature of the water bath to 25°C to ensure that the temperature of the core in the room is the same temperature as the core in the water bath. This water bath has a wire basket inside which is connected to a scale to determine the mass of the core in water.

3.5.1.3 Test Method

The BRD testing can be started by determining the dry mass of the vacuum-sealed asphalt core on the scale. Once the dry mass is recorded, place the vacuumed asphalt core into the wire basket in the water bath (see Figure 3.12). Wait at least one minute for the water to settle before recording the mass of the core in water. The core can be removed from the water bath once the mass is recorded. This process should be repeated for each asphalt core.

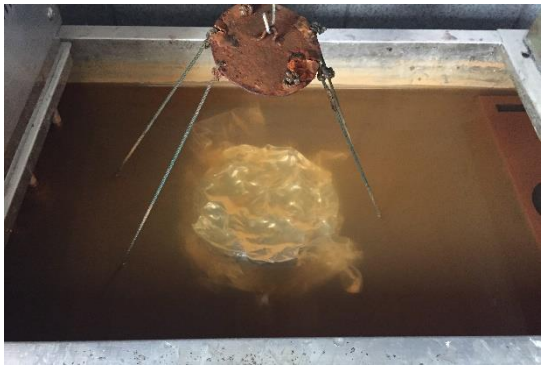

Figure 3.12: Vacuum-sealed asphalt core in water bath

3.5.1.4 Calculations

The Bulk Relative Density (BRD) of each asphalt core can be determined by using Equation 3.1:

$$BRD = \frac{A}{C-B} \qquad \text{Equation 3.1}$$

Where: A = Mass of core in air (g)

B = Mass of core in water (g)

C = Surface dry mass of core in air after water immersion (g) = A

3.5.1.5 Challenges

As previously mentioned in this chapter, two plastic bags were used to vacuum an asphalt core with, but since several cores had rough edges it resulted in the use of cling wrap instead of plastic bags. Using cling wrap on a few samples did not prove to be as effective as using vacuumed plastic bags to determine the BRD. When cling wrap is used the water infiltrates into the asphalt core and causes unreliable mass readings when submerged in the water tank. This then leads to inaccurate results with regards to the final void percentage calculation of each asphalt core.

3.5.2 RICE

The theoretical maximum specific gravity (*Gmm*) of an HMA sample can be described as the specific gravity of the mixture excluding all the air voids. This means that if the air voids are disregarded from an HMA sample, the combined specific gravity of the remaining aggregate and asphalt binder would be the theoretical maximum specific gravity. This theoretical maximum specific gravity can then be multiplied by the density of water to obtain the maximum theoretical density (RICE) of the sample.

The RICE is an important factor because it is used to calculate the air void percentage in a compacted HMA sample. The RICE is determined by taking a sample of loose HMA (not compacted), weighing it and then determining its volume by calculating the volume of water it displaces inside a flask. The theoretical maximum specific gravity (*Gmm*), is then determined by dividing the sample weight by its volume.

Since the RICE values for all the obtained asphalt cores were already known (information provided by road authorities), it was not necessary to perform this specific test.

3.5.3 VOIDS

Once the BRD for each core is calculated and the RICE values are known; the percentage of air void content for each core can be determined by using Equation 3.2:

$$Air\ Voids\ (\%) = \left(\frac{RICE - BRD}{RICE}\right) \cdot 100 \qquad \text{Equation 3.2}$$

3.6 PERMEABILITY TESTING

To determine the permeability of asphalt cores, the Marvil permeability and High Pressure Permeability (HPP) tests are chosen. The Marvil permeability test is chosen as this is the most widely used test in the industry; and the High Pressure Permeability test is chosen as it is the most recent and newly developed form of permeability testing which is based on the same principle of permeability testing than the Marvil. However, the High Pressure Permeability test takes pressure into account, which is not the case for the Marvil permeability test. These two tests are conducted in the laboratory at Stellenbosch University and the results are used to make conclusions about both these permeability tests for future use in the industry.

3.6.1 MARVIL PERMEABILITY TEST

The Marvil permeability test procedure set out in SANS 3001-BT12:2012 to determine the in-situ permeability of a bituminous surface, is designed for the specific use of the Marvil permeability apparatus on a road surface. Since several cores were obtained from the road surface, it was necessary to adapt this procedure for the use of laboratory testing instead of on-site testing. This meant that a mould had to be designed to fit the cores obtained from the road and provide an adequate adapted test procedure for laboratory Marvil permeability testing. The mould design as well as the adapted procedure will be discussed below.

3.6.1.1 Mould Design

Since the Marvil permeameter is designed to determine the in-situ water permeability of a bituminous road surface, an additional mould was required to test only the core of a specific road surface. The frame of the mould was thoroughly designed and then manufactured from wood and PVC pipes. This frame can be seen in Figure 3.13.

The mould was made from silicone rubber which is mixed with a catalyst and poured into the manufactured frame. It was left for 24 hours to set and finally create a silicone rubber mould which could then be used to place the cores in for the Marvil permeability test (see Figure 3.14).

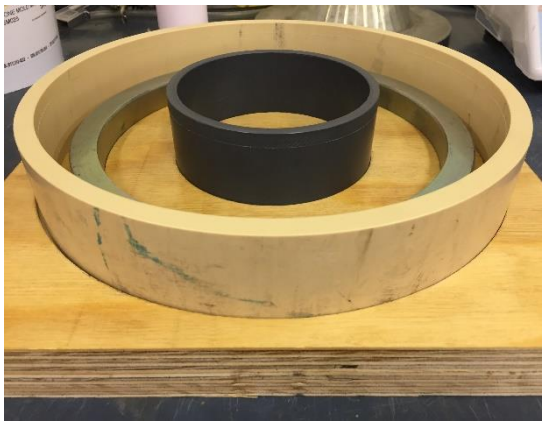

Figure 3.13: Manufactured mould frame

Figure 3.14: Silicone rubber mould

3.6.1.2 Latex Membrane Production

Latex membranes were made using liquid latex and PVC pipes, illustrated in Figure 3.15. These membranes are made by using an Ø75 mm pipe and dipping it into the liquid latex. All air bubbles should be removed from the layer once the layer is dipped. The dipped pipe then hangs until the layer of latex is dry, which takes about 2 hours. Once the layer has dried, the next layer can be applied. The membranes that were produced consisted of 10 layers of latex. Once the membrane is complete, it is cut into the required membrane sizes.

Figure 3.15: Liquid latex on PVC pipes

Based on preliminary experimentation, it was established that two membranes are needed for each core to prevent water from seeping through the sides of the core where it is in contact with the silicone rubber mould. It is important to manufacture a membrane of a smaller diameter than the

core (Ø150 *mm*), to ensure that the membranes fit snug around the core to prevent inaccurate permeability measurements (see Figure 3.16).

Figure 3.16: Core covered with latex membrane

3.6.1.3 Apparatus Setup

Once the core is covered with two latex membranes, the core can be placed inside the silicone rubber mould. The steel ring from the Marvil permeameter, which is covered with grease, can be placed inside the silicone rubber mould. An illustration of this can be seen in Figure 3.17.

Figure 3.17: Core placed inside silicone rubber mould

It is very important not to contaminate the surface of the core with grease, as this could interfere with the bituminous surface and lead to inaccurate permeability results.

Once all possible leaking surfaces are covered with grease, the cover can be placed on the steel ring while creating an air lock. The cover consists of an acrylic tube which has volume markings from 0 *mℓ* up to 600 *mℓ* in 50 *mℓ* increments. A clamp can then be placed over the steel ring where it meets the bottom of the cover to prevent any slipping on the surfaces. See Figure 3.18 for the final setup of the apparatus.

Figure 3.18: Marvil apparatus setup

3.6.1.4 Test Method

Once the apparatus setup is complete, the permeability testing can be conducted. To ensure that no leakages are present, it is advised that a non-permeable disk is used to do trials with before testing any specimens.

Fill the permeameter with water until the 0 *mℓ* mark is reached. This water level should be maintained for at least five minutes. This will ensure that the surface of the core is in uniform saturated condition before the test is started. A stopwatch will be used to measure time accurately.

Start the stopwatch after five minutes with the water level still at zero millilitres, and do not add any more water to the permeameter. Record the time it takes the water to reach each millilitre mark (50 *mℓ*, 100 *mℓ*, 150 *mℓ*, etc.) until the final mark of 600 *mℓ* is reached. Once this water level is reached, the test can be suspended. If two hours have passed without the permeameter reaching the 600 *mℓ* mark, the final water level reading will be measured and the test will be stopped at the end of two hours.

When the test is complete, remove the remaining water from the test apparatus by using a pipe to drain the water into a bottle. Take the entire test apparatus apart and remove the core from the silicone rubber mould. Ensure that all equipment is dry and grease-free before the next test is conducted.

For a step-by-step procedure of how to perform the Marvil permeability test, see Appendix A.1.

3.6.1.5 Calculations

The Marvil permeability at a specific millilitre mark can be calculated by using Equation 3.3:

$$P_M = 3{,}6 \cdot \frac{V_w}{t} \qquad \text{Equation 3.3}$$

Where: P_M = Marvil permeability (ℓ/h)

V_w = Volume of water ($m\ell$)

t = Time taken to reach millilitre mark (s)

3.6.1.6 Challenges

One of the challenges with the Marvil permeability test is when applying grease on the apparatus and accidentally applying it on the asphalt core as well, it could lead to grease contamination and influence the permeability results. To prevent this from happening it is necessary to handle grease with caution and only apply it on the Marvil apparatus and not on the asphalt core.

Another challenge that arose during testing was water seeping through the sides of the core where it was in contact with the silicone rubber mould. To prevent this from happening two latex membranes are needed to cover the sides of the core. It is necessary to keep a close eye on the test to check if any leakages occur at the sides, and then stop the test to apply another latex band if needed.

A small, but important factor to keep in mind is parallax with regards to reading off the millilitre marks on the acrylic tube as the water level drops during testing. Thus, it is necessary to be consistent in reading off the values in the same manner for every test.

The biggest challenge with the Marvil permeameter is to create a non-permeable seal between the top and bottom parts of the apparatus. At first, only grease was used to create a seal between these two surfaces, but the pressure of the water inside the apparatus during testing would constantly cause the seal to break and the top part of the apparatus would slip off, causing all the water to drain from the apparatus. After several attempts to fix this problem, the only solution was to manufacture a clamp and place it over the top and bottom parts of the apparatus before testing.

3.6.2 HIGH PRESSURE PERMEABILITY TEST

The High Pressure Permeability (HPP) apparatus was designed and developed by Ockert Renaldo Grobbelaar in 2016 at Stellenbosch University (Grobbelaar, 2016). This apparatus was used to test the permeability of different road seals, and was thus chosen to use for the testing of asphalt permeability for this research project. The HPP provides the opportunity to test the permeability of an asphalt layer at different pressures, which opens a wider possibility of results and discoveries with regards to asphalt permeability.

3.6.2.1 Mould Design

The existing High Pressure Permeability (HPP) apparatus consists of a stainless steel apparatus frame (see Figure 3.19) and silicone rubber inflatable seal. This inflatable seal was previously only used for testing on road seals, and thus had to be redesigned for the testing of asphalt cores. The new inflatable seal had to have a bigger diameter to ensure easier insertion and removal of an asphalt core.

The new inflatable seal was constructed by using an inner bicycle tube, covered with silicone rubber and wedging the seal between two galvanised plates. This was done by cutting two galvanised plates each with a thickness of 1,5 *mm*. The outer diameter of the plates was 197 *mm*, while the inner diameter was 110 *mm*. Three spacer blocks were glued to the bottom plate to ensure that the seal does not obstruct the free flow socket of the stainless-steel apparatus frame. Six bolts were also fitted to the two plates, to ensure that the inflatable seal is tightly fitted between the two plates.

Figure 3.19: Steel plates skeleton

Once the steel plate skeleton was complete, an inner bicycle tube with an extended valve was used. This tube was then inflated and submerged in water to test for any possible leakages. When no leaks were observed, the tube was deflated and folded into the required size. By using elastic bands around the bolts, it kept the bicycle tube in the required position before casting the silicone rubber mould. This is illustrated in Figure 3.20.

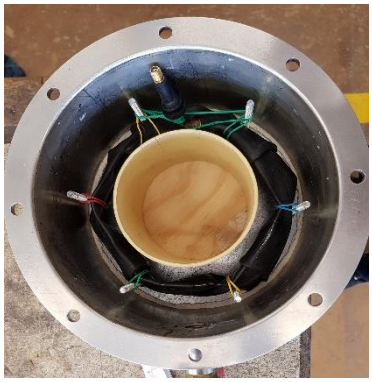

Figure 3.20: Final setup before mould casting

The mould was made from silicone rubber which is mixed with a catalyst and poured into the apparatus to cast the inflatable seal. Once the silicone rubber is poured, it is placed on a vibratory plate to ensure that all the small voids are filled with silicone rubber and to remove all trapped air. The inflatable seal was left for 24 hours to set where after the top plate was bolted tightly to the top of the mould, shown in Figure 3.21 and Figure 3.22. Once this was done, the mould was ready for high pressure asphalt core permeability testing.

Figure 3.21: Silicone rubber mould

Figure 3.22: Completed inflatable seal

3.6.2.2 Sample Preparation

The HPP apparatus is designed to fit an asphalt core with a 100 *mm* diameter. Since most of the samples that were acquired from the road authorities had a diameter of 150 *mm*, it was too large to fit into the apparatus and therefore it was necessary to core these samples down to a diameter of 100 *mm*. It was important to not have a core diameter of less than 96 *mm*, because then the core would be too small and once the inner tube is inflated for testing, it would not fit tightly enough to ensure that no water leaks through the sides. Thus, the asphalt cores had to be between 96 and 100 *mm* in diameter for the HPP test to be conducted accurately.

3.6.2.3 Apparatus Setup

Once the new inflatable seal is created, the apparatus can be set up for the high pressure permeability testing of an asphalt core. The test apparatus, as well as the core, should be thoroughly cleaned with a paint brush to ensure that the filter material does not create a pathway for a leak. This is also done to prevent any potential damage to the silicone rubber mould of the inflatable seal.

When the apparatus and core is free of any excess filter material, the core can be placed inside the silicone rubber mould, more or less five *mm* below the top of the inflatable seal. The inflatable seal should then be inflated to 300 *kPa* with a compressor and regulator, whilst some pressure is applied on top of the core to ensure that it stays in place. Always check that the pressure of the seal is greater than the pressures at which testing will be conducted.

Place the top section of the apparatus on the bottom section, with a rubber gasket between the two surfaces. Tighten the eight bolts and nuts firmly to ensure that no leakages take place between these two surfaces.

The complete setup of the High Pressure Permeability can be seen in Figure 3.23.

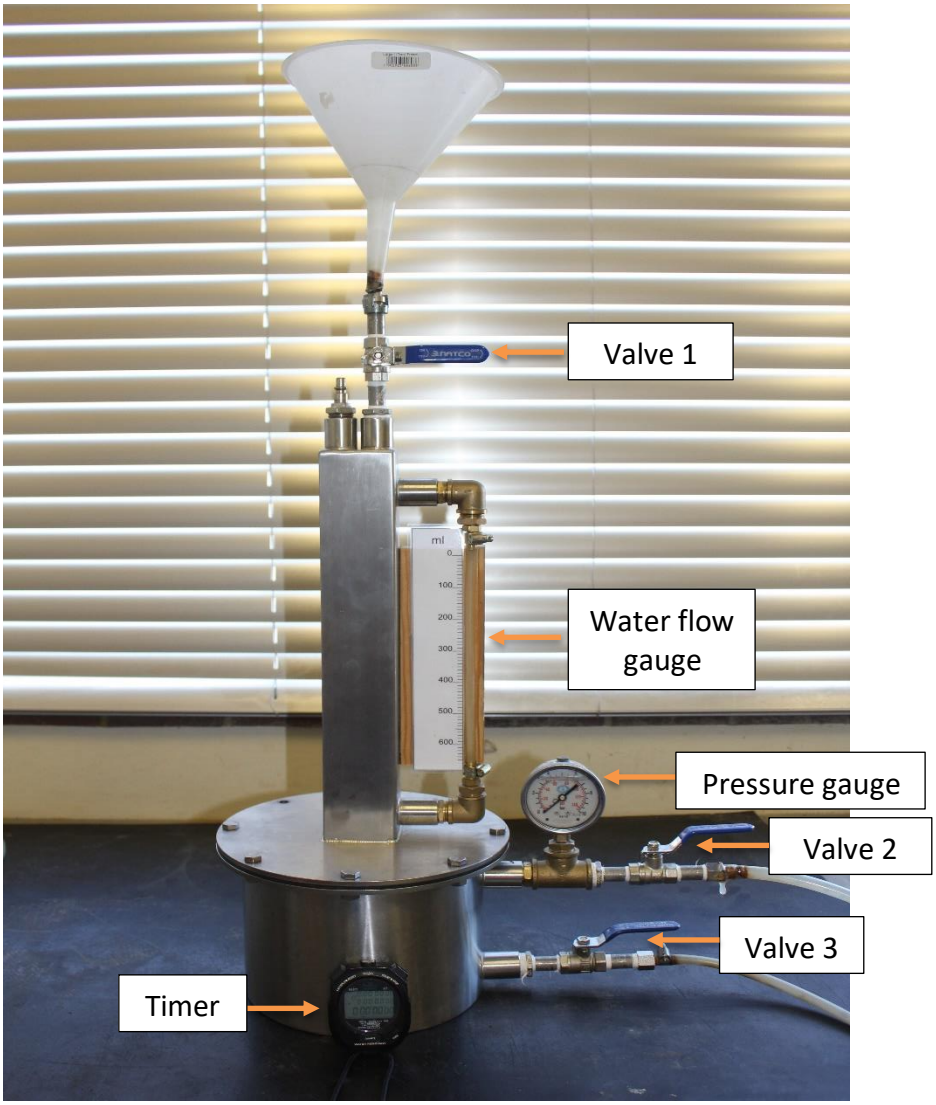

Figure 3.23: High pressure permeability apparatus setup

3.6.2.4 Test Method

To ensure that no leakages are present, it is advised that a non-permeable disk is used to do trials with before testing any specimens. Before starting the test, valve 2 and valve 3 should be closed, while valve 1 is kept open. Fill the apparatus with water until the zero-millilitre mark is reached.

Once the zero-millilitre mark is reached, valve 1 can be closed and the apparatus can be tilted to the side (see Figure 3.24) until all the water is out of the level indicator. While the apparatus is still tilted, open valve 2 and slowly lower the apparatus back to its original position until water flows out of valve 2. When water flows from valve 2, close this valve and place the apparatus back in its original position. This process is done to ensure that all air is forced out of the system.

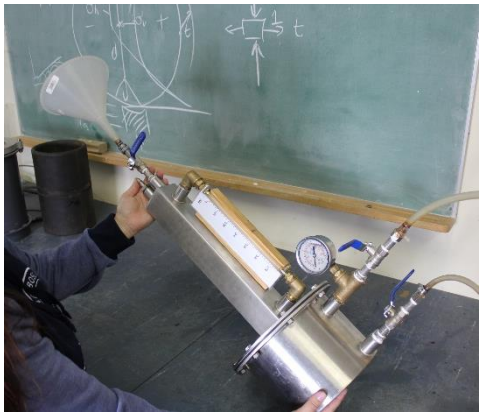

Figure 3.24: Tilting of apparatus

Now, valve 3 can be opened and the compressor can be set to 100 *kPa*. Apply this pressure by attaching the quick coupling nozzle to the apparatus. Once the pressure is applied, record the water level and start the stopwatch for 60 seconds. After one minute has passed, record the final water level and remove the applied pressure by disconnecting the compressor nozzle. Leave the apparatus to settle for another minute. This process is done as an initial wetting phase for the asphalt core.

Apply 100 *kPa* pressure by attaching the quick coupling nozzle again, record the water level and start the stopwatch. Apply this pressure for 20 minutes and record the water level every five minutes. Once 20 minutes have passed, record the last water level and remove the applied pressure. Repeat this process for the pressure at which testing is required. In this case, testing was done at 100 *kPa*, 150 *kPa* and 200 *kPa*.

If the asphalt core is very permeable and water flows through the core before 20 minutes have passed, record the time it takes to reach each individual water level mark until the level indicator is completely empty.

When testing is complete, the water can be drained from the apparatus and the seal can be deflated to remove the asphalt core. Before the next test is conducted, clean the apparatus thoroughly.

For a step-by-step procedure of how to perform the High Pressure Permeability (HPP) test, see Appendix B.1.

3.6.2.5 Calculations

The permeability of a core can be determined by calculating the rate at which water permeates through the core. The high pressure permeability at a specific millilitre mark can be calculated by using Equation 3.4:

$$P_{HP} = \frac{V_w}{t} \qquad \text{Equation 3.4}$$

Where: P_{HP} = High pressure permeability ($m\ell$/min)

V_w = Volume of water ($m\ell$)

t = Time taken to reach millilitre mark (min)

It should be noted that only the final three out of all the captured data points per test was used to calculate the permeability of each core at a specific pressure. This is done because in most cases there is still some settlement within the first few minutes of the test. Thus, only the last three data points for each applied pressure are used and plotted, which then leads to a more accurate representation of the asphalt core permeability.

3.6.2.6 Challenges

One of the challenges encountered during the high pressure permeability testing is with the inflatable seal. After several tests were conducted, the silicone rubber mould started to puncture. This is due to the fact that the asphalt cores have sharp edges, and every time the seal is inflated the edges of the asphalt starts to slowly cut into the silicone rubber mould. Eventually, this leads to a big puncture where testing has to be stopped, since it causes inaccurate permeability measurements. The entire mould then has to be rebuilt before any further testing can continue.

3.7 MOISTURE DAMAGE

To determine how moisture damage affects asphalt, it is necessary to perform a Moisture Induced Simulating Test (MIST) on the asphalt cores. Once the MIST conditioning is complete, it is important to see if the inter-connected voids in the asphalt core increases or not. To do this, CT-scans ought to be performed on the cores before and after MIST conditioning.

Another factor to be take into account when inducing moisture into an asphalt core, is to observe how the moisture affects the tensile strength of the core. This can be done by performing an Indirect Tensile Strength (ITS) test on the asphalt core before and after MIST conditioning.

The procedure for each of these three tests will be discussed in more detail below.

3.7.1 MOISTURE INDUCING SIMULATING TEST (MIST)

The MIST device was developed by Elias Twagira (2009) at Stellenbosch University to simulate field pulsing conditions which are caused by repeated traffic loads. This test procedure involves the saturation of an asphalt core in a tri-axial pressure cell while moisture is being pulsed onto the core.

3.7.1.1 Sample Preparation

The asphalt cores needed no sample preparation for the MIST conditioning. Once the high pressure permeability testing of the asphalt cores are completed, the cores are left to dry for at least 24 hours at room temperature before the MIST conditioning can commence.

3.7.1.2 Apparatus Setup

To start with MIST conditioning, the Water Heating Unit (WHU) has to be switched on to reach a temperature of 60°C. The WHU setup is illustrated in Figure 3.25. Once this temperature is reached, the asphalt core can be placed inside the tri-axial pressure cell which should then be sealed by tightening the six screws at the top of the cell. It is sealed to prevent any pressure loss during testing. The tri-axial pressure cell can then be connected to the MIST device to start with the MIST conditioning.

Figure 3.25: Water Heating Unit (WHU)

3.7.1.3 Test Method

The MIST conditioning can be started by setting the pulsing water pressure inside the tri-axial cell to 140 *kPa*. This specific pressure was identified by Jenkins and Twagira (2009) as a means of simulating hydrostatic pressure in the surfacing from fast traffic during wet conditions. The pressure can be regulated with the pressure gauge and pressure regulator on the MIST device. The MIST device can be switched on and once the tri-axial cell is filled with water, the stopwatch can be started. The MIST conditioning is done for a duration of six hours and two minutes, as suggested by Jenkins and Twagira (2009). The additional two minutes are to ensure that all cold water is flushed out of the system before testing is started.

The timer on the MIST device is set to open the first solenoid valve for 0.54 seconds to pressurise the cell, while the second valve is closed. Once 0.54 seconds have passed, the first valve closes, and the second valve opens for 1.40 seconds to relieve the pressure inside the tri-axial cell.

When the MIST conditioning is complete, the pulsing water pressure can be stopped, and the asphalt core can be removed from the tri-axial pressure cell.

The complete setup of the MIST apparatus can be seen in Figure 3.26. For a step-by-step procedure of how to perform the MIST, see Appendix C.1.

Figure 3.26: MIST device

3.7.1.4 Challenges

One of the challenges that was encountered with the MIST device was that the previous user used a mixture of soap and water in the MIST device for testing. This led to the device being filled with soapy water which was not adequate for this specific research project. If the soapy water was used as is, it would have a different pH level than clean water and could potentially influence the test results that followed after the MIST conditioning.

Thus, the entire system had to be flushed for several hours (see Figure 3.27), which led to a huge loss in water. This was undesirable considering the current drought that the region was facing. The pH level of the MIST device was tested several times while the system was being flushed to ensure that clean water (target pH-level of 7.0) was eventually inside the system and used for the MIST conditioning.

Figure 3.27: Flushing soapy liquid out of the MIST device

3.7.2 CT-SCANS

The CT Scanner Facility at Stellenbosch University is an open access laboratory that provides non-destructive X-ray computed tomography (CT) as well as a high performance image analysis service (Du Plessis et al., 2016). The high performance image analysis forms part of the Central Analytical Facilities (CAF) of the university.

The CT Scanner Facility has a walk-in cabinet micro-CT scanner system for scanning of large samples with a diameter between 10 *mm* and 300 *mm*. It also has a nano-CT scanner with the highest resolution for scanning of small samples with a diameter less than 10 *mm*.

The CT Scanner Facility was used to perform micro-CT scans on asphalt cores before and after MIST conditioning. These scans are used to determine if the MIST conditioning has an influence on the inter-connected voids of an asphalt core. The images that are produced by the CT-scans (see Figure 3.28) are analysed by means of comparing the before and after images to determine if the inter-connected voids increase after the MIST conditioning.

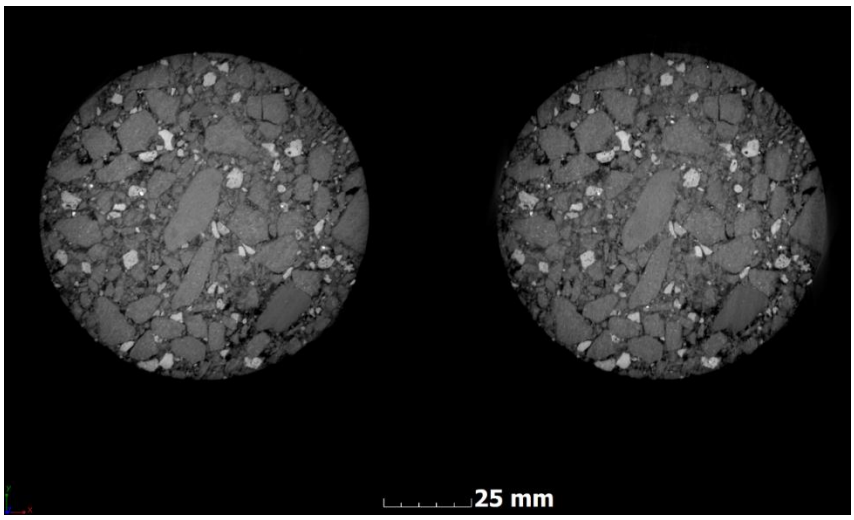

Figure 3.28: Asphalt core CT-scan before (left) and after (right) MIST conditioning

3.7.3 INDIRECT TENSILE STRENGTH (ITS) TESTING

The Indirect Tensile Strength (ITS) of an asphalt core is determined by measuring the resistance to failure of the cylindrical specimen when a load is applied to the curved sides of the core. An electronic load cell applies a vertical compressive load at a controlled rate of deformation to the loading device. This test is mostly used to estimate the potential rutting and cracking performance of an asphalt mixture.

3.7.3.1 Sample Preparation

Once all testing on the asphalt cores were concluded, the cores were left inside the Universal Testing Machine (UTM) for 24 hours at a temperature of 25°C. This temperature was chosen as a more elastic than viscous material behaviour was required during the testing of asphalt cores.

3.7.3.2 Apparatus Setup

Once the cores have been kept inside the UTM (see Figure 3.29) for 24 hours at 25°C, the asphalt cores can be used for ITS testing. Before testing can be started, it is necessary to measure the diameter, average height and mass of each asphalt core. Once these measurements are all recorded, the core can be placed on the loading device. The loading device is then placed on the moveable

shelf inside the UTM. The shelf inside the UTM is then raised until the top of the loading device makes contact with the bottom of the actuator, preventing any force from being applied to the core and loading device.

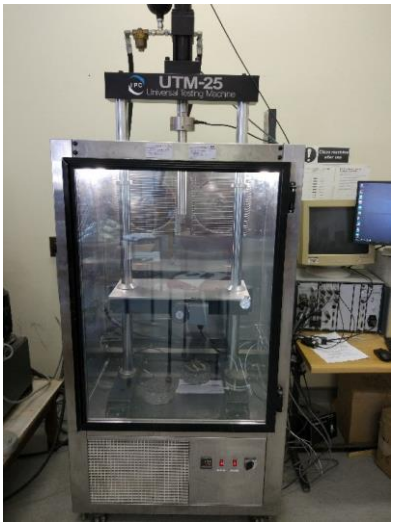

Figure 3.29: UTM for ITS testing

3.7.3.3 Test Method

When the test setup is complete, the software used for the testing can be loaded on the computer, while the necessary input parameters for the asphalt core are entered. These parameters include the average core height, core diameter as well as the loading rate of 50,8 *mm* per minute as recommended (ASTM International, 2012). The axial loading type can be set as actuator displacement.

The test is started once all the necessary parameters are entered and it was completed once the maximum load had been applied to the asphalt core. When the maximum load is achieved and breaking occurs (see Figure 3.30), the test is stopped and the shelf of the UTM is lowered.

The loading device with the asphalt core is removed from the UTM and the testing results are loaded onto the testing software and used for further calculations. This entire process is repeated for each asphalt core that is tested.

Figure 3.30: ITS testing of an asphalt core

For a step-by-step procedure of how to perform the ITS test, see Appendix D.1.

3.7.3.4 Calculations

The final ITS value for each asphalt core is calculated by using Equation 3.5:

$$ITS = \frac{2P}{\pi \cdot h \cdot d} \cdot (1\,000\,000) \qquad \text{Equation 3.5}$$

Where: ITS = Indirect Tensile Strength (kPa)

P = Maximum applied load (kN)

h = Average height of core (mm)

d = Diameter of core (mm)

3.7.3.5 Challenges

One of the only challenges that occurred during the ITS testing was that for each new core being tested, the core diameter and average core height needs to be imported into the computer software program. Sometimes this can be forgotten and lead to inaccurate results, thus it is very important to check that all parameters for each core is imported correctly into the software.

3.8 DATA VALIDATION

Once all test results were obtained, it was necessary to determine which results were viable enough to use in further calculations to reach the objectives stipulated for this project. The data used for further calculations were validated by means of doing the COLTO outlier test (SABS 1200, 1996).

3.8.1 OUTLIER TEST

Test results should be scanned for possible outliers to ensure that a test result is not inaccurate. If a test result proves to be an outlier, it needs to be rejected in all further use of the data. The sample mean and sample standard deviation will then be recalculated without the outlier and used for further calculations. The method below can be followed to identify possible outliers in test results (SABS 1200, 1996):

The value of T_o needs to be calculated by using Equation 3.6:

$$T_o = \frac{x_0 - \bar{x}_n}{S_n} \qquad \text{Equation 3.6}$$

Where: $\bar{x}_n$ = Arithmetic mean

S_n = Sample standard deviation

x_0 = Value of the test result that differs most from the mean (possible outlier)

Once T_o is calculated, compare its value with the value of T for the applicable value of "*n*", from Table 3.1. If the absolute value of T_o is greater than T, then x_0 is an outlier.

Table 3.1: Critical values of 'T' for outliers

1	2
Number of observations *n*	**Critical value** *T*
4	1,46
5	1,67
6	1,82
7	1,94
8	2,03
9	2,11
10	2,18
11	2,23
12	2,29
13	2,33
14	2,37
15	2,41
16	2,44
17	2,47
18	2,50
19	2,53
20	2,56

3.8.2 REGRESSION & ANOVA ANALYSIS

Regression analysis is used in research to draw further interpretations from the obtained data. Almost all the data sets typically include two or more independent variables that influence the outcome of the dependent variable (Rudman, 2019). The correlation factor R^2 is generally used in analysis, but this parameter alone could lead to biased results if not interpreted correctly.

It is incorrectly assumed that if the correlation between a variable and a dependent is low, that this variable is negligible. However, another useful and compatible tool to correlation is to use ANOVA analysis (Rudman, 2019). This statistical method is used for the research in this thesis (Chapter 5), as it yields values that can be tested to determine if a significant relationship exists between variables. ANOVA (or MANOVA if there are two ore more dependent variable) can be defined as a statistical analysis which is used to evaluate the significance of the effect of one or more independent variables (Rudman, 2019).

For ANOVA statistical analysis the P-value can be used to determine if a variable is significant in predicting the behaviour of a model. "The main difference between the P-value to the R^2 is that the R^2 is only an estimate of the strength of the relationship between the model and the variables under consideration and cannot provide a hypothesis test for this relationship" (Rudman, 2019).

Globally, a P-value of 0.05 can be seen as the threshold to measure the statistical significance of a model (Rudman, 2019). A higher P-value can also be used for benchmarking, taking into account that it is a measure of confidence intervals.

CHAPTER 4 - RESULTS

4.1 INTRODUCTION

This chapter presents the results that were obtained during the execution of the experimental research methodology as presented in Chapter 3. Marvil permeability, High Pressure Permeability (HPP), MIST conditioning and ITS testing form the basis of the results. These results are interpreted to conclude the laboratory findings for this study. The layout for this results chapter can be seen in Figure 4.1.

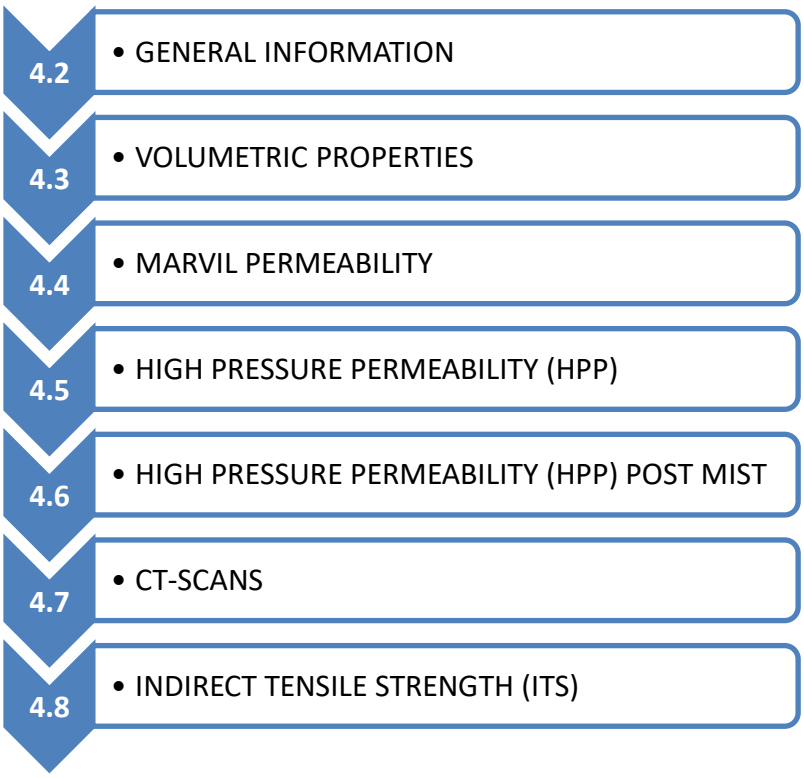

Figure 4.1: Results layout

4.2 GENERAL INFORMATION

To reach the objectives for this research project, it was necessary to obtain asphalt cores that could be used for laboratory testing. These cores are from different sources such as Raubex, N3 Toll Concession (N3TC), the N7 highway as well as Much Asphalt. In this chapter a brief overview of these sources will be given, as well as a description of the asphalt mixtures obtained from each source.

4.2.1 RAUBEX

Stellenbosch University received a total of 19 asphalt cores from Raubex Group Ltd. These 19 cores were obtained from the N3 highway near Harrismith in the Free State at three different sections on the road. The mix type for Section 1, Section 2 and Section 3 is TRH 8 with A-E2 binder, and a binder content of approximately 3.9 %.

4.2.2 N3TC

The N3 Toll Concession (N3TC) sent Stellenbosch University a total of 17 asphalt cores to be used for laboratory testing. These cores were from three different mixture types:

- **MIX Cd** – BR SABITA 19 mix using 100 % dolerite aggregate (possible slight contamination in joints of parent rock) with approximately 6.3 % binder used;
- **MIX Cp** – BR SABITA 19 mix using dolerite coarse aggregate and BOF steel slag (ex. Newcastle) fine (<3 mm) aggregate with approximately 6.7 % binder used; and
- **MIX Ev** – 13mm max size continuously graded COLTO mix with A-E2 binder (TRH 8 Fine Medium). Aggregate is approximately 75 % dolerite and 25 % EAF steel slag (ex. Van der Bijl Park).

4.2.3 N7

To obtain asphalt cores to use for laboratory testing, it was necessary to drill cores from the N7 highway. Five cores were obtained and used for further laboratory testing. The asphalt cores were drilled between the wheel paths (BWP) as well as from the outer wheel path (OWP).

These asphalt cores consist of a UTFC top layer with large aggregates and a continuously graded COLTO medium bottom layer. However, for this research project the cores are not separated, but tested in this combined state.

4.2.4 MUCH ASPHALT

Only four asphalt cores were obtained from Much Asphalt to use for further laboratory testing. These cores are not drilled from the road, but were mixed, compacted and prepared in their laboratory. Two of these cores are a semi-gap graded mix, while the other two are a COLTO medium mix.

4.3 VOLUMETRIC PROPERTIES

To determine the air void content (VIM) of an asphalt core, it is necessary to acquire the maximum theoretical relative density (RICE) along with the bulk relative density (BRD) for each asphalt core.

The BRD and RICE values are determined by means of following the procedures set out in Chapter 3.5.1 and Chapter 3.5.2 respectively. Once these values are obtained, the air void percentage for each asphalt core can be determined by using Equation 3.2.

The volumetric properties obtained for all the asphalt cores used in this research project will be discussed and presented in the following sections.

4.3.1 RAUBEX

The air void content for the Raubex asphalt cores are determined for the three road sections from which the cores were obtained. These air void content values, together with the BRD and RICE values for each core, are calculated and tabulated in Table 4.1, as well as a few comments regarding the cores.

Table 4.1: Raubex volumetric properties

	CORE	BRD (kg/m³)	RICE (kg/m³)	% VOIDS	COMMENTS
SECTION 1	A	2641,23	3021,00	12,57	
	B	2307,48		23,62	High void % could be due to cling wrap used during BRD determination.
	D	2633,38		12,83	
	E	2276,67		24,64	High void % could be due to cling wrap used during BRD determination.
	F	2565,98		15,06	
	G	2548,47		15,64	
	L	2706,26		10,42	
SECTION 2	C	2072,65	3018,00	31,32	High void % could be due to cling wrap used during BRD determination.
	H	2796,66		7,33	Cracked surface noted during visual inspection.
	I	2665,96		11,66	
	J	2692,37		10,79	
	K	2500,09		17,16	Cracked surface noted during visual inspection.
	M	2611,29		13,48	
SECTION 3	N	2649,55	3024,00	12,38	
	O	2743,22		9,29	
	P	2659,07		12,07	
	Q	2738,25		9,45	
	R	2695,70		10,86	
	S	2701,35		10,67	

From Table 4.1 it is evident that Core B and Core E from Section 1, as well as Core C from Section 2 contain a very high air void content. It should be considered that these high air void percentages could be caused by the use of cling wrap instead of vacuum-sealed plastic bags to cover the asphalt cores with during BRD testing. These three cores had sharp edges and caused the vacuum-sealed bags to puncture, thus cling wrap had to be used as an alternative.

Another comment in Table 4.1 to take note of is the comments regarding Core H and Core K in Section 2. During the initial visual inspection it was noted that these two cores already had cracks on their surface. An example of the cracks noted on Core H can be seen in Figure 4.2. Thus, it was assumed that Core H and Core K would portray a high permeability because of their cracked surfaces.

Figure 4.2: Cracked surface of Core H noted during visual inspection

Overall, Table 4.1 indicates that Section 3 has the lowest average air void percentage, without any irregularities noted during the visual inspection, and thus it can be expected that this section will reveal a lower permeability than the other two sections. This can be explained by referring to Chapter 2 which states that an asphalt mixture with lower individual air voids leads to the pavement having a decreased permeability.

4.3.2 N3TC

Since the asphalt cores acquired from the N3TC are double layered asphalt cores (see Figure 3.3), these double layered cores had to be separated and both these asphalt layers could be used to determine the various volumetric properties. The air void content for the 12 top layer asphalt cores, as well as the 12 bottom layer asphalt cores can be determined. These air void content values, together with the BRD and RICE values for each core, are calculated and tabulated in Table 4.2.

Table 4.2: N3TC volumetric properties

		CORE	BRD (kg/m³)	RICE (kg/m³)	% VOIDS
TOP ASPHALT LAYER	MIX Cd	1	2544,53	2840,00	10,40
		2	2544,23		10,41
		3	2635,94		7,19
		4	2543,75		10,43
		5	2550,29		10,20
		6	2588,51		8,86
	MIX Cp	7	2771,94	2840,00	2,40
		8	2730,89		3,84
		9	2731,79		3,81
		10	2702,91		4,83
		11	2694,97		5,11
		12	2734,12		3,73
BOTTOM ASPHALT LAYER	UNKNOWN MIX	1	2794,41	2840,00	1,61
		2	2674,59		5,82
		3	2693,21		5,17
		4	2788,93		1,80
		5	2755,07		2,99
		6	2732,06		3,80
		7	2805,35		1,22
		8	2766,67		2,58
		9	2798,95		1,45
		10	2785,78		1,91
		11	2819,07		0,74
		12	2781,20		2,07

The top asphalt layer consists of two mixture types, these types can be identified as Mix Cd and Mix Cp, while the type of mixture for the bottom asphalt layer is unknown. From Table 4.2 it is evident that the bottom asphalt layer has a considerable lower average air void percentage than the top asphalt layer. It can therefore be expected that the top layer will display higher permeability values than the bottom asphalt layer.

When considering only the top asphalt layer, it can be seen in Table 4.2 that Mix Cd has a higher average air void percentage than Mix Cp, thus leading to the conclusion that Mix Cp will be less permeable than Mix Cd.

Overall, the N3TC cores have a notably lower air void content than the Raubex asphalt cores. This can be explained by the fact that the N3TC cores have a different mixture type than the Raubex asphalt cores.

4.3.3 N7

The air void content for the asphalt cores obtained from the N7 highway are determined for each core. These air void content values, together with the BRD and RICE values for each core, are calculated and tabulated in Table 4.3, as well as a few comments regarding the cores.

Table 4.3: N7 volumetric properties

CORE	BRD (kg/m³)	RICE (kg/m³)	% VOIDS	COMMENTS
V	2423,40	2514,00	3,60	Core drilled BWP.
W	2484,23	2527,00	1,69	Core drilled from OWP.
X	2466,05	2527,00	2,41	Core drilled from OWP.
Y	2409,60	2527,00	4,65	Core drilled from OWP.
Z	2420,65	2514,00	3,71	Core drilled BWP.

According to Table 4.3, Core V and Core Z are drilled between the wheel paths (BWP), while the remaining cores are drilled in the outer wheel path (OWP). The core with the highest air void content, Core Y, was drilled in the wheel path and therefore it is assumed that this core will have the highest overall permeability.

In general, the cores from the N7 highway portray a very low average air void percentage and it is thus anticipated that these cores will have a relatively low permeability.

4.3.4 MUCH ASPHALT

The air void content for the asphalt cores obtained from Much Asphalt are determined for each core. These air void content values, together with the BRD and RICE values for each core, are calculated and tabulated in Table 4.4.

Table 4.4: Much Asphalt volumetric properties

	CORE	BRD (kg/m³)	RICE (kg/m³)	% VOIDS
SEMI-GAP GRADED	1	2418,02	2480,00	2,50
	2	2418,85	2480,00	2,47
COLTO MEDIUM	5	2483,60	2541,00	2,26
	6	2479,12	2541,00	2,44

The four cores obtained from Much Asphalt consisted of two different asphalt mixture types. These mixtures are semi-gap graded and COLTO medium; two cores of each mix type. Core 1 and Core 2 are semi-gap graded, while Core 5 and Core 6 are COLTO medium. According to Table 4.4 both these mix types have a very low air void percentage. It is thus assumed that this will lead to a relatively low permeability in all four of the asphalt cores.

4.4 MARVIL PERMEABILITY

The Marvil permeameter is designed to determine the in-situ water permeability of a bituminous road surface. For the purpose of this research project it is necessary to determine the Marvil permeability of asphalt cores obtained from different sources. The Marvil permeability test as set-out in Chapter 3.6.1 is used to determine the permeability of the asphalt cores from Raubex, N3TC, the N7 highway as well as the cores from Much Asphalt. A summary of the results obtained from the Marvil permeability for these cores will be discussed in the following sections.

4.4.1 RAUBEX

The results obtained from the Marvil permeability test of the Raubex asphalt cores can be seen in Figure 4.3. Figure 4.3 gives an indication of the average, 90th percentile (top of pin) and 10th percentile (bottom of pin) from the data collected for three different road sections. According to the outlier test explained in Chapter 3.8.1, Core G in Section 1 and Core H in Section 2 are identified as outliers for the Marvil permeability test. The Marvil permeability results for these cores are omitted from any final result calculations (including the results shown in Figure 4.3).

The Marvil data collected from all the asphalt cores are plotted, and from this data it is evident that for the Raubex asphalt cores the millilitre interval with the highest consistency based on a linear relationship differs for all three road sections. For Section 1 the millilitre interval is at 100-millilitres; for Section 2 the millilitre interval is at 150-millilitres; and for Section 3 the millilitre interval is at 400-millilitres. These statements are proven and shown in Appendix E.1 (Figure 8.1 - Figure 8.3).

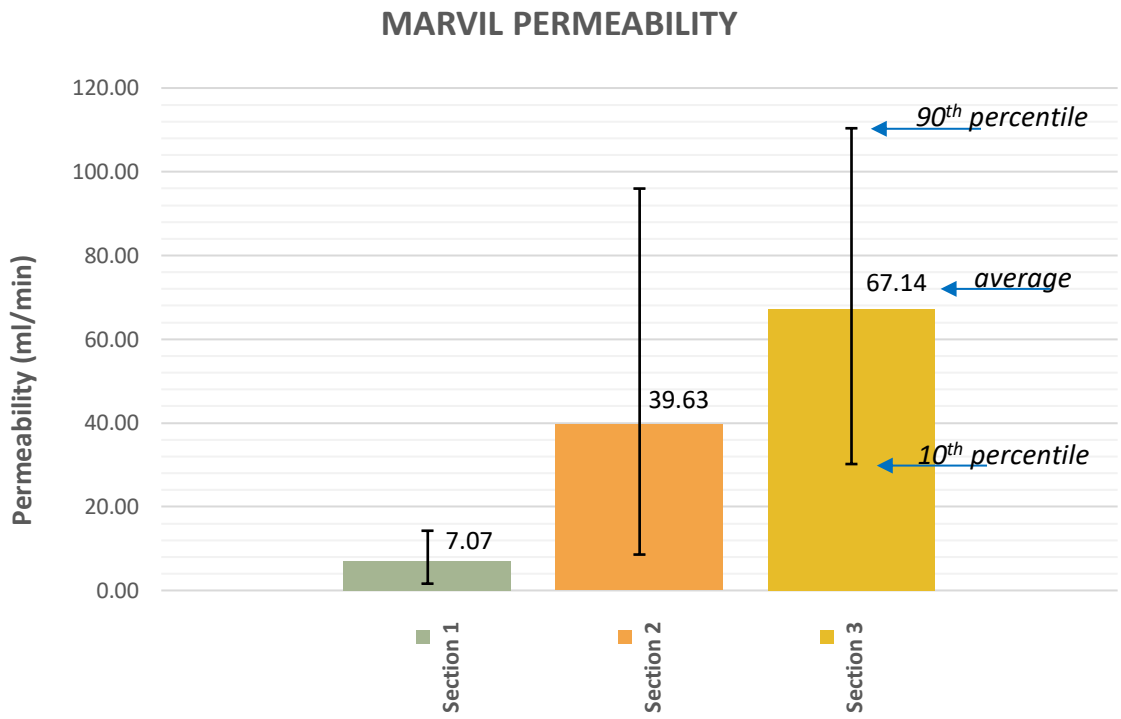

Figure 4.3: Permeability results for Sections

Figure 4.3 show that Section 1 has an average permeability of 7.07 *mℓ/min* for the six tested asphalt cores, excluding the outlier. The average permeability for the five asphalt cores tested in Section 2 is 39.63 *mℓ/min* (excluding outlier), while the average for Section 3 is at a high of 67.14 *mℓ/min.* The

Marvil permeability results for Section 2 and Section 3 are relatively high compared to the low permeability of Section 1.

Thus, according to the Marvil permeability test for the Raubex asphalt cores, Section 1 is the least permeable of all three sections, while Section 3 has the highest overall permeability. This conclusion does not coincide with the statement made in Chapter 4.3.1, which states that Section 3 will be the least permeable of all three sections due to its lower average air void percentage. A possible explanation for this can be the possibility of more inter-connected voids in the cores from Section 3.

For more detailed results regarding the Marvil permeability of each individual asphalt core for these three sections, see Appendix E.1 (Figure 8.4 – Figure 8.8).

4.4.2 N3TC

The results obtained for the Marvil permeability test of the N3TC asphalt cores can be seen in Figure 4.4. Figure 4.4 gives an indication of the average, 90th percentile (top of pin) and 10th percentile (bottom of pin) from the data collected for Mix Cd and Mix Cp. According to the outlier test explained in Chapter 3.8.1, there are no outliers with regards to the Marvil permeability test for Mix Cd and Mix Cp.

The Marvil data collected from all the asphalt cores are plotted, and from this data it is evident that at the 450-millilitre interval the highest consistency based on a linear relationship exists. This statement is proven and shown in Figure 8.9 in Appendix E.2. Thus, all the final results for the Marvil permeability for Mix Cd and Mix Cp are taken at the 450-millilitre interval.

No Marvil permeability testing is done on Mix Ev, as these asphalt cores are too small (100 *mm* diameter) to fit into the adjusted laboratory Marvil apparatus which was only usable for cores with a 145 to 150 *mm* diameter.

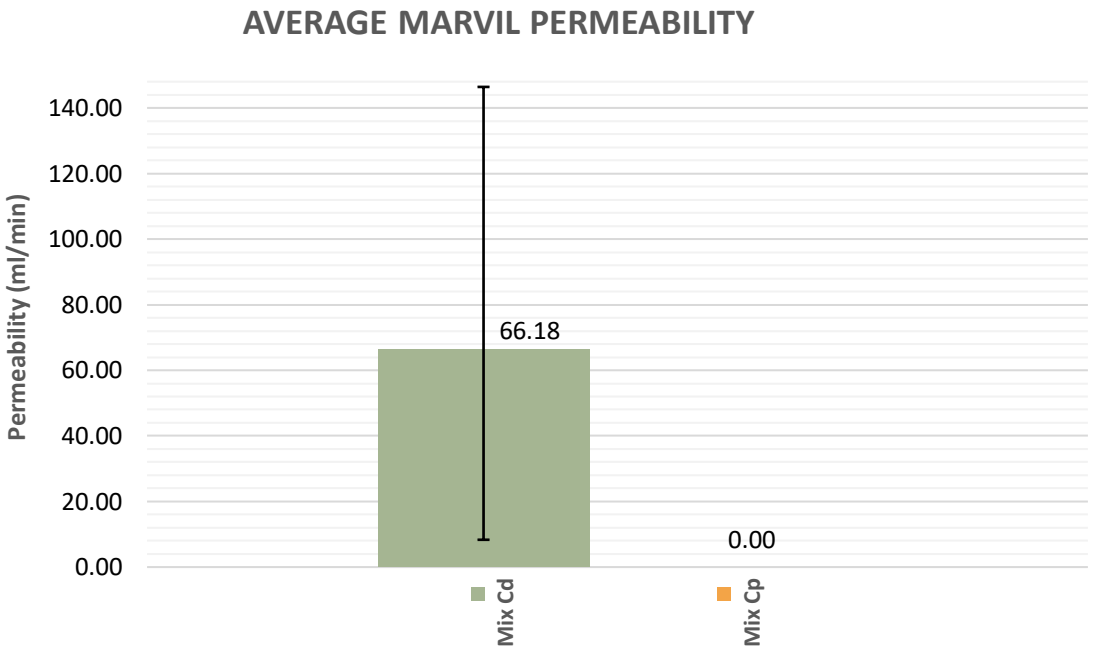

Figure 4.4: Permeability results for Mixes

Figure 4.4 show that Mix Cd has an average permeability of 66.18 *mℓ/min* for the six tested asphalt cores. This value is relatively high compared to the permeability of Mix Cp, which has an average of 0.00 *mℓ/min*. Thus, according to the Marvil permeability test for the N3TC asphalt cores, Mix Cd is more permeable than Mix Cp. This conclusion coincides with the statement made in Chapter 4.3.2, which states that Mix Cp will be less permeable due to its lower average air void percentage.

More detailed results of the Marvil permeability with regards to each individual asphalt core for Mix Cd and Mix Cp can be found in Appendix E.2 (Figure 8.10 - Figure 8.11).

4.4.3 N7

The results obtained for the Marvil permeability test of the N7 highway asphalt cores can be seen in Figure 4.5. Figure 4.5 gives an indication of the average, 90th percentile (top of pin) and 10th percentile (bottom of pin) from the data collected for the asphalt cores drilled from the N7 highway.

According to the outlier test explained in Chapter 3.8.1, there are no outliers with regards to the Marvil permeability test for the N7 cores.

All the final results for the Marvil permeability for the N7 highway cores were not calculated at a specific millilitre interval, as these cores displayed such a low permeability that not even the first millilitre interval of 50 *mℓ* was reached.

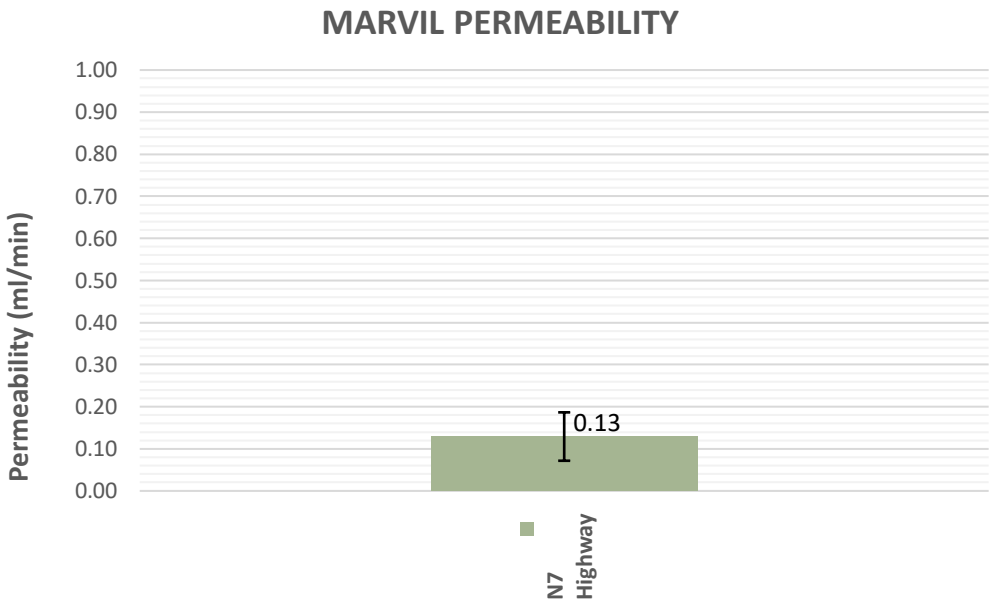

Figure 4.5: Permeability results of N7, Cape Town

Figure 4.5 indicates that the five asphalt cores from the N7 highway has an average permeability of only 0.13 *mℓ/min*. This is extremely low and leads to the conclusion that these cores are essentially impermeable. This conclusion coincides with the statement made in Chapter 4.3.3, which states that the N7 asphalt cores will have a very low permeability due to its low average air void content.

More detailed results of the Marvil permeability with regards to each individual asphalt core from the N7 highway can be found in Appendix E.3 (Figure 8.12).

4.4.4 MUCH ASPHALT

The results obtained for the Marvil permeability test of the Much Asphalt cores can be seen in Figure 4.6. Figure 4.6 gives an indication of the average, 90th percentile (top of pin) and 10th percentile (bottom of pin) from the data collected for the asphalt cores. According to the outlier test explained in Chapter 3.8.1, Core 5 is identified as an outlier with regards to the Marvil permeability test. The

permeability result for this core is omitted from any final result calculations (including the results shown in Figure 4.6).

The Marvil data collected from all the asphalt cores are plotted, and from this data it is evident that at the 150-millilitre interval the highest consistency based on a linear relationship exists. This statement is proven and shown in Figure 8.13 in Appendix E.4. Thus, all the final results for the Marvil permeability of the Much Asphalt cores are taken at the 150-millilitre interval.

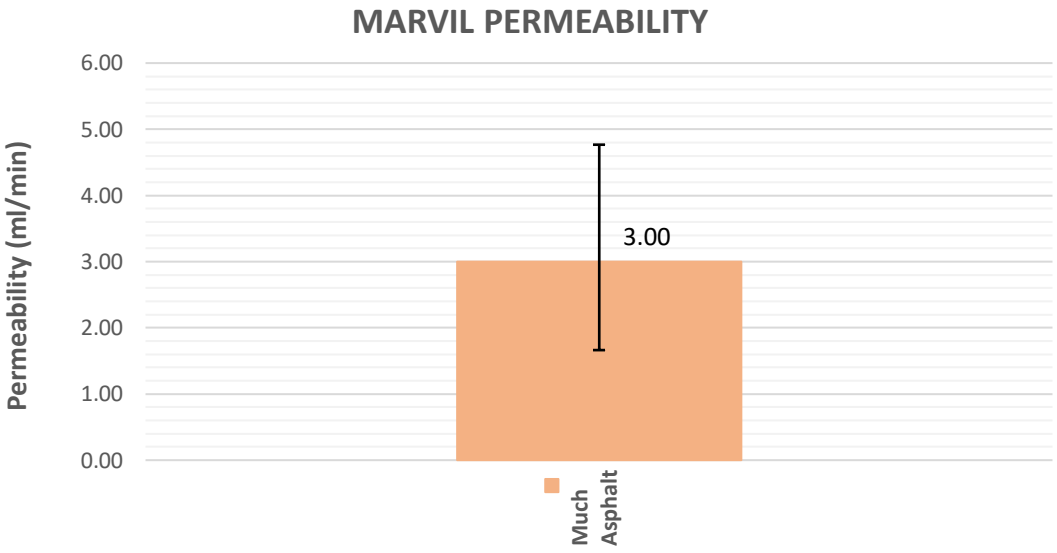

Figure 4.6: Permeability results of Much Asphalt

Figure 4.6 indicates that the four asphalt cores from Much Asphalt have an average permeability of only 3.00 *mℓ/min*. This is relatively low and leads to the conclusion that these cores are impermeable. This conclusion coincides with the statement made in Chapter 4.3.4, which states that the Much Asphalt cores will have a relatively low permeability due to its low average air void content.

More detailed results of the Marvil permeability with regards to each individual asphalt core from Much Asphalt can be found in Appendix E.4 (Figure 8.14 – Figure 8.15).

4.5 HIGH PRESSURE PERMEABILITY (HPP)

The High Pressure Permeability (HPP) apparatus provides the opportunity to test the permeability of an asphalt layer at different pressures, which opens a wider possibility of results and discoveries with regards to asphalt permeability.

For the purpose of this research project it is necessary to determine the HPP of asphalt cores obtained from different sources at three different pressures, namely: 100, 150 and 200 kPa. The HPP test as set-out in Chapter 3.6.2 is used to determine the permeability of the asphalt cores from Raubex, N3TC, the N7 highway as well as the cores from Much Asphalt. A summary of the results obtained for the HPP of these cores at the various pressures is discussed in the following sections.

4.5.1 RAUBEX

The results obtained for the HPP tests can be seen in Figure 4.7. Figure 4.7 gives an indication of the average, 90^{th} percentile (top of pin) and 10^{th} percentile (bottom of pin) for the data collected for each mix at their various pressures: 100, 150 and 200 *kPa*. According to the outlier test explained in Chapter 3.8.1, Core A of Section 1 is identified as an outlier with regards to the HPP test for the pressure of 200 *kPa*. Core H of Section 2 and Core P of Section 3 are also identified as outliers for the pressures of 100, 150 and 200 *kPa*. All the obtained data for these three cores are omitted from all final results, including the results shown in Figure 4.7.

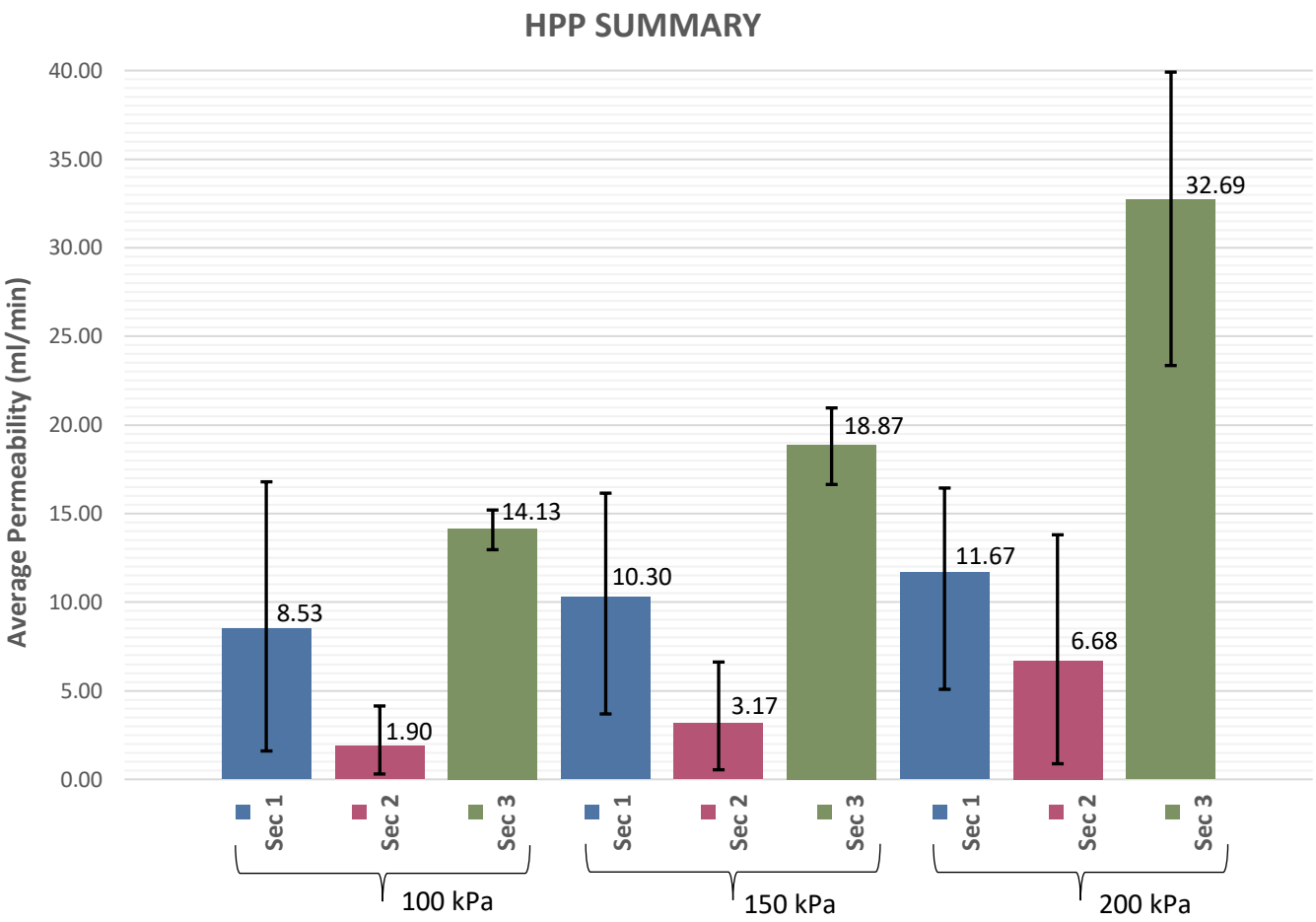

Figure 4.7: HPP Section results (3 pressure repeats for each)

Figure 4.7 indicates that the permeability of an asphalt mix increases with an increase in the pressure being applied. As the testing pressure increases from 100 *kPa* to 200 *kPa*, the rate at which water flows through the asphalt core also increases significantly. This statement is evident in all three sections.

From Figure 4.7 it is also evident that Section 3 displays the highest average permeability with regards to the HPP test for the three various pressures. Section 2 displays the lowest average permeability, which means that this section is less permeable than both Section 1 and Section 3. This observation does not correspond with the statement made in Chapter 4.3.1, which states that Section 3 will be the least permeable due to its lower average air void percentage. But, instead of Section 3 displaying the lowest permeability, Section 2 displays the lowest permeability with regards to the HPP test. This occurrence will be thoroughly investigated and discussed in Chapter 5.

The results shown in Figure 4.7 does not fully coincide with the Marvil test results for the individual sections. A possible reason for this could be due to the HPP using pressure to force water through the core, while the Marvil only takes natural water pressure into account.

More detailed results for the HPP test with regards to each individual core of Section 1, Section 2 and Section 3 can be found in Appendix F.1, Appendix F.2 and Appendix F.3 respectively.

4.5.2 N3TC

The results obtained for the HPP tests can be seen in Figure 4.8. Figure 4.8 gives an indication of the average, 90th percentile (top of pin) and 10th percentile (bottom of pin) for the data collected for each mix at their various pressures: 100, 150 and 200 *kPa*. According to the outlier test explained in Chapter 3.8.1, Core 10 of Mix Cp is identified as an outlier with regards to the HPP test for the pressures of 100, 150 and 200 *kPa*. All the obtained data for this core is omitted from all final results, including the results shown in Figure 4.8.

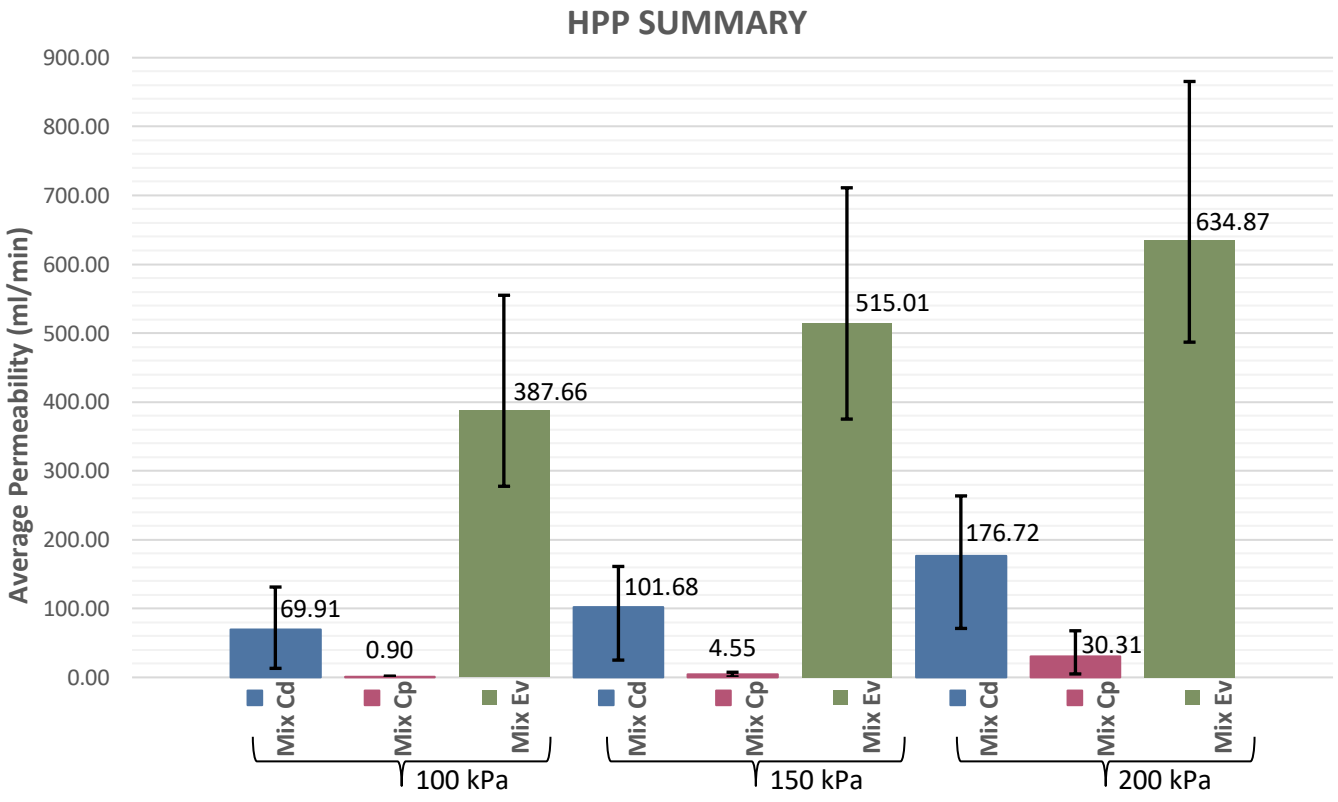

Figure 4.8: HPP Mix results (3 pressure repeats for each)

Figure 4.8 indicates that the permeability of an asphalt mix increases with an increase in the pressure being applied. As the testing pressure increases from 100 to 200 *kPa*, the rate at which water flows through the asphalt core increases drastically.

From Figure 4.8 it is also evident that Mix Ev displays the highest average permeability with regards to the HPP test for the three pressures. Mix Cp displays the lowest average permeability, which means that it is less permeable than both Mix Cd and Mix Ev. This conclusion corresponds with the statement made in Chapter 4.3.2, which states that Mix Cp will be the least permeable due to its lower average air void percentage.

More detailed results for the HPP test with regards to each individual core of Mix Cd, Mix Cp and Mix Ev can be found in Appendix F.4, Appendix F.5 and Appendix F.6 respectively.

4.5.3 N7

The results obtained for the HPP tests can be seen in Figure 4.9. Figure 4.9 gives an indication of the average, 90^{th} percentile (top of pin) and 10^{th} percentile (bottom of pin) for the data collected for each mix at their various pressures: 100, 150 and 200 *kPa*. According to the outlier test explained in Chapter 3.8.1, there are no outliers with regards to the HPP test for the N7 cores. Thus, no omissions with regards to the HPP data must be made.

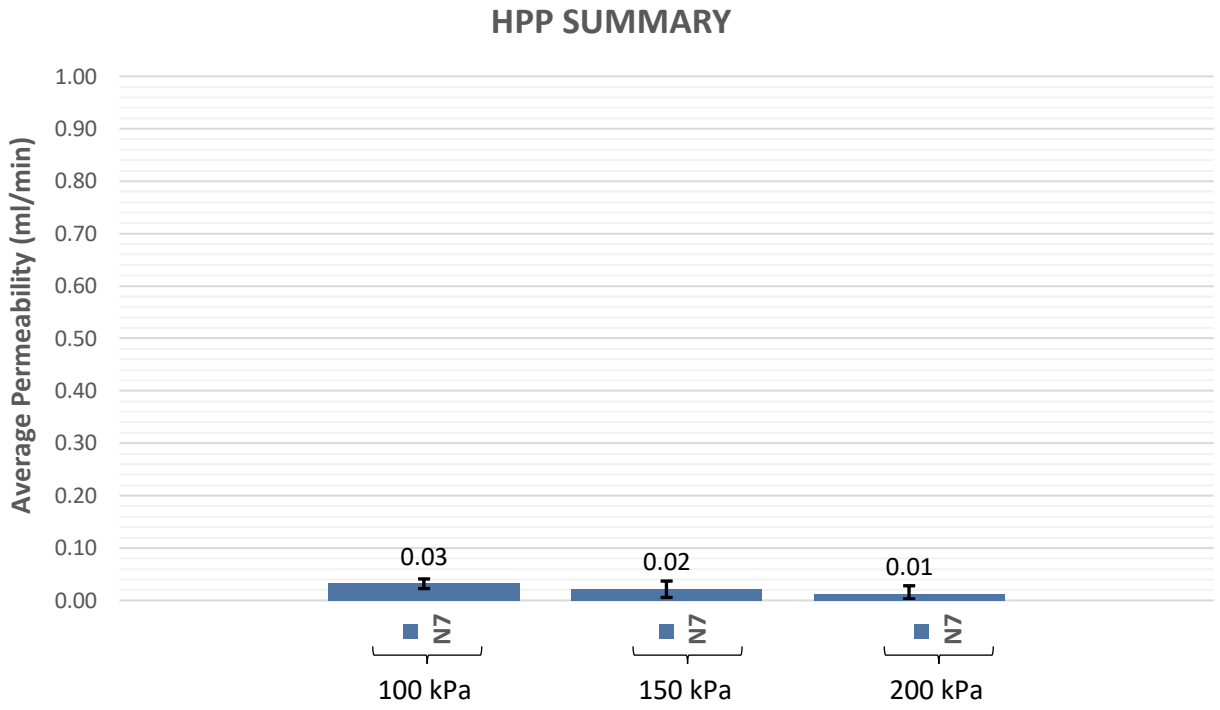

Figure 4.9: HPP results for N7 (3 pressure repeats for each)

Figure 4.9 indicates that the permeability of the asphalt mix decreases with an increase in the pressure being applied. However, this statement cannot be accepted for these asphalt cores, as the permeability of the N7 cores are so low that the cores are deemed impermeable and comparisons are inappropriate.

In conclusion, these cores display an extremely low permeability at all three pressures applied and can thus be classified as a good asphalt mixture with regards to the cores being impermeable. This conclusion corresponds with the statement made in Chapter 4.3.3, which states that the N7 asphalt cores will have a very low permeability due to its low average air void content.

More detailed results for the HPP test with regards to each individual asphalt core of the N7 highway can be found in Appendix F.7.

4.5.4 MUCH ASPHALT

The results obtained for the HPP tests can be seen in Figure 4.10. Figure 4.10 gives an indication of the average of the data collected for each mix at their various pressures: 100, 150 and 200 *kPa*. According to the outlier test explained in Chapter 3.8.1, there are no outliers with regards to the HPP test for the Much Asphalt cores. Thus, no omissions with regards to the HPP data must be made.

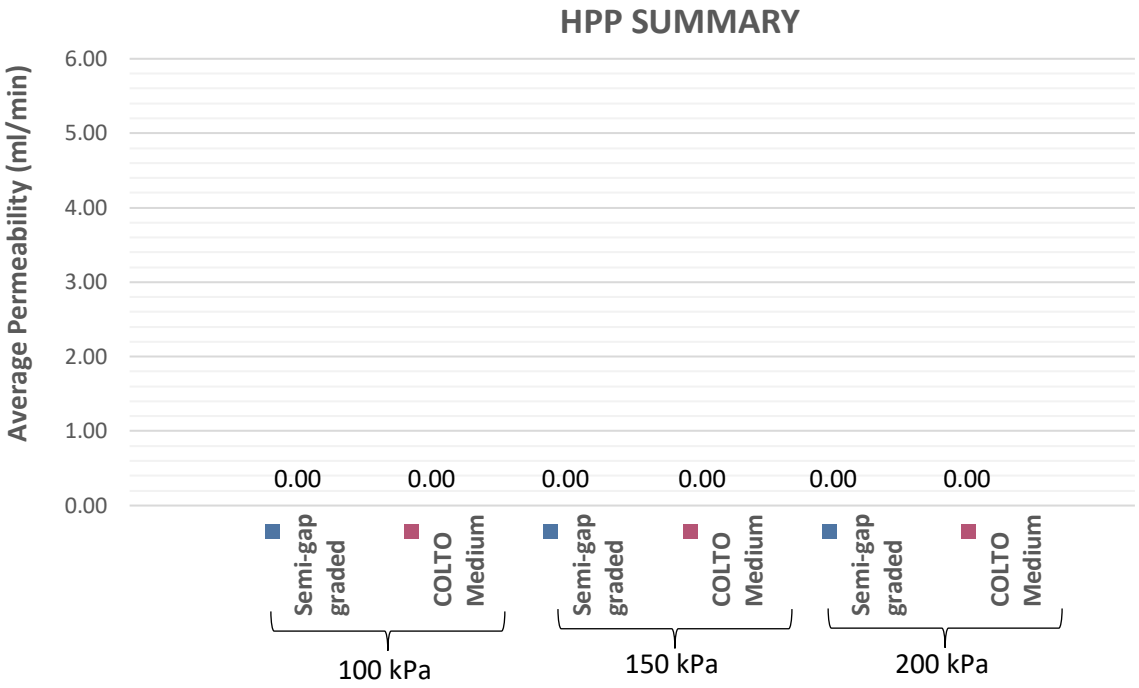

Figure 4.10: HPP mix results for Much Asphalt cores (3 pressure repeats for each)

Figure 4.10 indicates that the permeability of the asphalt cores from Much Asphalt are all zero, which indicates that these cores are impermeable at all three pressures. Thus, these cores can be classified as a good asphalt mixture with regards to the cores being impermeable. This conclusion corresponds with the statement made in Chapter 4.3.4, which states that the Much Asphalt cores will have a very low permeability for both mixes due to its low average air void content.

More detailed results for the HPP test with regards to each individual asphalt core of Much Asphalt for the semi-gap graded and COLTO medium mixes can be found in Appendix F.8 and Appendix F.9 respectively.

4.6 HIGH PRESSURE PERMEABILITY (HPP) POST MIST

The MIST device developed by Elias Twagira (2009) at Stellenbosch University is used to simulate field pulsing conditions which are caused by repeated traffic loads. This test procedure involves the saturation of an asphalt core in a tri-axial pressure cell while moisture is being pulsed onto the core. The procedure for the MIST conditioning of an asphalt core can be found in Chapter 3.7.1.

For the purpose of this research project it is necessary to determine the HPP of asphalt cores before and after MIST conditioning to determine if inducing moisture into an asphalt core has an effect on its permeability. The HPP test as set-out in Chapter 3.6.2 is used to determine the permeability of the asphalt cores from Raubex and the N3TC before and after MIST conditioning at the relevant pressure, namely: 100, 150 and 200 *kPa*. A summary of the results obtained for the HPP test of these cores before and after MIST conditioning at the various pressures will be discussed in the following chapter.

4.6.1 RAUBEX

The results obtained for the HPP tests after MIST conditioning can be seen in the graphs below. Figure 4.11, Figure 4.12 and Figure 4.13 gives an indication of the average, maximum (top of pin) and minimum (bottom of pin) for the data collected for each mix at their various pressures: 100, 150 and 200 *kPa*. Only two cores for each mix of the Raubex asphalt cores are used for MIST conditioning. These results reflect the effect that MIST conditioning has on the permeability of the various asphalt cores.

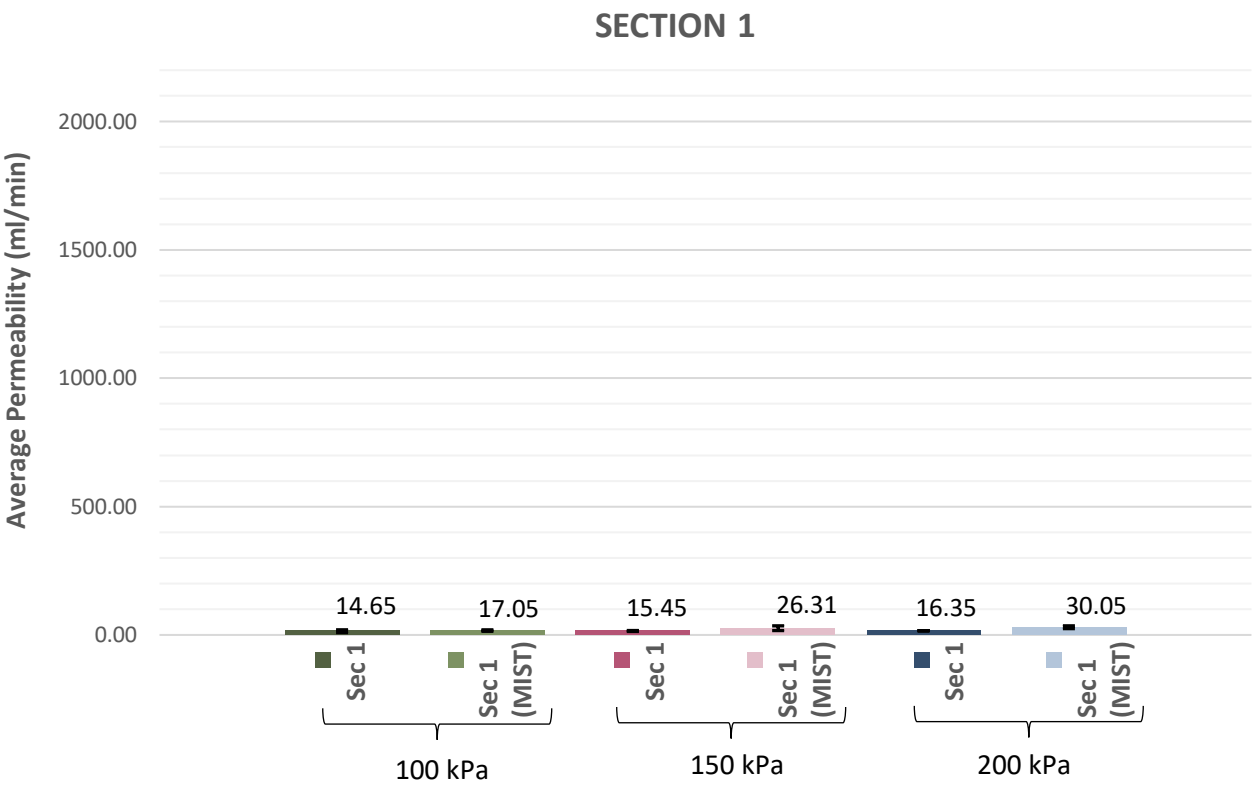

Figure 4.11: HPP results for Section 1 (before and after MIST)

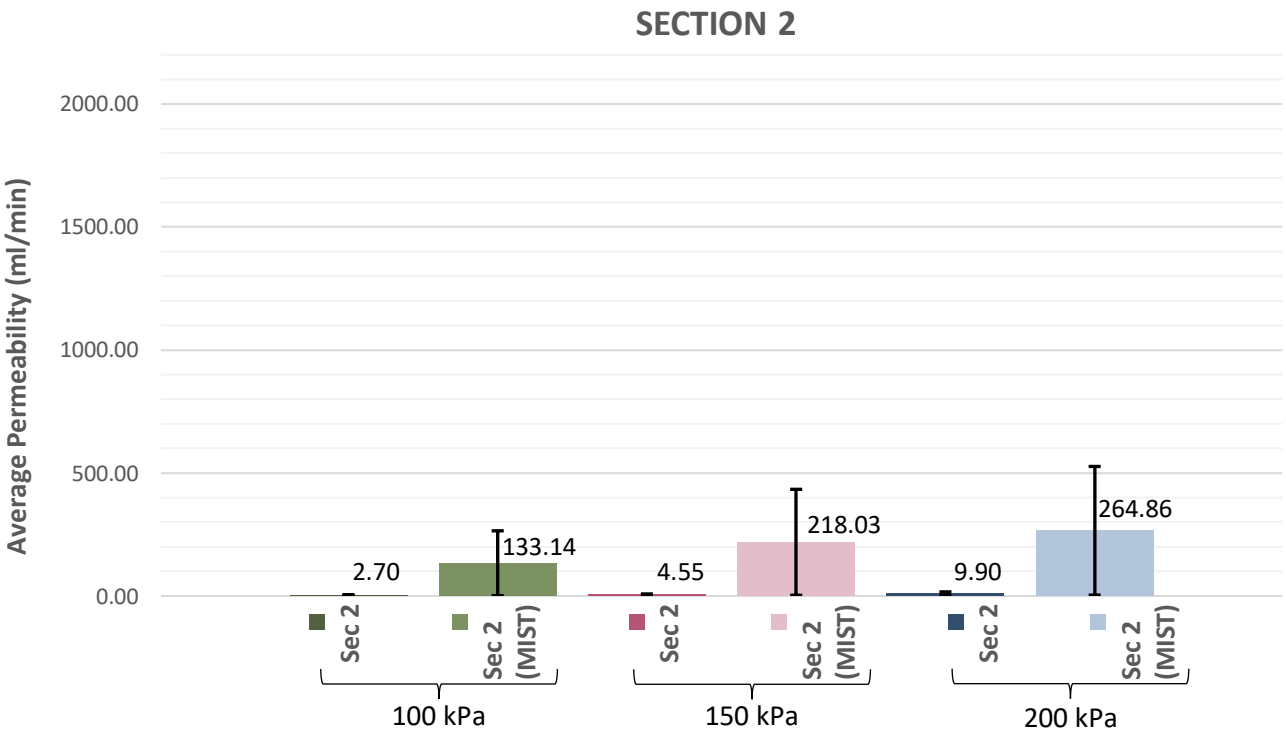

Figure 4.12: HPP results for Section 2 (before and after MIST)

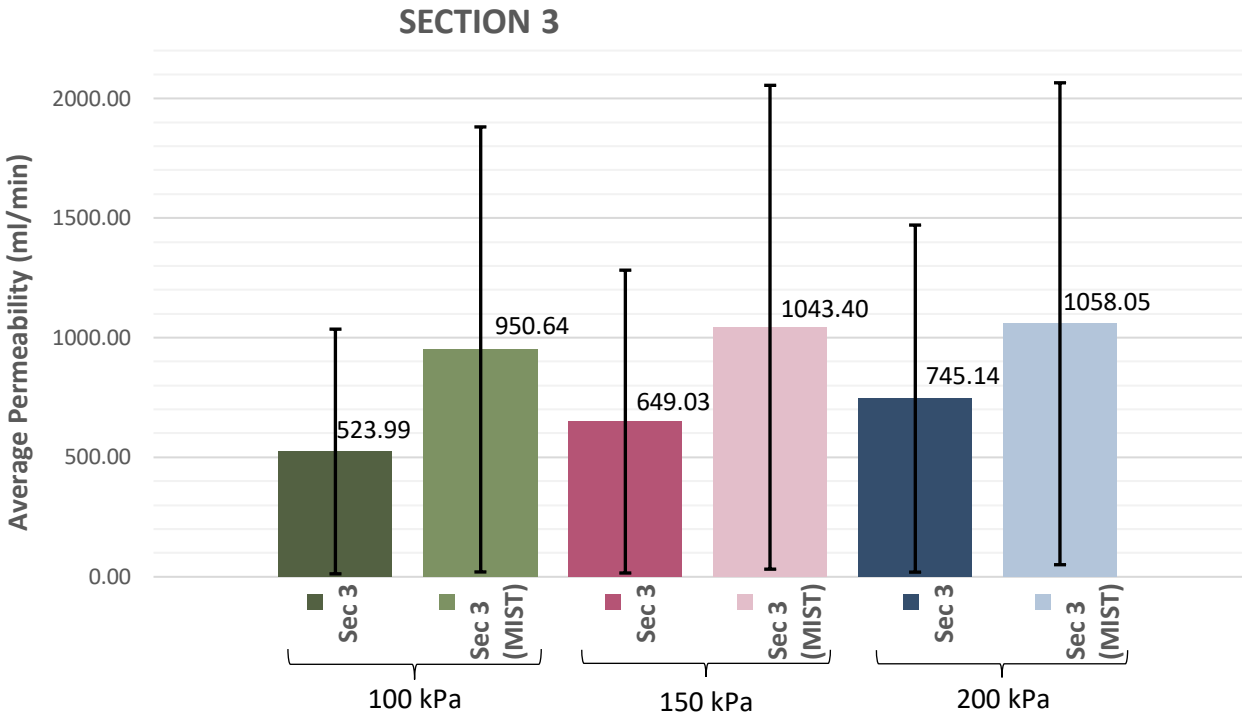

Figure 4.13: HPP results for Section 3 (before and after MIST)

From Figure 4.11 it is evident that for Section 1 the MIST conditioning causes an increase in the average permeability at pressures of 100, 150 and 200 *kPa*. Thus, the conclusion can be drawn that for Section 1, the permeability of the asphalt cores increase after MIST conditioning.

According to Figure 4.12 and Figure 4.13, the same conclusion can be made for Section 2 and Section 3. These two sections also display an increase in the HPP of the asphalt cores after MIST conditioning at the various pressures.

Overall, it can be concluded that MIST conditioning causes an increase in the HPP of the Raubex asphalt cores. Thus, MIST conditioning causes moisture damage in the asphalt cores.

More detailed results of each core for the High Pressure Permeability (HPP) tests after MIST conditioning for Section 1, Section 2 and Section 3 can be found in Appendix G.1, Appendix G.2 and Appendix G.3 respectively.

4.6.2 N3TC

The results obtained for the HPP tests after MIST conditioning can be seen in Figure 4.14, Figure 4.15 and Figure 4.16. These figures give an indication of the average, maximum (top of pin) and minimum (bottom of pin) for the data collected for each mix at their various pressures: 100, 150 and 200 *kPa*. Only three cores for each mix of the N3TC asphalt cores are used for MIST conditioning. These results reflect the effect that MIST conditioning has on the permeability of the various asphalt cores.

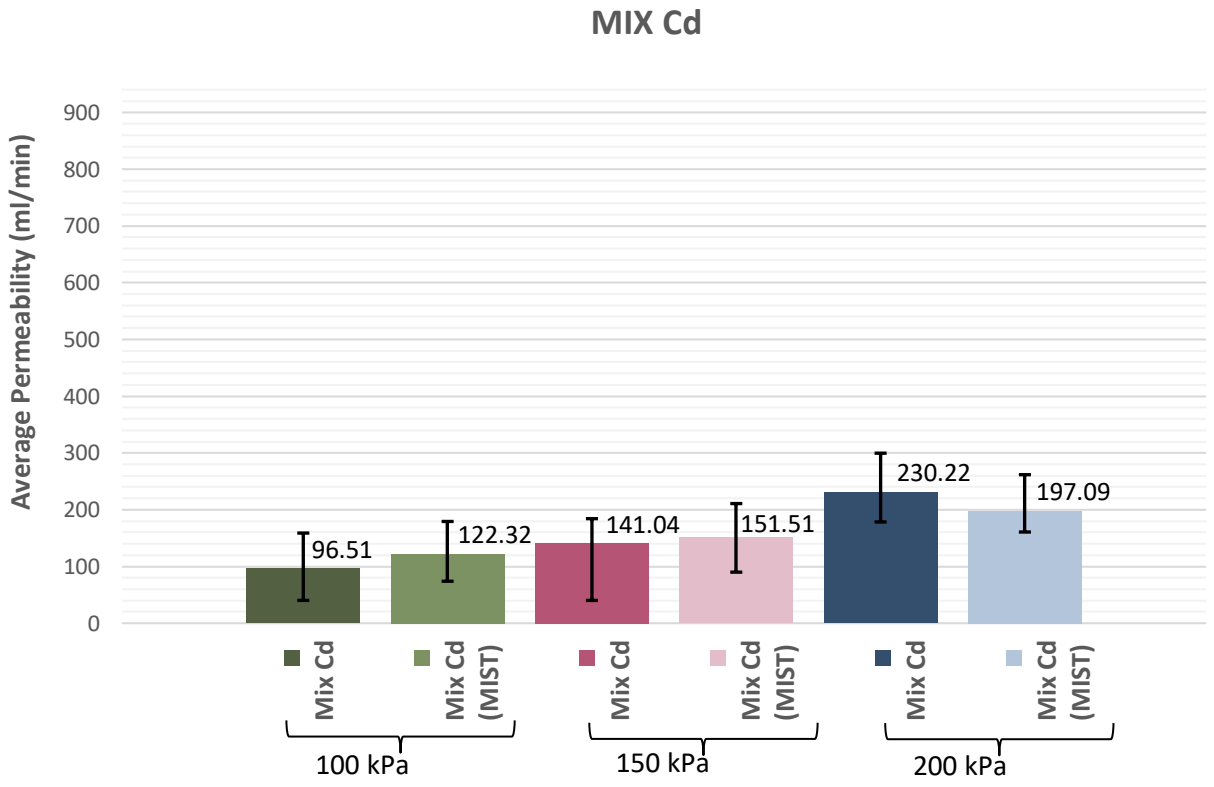

Figure 4.14: HPP results for Mix Cd (before and after MIST)

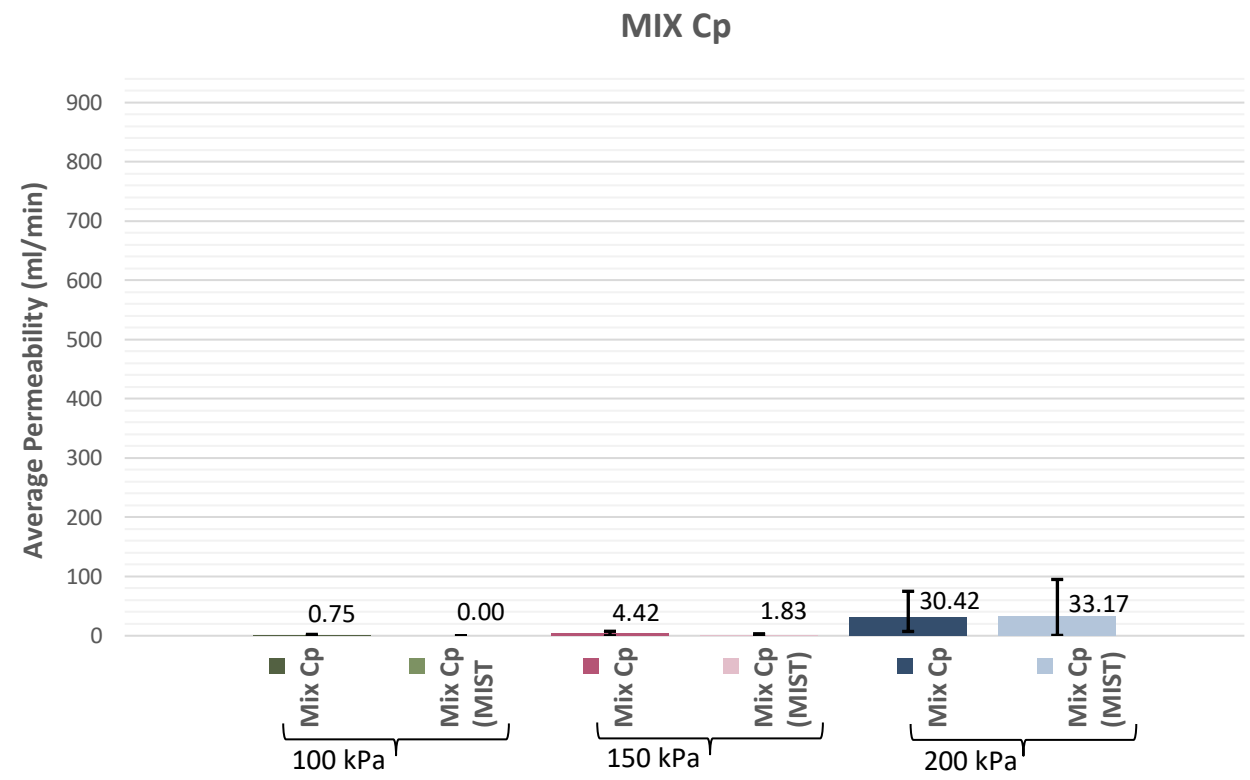

Figure 4.15: HPP results for Mix Cp (before and after MIST)

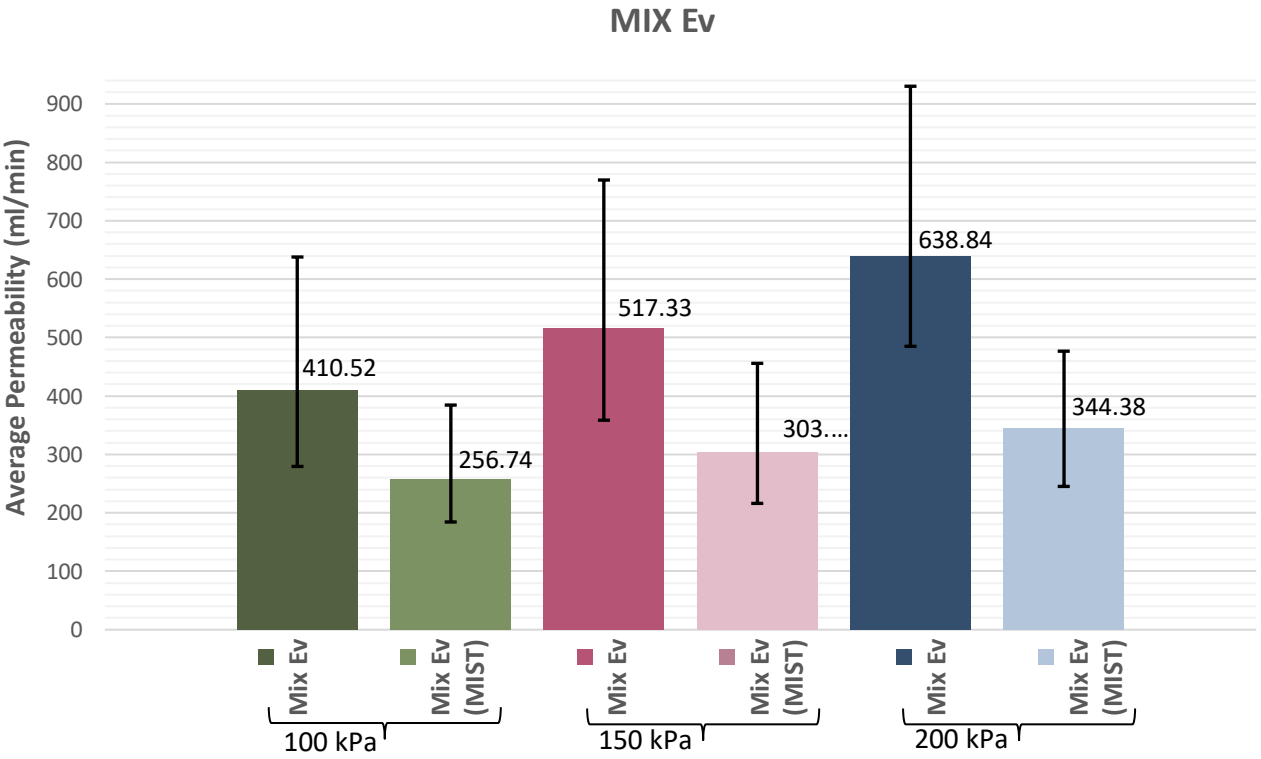

Figure 4.16: HPP results for Mix Ev (before and after MIST)

From Figure 4.14 it is evident that for Mix Cd the MIST conditioning causes an increase in the average permeability at pressures of 100 and 150 kPa. At 200 *kPa* a slight decrease in the average permeability can be noticed.

From Figure 4.15 it can be seen that the permeability before and after MIST conditioning remains more or less the same for Mix Cp. This can be due to the fact that Mix Cp is identified as a good mix with low permeability. Thus, noticing a difference before and after MIST conditioning can be difficult.

However, Mix Ev displays a large drop in the average permeability according to Figure 4.16. The reason for this drop is not clear. Further investigation is necessary. The possibility that the pressure pulsing of the MIST has redistributed the binder, although unlikely, cannot be ruled out.

More detailed results of each core for the High Pressure Permeability (HPP) tests after MIST conditioning for Mix Cd, Mix Cp and Mix Ev can be found in Appendix G.4, Appendix G.5 and Appendix G.6 respectively.

4.7 CT-SCANS

CT-scans are performed at the CT Scanner Facility at Stellenbosch University on Mix Cd and Mix Cp of the asphalt cores sourced by the N3TC. Due to financial constraints the CT-scans are only performed on Mix Cd and Mix Cp from the N3TC. These micro-CT scans are performed on the asphalt cores before and after MIST conditioning to detect the impact that the MIST would have on the inter-connected voids of an asphalt core. The assumption is made that the inter-connected voids of an asphalt core after MIST conditioning would increase, thus leading to a more permeable asphalt core.

Figure 4.17 and Figure 4.18 gives an indication of the void percentages that are measured for each core by use of the *myVGL3.1* software program after CT-scanning is complete. These voids are measured by means of identifying “imperfections” within the entire asphalt core and representing it as the void percentage.

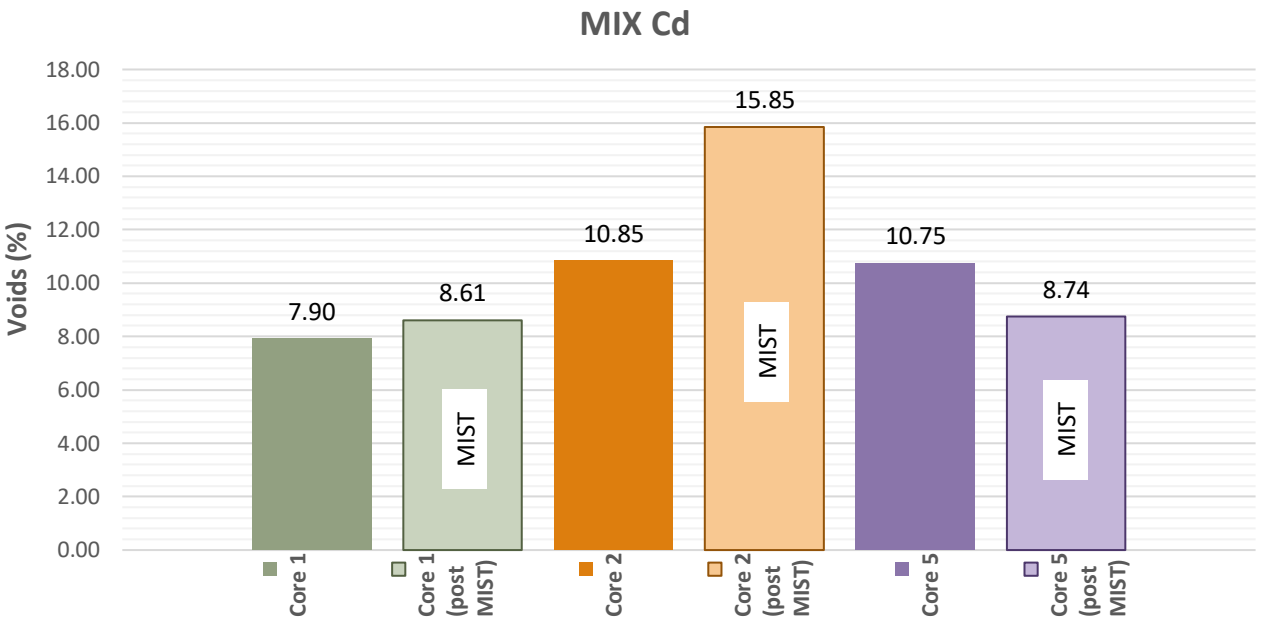

Figure 4.17: Void % of Mix Cd (from CT-scans)

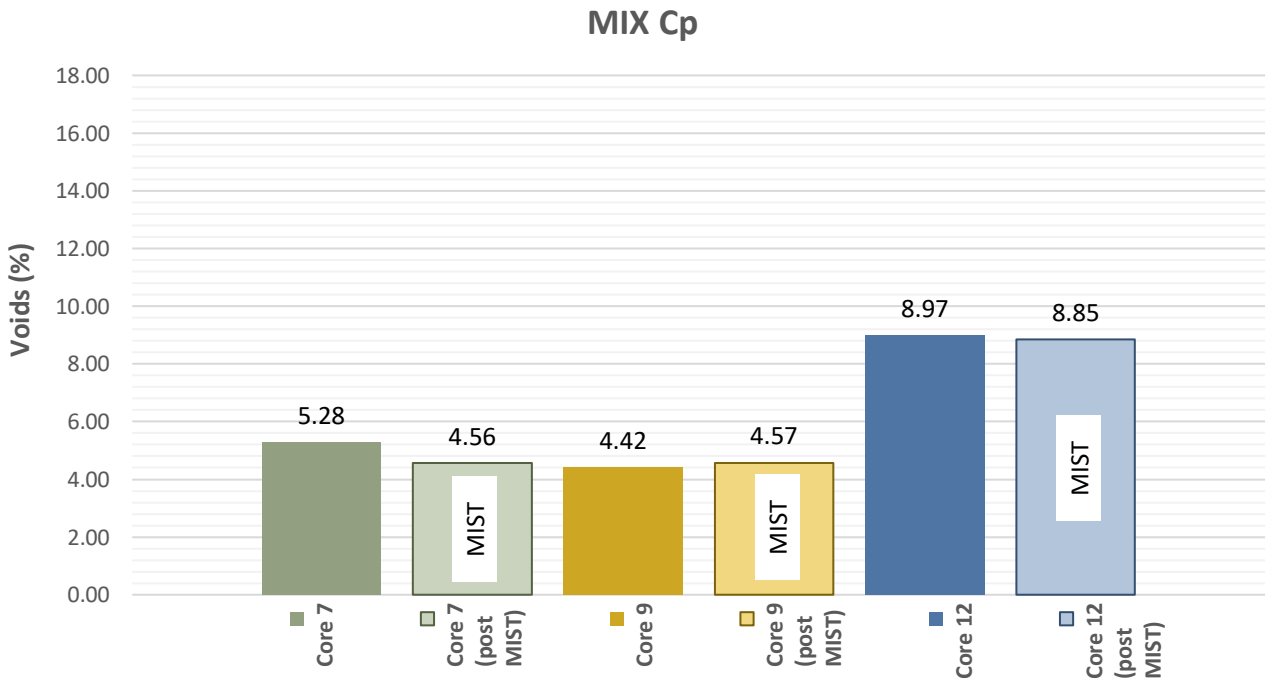

Figure 4.18: Void % of Mix Cp (from CT-scans)

Asphalt mixtures with minimal air voids that are not inter-connected, are essentially impermeable. When air voids increase beyond a critical value, they become larger and inter-connected.

From Figure 4.17 it is evident that the air void percentage for Core 1 and Core 2 increase significantly. This also indicates that the MIST conditioning increases the inter-connected voids. However, Core 5 displays a slight decrease in air void percentage. According to Figure 8.77 in Appendix H.1, there is a definite increase noted in the inter-connected voids of Core 5, but this is not shown in the void percentage.

As per Figure 4.18, the air void percentages for the cores from Mix Cp remain constant. There is no drastic increase or decrease in the air void percentages after MIST conditioning. This is expected, as Mix Cp was identified as a very good asphalt mixture with low air voids and a low overall permeability.

In Figure 4.19 below it is evident that the inter-connected voids for Core 1 increased from before MIST conditioning (left) to after MIST conditioning (right). It is also found that the inter-connected voids for Core 2 and Core 5 increased, which can be seen in Appendix H.1. There is no noticeable increase in the inter-connected voids in Core 7, 9 and 12, which can be confirmed in Appendix H.2.

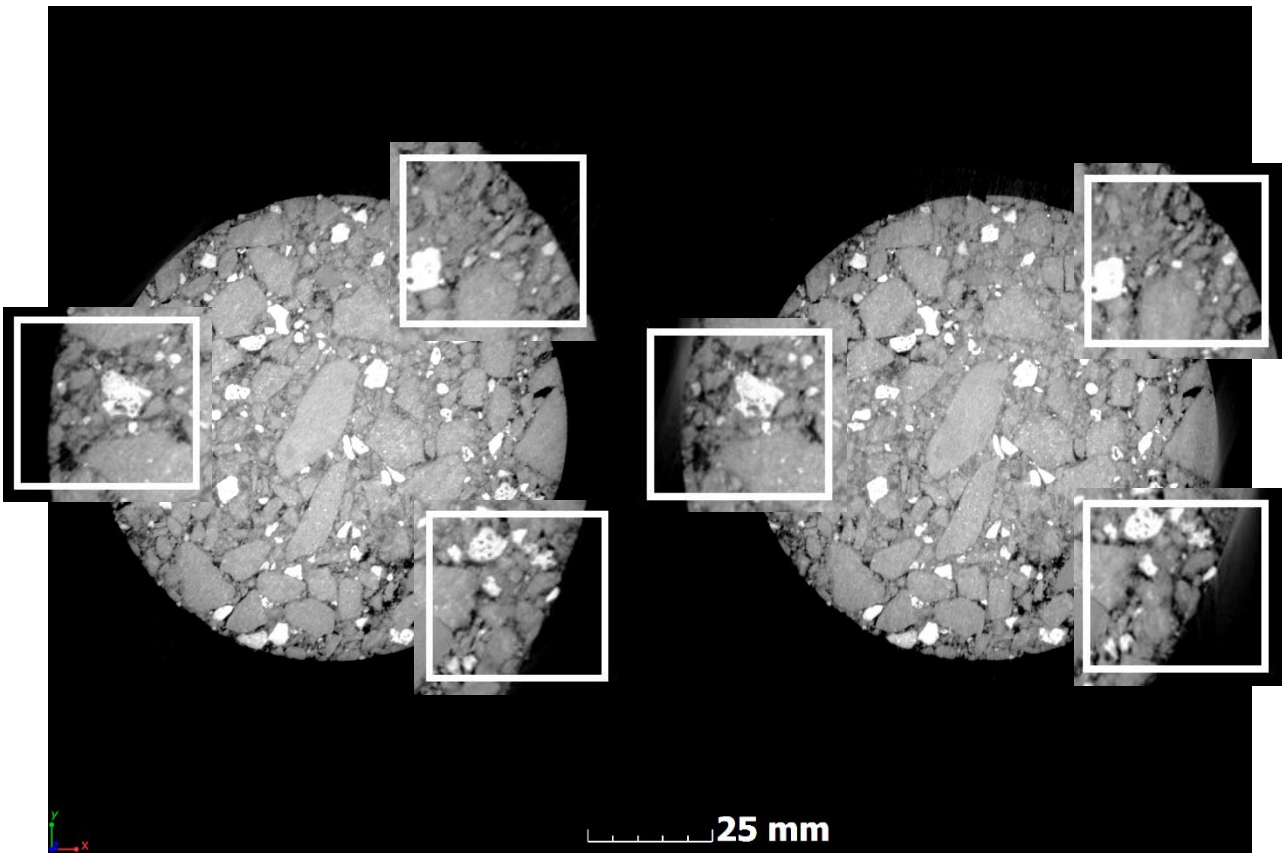

Figure 4.19: Core 1 inter-connected voids before MIST (left) and after MIST (right)

4.8 INDIRECT TENSILE STRENGTH (ITS)

The Indirect Tensile Strength (ITS) of an asphalt core is determined by measuring the resistance to failure of the cylindrical specimen when a load is applied to the curved sides of the core. This test is mostly used to estimate the potential cracking resistance or shear strength of an asphalt mixture. For the purpose of this research project, the ITS is also needed to determine if inducing moisture into an asphalt core by means of MIST conditioning has an influence on its tensile strength. To test the ITS of the asphalt cores, the procedure set out in Chapter 3.7.3 is followed.

Only the ITS of the asphalt cores from Raubex and N3TC are tested, as these cores are the only cores on which MIST conditioning was performed. The results and conclusions with regards to the ITS values obtained from these two sources will be discussed in more detail below.

4.8.1 RAUBEX

12 cores from the Raubex asphalt cores are used for ITS testing. For each of the three road sections, four cores are tested while half of those cores were exposed to MIST conditioning. Before the ITS testing is started, the core diameter and average core thickness are acquired for each asphalt core. These parameters are required by the software that will be used during testing. A summary of these parameters as well as the final ITS test results for the Raubex asphalt cores can be seen in Table 8.16 in Appendix I.1.

Figure 4.20, Figure 4.21 and Figure 4.22 indicate the ITS values obtained for the asphalt cores from Section 1, Section 2 and Section 3 respectively. These figures also indicate which cores were exposed to MIST conditioning before ITS testing.

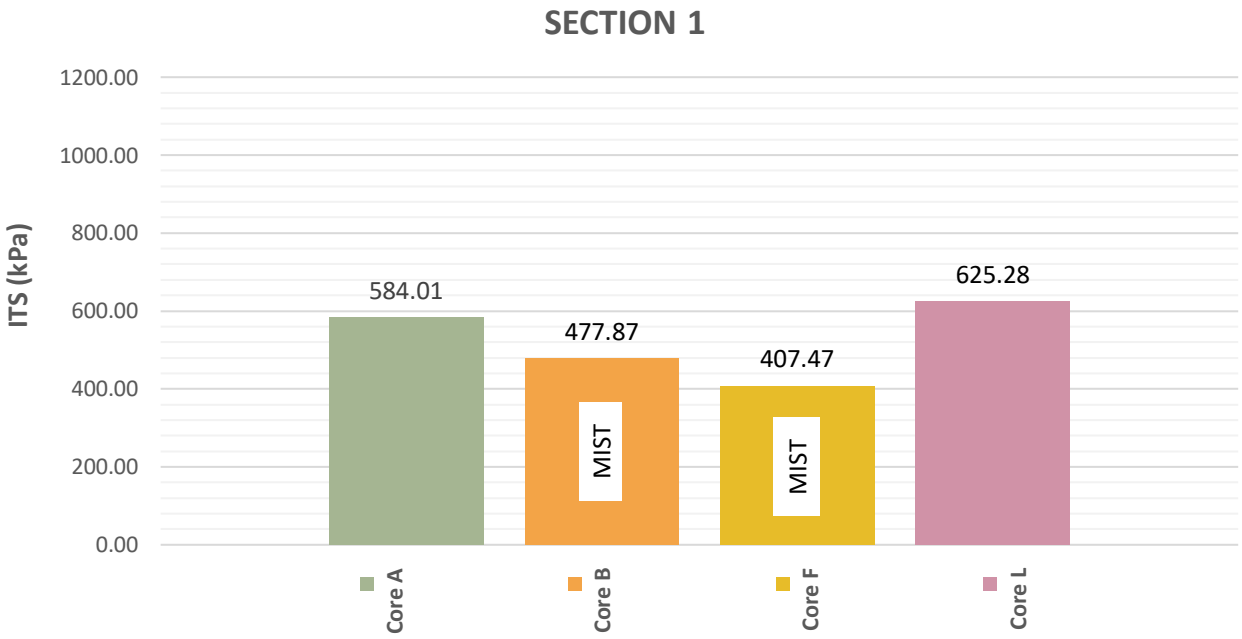

Figure 4.20: ITS results for Section 1 tested at 25°C

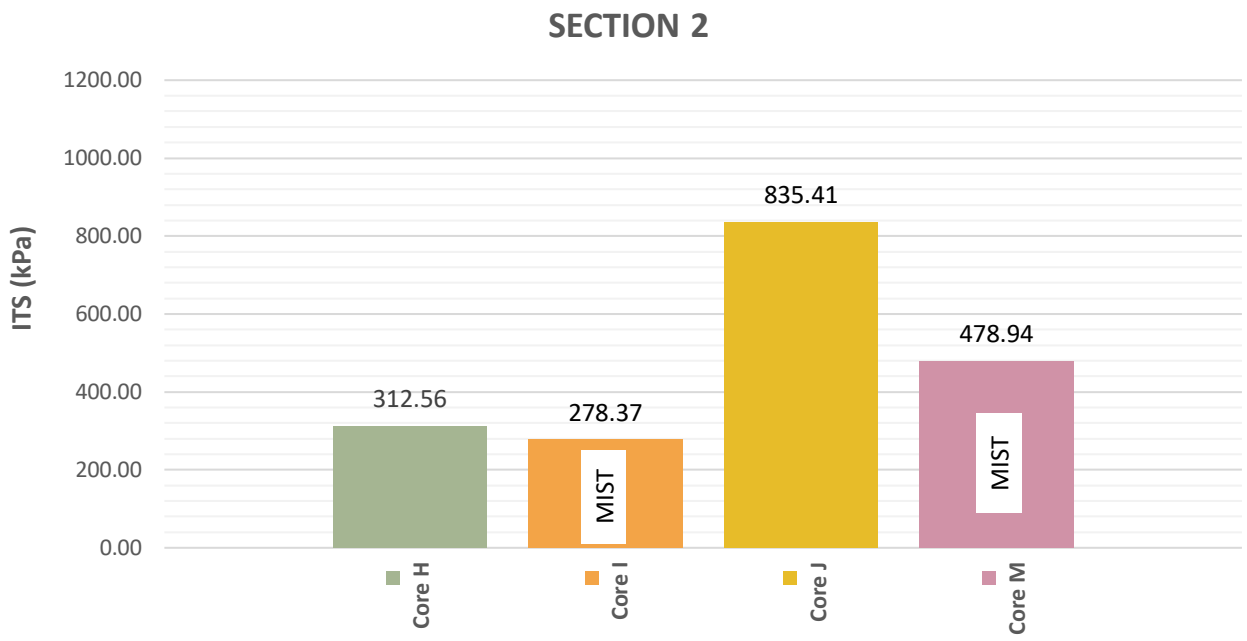

Figure 4.21: ITS results for Section 2 tested at 25°C

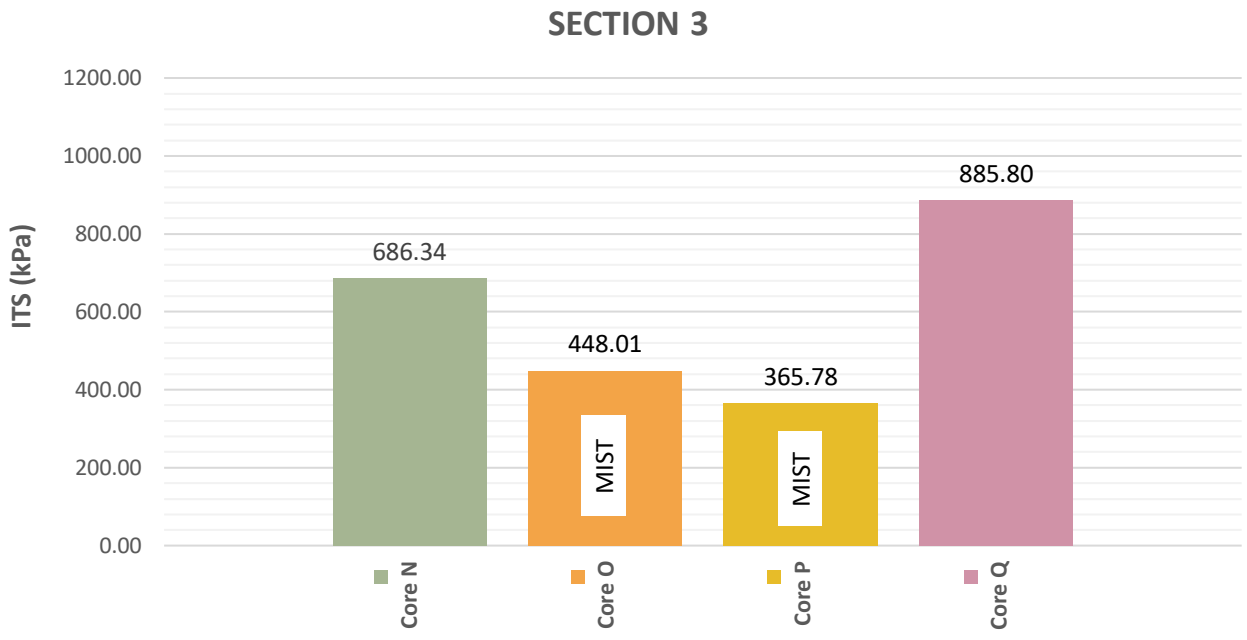

Figure 4.22: ITS results for Section 3 tested at 25°C

From these three figures shown above, it can be interpreted that MIST conditioning has a negative impact on the tensile strength of an asphalt core. In all three the road sections from the Raubex asphalt cores it can be seen that the cores exposed to moisture damage by means of MIST conditioning, display the lowest overall ITS values.

In Figure 4.21 an exception to the abovementioned interpretation can be seen where Core H displays a very low ITS value. This can be explained by referring back to Figure 4.2 and the comment section of Table 4.1 in Chapter 4.3.1. Here it is explained that during the visual inspection of the asphalt cores, Core H displayed a severely cracked surface. A cracked surface can lead to a low ITS value and can thus be ignored with regards to the abovementioned interpretation.

According to the results obtained from the ITS testing of the Raubex asphalt cores, it can be concluded that when moisture is induced into the asphalt core by means of MIST conditioning, the tensile strength of the core decreases.

4.8.2 N3TC

17 cores from the N3TC asphalt cores are used for ITS testing. For each of the three mixtures (Mix Cd, Mix Cp and Mix Ev), all of the obtained cores are tested while half of those cores were exposed to MIST conditioning. Before the ITS testing is started, the core diameter and average core thickness are acquired for each asphalt core, as these parameters are required by the software that will be used during testing. A summary of these parameters as well as the final ITS test results for the N3TC asphalt cores can be seen in Table 8.17 in Appendix I.2.

Figure 4.23, Figure 4.24 and Figure 4.25 indicate the ITS values obtained for the asphalt cores from Mix Cd, Mix Cp and Mix Ev respectively. These figures also indicate which cores were exposed to MIST conditioning before ITS testing.

Core 10 from Mix Cp is excluded from ITS testing as this core was incorrectly cored by the drill operator. The core was slightly deformed and could not be used for any ITS testing (see Figure 8.35 Appendix F.5)

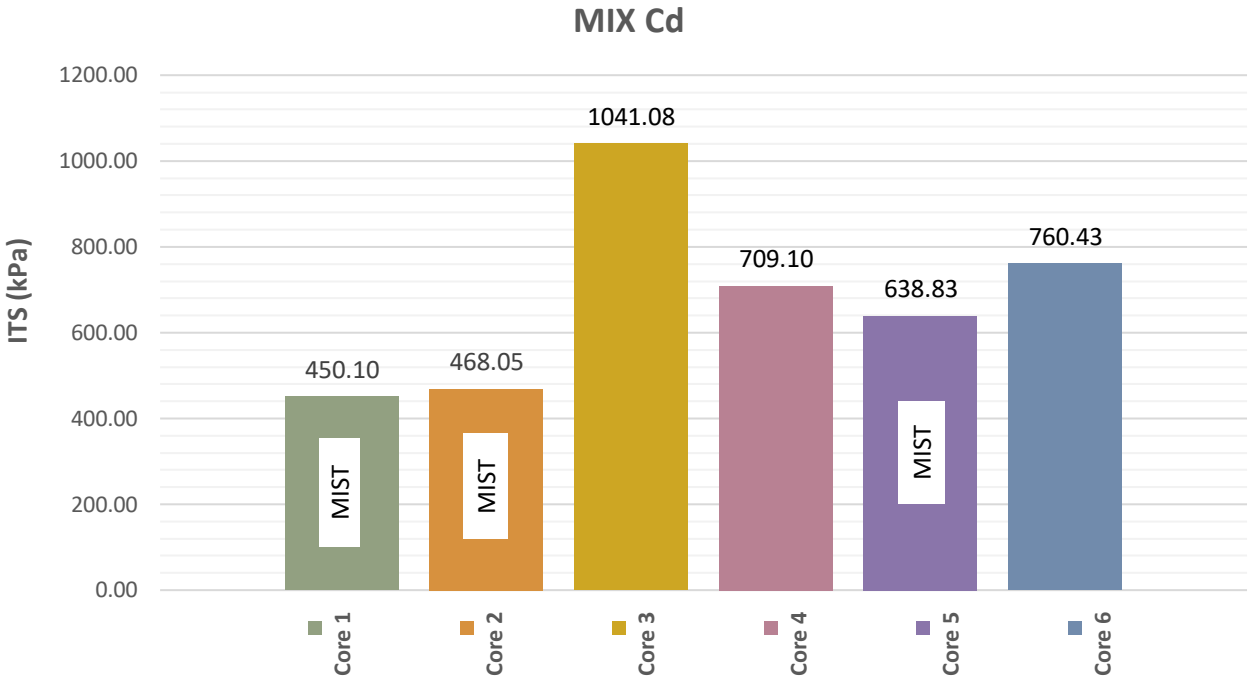

Figure 4.23: ITS results for Mix Cd tested at 25°C

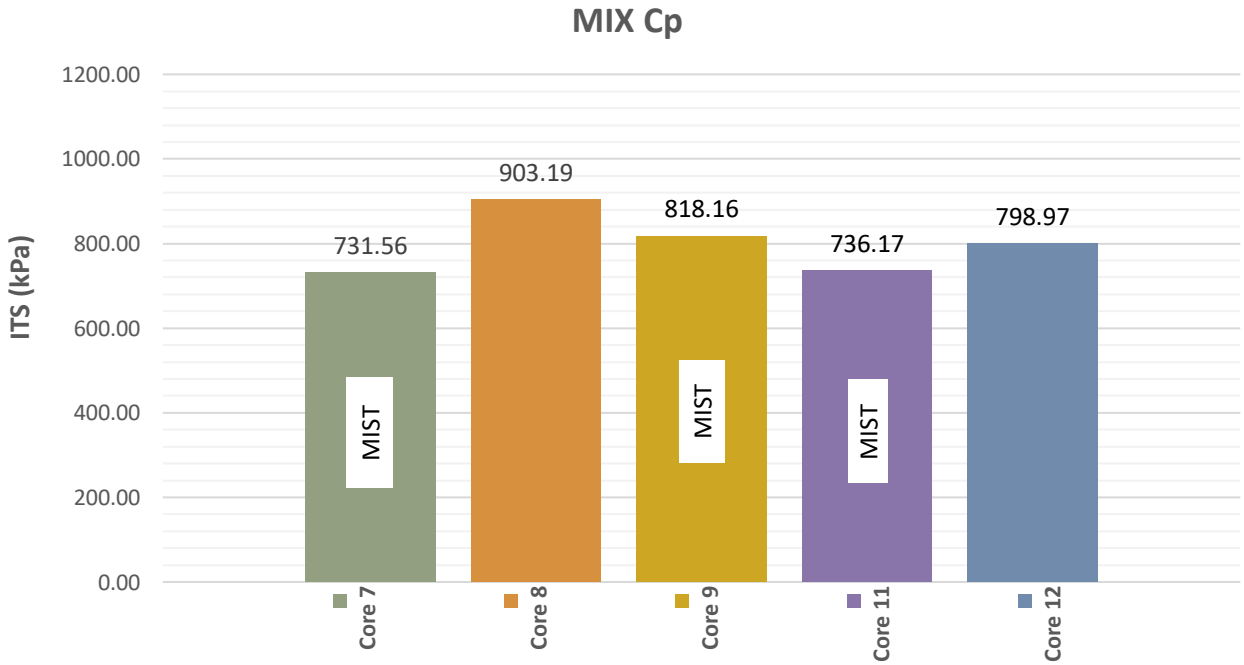

Figure 4.24: ITS results for Mix Cp tested at 25°C

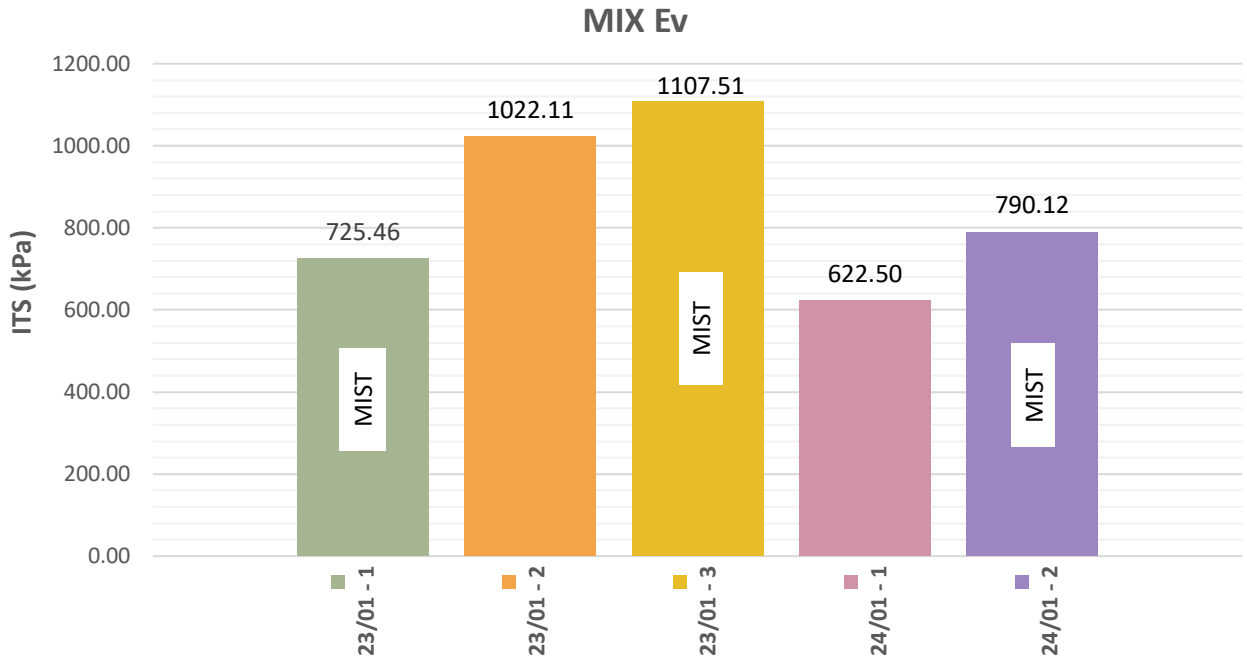

Figure 4.25: ITS results for Mix Ev tested at 25°C

From Figure 4.23 it can be interpreted that MIST conditioning has an impact on the tensile strength of an asphalt core of Mix Cd. This indicates that an asphalt core from Mix Cd which is exposed to moisture damage by means of MIST conditioning, displays a lower overall ITS value.

The same abovementioned interpretation can however not be made for Mix Cp and Mix Ev. A conclusion with regards to the impact of MIST conditioning on an asphalt core cannot be made. This is due to the fact that the ITS values obtained in Figure 4.24 are within close proximity of one another. Thus, a clear and viable conclusion cannot be made.

With regards to Mix Ev, the results obtained in Figure 4.25 display the opposite of the conclusion made for Mix Cd. It is unclear why the ITS values of Mix Ev are widely spread, and why a core with MIST conditioning displays the highest overall tensile strength. In order to be able to draw a reliable conclusion, more tests are needed.

Thus, in conclusion, no clear relationship between MIST conditioning and tensile strength can be made for Mix Cp and Mix Ev. But, Mix Cd conform to the statement that if moisture is induced into the asphalt core by means of MIST conditioning, the tensile strength of the core decreases.

4.9 SUMMARY

In Chapter 4 the different volumetric properties of all the asphalt cores are identified. These properties include the BRD's, RICE values and the void content of each core. Once these properties are known, the cores are used in their natural state to test their various permeabilities by means of the Marvil and HPP. The HPP testing is conducted at 100, 150 and 200 *kPa*.

Once all the permeability tests are complete on the asphalt cores in their natural state, a few cores are identified to be used for MIST conditioning. Once MIST conditioning is completed on the selected cores, these cores are used to investigate the HPP after moisture has been induced into the core.

To determine the effect that the MIST conditioning has on the inter-connected voids of an asphalt core, CT-scans are done at the CT-Scanner facility. The results from the CT-scans prove that the MIST conditioning causes an increase in the inter-connected voids of an asphalt core.

To determine the effect on the tensile strength of an asphalt core after moisture has been induced into the asphalt core (by means of MIST conditioning), ITS tests are conducted on these cores. Most of the asphalt cores displayed a decrease in tensile strength after MIST conditioning.

CHAPTER 5 - INTERPRETATION

5.1 INTRODUCTION

This chapter presents the interpretations made with regards to the Marvil, HPP and air voids of the asphalt cores. An interpretation with regards to the permeability of the Marvil versus the HPP will be made; as well as interpretations with regards to the Marvil and HPP versus the air voids. These interpretations are made to achieve the secondary objectives of this research project. The outline for this chapter can be seen in Figure 5.1.

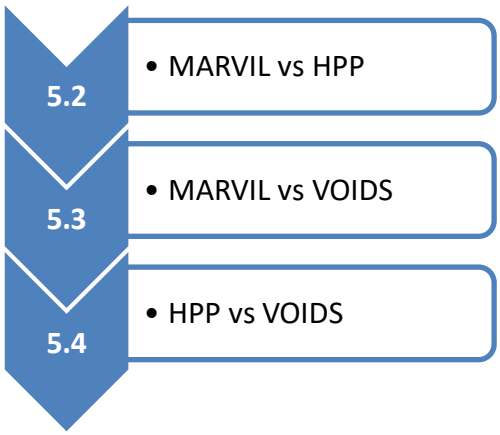

Figure 5.1: Interpretation layout

5.2 MARVIL VERSUS HIGH PRESSURE PERMEABILITY (HPP)

To meet the secondary objective of determining whether there is a correlation between the permeability results of the Marvil and the HPP (at its various pressures, namely: 100, 150 and 200 *kPa*), it is necessary to acquire adequate data to make a viable conclusion in this regard. Thus, the asphalt cores from Raubex, N3TC (top and bottom layer asphalt cores) and the N7 highway are tested and used to draw a viable conclusion.

The permeability results for the Marvil and HPP of these cores can be seen in Table 5.1 (Raubex), Table 5.2 (N3TC top layer asphalt cores), Table 5.3 (N3TC bottom layer asphalt cores) and Table 5.4 (N7 highway). The values highlighted in red were previously identified as outliers for the various

tests and will be ignored when drawing conclusions. The results displayed in these tables are graphically represented in Appendix J.1, Appendix J.2, Appendix J.3 and Appendix J.4 respectively. The graphs displayed in the appendices give a visual representation of the results and provide a more reliable manner to make a conclusion with regards to this objective.

To support the conclusions made in Chapter 5.2, an ANOVA statistical analysis is performed on the relevant variables. The results from this analysis can be seen in Appendix M.

5.2.1 RAUBEX

The permeability results for the Marvil and the HPP of the Raubex asphalt cores are presented in Table 5.1.

Table 5.1: Raubex - Marvil vs HPP

		PERMEABILITY (mℓ/min)			
		Marvil	**HPP: 100 kPa**	**HPP: 150 kPa**	**HPP: 200 kPa**
SECTION 1	Core A	22,30	4,40	8,80	144,14
	Core B	5,94	20,00	17,20	16,20
	Core F	0,83	9,30	13,70	16,50
	Core L	6,24	0,40	1,50	2,30
SECTION 2	Core H	500,00	1980,20	2023,61	1980,20
	Core I	14,98	5,10	8,00	16,40
	Core J	6,06	0,30	0,40	0,25
	Core M	12,36	0,30	1,10	3,40
SECTION 3	Core N	118,23	14,40	21,40	37,97
	Core O	42,78	12,60	16,00	19,70
	Core P	102,56	1035,38	1282,05	1470,59
	Core Q	17,61	15,40	19,20	40,40

From Table 5.1 (and Appendix J.1) follows that the asphalt cores from Raubex display a widespread permeability ranging from very low to very high for the Marvil and HPP. The only exception on this statement is with regards to Core N, where a very high Marvil permeability exists, but the HPP is relatively low. This inconsistency can be explained by means of referring to the detail that for the Marvil permeability test the asphalt core had a diameter of 150 *mm*. For HPP testing it was necessary for the core to be smaller, and thus it was cored down to 102 *mm*. The possibility exists that the edges of the core had more inter-connected voids which led to a higher Marvil permeability, and once the edges were cored off, only the center part of the core was left; leading to a lower

permeability during HPP testing. Another possibility exists that during Marvil testing water could have leaked through the sides of the core where it met the silicone rubber mould, leading to a high Marvil permeability reading.

It should be noted that the permeability of Core A at 200 *kPa* is identified as an outlier. This can lead to the assumption that the test results can be extremely sensitive when testing under a high pressure.

However, for the remaining cores a relationship between the Marvil and HPP can be observed. This statement is supported by referring to Figure 5.2, which indicates that a linear relationship exists between the Marvil and HPP at pressures of 100 and 150 *kPa*. At 200 *kPa*, the data is too variable and sensitive, and no relationship exists, thus is was not included in the analysis.

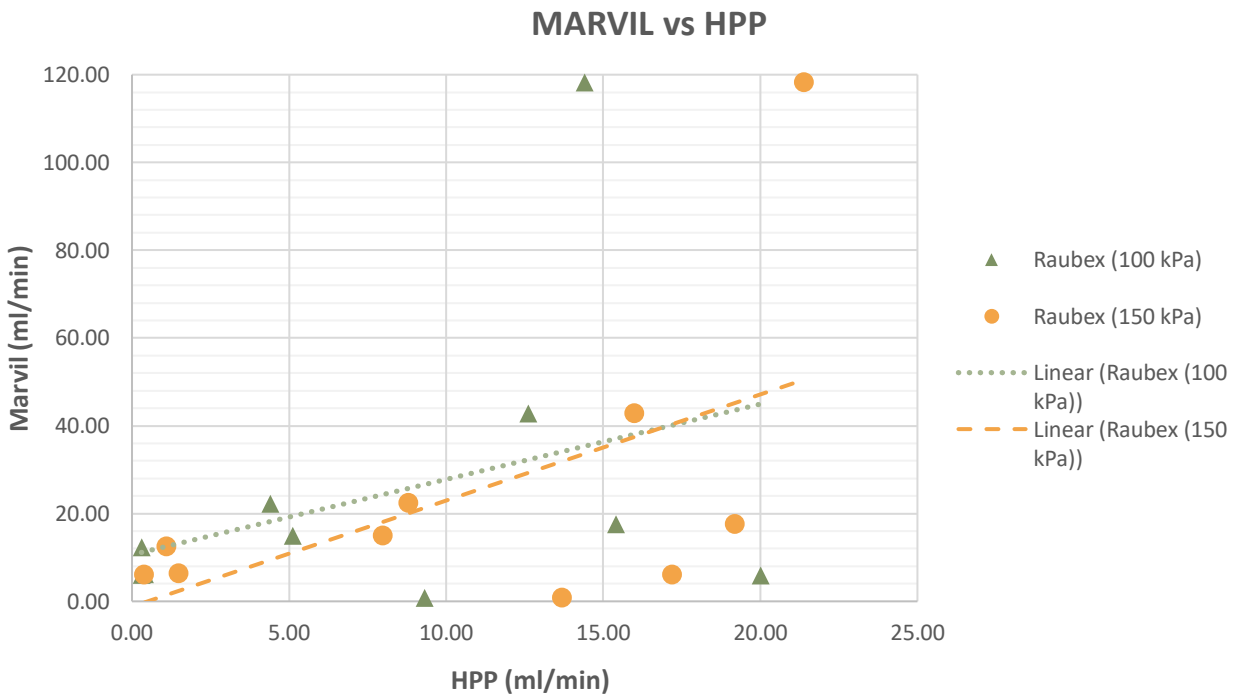

Figure 5.2: Raubex cores – comparative analysis of permeability tests

Even though it is evident from Figure 5.2 that the data is relatively widespread, a linear relationship can still be noted. Thus, in conclusion, for varying asphalt core permeabilities, a correlation between the Marvil and HPP occurs at testing pressures of 100 and 150 *kPa*. It is recommended that testing at 200 *kPa* be avoided.

5.2.2 N3TC

The permeability results for the Marvil and the HPP of the N3TC top layer asphalt cores are presented in Table 5.2.

Table 5.2: N3TC - Marvil vs HPP

		PERMEABILITY (*mℓ/min*)			
		Marvil	**HPP: 100 kPa**	**HPP: 150 kPa**	**HPP: 200 kPa**
MIX Cd	Core 1	102,66	90,36	137,99	178,47
	Core 2	190,14	158,88	184,28	299,63
	Core 3	0,00	0,00	0,00	4,50
	Core 4	48,47	103,61	136,71	137,69
	Core 5	16,67	40,29	100,85	212,58
	Core 6	39,13	26,31	50,24	227,49
MIX Cp	Core 7	0,00	0,00	7,50	75,00
	Core 8	0,00	1,00	2,00	3,50
	Core 9	0,00	2,25	5,75	9,00
	Core 10	0,00	109,87	200,20	265,37
	Core 11	0,00	1,25	7,50	56,80
	Core 12	0,00	0,00	0,00	7,25

The top layer asphalt cores from the N3TC exhibit a high overall permeability for Mix Cd and a very low overall permeability for Mix Cp with regards to the Marvil and HPP. Table 5.2 (Appendix J.2) indicates that the Marvil permeability varies from very low to high. The HPP also displays very low to high permeabilities accordingly, however, at the pressure of 200 *kPa* a wide variability of permeability results is noticed. This variability indicates that at the HPP testing pressure of 200 *kPa*, a sensitivity with regards to the permeability in asphalt cores is noticed.

The asphalt cores displaying a high Marvil permeability also display a high permeability at the pressures of 100 and 150 *kPa* for the HPP. Thus, in conclusion, for asphalt cores of Mix Cd, with low to high permeabilities, a correlation exists between the Marvil and HPP, except at the pressure of 200 *kPa*, where inconsistencies can be noticed.

From Table 5.2 (Appendix J.2) it can be observed that the Marvil permeabilities for Mix Cp are all zero, meaning that during the Marvil permeability testing these cores were identified as impermeable. The HPP also displays a very low permeability for these cores, however, at the pressure of 200 *kPa* a spike in permeability can be noticed for Core 7 and Core 11. This indicates that at the highest testing pressure of 200 *kPa*, a sensitivity with regards to permeability in asphalt

cores can be identified. Thus, for a low Marvil permeability, a low permeability for the pressure of 100 and 150 *kPa* can be identified in the HPP, with inconsistent permeability measurements at 200 *kPa*. A conclusion can be made that for the cores of Mix Cp, with a very low overall permeability, a correlation between the Marvil and HPP exists, except at a pressure of 200 *kPa*.

The conclusions made for Mix Cd and Mix Cp are supported by the analysis done in Figure 5.3. From this analysis (and the statistical analysis) it is proven that a linear relationship exists between the permeability results of the Marvil and the HPP for both pressure of 100 and 150 *kPa*. Since the permeability data at 200 kPa is too variable, it was not included in this analysis.

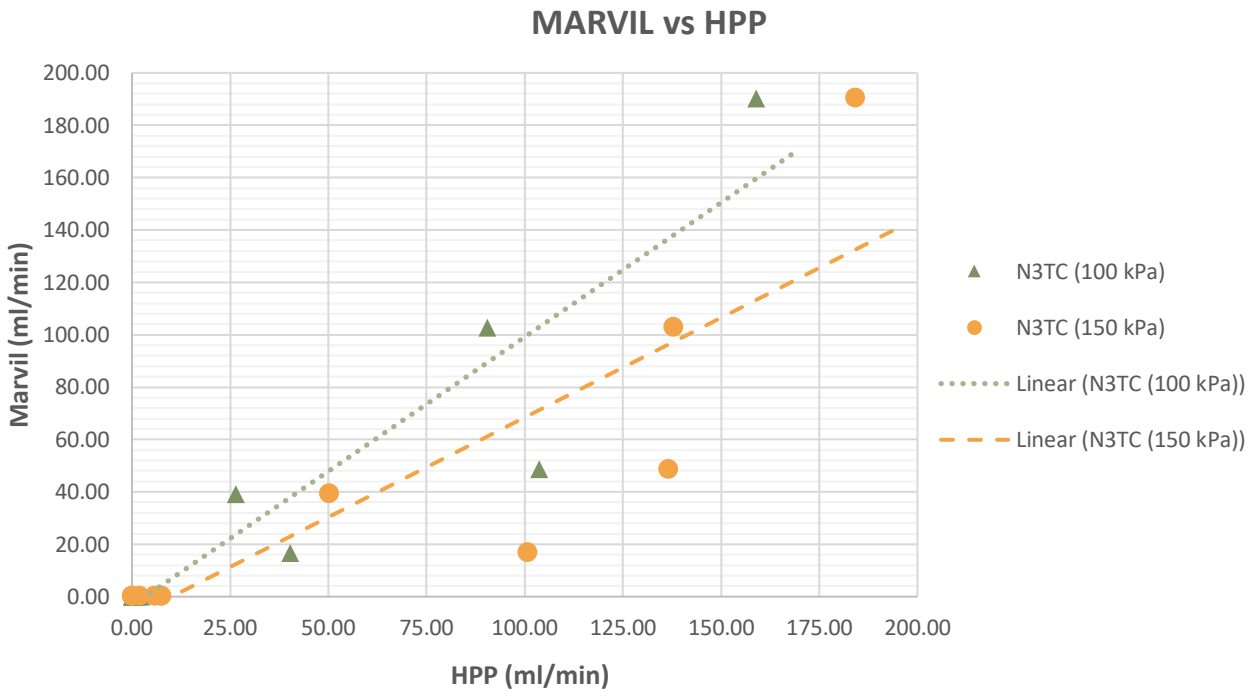

Figure 5.3: N3TC cores – comparative analysis of permeability tests

Thus, in conclusion, for the cores from the N3TC top asphalt layer a clear correlation between the Marvil and HPP exists at testing pressures of 100 and 150 *kPa*.

5.2.3 N3TC (BOTTOM LAYER ASPHALT CORES)

The permeability results for the Marvil and the HPP of the N3TC bottom layer asphalt cores are presented in Table 5.3.

Table 5.3: N3TC bottom layer asphalt cores - Marvil vs HPP

	PERMEABILITY (*mℓ/min*)			
	Marvil	**HPP: 100 kPa**	**HPP: 150 kPa**	**HPP: 200 kPa**
Core 1	0,21	2,00	2,75	10,50
Core 2	2,15	6,00	27,50	55,90
Core 3	0,17	5,25	5,25	10,50
Core 4	0,14	0,00	0,00	0,00
Core 5	0,17	0,00	0,00	0,00
Core 6	0,17	5,00	7,50	9,50
Core 7	0,13	0,00	0,00	0,00
Core 8	0,08	0,00	0,25	1,00
Core 9	0,08	0,00	0,00	0,00
Core 10	0,08	0,00	0,25	0,50
Core 11	0,14	0,00	0,00	0,50
Core 12	0,13	0,00	0,00	0,50

The bottom layer asphalt cores from the N3TC display a very low permeability with regards to the Marvil and HPP. Table 5.3 (Appendix J.3) show that there is no clear correlation between the permeability of the Marvil and HPP. This statement is supported by the analysis done for all the asphalt cores of the bottom layer from the N3TC in Figure 5.4.

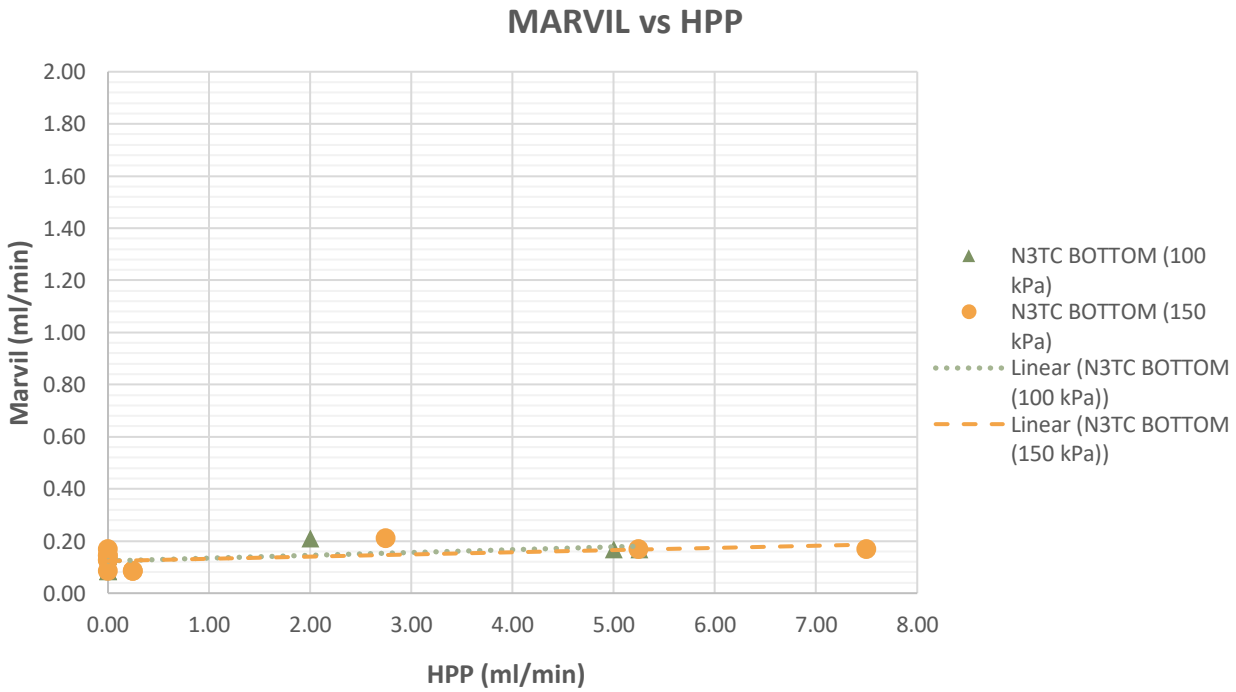

Figure 5.4: N3TC (bottom) cores – comparative analysis of permeability tests

Figure 5.4 gives a clear indication that there is no correlation between the Marvil and HPP at either 100 or 150 *kPa*. Since it was previously proven that testing at a pressure of 200 *kPa* leads to inconsistencies and variability in the permeability results, this pressure was excluded from the analysis.

Thus, the conclusion can be made that for the N3TC bottom layer asphalt cores, which is virtually impermeable, no correlation exists between the Marvil and HPP.

5.2.4 N7

The permeability results for the Marvil and the HPP of the N7 highway asphalt cores are presented in Table 5.4.

Table 5.4: N7 - Marvil vs HPP

	PERMEABILITY (*mℓ/min*)			
	Marvil	**HPP: 100 kPa**	**HPP: 150 kPa**	**HPP: 200 kPa**
Core 1	0,17	0,04	0,04	0,03
Core 2	0,13	0,04	0,00	0,00
Core 3	0,06	0,05	0,04	0,03
Core 4	0,09	0,02	0,01	0,01
Core 5	0,20	0,03	0,02	0,01

The asphalt cores from the N7 highway exhibit a very low permeability with regards to the Marvil and HPP. The permeability of these cores is so low that it can be considered impermeable. From Table 5.4 (Appendix J.4) follows that no correlation between the permeability of the Marvil and the HPP occurs.

With a low Marvil permeability, a low permeability for the various pressures can also be noted in the HPP. But, even though a low permeability can be noted for the Marvil and HPP, no clear relationship between these permeabilities exist. This statement is supported by the analysis done in Figure 5.5.

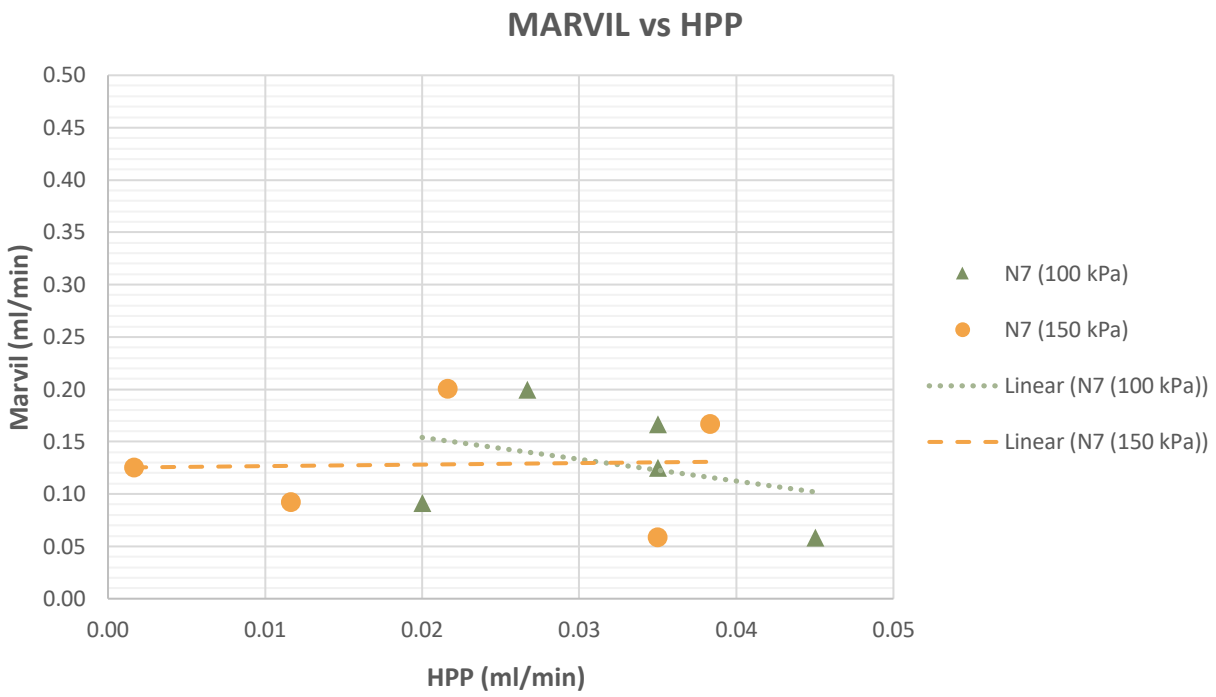

Figure 5.5: N7 cores – comparative analysis of permeability tests

From Figure 5.5 it is proven that the data for the Marvil and HPP at its various pressures are relatively widespread, which indicates that no relationship occurs. Thus, the conclusion can be made that for the N7 highway asphalt cores, with a very low permeability, no correlation between the Marvil and HPP exists.

5.3 MARVIL VERSUS VOIDS

To meet the secondary objective of determining whether there exists a correlation between the Marvil permeability results and the air void percentage of an asphalt core, it is necessary to acquire adequate data to make a viable conclusion. Thus, the asphalt cores from Raubex, N3TC (top and bottom cores) and the N7 highway are tested and interpreted to help draw a conclusion with regards to this statement.

The Marvil permeability results, together with the respective air void percentage for each core can be seen in Table 5.5 (Raubex), Table 5.6 (N3TC top asphalt cores), Table 5.7 (N3TC bottom asphalt cores) and Table 5.8 (N7). These tables are arranged in the manner of increasing air void percentage, thus providing the opportunity to draw conclusions by referring to the increase of air void content

in an asphalt mixture. It is assumed that as the air void percentage increases the Marvil permeability will also increase.

The values highlighted in red were previously identified as outliers for the various tests and will be ignored when drawing conclusions. The results displayed in these tables are graphically represented in Appendix K.1, Appendix K.2, Appendix K.3 and Appendix K.4 respectively. The graphs displayed in the appendices give a visual representation of the results and provide a more reliable manner to make a conclusion with regards to this objective.

To support the conclusions made in Chapter 5.3, an ANOVA statistical analysis is performed on the relevant variables. The results from this analysis can be seen in Appendix N.

5.3.1 RAUBEX

The permeability results for the Marvil and the air void percentages of the Raubex asphalt cores are presented in Table 5.5.

Table 5.5: Raubex - Marvil vs Voids

		Marvil (*mℓ/min*)	Voids (%)
SECTION 1	Core L	6,24	10,42
	Core A	22,30	12,57
	Core F	0,83	15,06
	Core B	5,94	23,62
SECTION 2	Core H	500,00	7,33
	Core J	6,06	10,79
	Core I	14,98	11,66
	Core M	12,36	13,48
SECTION 3	Core O	42,78	9,29
	Core Q	17,61	9,45
	Core P	102,56	12,07
	Core N	118,23	12,38

From Table 5.5 (and Appendix K.1) follows that the asphalt cores from Raubex display a widespread permeability ranging from very low to very high for the Marvil. The air void percentages vary from 7.33 % up to 15.06 % for the three different sections. These air void percentages are relatively high, thus a high Marvil permeability is expected.

However, no clear relationship can be seen in any of the road sections of the Raubex asphalt cores. It was previously assumed that as the air void percentage increases, the Marvil permeability would

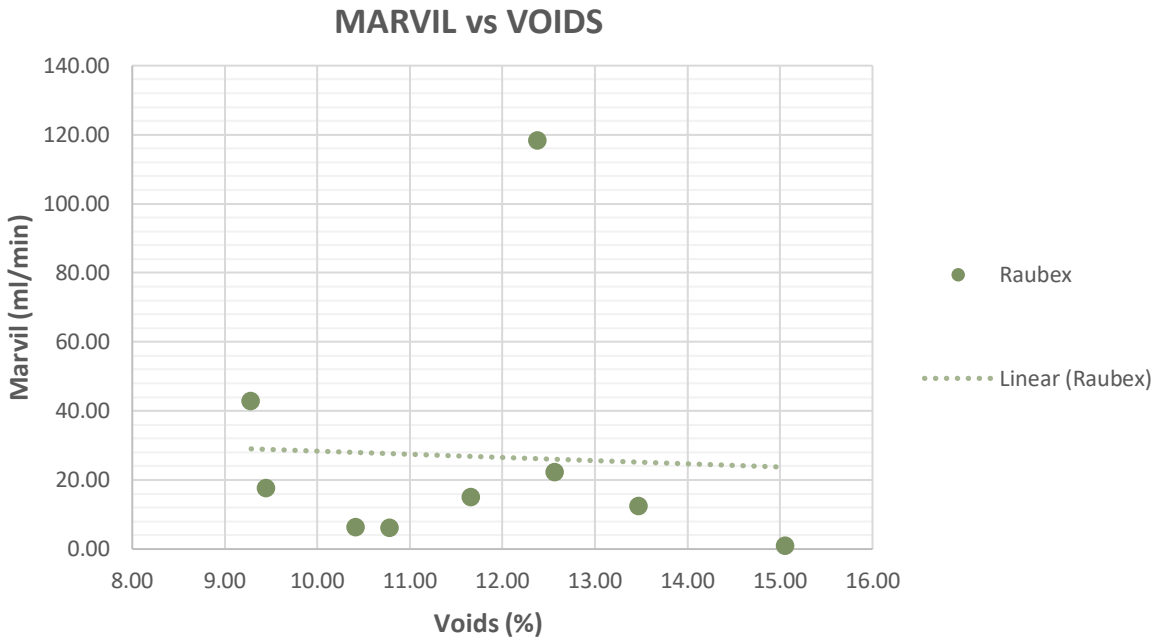

Figure 5.6: Raubex cores – comparative analysis of permeability versus voids

also increase. For these specific cores no clear increase can be noted in the Marvil permeability with regards to an increase in the air void percentage. This statement is proven in Figure 5.6 by the analysis done for the Marvil versus the air void percentages of the Raubex asphalt cores.

From Figure 5.6 it is proven that no relationship exists between the Marvil permeability and the air void percentages for these asphalt cores. Thus, in conclusion, the asphalt cores from Raubex present no clear correlation between the increase of air void content and increased Marvil permeability.

5.3.2 N3TC

The permeability results for the Marvil and the air void percentages of the N3TC top layer asphalt cores are presented in Table 5.6.

Table 5.6: N3TC - Marvil vs Voids

		Marvil (*mℓ/min*)	Voids (%)
MIX Cd	Core 3	0,00	7,19
	Core 6	39,13	8,86
	Core 5	16,67	10,20
	Core 1	102,66	10,40
	Core 2	190,14	10,41
	Core 4	48,47	10,43
MIX Cp	Core 7	0,00	2,40
	Core 12	0,00	3,73
	Core 9	0,00	3,81
	Core 8	0,00	3,84
	Core 10	0,00	4,83
	Core 11	0,00	5,11

From Table 5.6 (and Appendix K.2) follows that the top layer asphalt cores from the N3TC exhibit a high Marvil permeability for Mix Cd and a very low Marvil permeability (impermeable) for Mix Cp. The air void percentages for Mix Cd vary from 7.19 % up to 10.43 % and from 2.40 % up to 5.11 % for Mix Cp. The air void percentages for Mix Cd is relatively high, thus a higher Marvil permeability is expected. With the air void percentage for Mix Cp being relatively low, a low Marvil permeability is expected; which is proven with regards to the Marvil permeability being zero for all these cores.

However, no clear linear relationship can be observed in the asphalt cores for Mix Cd. It was previously assumed that as the air void percentage increases, the Marvil permeability would also increase. For these specific cores no clear increase can be noticed in the Marvil permeability with regards to an increase in the air voids. Thus, in conclusion, the asphalt cores from Mix Cd present no clear linear relationship between the increase of air void content and Marvil permeability.

It can be seen that the cores of Mix Cp are impermeable with regards to the Marvil. The assumption can be made that the lower the air void content, the lower the Marvil permeability will be. Thus, in conclusion, the asphalt cores from Mix Cp indicate that a very low air void percentage (less than 5.11 %) leads to essential impermeability with regards to the Marvil.

To support the conclusions made for these two mixtures, an analysis is done and interpreted with regards to all the asphalt cores from the N3TC top layer asphalt cores. This analysis can be seen in Figure 5.7.

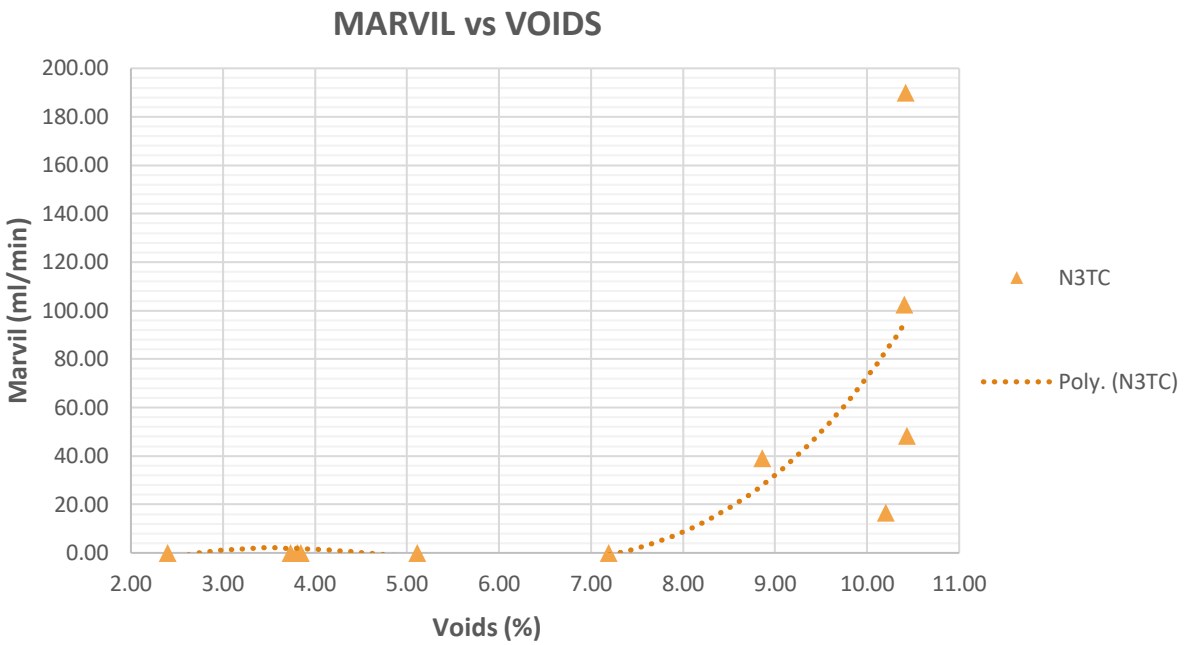

Figure 5.7: N3TC cores – comparative analysis of permeability versus voids

Figure 5.7 supports the conclusion that no clear linear relationship exists between the Marvil permeability and air void percentages for these cores. However, a non-linear relationship can be noted, which is identified as a 3rd order polynomial relationship for the N3TC top layer asphalt cores.

5.3.3 N3TC (BOTTOM LAYER ASPHALT CORES)

The permeability results for the Marvil and the air void percentages of the N3TC bottom layer asphalt cores are presented in Table 5.7.

Table 5.7: N3TC bottom layer asphalt cores - Marvil vs Voids

	Marvil (*mℓ/min*)	Voids (%)
Core 11	0,14	0,74
Core 7	0,13	1,22
Core 9	0,08	1,45
Core 1	0,21	1,61
Core 4	0,14	1,80
Core 10	0,08	1,91
Core 12	0,13	2,07
Core 8	0,08	2,58
Core 5	0,17	2,99
Core 6	0,17	3,80
Core 3	0,17	5,17
Core 2	2,15	5,82

Table 5.7 (and Appendix K.3) indicates that the bottom layer asphalt cores from the N3TC exhibit a very low Marvil permeability. These cores display such a low permeability that it can be classified as impermeable. The air void percentages for these cores vary from 0.74 % up to 5.82 %. The air void percentages for these cores are very low, thus a low Marvil permeability is expected; which is proven in Table 5.7 with regards to the Marvil permeability being close to zero for all the cores.

Thus, in conclusion, the bottom layer asphalt cores from the N3TC indicate that a very low air void percentage (less than 5.82 %) leads to very low permeability with regards to the Marvil.

To establish if there exists a correlation between the Marvil permeability and the air void content, further analysis is performed. This analysis can be observed in Figure 5.8.

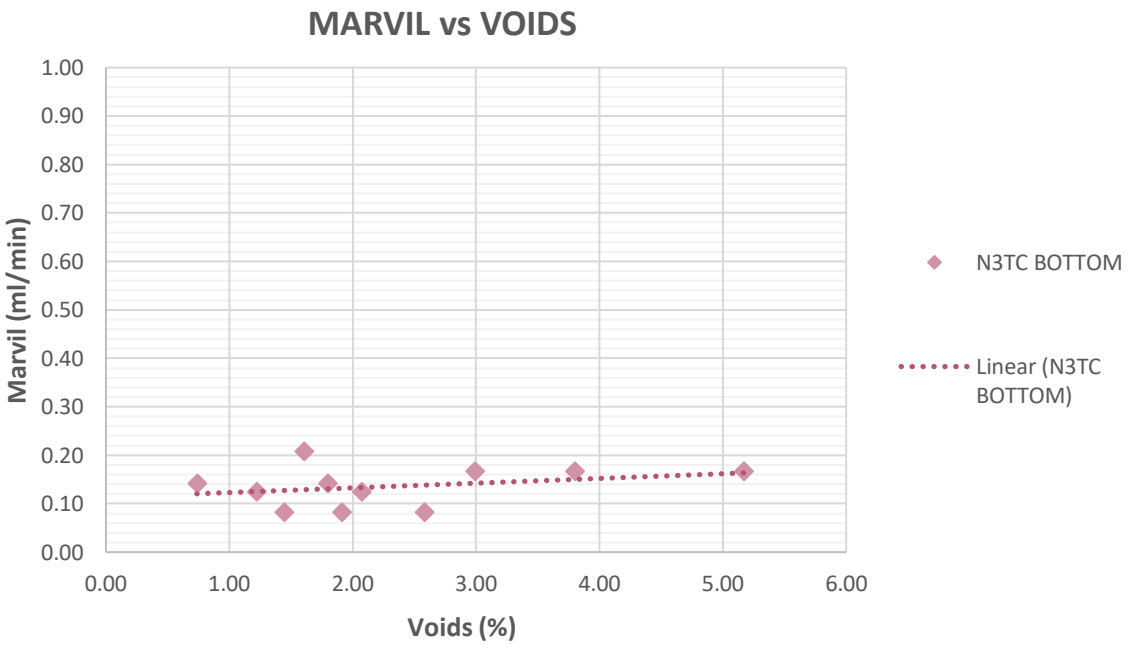

Figure 5.8: N3TC (bottom) cores – comparative analysis of permeability versus voids

Figure 5.8 indicates that no linear relationship occurs between the Marvil permeability and air void percentages for the N3TC bottom layer asphalt cores. Thus, the statement stating that the Marvil permeability will increase as the air void percentage increases, cannot be supported or proven in this regard.

5.3.4 N7

The permeability results for the Marvil and the air void percentages of the N7 highway asphalt cores are presented in Table 5.8.

Table 5.8: N7 - Marvil vs Voids

	Marvil (*mℓ/min*)	Voids (%)
Core 2	0,13	1,69
Core 3	0,06	2,41
Core 1	0,17	3,60
Core 5	0,20	3,71
Core 4	0,09	4,65

The asphalt cores from the N7 highway display a very low Marvil permeability in Table 5.8 (and Appendix K.4). The air void percentages for these cores vary from 1.69 % up to 4.65 %. The air void content for these cores are very low, thus a low Marvil permeability is expected; which is confirmed in Table 5.8 with regards to the Marvil permeability being close to zero for all the asphalt cores.

Thus, in conclusion, the asphalt cores from the N7 highway specify that a very low air void percentage (less than 4.65 %) leads to a very low (impermeable) Marvil permeability.

To determine if there exists a correlation between the Marvil permeability and the air void content for these cores, further analysis is performed. This analysis can be seen in Figure 5.9.

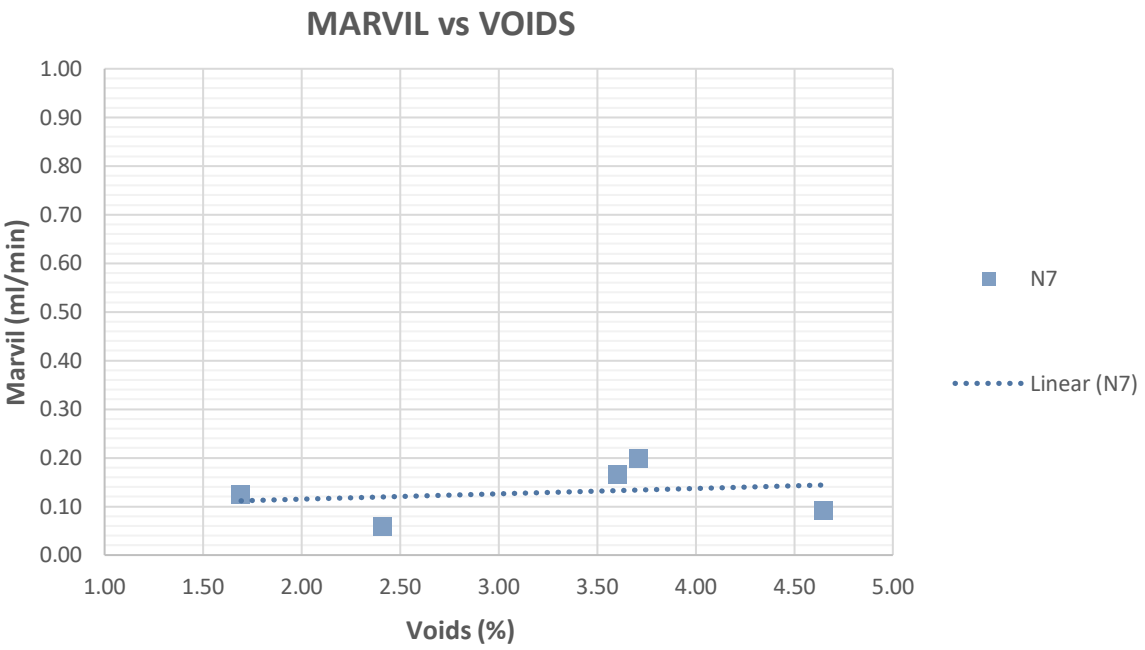

Figure 5.9: N7 cores – comparative analysis of permeability versus voids

From Figure 5.9 it is evident that no linear relationship exists between the Marvil permeability and air void percentages for the N7 highway asphalt cores. Thus, in conclusion, the statement suggesting that the Marvil permeability will increase as the air void percentage increases is proven untrue.

5.4 HIGH PRESSURE PERMEABILITY (HPP) VERSUS VOIDS

In order to meet the secondary objective of determining whether there exists a correlation between the HPP results and the air void percentage of an asphalt core, it is necessary to acquire adequate data to make a viable conclusion. Thus, the asphalt cores from Raubex, N3TC (top and bottom layer cores) and the N7 highway are tested and interpreted to help draw a conclusion with regards to this statement.

The HPP results, together with the respective air void percentages for each core can be seen in Table 5.9 (Raubex), Table 5.10 (N3TC top asphalt cores), Table 5.11 (N3TC bottom asphalt cores) and Table 5.12 (N7). These tables are arranged in the manner of increasing air void percentage, thus providing the opportunity to draw conclusions by referring to the increase of air void percentage in an asphalt mixture. It is assumed that as the air void percentage increases the HPP will also increase.

The values highlighted in red was previously identified as outliers for the various tests and will be ignored when drawing conclusions. The results displayed in these tables are graphically represented in Appendix L.1, Appendix L.2, Appendix L.3 and Appendix L.4 respectively. The graphs displayed in the appendices give a visual representation of the results and provide a more reliable manner to make a conclusion with regards to this objective.

To support the conclusions made in Chapter 5.4, an ANOVA statistical analysis is performed on the relevant variables. The results from this analysis can be seen in Appendix O.

5.4.1 RAUBEX

The permeability results for the HPP (at 100, 150 and 200 *kPa*) and the air void percentages of the Raubex asphalt cores are presented in Table 5.9.

Table 5.9: Raubex - HPP vs Voids

		PERMEABILITY (*mℓ/min*)			
		100 kPa	**150 kPa**	**200 kPa**	**Voids (%)**
SECTION 1	Core L	0,40	1,50	2,30	10,42
	Core A	4,40	8,80	144,14	12,57
	Core F	9,30	13,70	16,50	15,06
	Core B	20,00	17,20	16,20	23,62
SECTION 2	Core H	1980,20	2023,61	1980,20	7,33
	Core J	0,30	0,40	0,25	10,79
	Core I	5,10	8,00	16,40	11,66
	Core M	0,30	1,10	3,40	13,48
SECTION 3	Core O	12,60	16,00	19,70	9,29
	Core Q	15,40	19,20	40,40	9,45
	Core P	1035,38	1282,05	1470,59	12,07
	Core N	14,40	21,40	37,97	12,38

From Table 5.9 (and Appendix L.1) follows that the asphalt cores from Raubex display a widespread permeability for the HPP test. The air void percentages also vary from 7.33 % up to a maximum of 15.06 % for the three sections. These air void percentages are relatively high, thus a high HPP result is expected.

It can be assumed that as the air void percentage increases, the HPP will also increase. It can be seen in Table 5.9 that as the air void percentages for Section 1 and Section 3 increase, the HPP also

increases at the pressures of 100 and 150 *kPa*. However, at 200 *kPa* some irregularities occur due to the cores' sensitivity to this high pressure.

For Section 2, however, the same observation cannot be made. No clear relationship can be seen in this road section with regards to the HPP and air void content. It was previously assumed that as the air void percentage increases, the HPP would also increase. For these specific cores in Section 2, no clear increase can be noted in the HPP with regards to an increase in the air void content. Thus, in conclusion, the asphalt cores from Section 2 present no clear correlation between the increase of air void content and increased permeability of the HPP. This statement is proven by the analysis done in Figure 5.10.

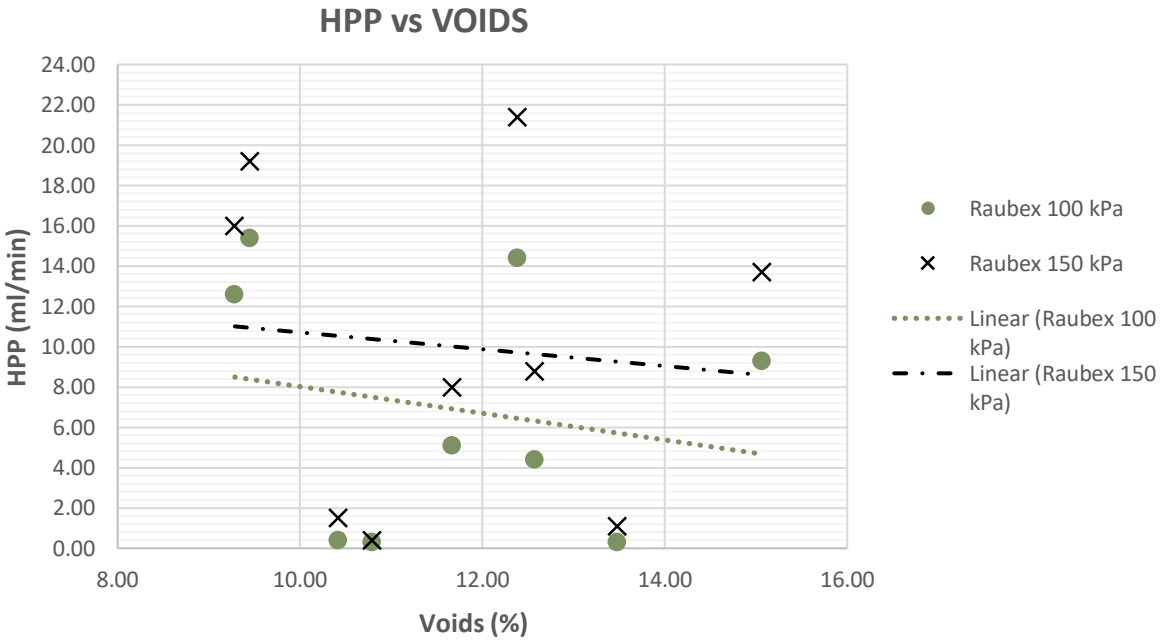

Figure 5.10: Raubex cores – comparative analysis of high pressure permeability versus voids

The analysis in Figure 5.10 includes the data from all three sections to draw a clear conclusion about the overall state of the Raubex asphalt cores. According to Figure 5.10 the data is relatively widespread, and no relationship exists between the air void content and the HPP at 100 and 150 *kPa*. Thus, the assumption that the HPP will increase as the air void percentages increase is proven untrue.

5.4.2 N3TC

The permeability results for the HPP (at 100, 150 and 200 *kPa*) and the air void percentages of the N3TC top layer asphalt cores are presented in Table 5.10.

Table 5.10: N3TC - HPP vs Voids

		PERMEABILITY (*mℓ/min*)			
		100 kPa	**150 kPa**	**200 kPa**	**Voids (%)**
MIX Cd	Core 3	0,00	0,00	4,50	7,19
	Core 6	26,31	50,24	227,49	8,86
	Core 5	40,29	100,85	212,58	10,20
	Core 1	90,36	137,99	178,47	10,40
	Core 2	158,88	184,28	299,63	10,41
	Core 4	103,61	136,71	137,69	10,43
MIX Cp	Core 7	0,00	7,50	75,00	2,40
	Core 12	0,00	0,00	7,25	3,73
	Core 9	2,25	5,75	9,00	3,81
	Core 8	1,00	2,00	3,50	3,84
	Core 10	109,87	200,20	265,37	4,83
	Core 11	1,25	7,50	56,80	5,11

From Table 5.10 (and Appendix L.2) follows that the top layer asphalt cores from the N3TC exhibit a high HPP for Mix Cd and a lower overall HPP for Mix Cp. The air void percentage for Mix Cd varies from 7.19 % up to 10.43 % and from 2.40 % up to 5.11 % for Mix Cp. The air void percentages for Mix Cd are relatively high, thus a higher HPP is expected. With the air void percentage for Mix Cp being relatively low, a low HPP can be expected.

It is assumed that as the air void percentage increases, the HPP will also increase. For Mix Cd this statement is proven true for the HPP at 100 and 150 *kPa* (except for core 4). It can be seen in Table 5.10 that as the air void percentage for Mix Cd increases, the HPP also increases at the pressures of 100 and 150 *kPa*. However, at 200 *kPa* some irregularities occur due to the cores' sensitivity to this high pressure, which leads to a high variability in the results. Thus, in conclusion, the asphalt cores from Mix Cd present a possible correlation between the increase of air void content and increased HPP at pressures of 100 and 150 *kPa*, but variability exists at 200 *kPa*.

For Mix Cp, however, the same reflection cannot be made. No clear relationship can be seen in this road section with regards to the HPP and air void content. It was previously assumed that as the air

void percentage increases, the HPP would also increase. For these specific cores in Mix Cp, no clear increase can be noted in the HPP with regards to an increase in the air void content. Thus, in conclusion, the asphalt cores from Mix Cp present no noticeable correlation between the increase of air void content and increased HPP for cores with an air void content less than 5.11 %.

To support the conclusions made with regards to Mix Cd and Mix Cp, an additional analytical analysis is performed. This analysis can be observed in Figure 5.11.

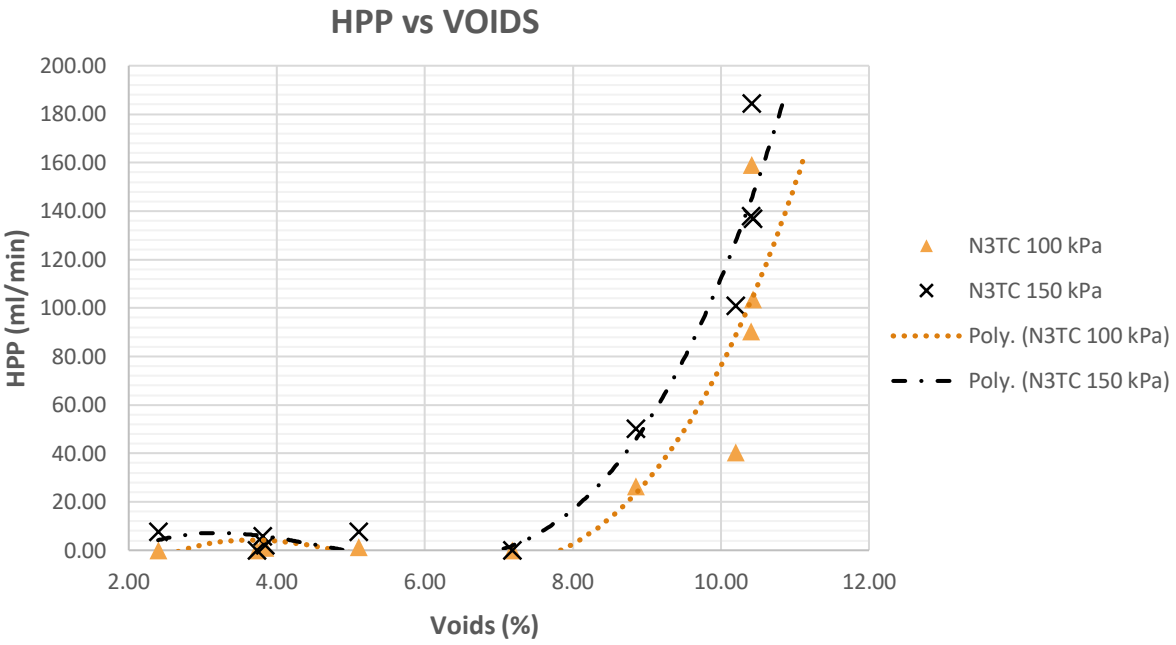

Figure 5.11: N3TC cores – comparative analysis of high pressure permeability versus voids

The analysis in Figure 5.11 includes the data from both Mix Cd and Mix Cp. The analysis is not done at a pressure of 200 kPa, as this high pressure leads to inconsistencies and variability in the data. From Figure 5.11 it can be concluded that no clear linear relationship exists between the HPP and air void percentages for these cores. However, a non-linear relationship can be noted, which is identified as a 3rd order polynomial relationship for the N3TC top layer asphalt cores. Thus, the assumption that the HPP will increase as the air void percentages increase is proven to be accurate.

5.4.3 N3TC (BOTTOM LAYER ASPHALT CORES)

The permeability results for the HPP (at 100, 150 and 200 *kPa*) and the air void percentages of the N3TC bottom layer asphalt cores are presented in Table 5.11.

Table 5.11: N3TC bottom layer asphalt cores - HPP vs Voids

	PERMEABILITY (*mℓ/min*)			
	100 kPa	**150 kPa**	**200 kPa**	**Voids (%)**
Core 11	0,00	0,00	0,50	0,74
Core 7	0,00	0,00	0,00	1,22
Core 9	0,00	0,00	0,00	1,45
Core 1	2,00	2,75	10,50	1,61
Core 4	0,00	0,00	0,00	1,80
Core 10	0,00	0,25	0,50	1,91
Core 12	0,00	0,00	0,50	2,07
Core 8	0,00	0,25	1,00	2,58
Core 5	0,00	0,00	0,00	2,99
Core 6	5,00	7,50	9,50	3,80
Core 3	5,25	5,25	10,50	5,17
Core 2	6,00	27,50	55,90	5,82

From Table 5.11 (and Appendix L.3) follows that the bottom layer asphalt cores from the N3TC exhibit a low overall HPP. The air void percentages for these asphalt cores vary from 0.74 % up to 5.82 %. The air void percentage of these cores are relatively low, thus a low HPP can be expected; which is proven in Table 5.11 with regards to the HPP being close to zero for most of the cores.

It can be assumed that as the air void percentage increase, the HPP permeability will also increase. For these asphalt cores this statement is proven true, as a possible relationship can be noticed with regards to the HPP and air void content. This conclusion is confirmed in Figure 5.12.

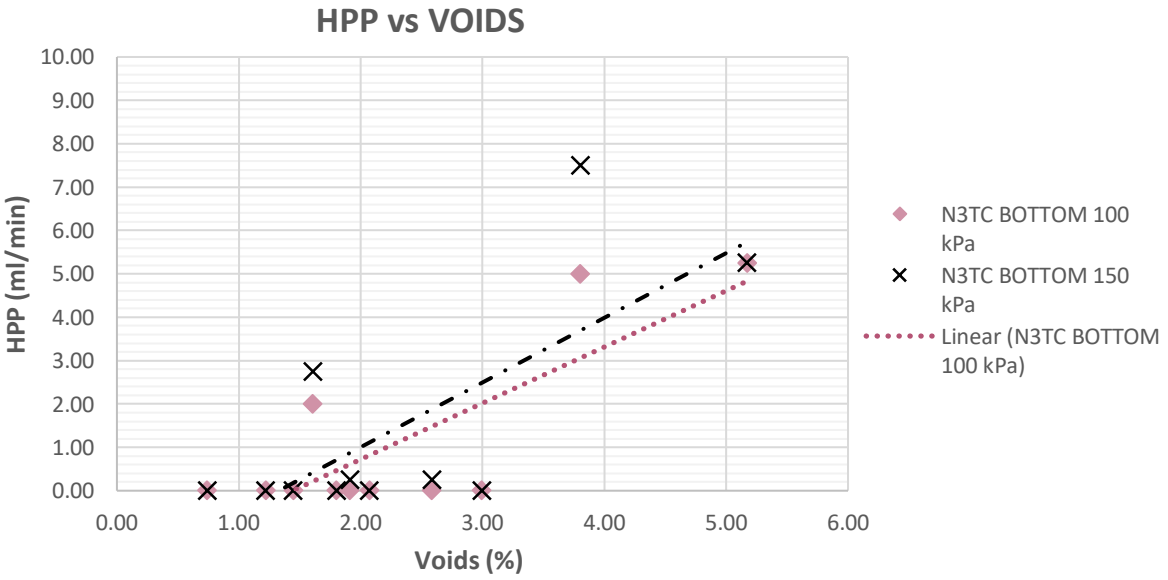

Figure 5.12: N3TC (bottom) cores – comparative analysis of high pressure permeability versus voids

For these specific cores, an increase can be noted in the HPP with regards to an increase in the air void content at the various pressures in Figure 5.12. Thus, in conclusion, the bottom layer asphalt cores from the N3TC present a clear linear relationship between the HPP (at 100 and 150 *kPa*) and air void content. Thus, the assumption that the permeability will increase as the air void content increases is verified as true for these cores.

5.4.4 N7

The permeability results for the HPP (at 100, 150 and 200 *kPa*) and the air void percentages of the N7 highway asphalt cores are presented in Table 5.12.

Table 5.12: N7 - HPP vs Voids

	PERMEABILITY (*mℓ/min*)			
	100 kPa	**150 kPa**	**200 kPa**	**Voids (%)**
Core 2	0,04	0,00	0,00	1,69
Core 3	0,05	0,04	0,03	2,41
Core 1	0,04	0,04	0,03	3,60
Core 5	0,03	0,02	0,01	3,71
Core 4	0,02	0,01	0,01	4,65

Table 5.12 (and Appendix L.4) indicates that the asphalt cores from the N7 highway display a low overall HPP. The air void percentages for these asphalt cores vary from 1.69 % up to 4.65 %. The air void percentages for these asphalt cores are relatively low, thus a low HPP can be anticipated; which is proven true in Table 5.12 with regards to the HPP being close to zero for all the cores.

It can be assumed that as the air void percentages increase, the HPP will also increase. For these asphalt cores this statement cannot be proven accurate, as no clear correlation can be noted with regards to the HPP and air void content. For these specific cores, no clear increase can be seen in the HPP with regards to an increase in the air voids at any of the various pressures. This statement is proven by an analysis performed on the N7 highway asphalt cores, and can be seen in Figure 5.13.

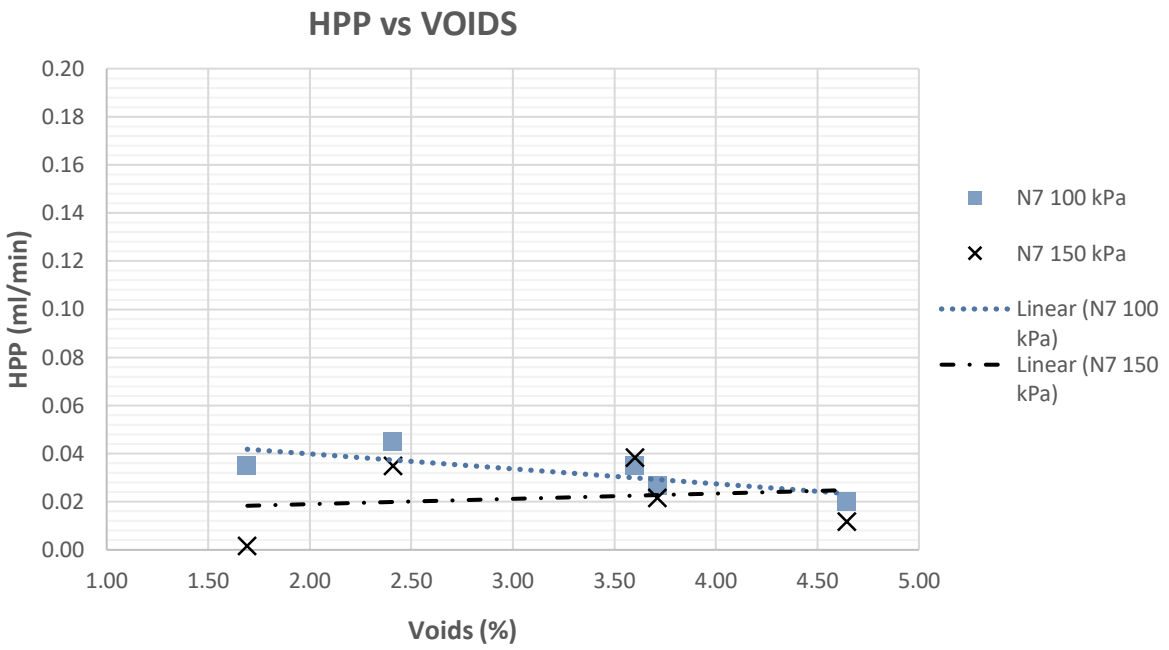

Figure 5.13: N7 cores – comparative analysis of high pressure permeability versus voids

Figure 5.13 indicates that no relationship of any kind is present between the HPP (at 100 and 150 kPa) and the air void content for the N7 asphalt cores. For these specific cores, no clear increase can be noted in the HPP with regards to an increase in the air voids at any of the pressures. Thus, the assumption that the permeability will increase as the air void content increases is verified as false for these cores.

5.5 SUMMARY

With regards to the Marvil versus the HPP apparatus, a clear correlation exists between the permeability results obtained from these tests for the Raubex and N3TC top asphalt layer cores. However, inconsistencies exist when testing at a pressure of 200 *kPa* and leads to a high variability in the results. No clear correlation is noted for the N3TC bottom asphalt layer or the N7 highway cores.

Regarding the Marvil versus the air void percentage, it can be concluded that for an asphalt core with an air void percentage of 5.82 % or less, a very low (impermeable) Marvil permeability can be expected. However, for asphalt cores with an air void percentage of 7.19 % or higher, inconsistent Marvil permeabilities are obtained. Thus, no clear linear correlation exists between the Marvil permeability and air void percentage for cores with these high air void percentages.

However, for the N3TC top layer asphalt cores a 3rd order polynomial relationship is identified between the Marvil permeability and air void content.

With regards to the HPP versus the air void content, it can be concluded that for asphalt cores with a low air void percentage of 5.82 % or less, no clear correlation exists between the HPP and air void content for these low air void percentages. However, for asphalt cores with and air void percentage of 7.19 % or higher, a relationship can be noted between the air void content and HPP of an asphalt core at 100 and 150 *kPa*. This implies that as the air void content increases, the HPP also increases at pressures of 100 and 150 *kPa*. But, at the pressure of 200 *kPa* a high variably in the HPP results can be noticed, and lead to inconsistencies.

It is also proven that no clear relationship exists between the HPP and air void content for the Raubex and N7 highway asphalt cores. However, a linear relationship is established for the N3TC bottom layer asphalt cores and a 3rd order polynomial relationship is identified between the HPP permeability and air void percentages for the N3TC top layer asphalt cores.

CHAPTER 6 - DEVELOPMENT OF ASPHALT PERMEABILITY CLASSIFICATION RANGES

6.1 INTRODUCTION

The following chapter presents the development of the asphalt permeability classification ranges for the Marvil and HPP. No previous permeability classification range was developed for the Marvil within laboratory conditions, only for in-field testing, which is set out in SANS 3001-BT12. Thus, a permeability classification range for the Marvil is developed for laboratory testing conditions. This classification range matrix will be discussed in more detail below in Chapter 6.2.

Again, no previous permeability classification range for asphalt had been developed for the HPP either. Thus, it was necessary to develop a classification range for the HPP to give an indication of whether the specific asphalt core being tested has a high or low permeability. This grading matrix will also be discussed in more detail below in Chapter 6.3.

6.2 MARVIL PERMEABILITY CLASSIFICATION RANGE

Since there is only an asphalt permeability classification range developed for in-field Marvil testing as set out by SANS 3001-BT12 (discussed in Chapter 2.17.4.2), it was necessary to develop a permeability classification range for the laboratory testing of asphalt. Laboratory testing requires different testing conditions than in-field testing, as well as a longer testing period (two hours, as opposed to three minutes). The abovementioned factors were taken into account when the permeability classification range for laboratory testing, which can be seen in Table 6.1, was developed.

Table 6.1: Marvil permeability classification range

Good	< 16.50 mℓ/min
Moderate	Between 16.50 and 50.00 mℓ/min
Warning (Poor)	> 50.00 mℓ/min

The classification range developed in Table 6.1 is developed by means of using the asphalt permeability classification range set out by SANS 3001-BT12 (SANS 3001-BT12, 2012). This range set out in SANS 3001-BT12 is used to determine the in-field permeability of an asphalt surface measured in litres per hour (*ℓ/h*) and are then converted to millilitres per minute (*mℓ/min)* for the laboratory use of the Marvil permeability test.

From Table 6.1 follows that for an asphalt core to be classified as "good" with a low permeability, the Marvil permeability has to be below 16.50 *mℓ/min*. For an asphalt core to be classified as "moderate" with a warning permeability, the Marvil permeability should be between 16.50 and 50.00 *mℓ/min*. An asphalt core is classified as "warning" with a high permeability when its Marvil permeability result exceeds 50.00 *mℓ/min*.

6.3 HPP PERMEABILITY CLASSIFICATION RANGE

As there is no asphalt permeability classification range previously developed for the HPP, it was necessary to develop an asphalt permeability classification range for testing at high pressures.

Since no correlation was found to the permeability of asphalt at a testing pressure of 200 *kPa* in either Chapter 4 or Chapter 5, no permeability classification range was developed for this pressure. It is therefore recommended that asphalt permeability testing should only be done at 100 and 150 *kPa*.

The classification range developed in Table 6.2 is developed by means of using the seal permeability classification set out by Ockert Grobbelaar in 2016 (Grobbelaar, 2016). Grobbelaar stated that a seal can be classified as a "warning (poor)" permeability if the water level inside the HPP drops below the minimum mark of the water level indicator during the testing period. This means that if 650 *mℓ* permeates through the seal in 20 minutes at a pressure of 100 *kPa*, the seal has a "warning (poor)" permeability. The same principle is used for the permeability of an asphalt core at 100 *kPa*.

By using all the data from the HPP tests at 100 and 150 *kPa*, it was found that minimum permeability increase of 16 % can be expected from the HPP pressure increase at 100 *kPa* up to 150 *kPa*. Thus, the classification range from 100 *kPa* is increased with 16 % for testing at 150 *kPa*. These factors were all taken into account when the permeability classification range for the HPP, which can be seen in Table 6.2, was developed.

Table 6.2: HPP permeability classification range

	100 kPa	150 kPa
Good	< 8.00 mℓ/min	< 9.50 mℓ/min
Moderate	Between 8.00 and 32.50 mℓ/min	Between 9.50 and 38.00 mℓ/min
Warning (Poor)	> 32.50 mℓ/min	> 38.00 mℓ/min

Table 6.2 indicates that for testing permeability at 100 *kPa*, an asphalt core's permeability is classified as "good" (low permeability) if it is below 8.00 *mℓ/min*. An asphalt core is classified as "moderate" when the permeability is between 8.00 and 32.50 *mℓ/min*. For an asphalt core to be labelled as "warning", the permeability should exceed 32.50 *mℓ/min* at 100 *kPa*.

Table 6.2 also shows that when testing with the HPP at a pressure of 150 *kPa*, an asphalt core's permeability can be classified as "good" (low permeability) if it is below 9.50 *mℓ/min*. The permeability of an asphalt core is labelled as "moderate" when the permeability is between 9.50 and 38.00 *mℓ/min*. If the permeability at 150 *kPa* exceeds 38.00 *mℓ/min*, the asphalt core is classified as "warning".

6.4 SUMMARY

An asphalt permeability classification range is developed for Marvil laboratory testing. This classification range can be used to identify whether the permeability of asphalt cores is low, moderate or high. An asphalt permeability classification range is also developed for HPP testing. This permeability classification range is developed for testing at 100 and 150 *kPa*. It is advised that high pressure permeability not be conducted at 200 *kPa*, as this pressure causes inconsistencies in the results. Thus, the permeability classification range provide a manner of classifying an asphalt core's permeability as good, moderate or warning for testing at 100 and 150 *kPa*.

CHAPTER 7 - CONCLUSIONS & RECOMMENDATIONS

7.1 INTRODUCTION

This chapter provides a summary of the primary and secondary objectives. In addition, the findings, conclusions and recommendations made from the literature review and laboratory testing are also presented.

7.2 CONCLUSIONS

The following conclusions are drawn based on the objectives stated in Chapter 1, linked to the findings of the research.

7.2.1 PRIMARY OBJECTIVE

The primary objective of this research study is to analyse the permeability of asphalt cores by means of the laboratory Marvil and High Pressure Permeability (HPP) tests, and through this to determine the influence of pressure on the permeability of asphalt. By evaluating the permeability of asphalt at low and high pressures, a better understanding and more realistic conclusion could be made with regards to moisture damage in asphalt cores.

This objective was achieved by conducting several permeability tests in the laboratory, such as the Marvil and HPP on numerous asphalt cores provided by Raubex, N3TC, N7 highway and Much Asphalt. All of these tests were successfully executed. From the HPP tests that were performed on the asphalt cores, it was concluded that the permeability increased as the pressure increased. Thus, a higher testing pressure will lead to a higher permeability, confirming a trend that was intuitively anticipated.

MIST conditioning was also performed on selected asphalt cores to evaluate the influence it has on the HPP. To evaluate this influence more closely, CT-scans were performed on these cores. The CT-

scans enabled the volumetric structure of the voids before and after MIST tests to be examined. From the CT-scans it was evident that MIST conditioning increased the inter-connected voids.

From the ITS tests conducted on the asphalt cores it was also evident that most of the asphalt cores displayed a decrease in tensile strength after MIST conditioning.

7.2.2 SECONDARY TASK & OBJECTIVE (i)

This secondary task and objective was to determine the volumetric properties of various asphalt cores from different sources. This objective was achieved by means of determining the volumetric properties of the asphalt cores with BRD and RICE testing. Once these properties were acquired, it was used to determine the air void content for every asphalt core.

The BRD test results indicated that when using cling wrap instead of a vacuum-sealed plastic bag to cover the asphalt cores with, a much higher air void content was determined. Thus, it can be concluded that a vacuum-sealed plastic bag should be used for BRD testing since it provides more accurate results, given that the higher air void content was commensurate with higher permeability.

7.2.3 SECONDARY TASK & OBJECTIVE (ii)

This secondary task and objective was to determine if a correlation exists between the permeability of the Marvil and HPP (at its various pressures of 100, 150 and 200 *kPa*). This objective was achieved by comparing results obtained from the Marvil and HPP and using these results to perform additional analytical analyses and determine if a correlation exists.

For this objective it was concluded that a clear correlation exists between the permeability results of the Marvil versus the HPP for the Raubex and N3TC top layer asphalt cores. However, a correlation only exists for the HPP at 100 and 150 *kPa* testing pressure, but at a pressure of 200 *kPa* inconsistencies exist leading to high variability in the results. It is postulated that testing pressures of 200 *kPa* and above lead to a great risk of leakage and other secondary effects during testing.

From the analysis it was also established that no relationship occurs between the Marvil and HPP for the N3TC bottom layer asphalt cores or the N7 highway cores.

7.2.4 SECONDARY TASK & OBJECTIVE (iii)

This secondary task and objective was to determine if a correlation exists between the Marvil permeability results and the air void percentage of an asphalt core. This objective was achieved by plotting the Marvil permeability results against the increasing air void content for the asphalt cores. These plots were used to compare the results and draw the relevant conclusions. An additional analytical analysis was performed to determine whether a relationship between the Marvil and air void content exists.

For this objective it was concluded that for asphalt cores with an air void content of 5.82 % or less, low Marvil permeability results are obtained, as can be expected. It was also found that for asphalt cores with an air void content of 7.19 % or higher, inconsistent and unreliable Marvil permeability results are obtained.

From the analysis it was found that no clear linear correlation exists between the Marvil permeability and air void percentage for the asphalt cores tested. Except, for the N3TC top layer asphalt cores a 3rd order polynomial relationship is identified between the Marvil permeability and air void percentages.

7.2.5 SECONDARY TASK & OBJECTIVE (iv)

This secondary task and objective was to determine if a correlation exists between the HPP results (at 100, 150 and 200 *kPa*) and the air void percentage of an asphalt core. This objective was achieved by plotting the HPP results for the various pressures as the air void content of the asphalt cores increased. An additional analytical analysis was performed to determine whether a relationship between the HPP and air void content exists.

For this objective it was concluded that for asphalt cores with an air void content of 7.19 % or more, a clear correlation exists between the air void content and the HPP results of an asphalt core at 100 and 150 *kPa*. As the air void content of an asphalt core increases, so does the HPP at pressures of 100 and 150 *kPa*. However, no correlation exists at a pressure of 200 *kPa*, and it is thus advised that no HPP testing of an asphalt core be done at this pressure.

For this objective it was also proven that no correlation exists with regards to the HPP and an asphalt core with an air void content of 5.82 % or less. For asphalt cores with a low air void content the HPP results were inconsistent and no clear trend could be found.

It is also proven that no relationship exists between the HPP and air void content for the Raubex and N7 highway asphalt cores. However, a linear relationship is recognized for the N3TC bottom layer asphalt cores and a 3rd order polynomial relationship is identified between the HPP permeability and air void percentages for the N3TC top layer asphalt cores.

7.2.6 SECONDARY TASK & OBJECTIVE (v)

This secondary task and objective was to develop asphalt permeability classification ranges for the Marvil and HPP under laboratory conditions. This objective was achieved by using the previous classification for in-field Marvil permeability testing set out by SANS 3001-BT12. This classification was adjusted for laboratory Marvil testing and used to determine a classification range for the HPP at 100 and 150 *kPa*.

For this objective it was concluded that for the Marvil permeability test an asphalt core can be classified as “good” with a low permeability if the permeability is below 16.50 *mℓ/min*. An asphalt core can be classified as “moderate” if the permeability is between 16.50 and 50.00 *mℓ/min*. Lastly, an asphalt core can be classified as “warning (poor)” with a high permeability if the Marvil permeability result exceeds 50.00 *mℓ/min*.

For this objective it was also concluded that for the HPP test at 100 *kPa* an asphalt core can be classified as “good” with a low permeability if it is below 8.00 *mℓ/min*. An asphalt core can be classified as “moderate” if the permeability is between 8.00 and 32.50 *mℓ/min*. Lastly, an asphalt core can be labelled as “warning (poor)” if the permeability is more than 32.50 *mℓ/min* at 100 *kPa.*

For the HPP test at a pressure of 150 *kPa,* an asphalt core can be classified as “good” with a low permeability if it is below 9.50 *mℓ/min*. An asphalt core can be classified as “moderate” if the permeability is between 9.50 and 38.00 *mℓ/min*. Lastly, an asphalt core can be labelled as “warning”, indicating a high permeability, if the permeability exceeds 38.00 *mℓ/min* at a pressure of 150 *kPa.*

7.3 RECOMMENDATIONS

This research study was successfully executed. However, ample room for improvement remains for further testing with regards to asphalt permeability and moisture damage. Thus, for future research the following recommendations are provided:

i. For BRD testing of asphalt cores, vacuum-sealed plastics bags should be used instead of cling wrap.

ii. To build an additional mould for the Marvil permeameter which can accommodate 100 *mm* diameter asphalt cores.

iii. The level indicator on the Marvil apparatus should be reduced to 10 *mℓ* increments instead of 50 *mℓ*. This will provide more accurate and precise measurements.

iv. The laboratory Marvil permeability test should preferably be used for permeability testing of asphalt cores with an air void percentage of 6 % or less. The boundary for the maximum air void content needs to be verified with additional research.

v. The level indicator of the HPP test apparatus should be reduced to 2.50 *mℓ* intervals instead of 10 *mℓ* intervals. This will ensure more sensitive and detailed results.

vi. Design and develop a longer-lasting inner mould for the HPP, as the silicone rubber mould tends to break and tear after only a few tests.

vii. It is recommended that HPP testing should only be done at pressures of 100 and 150 *kPa* to obtain reliable and accurate results.

viii. Do not test asphalt core permeability with the HPP at a pressure of 200 *kPa* or higher, as this leads to inaccurate results.

ix. The HPP test should preferably be used on asphalt cores with an air void content greater than 7 % at pressure of 100 and 150 *kPa*. The boundary for the minimum air void content needs to be verified with additional research.

x. Use a larger pressure cell for the MIST conditioning which can fit more than one asphalt core on the surface thereof.

xi. To obtain more comparable results, it is recommended that a standard test procedure should specify that asphalt cores being tested should have the same thickness.

xii. Recommended permeability limits are provided in Table 7.1.

Table 7.1: Permeability limits

TEST	GOOD	MODERATE	WARNING (POOR)
Marvil (*mℓ/min*)	< 16.50	16.50 – 50.00	> 50.00
HPP 100 kPa (*mℓ/min*)	< 8.00*	8.00* – 32.50	> 32.50
HPP 150 kPa (*mℓ/min*)	< 9.50*	9.50* – 38.00	> 38.00

* Further research needed

CHAPTER 8 - REFERENCES

Allen, D. L., Schultz, D. B. & Fleckenstein, L. J., 2001. *Development and Proposed Implementation of a Field Permeability Test for Asphalt Concrete,* Kentucky: Kentucky Transportation Center.

Annandale, W., 2012. *Permeability of Surfacing Seals,* Stellenbosch: Stellenbosch University.

Asphalt Institute, 2007. *The Asphalt Handbook.* Seventh ed. United States of America: Asphalt Institute.

ASTM International, 2012. *Standard Test Method for Indirect Tensile (IDT) Strength of Bituminous Mixtures,* Pennsylvania: ASTM International.

Awadalla, M., 2015. *Field and Laboratory Investigation of Asphalt Pavement Permeability ,* Ottawa: Carleton University .

Brovold, F. N. & Majidzadeh, K., 1968. *State of the Art: Effect of Water on Bitumen-Aggregate Mixtures,* Washington D.C.: Transportation Research Board.

Brown, E. R., Hainin, M. R., Cooley, A. & Hurley, G., 2004. *Relationship of Air Voids, Lift Thickness, and Permeability in Hot Mix Asphalt Pavements,* Washington D.C.: Transportation Research Board.

California Department of Transport, 2000. *Method of test for moisture vapour susceptibility of bituminous mixtures,* California: California Department of Transportation.

Chadbourn, B. A., Skok, E. L., Crow, B. L. & Spindler, S., 1999. *The Effect of Voids in Mineral Aggregate (VMA) on Hot-Mix Asphalt Pavements,* Minnesota: Minnesota Department of Transportation.

Cheng, D., Little, D., Lytton, L. & Holste, J., 2002. Surface Energy Measurement of Asphalt and its application to predicting Fatigue and Healing in Asphalt Mixtures. *Journal of the Transport Research Board,* Issue 1810, pp. 44-53.

De Sombre, R., Newcomb, D. E., Chadbourn, B. & Voller, V., 1998. Parameters to Define the Laboratory Compaction Temperature Range of Hot-Mix Asphalt. *Association of Asphalt Paving Technologists,* Volume 67, p. 125.

Dictionary.com, 2015. *Dictionary.com.* [Online] Available at: http://dictionary.reference.com/browse/amine [Accessed 21 June 2018].

Douries, W., 2004. *Factors influencing Asphalt Compactibility and its Relation to Asphalt Rutting Performance,* Stellenbosch: Stellenbosch University (Undergraduate Thesis).

Du Plessis, A., Le Roux, S. G. & Guelpa, A., 2016. *The CT Scanner Facility at Stellenbosch University: An open X-ray computed tomography laboratory,* Stellenbosch: s.n.

European Asphalt Pavement Association, 2011. *The Asphalt Paving Industry: A Global Perspective,* Brussels: European Asphalt Pavement Association.

Faghri, M. & Sadd, M. H., 2002. *Performance Improvement of Open-Graded Asphalt Mixes,* Kingston: University of Rhode Island Transportation Center.

Fromm, H., 1974. *The Mechanisms of Asphalt Stripping from Aggregate Surfaces,* Chicago: Association of Asphalt Paving Technologists.

Garber, N. J. & Hoel, L. A., 2009. *Traffic and Highway Engineering.* 4th ed. Toronto: Cengage Learning.

Greyling, A., Van Zyl, G. & Jenkins, J. J., 2015. *Grey water resistant asphalt study Volume 3: Literature review report,* Cape Town: BVi Consulting Engineers.

Grobbelaar, O. R., 2016. *Towards the development of a standard test protocol: Permeability of Chip seals under pressure,* Stellenbosch: Stellenbosch University.

Hughes, R., Lamb, D. & Pordes, O., 1960. Adhesion in bitumen Macadam. *Journal of Applied Chemistry,* Volume 10.

Huner, L. M. & Brown, E. R., 2001. *Effects of re-heating and compaction temperature on hot mix asphalt volumetrics,* Alabama: National Center for Asphalt Technology Auburn University.

Hunter, E. R. & Ksaibati, K., 2002. *Evaluating Moisture Susceptibility of Asphalt Mixes,* Wyoming: Department Civil and Architectural Engineering.

Jenkins, K. J., 2016. *Hitchhikers guide to Pavement Engineering,* Stellenbosch: SANRAL.

Jenkins, K. J. & Twagira, M., 2009. *Moisture damage on bituminous stabilized materials using a MIST device,* Stellenbosch: Stellenbosch University.

Kiggundu, B. & Roberts, F., 1998. *The Success/Failure of Methods used to Predict the Stripping Potential in the Performance of Bituminous Pavement Mixtures,* s.l.: TRB.

Lancellotta, R., 2008. *Geotechnical Engineering.* 2nd ed. s.l.:CRC Press.

Little, D. N. & Jones IV, D. R., 2003. *Chemical and Mechanical Processes of Moisture Damage in Hot-Mix Asphalt Pavements,* San Diego: Transportation Research Board of the National Academies.

Maupin, G. W., 2000. *Investigation of Test Methods, Pavements and Laboratory Design Related to Asphalt Permeability,* Virginia: Virginia Transportation Research Council.

NCHRP, N. C. H. R. B., 2011. *A Manual for Design of Hot Mix Asphalt with Commentary,* Washington D.C.: Transportation Research Board.

Nel, C. L. M., 2017. *Identifying Gradings and Binder Combinations for Improving the Grey Water Resistance of Asphalt,* Stellenbosch: Stellenbosch University (Master's Thesis).

Read, J. & Whiteoak, D., 2003. *The Shell Bitumen Handbook.* Fifth ed. London: Thomas Telford Publishing.

Redivo, S., 2012. *Correlation of Asphalt Surfacing Permeability of Laboratory and Field Prepared Specimens,* Stellenbosch: Stellenbosch University (Master's Thesis).

Robertson, R., 2000. *Chemical properties of Asphalts and their Effects on Pavement Performance,* Washington D.C.: National Research Council.

Rudman, C. E., 2019. *Aspects of Self-Cementation of Recycled Concrete Aggregate when Applied in Roads,* Stellenbosch: Stellenbosch University (PhD Dissertation Draft).

SABITA Manual 35/TRH 8, 2016. *Design and Use of Asphalt in Road Pavements,* Cape Town: SABITA.

SABS 1200, 1996. *Standardized Specification for Civil Engineering Construction: Roads (General),* Pretoria: SABS.

SANS 3001-BT12, 2012. *Determination of the in situ permeability of a bituminous surfacing (Marvil test),* Pretoria: SABS.

SAPEM Chapter 1, 2014. *South African Pavement Engineering Manual: Introduction,* Pretoria: SANRAL.

SAPEM Chapter 2, 2014. *South African Pavement Engineering Manual: Pavement Composition and Behaviour,* Pretoria: SANRAL.

SAPEM Chapter 4, 2014. *South African Pavement Engineering Manual: Standards,* Pretoria: SANRAL.

SAPEM Chapter 9, 2014. *South African Pavement Engineering Manual: Utilisation of Materials and Design,* Pretoria: SANRAL.

Schmidt, R. & Graf, P., 1972. The effect of water on the resilient modulus of asphalt treated mixes. *Association of Asphalt Paving Technologists,* Volume 41, pp. 118-162.

Scott, J., 1978. Adhesion and Disbonding Mechanisms of Asphalt used in Highway Construction and Maintenance. *Association of Asphalt Paving Technologists,* Volume 47, pp. 19-48.

Tarefder, R. A. & Zaman, A. M., 2010. Nanoscale Evaluation of Moisture Damage in Polymer Modified Asphalts. *Journal of Materials in Civil Engineering,* 22(7), pp. 714-725.

Tarrer, A. & Wagh, V., 1991. *The Effect of the Physical and Chemical Characteristics of Aggregate on Bonding,* Washington D.C.: National Research Council.

Taute, A., Verhaeghe, B. M. & Visser, A. T., 2001. *Interim Guidelines for the Design of Hot-Mix Asphalt in South Africa,* Pretoria: SANRAL, CSIR, SABITA.

Terrel, R. & Al-Swailmi, S., 1994. *Water Sensitivity of Asphalt-Aggregate Mixes: Test Selection,* Washington D.C.: National Research Council.

Terrel, R. & Shute, J., 1989. *Report on water sensitivity,* Washington D.C.: National Research Council.

TMH 9, 1992. *Pavement Management Systems: Standard Visual Assessment Manual for Flexible Pavements,* Pretoria: Department of Transport.

TRH 8, 1987. *Design and Use of Hot-Mix Asphalt in Pavements,* Pretoria: Department of Transport.

Twagira, E. M., 2009. *Influence of Durability Properties on Performance of Bitumen Stabilized Materials,* Stellenbosch: Stellenbosch University (PhD Dissertation).

Weston, J., 2005. *Washington State Department of Transportation.* [Online] Available at: https://www.wsdot.wa.gov/NR/rdonlyres/BB595DA7-99F9-4D73-A4B4-844FFDB5A784/0/FactorsAffectingHMAPermeabilityTN.pdf
[Accessed 5 October 2018].

Zaniewski, J. P., 2013. *Hot Mix Asphalt Concrete Density, Bulk Specific Gravity, and Permeability,* Morgantown, West Virginia: Department of Civil and Environmental Engineering.

APPENDIX A METHODOLOGY – MARVIL

A.1 STEP-BY-STEP PROCEDURE

1. Firstly, the core is placed inside the silicone rubber mould.
2. The inside of the gap in the silicone rubber mould is then smeared with grease to prevent any water from seeping through.
3. The steel ring is then placed in this gap.
4. The top of this steel ring should also be covered with grease as well as the bottom of the cover. Be sure that no grease is on the surface of the core, as this may influence the results and also lead to damage of the bituminous surface.
5. Place the cover on top of the steel ring and wiggle it slightly to help the grease lock and prevent any leaking.
6. Place the clamp over the steel ring where it meets the bottom of the cover to prevent any slip.
7. Fill the permeameter with water until the 0 *mℓ* mark is reached. Maintain the water level at 0 *mℓ* for 5 minutes. This is done to ensure that the surface of the core is in a uniform saturated condition before the test is started.
8. Start the stopwatch after 5 minutes with the water level at 0 *mℓ* and do not add any more water.
9. Record the time taken for the water level to reach each millilitre mark (50 *mℓ*, 100 *mℓ*, 150 *mℓ*, etc.) until it reaches the final mark of 600 *mℓ*.
10. If 2 hours have passed without the permeameter reaching 600 *mℓ*, take the final reading and stop the test at the end of 2 hours.
11. Once the test is completed, remove remaining water from test apparatus by using a pipe to drain the water into a bottle.
12. Take the whole test apart and remove the sample from the silicone rubber mould.

13. Clean the grease from the silicone rubber mould, the steel ring and the cover of the permeameter.
14. Ensure that all the equipment is dry and contains no grease before the next test is conducted.

APPENDIX B METHODOLOGY – HPP

B.1 STEP-BY-STEP PROCEDURE

1. Firstly, the test apparatus should be thoroughly cleaned with a paint brush to ensure that the filter material does not create a pathway for a water leak or damage the silicone rubber mould of the inflatable seal.
2. Place the core inside the silicone rubber mould and then inflate the seal to 300 *kPa*.
3. Place the rubber between the top and bottom section of the apparatus and then place the top section of the apparatus on the rubber.
4. Tighten the bolts of the apparatus to lock the two sections of the apparatus together.
5. Close valve 2 and open valve 1 to fill the apparatus with water until the 0 *mℓ* mark is reached.
6. Tilt the apparatus to the side until all the water is out of the level indicator and then open valve 2. Slowly lower the apparatus back to its original position until water flows out of valve 2, which should then be closed. Lower the apparatus to its original position. This is done to force all air out of the system.
7. Close valve 1 and make sure that valve 3 is completely open.
8. Set the compressor to 100 *kPa* and apply this pressure by attaching the quick coupling nozzle to the apparatus. Record the water level and start the stopwatch for 1 minute. After 1 minute has passed, record the final water level and remove the pressure. This is done as an initial wetting of the core.
9. Leave the apparatus to settle for another minute and then apply 100 *kPa* pressure by attaching the quick coupling nozzle to the apparatus. Record the water level and start the stopwatch. Apply this pressure for 20 minutes and record the water level every 5 minutes.
10. After 20 minutes record the last reading and remove the pressure by disconnecting the compressor nozzle.
11. Repeat step 9 and 10 for 150 *kPa* as well as 200 *kPa*.

12. If the core is very permeable and water flows through before the 20 minute mark is reached, record the time it takes for the water level to reach 100 *mℓ*, 200 *mℓ*, 300 *mℓ*, etc. until it is completely empty.
13. Once the test has been conducted for 100 *kPa*, 150 *kPa* and 200 *kPa* the water can be drained from the apparatus, the seal can be deflated and thoroughly cleaned before the next test is conducted.

APPENDIX C METHODOLOGY - MIST

C.1 STEP-BY-STEP PROCEDURE

The MIST device was developed to simulate field pulsing conditions which are caused by repeated traffic loads. This test procedure involves the saturation of a material specimen in a tri-axial pressure cell while moisture is being pulsed into the specimen.

1. Firstly, the water heating unit (WHU) is switched on to reach a temperature of 60°C.
2. Once this temperature is reached, the core is placed inside the tri-axial pressure cell which is then sealed by tightening the six screws at the top of the cell.
3. The pulsing water pressure in the tri-axial cell is then set to 150 *kPa* and is regulated with the pressure gauge and pressure regulator.
4. The ON-OFF timer is set to open the first solenoid valve for 0.54 seconds to pressurise the cell while the second valve is closed.
5. Once 0.54 seconds have passed, the first valve closes and the second valve open for 1.40 seconds to relieve the pressure inside the tri-axial cell.
6. This test was conducted for a total of 6 hours and 2 minutes.
7. Once the test is complete, the pulsing water pressure is stopped and the core is removed from the tri-axial pressure cell.

APPENDIX D METHODOLOGY – ITS TEST

D.1 STEP-BY-STEP PROCEDURE

1. Firstly, the height, diameter and weight of each core is recorded.
2. Once these measurements are all recorded, the specimen is placed on the loading apparatus.
3. The loading apparatus is then placed on the shelf inside the Universal Testing Machine (UTM).
4. The shelf inside the UTM is then raised until the top of the loading apparatus makes contact with the bottom of the actuator, preventing any force from being applied to the core and loading apparatus.
5. The testing software is then loaded on the computer, while the necessary input parameters for the core are entered. These parameters include the specimen height, the loading rate of 50.8 *mm* per minute as well as the axial loading type (which is actuator displacement).
6. The test is then started and is completed once the maximum load has been applied to the core.
7. Once the maximum load is achieved, the test is stopped, and the shelf is then lowered, and the loading apparatus removed.
8. The results from the test is then loaded onto the testing software and used for further calculations.
9. This entire process is repeated for each core.

APPENDIX E RESULTS – MARVIL PERMEABILITY

E.1 RAUBEX

The Marvil data collected from all the asphalt cores are plotted, and from this data it is evident that for the Raubex asphalt cores the millilitre interval with the highest consistency based on a linear relationship differs for all three road sections. For Section 1 the millilitre interval is at 100-millilitres (Figure 8.1); for Section 2 the millilitre interval is at 150-millilitres (Figure 8.2); and for Section 3 the millilitre interval is at 400-millilitres (Figure 8.3).

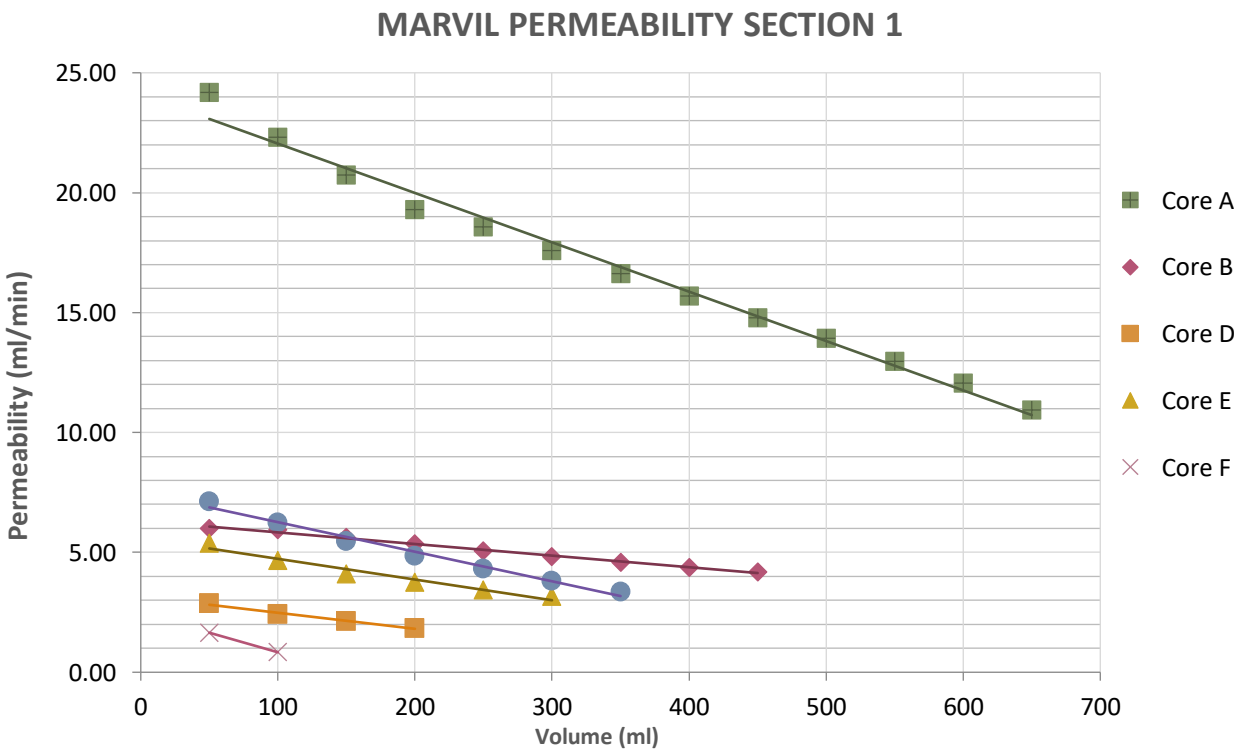

Figure 8.1: Linear relationship for asphalt core permeability (Section 1)

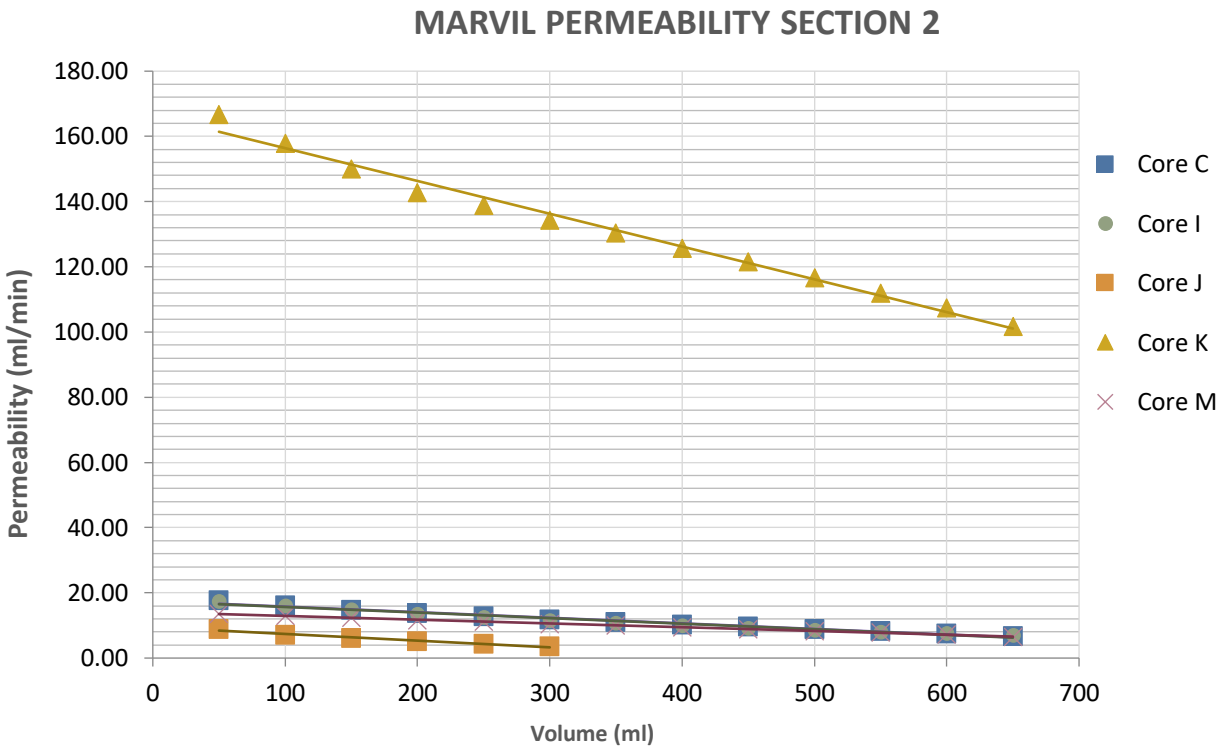

Figure 8.2: Linear relationship for asphalt core permeability (Section 2)

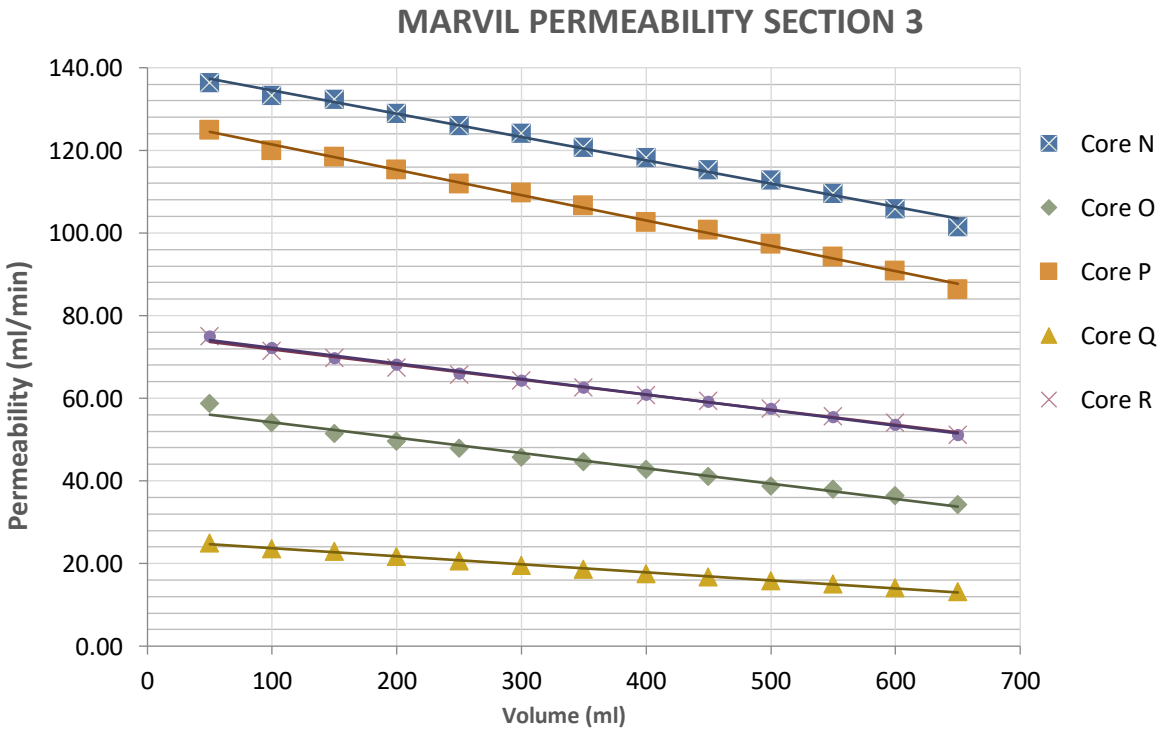

Figure 8.3: Linear relationship for asphalt core permeability (Section 3)

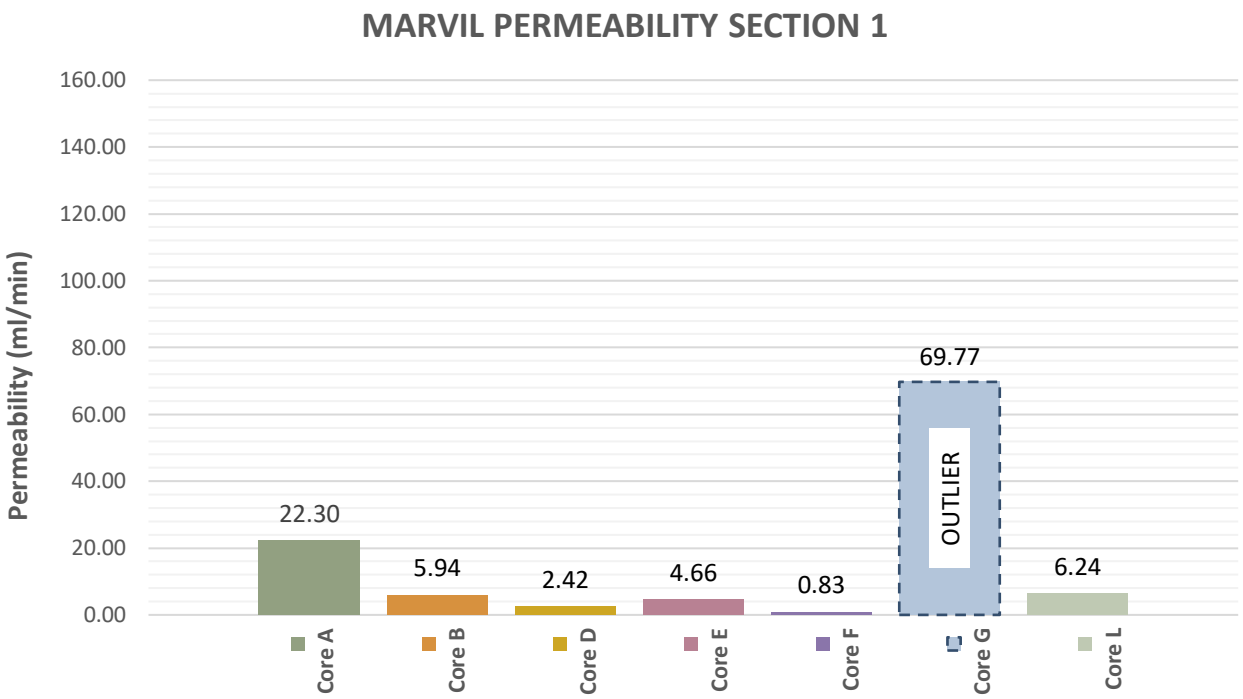

Figure 8.4: Marvil permeability for Section 1 asphalt cores

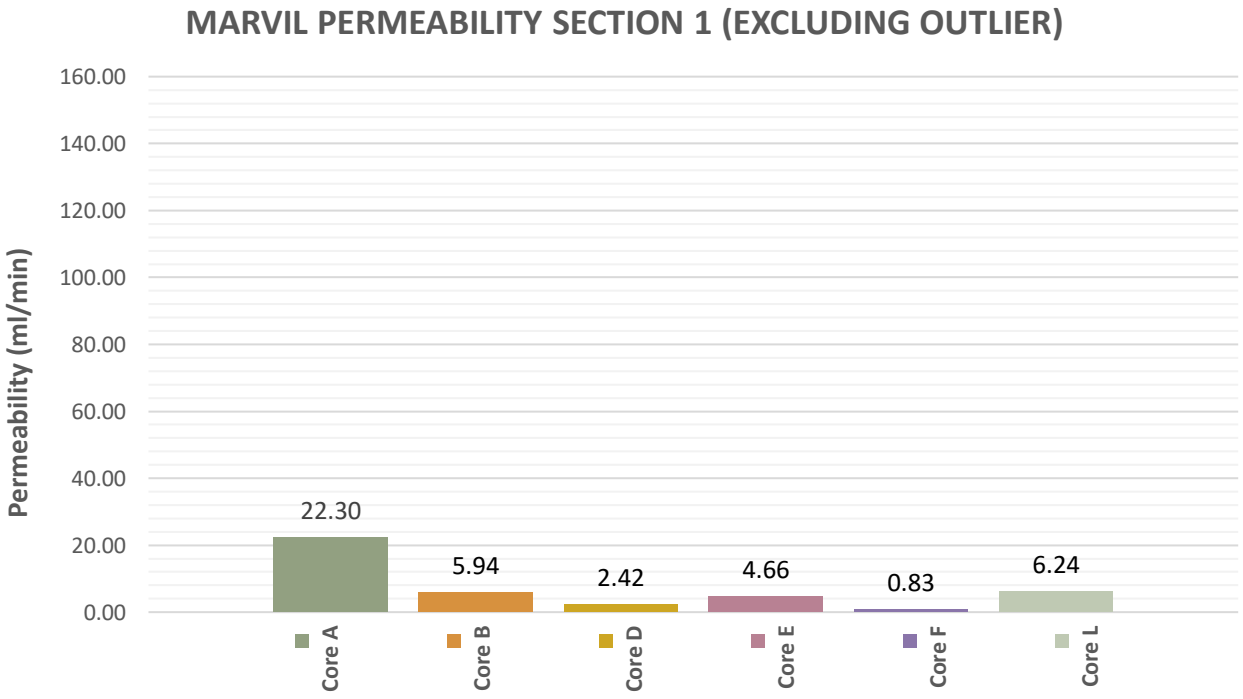

Figure 8.5: Marvil permeability for Section 1 asphalt cores (excluding outlier)

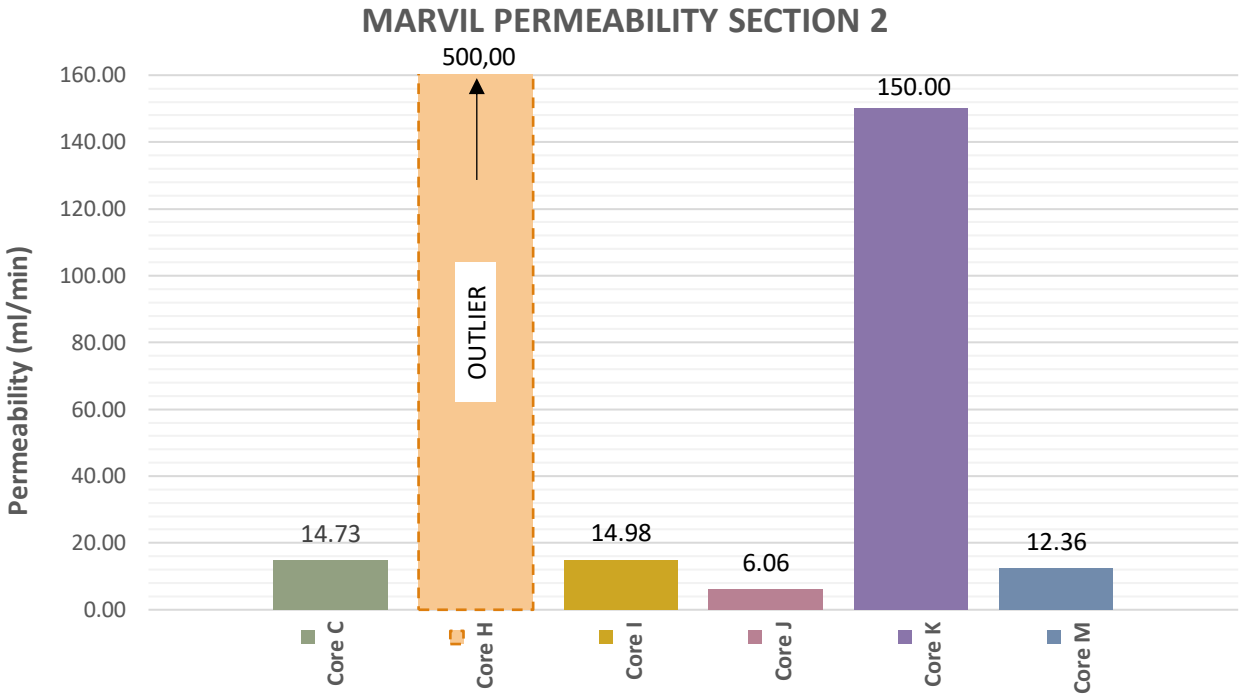

Figure 8.6: Marvil permeability for Section 2 asphalt cores

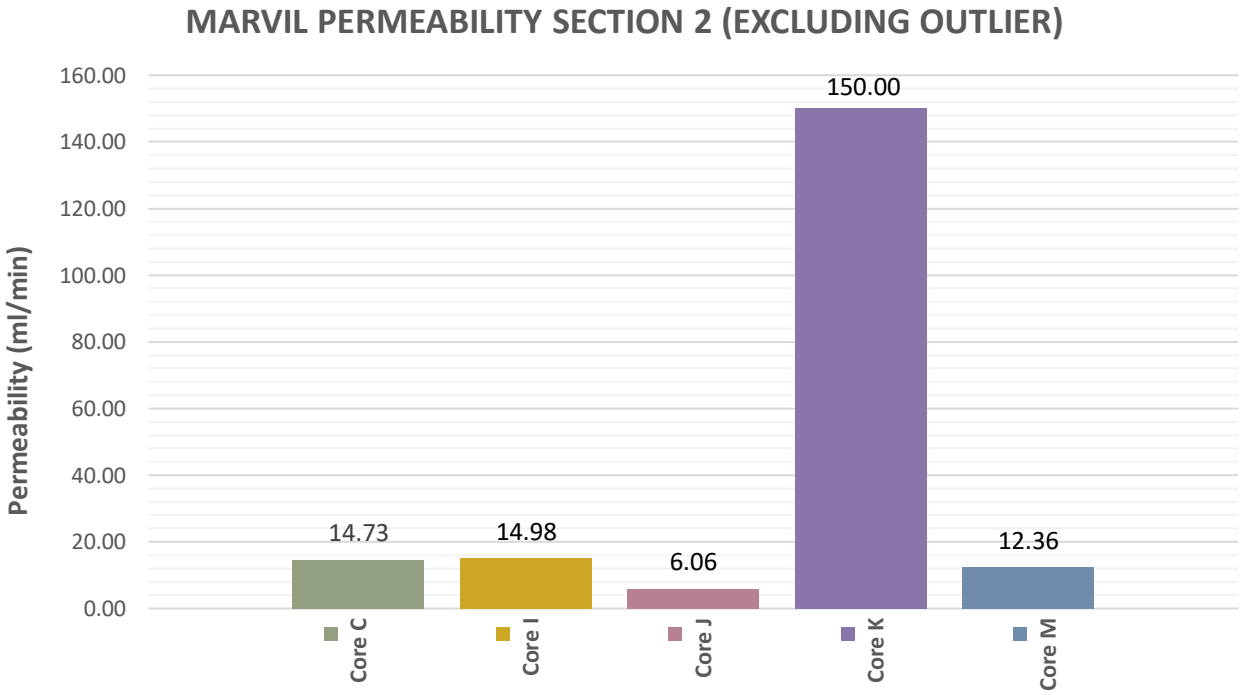

Figure 8.7: Marvil permeability for Section 2 asphalt cores (excluding outlier)

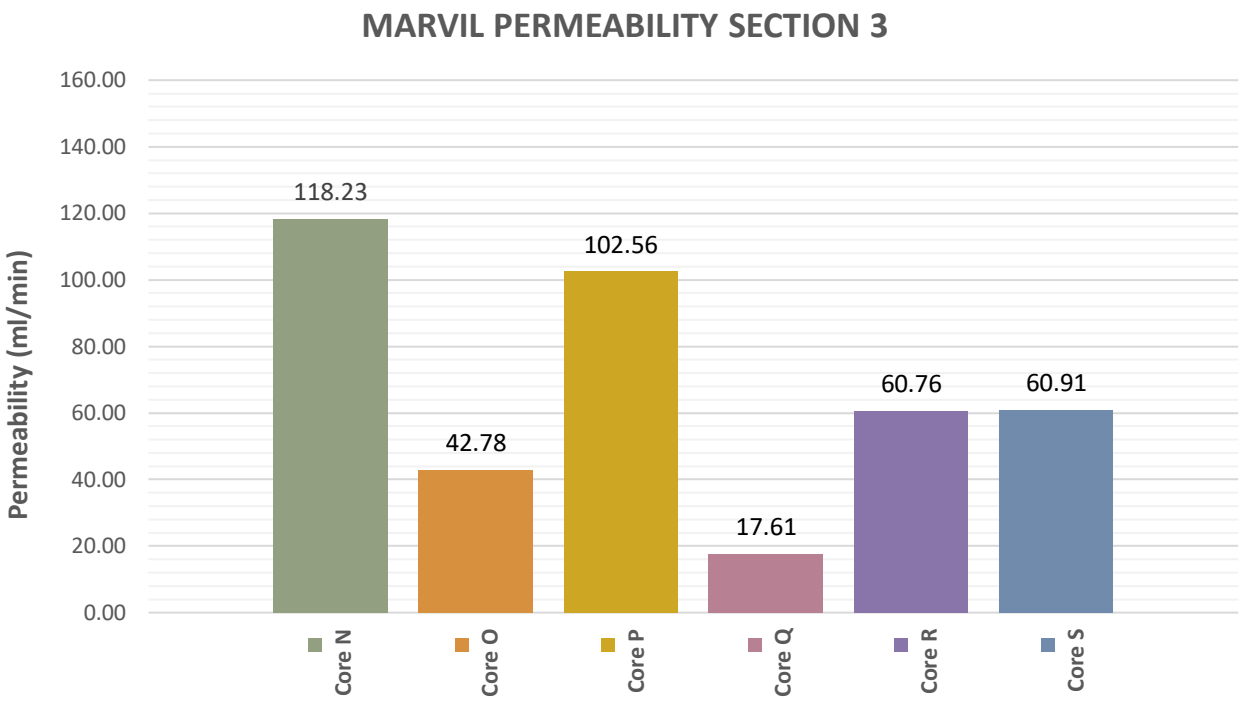

Figure 8.8: Marvil permeability for Section 3 asphalt cores

E.2 N3TC

The Marvil data collected from all the asphalt cores are plotted below, and from this data it is evident that at the 450-millilitre interval the highest consistency based on a linear relationship exists. The linear relationship graph is only done for Mix Cd (Figure 8.9), as the permeability for every core in Mix Cp was simply zero millilitres per minute.

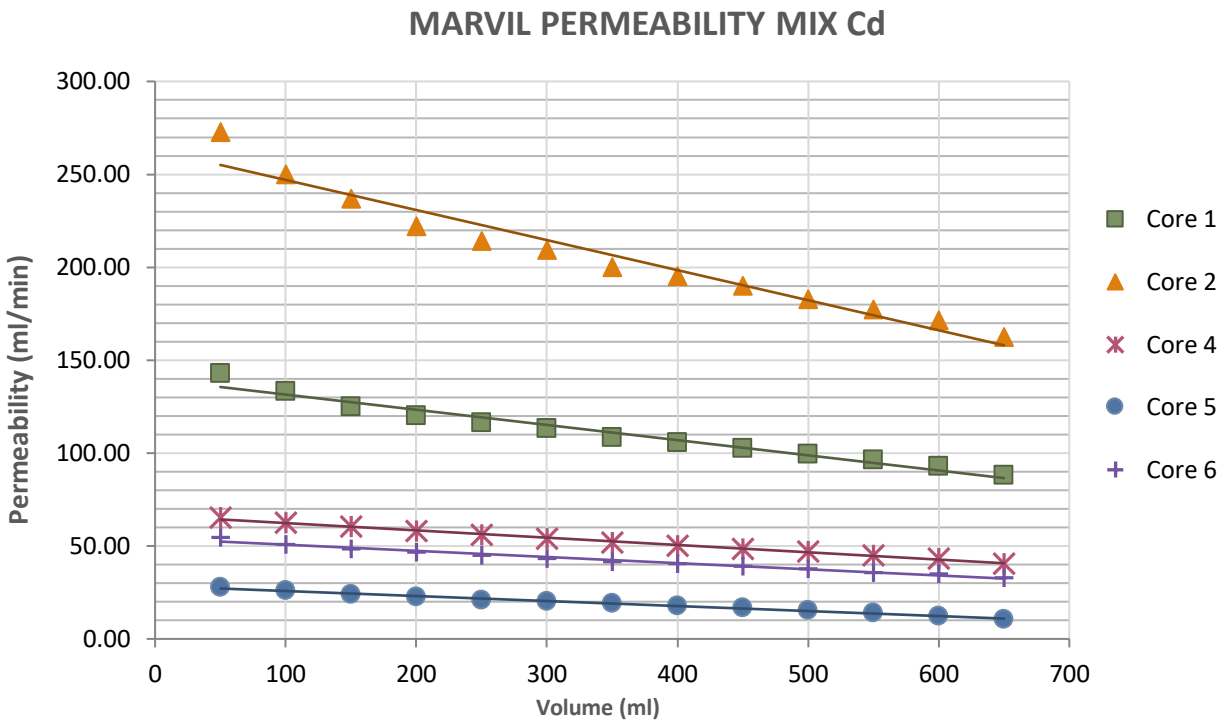

Figure 8.9: Linear relationship for asphalt core permeability (Mix Cd)

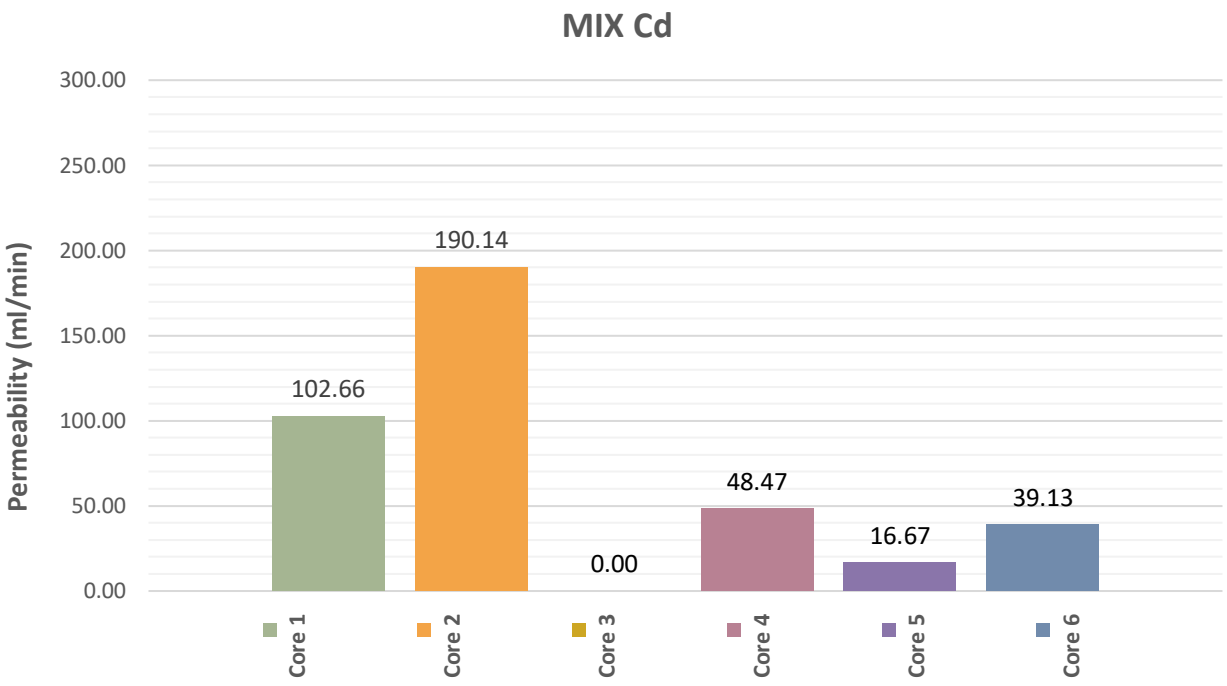

Figure 8.10: Marvil permeability for Mix Cd asphalt cores

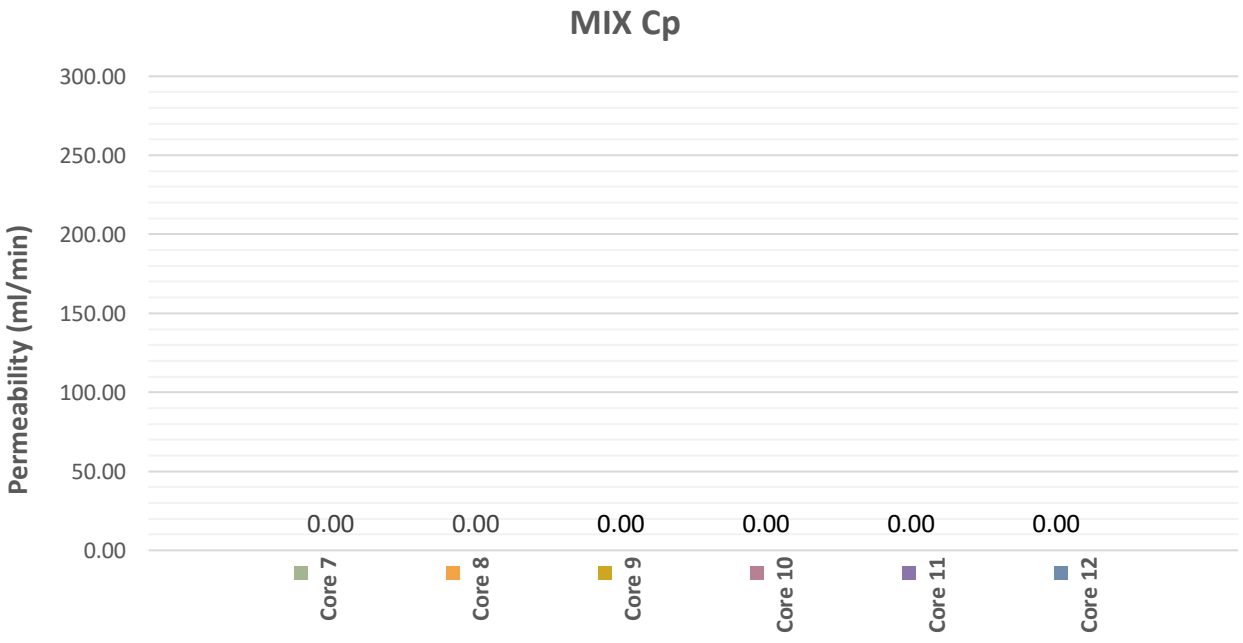

Figure 8.11: Marvil permeability for Mix Cp asphalt cores

E.3 N7

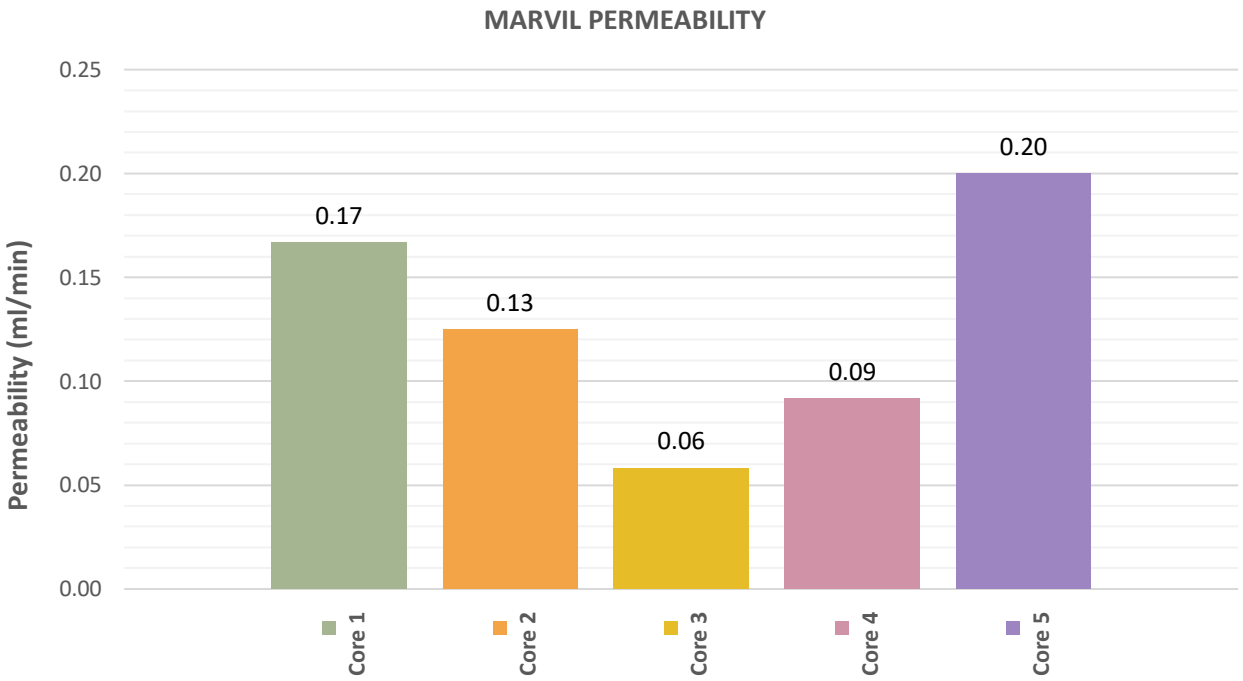

Figure 8.12: Marvil permeability for N7 asphalt cores

E.4 MUCH ASPHALT

The Marvil data collected from all the asphalt cores are plotted below, and from this data it is evident that at the 150-millilitre interval the highest consistency based on a linear relationship exists. This can be seen in Figure 8.13.

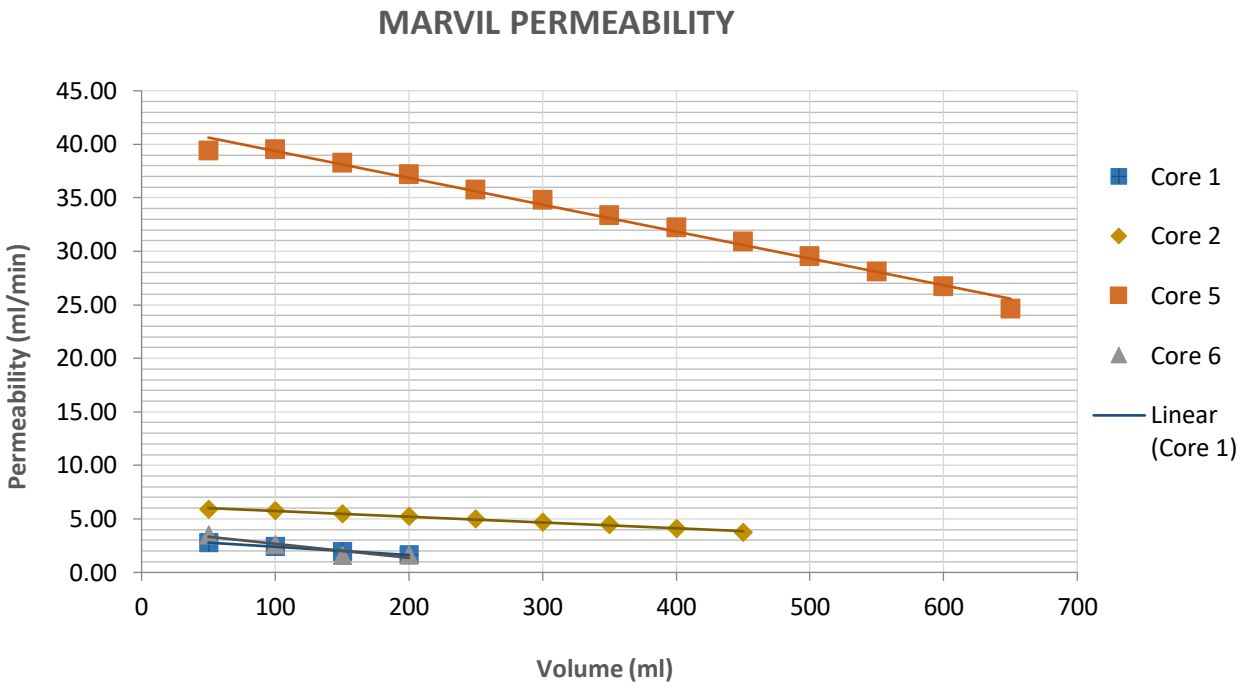

Figure 8.13: Linear relationship for asphalt core permeability

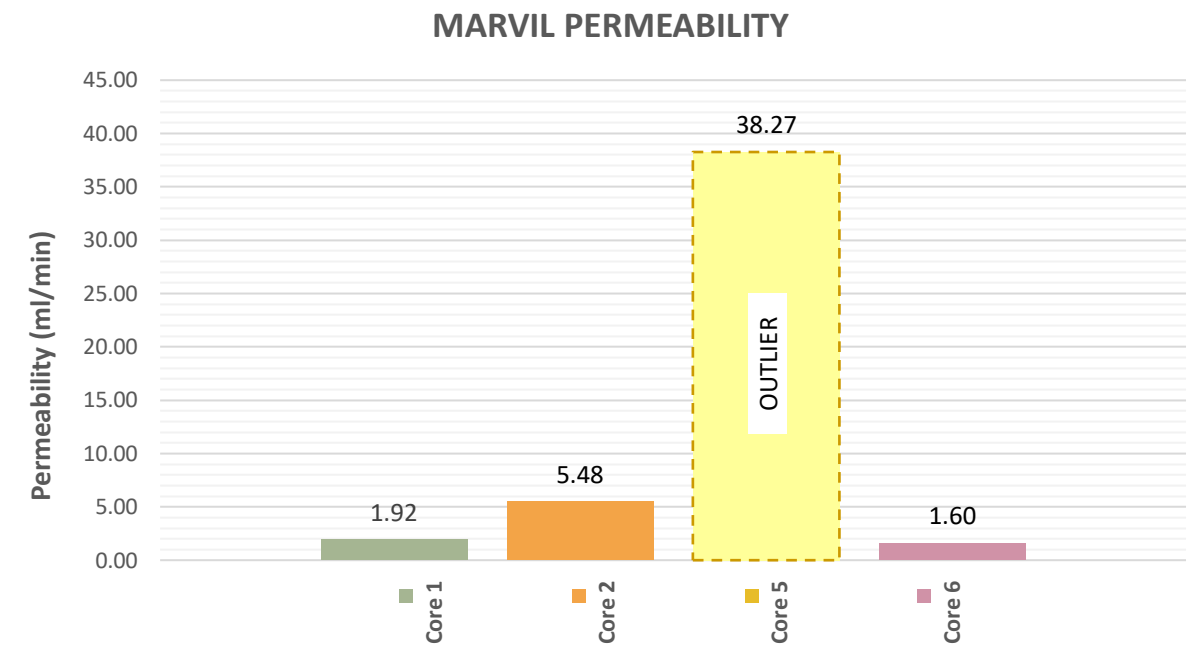

Figure 8.14: Marvil permeability for Much Asphalt cores

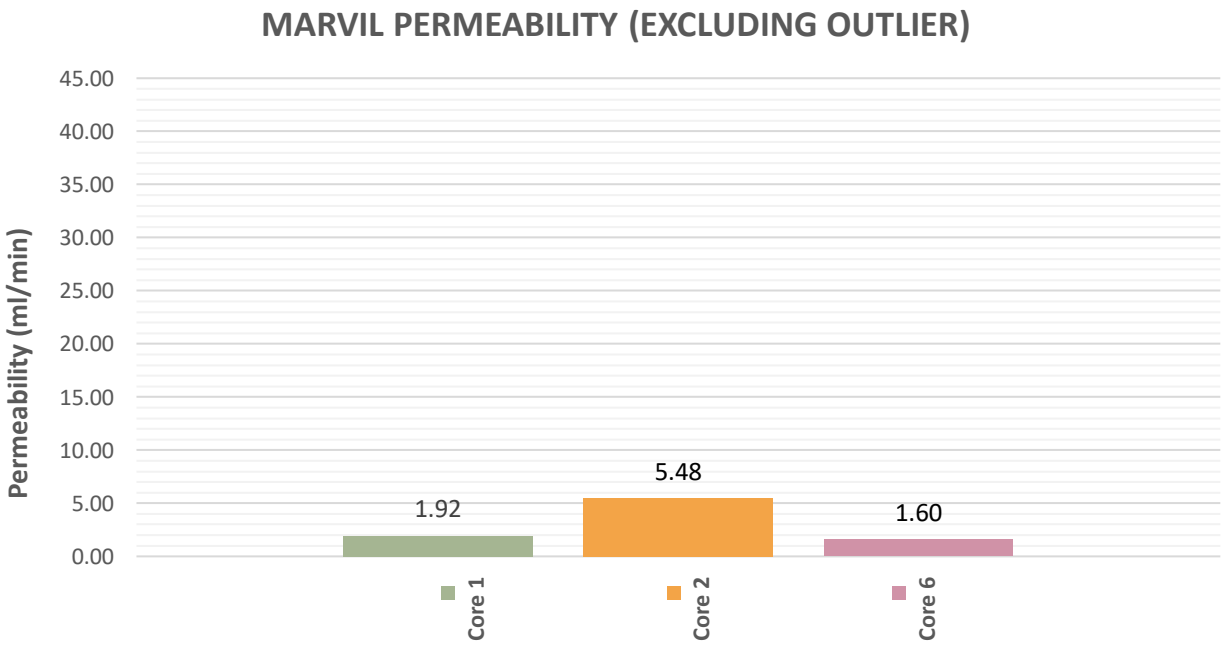

Figure 8.15: Marvil permeability for Much Asphalt cores (excluding outlier)

APPENDIX F RESULTS – HPP

F.1 RAUBEX – SECTION 1

Table 8.1: HPP permeability results for Section 1

Core	Permeability *(mℓ/min)*		
	100 kPa	150 kPa	200 kPa
A	4,40	8,80	144,14
B	20,00	17,20	16,20
F	9,30	13,70	16,50
L	0,40	1,50	2,30

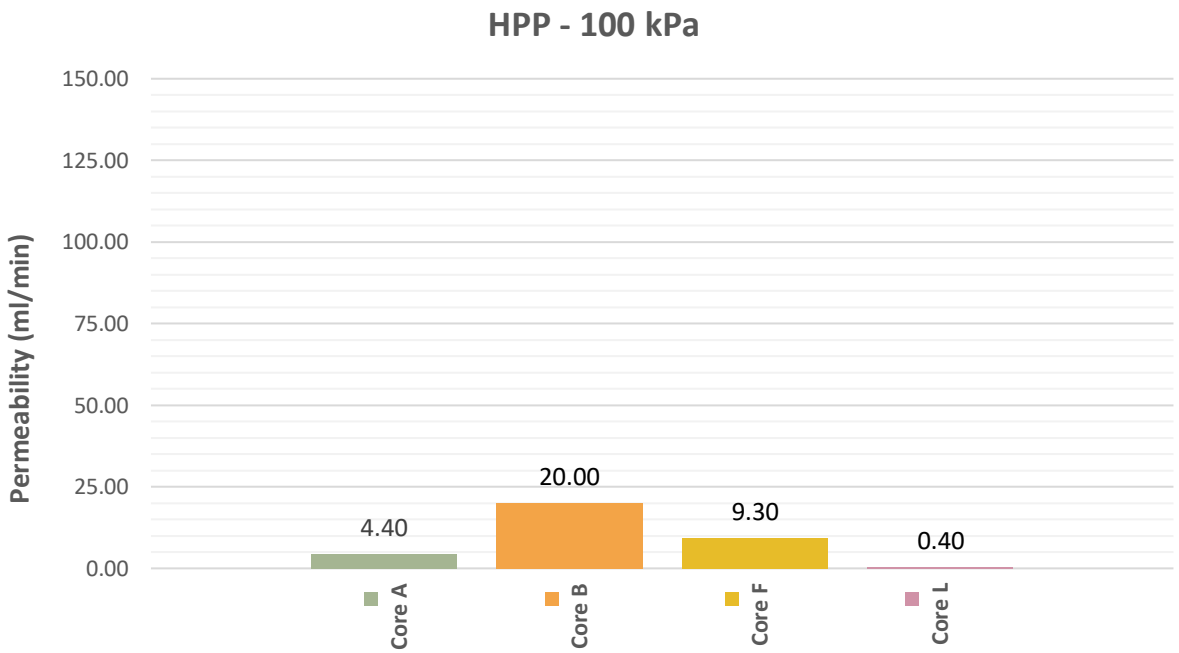

Figure 8.16: HPP permeability at 100 kPa

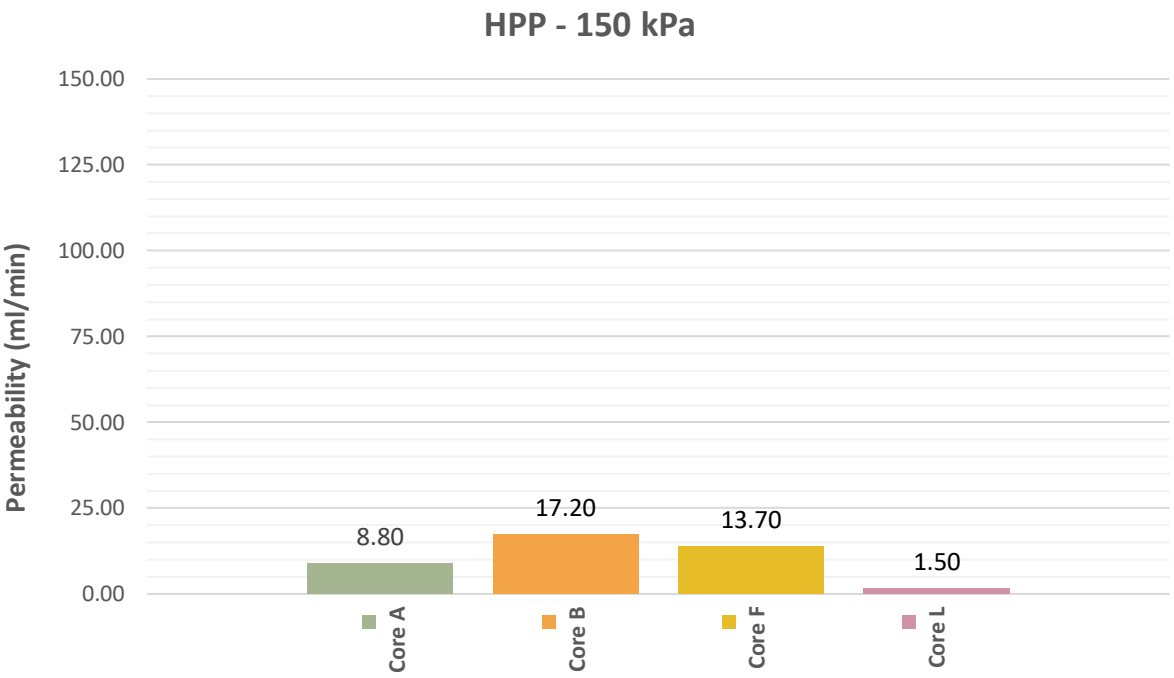

Figure 8.17: HPP permeability at 150 kPa

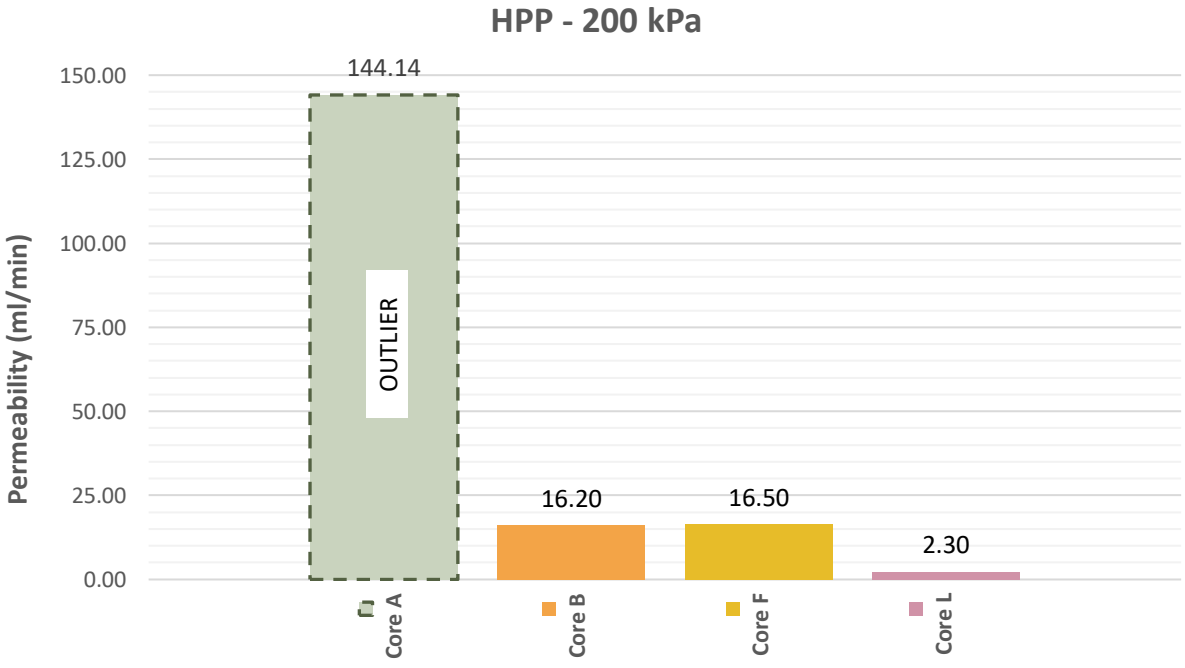

Figure 8.18: HPP permeability at 200 kPa

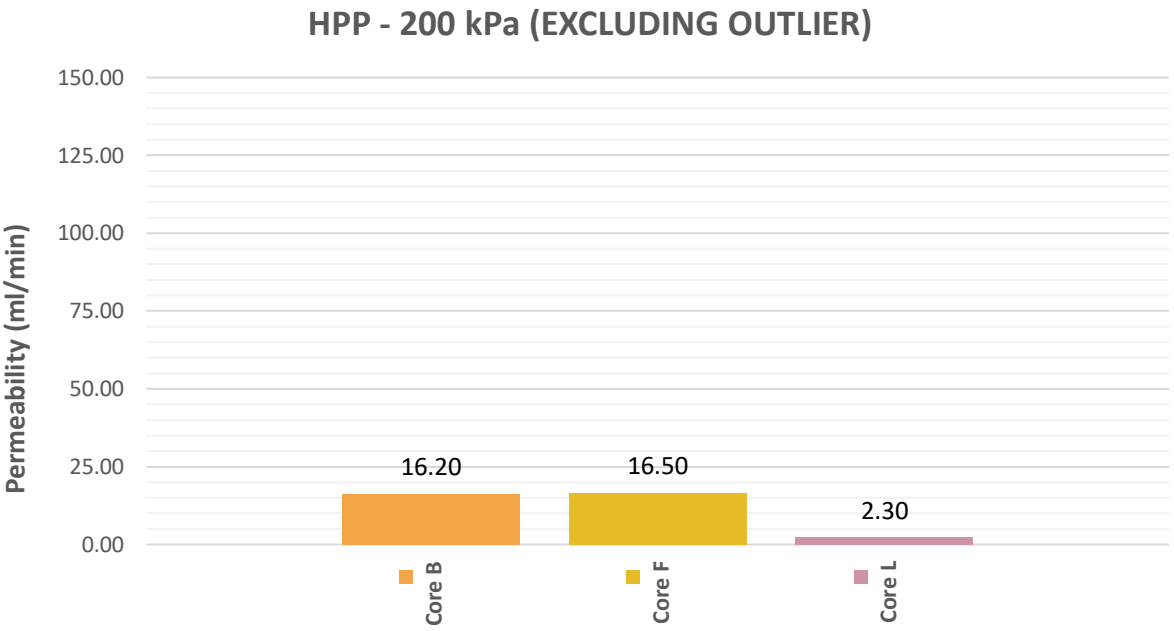

Figure 8.19: HPP permeability at 200 kPa (excluding outlier)

F.2 RAUBEX – SECTION 2

Table 8.2: HPP permeability results for Section 2

Core	Permeability *(mℓ/min)*		
	100 kPa	**150 kPa**	**200 kPa**
H	1980,20	2023,61	1980,20
I	5,10	8,00	16,40
J	0,30	0,40	0,25
M	0,30	1,10	3,40

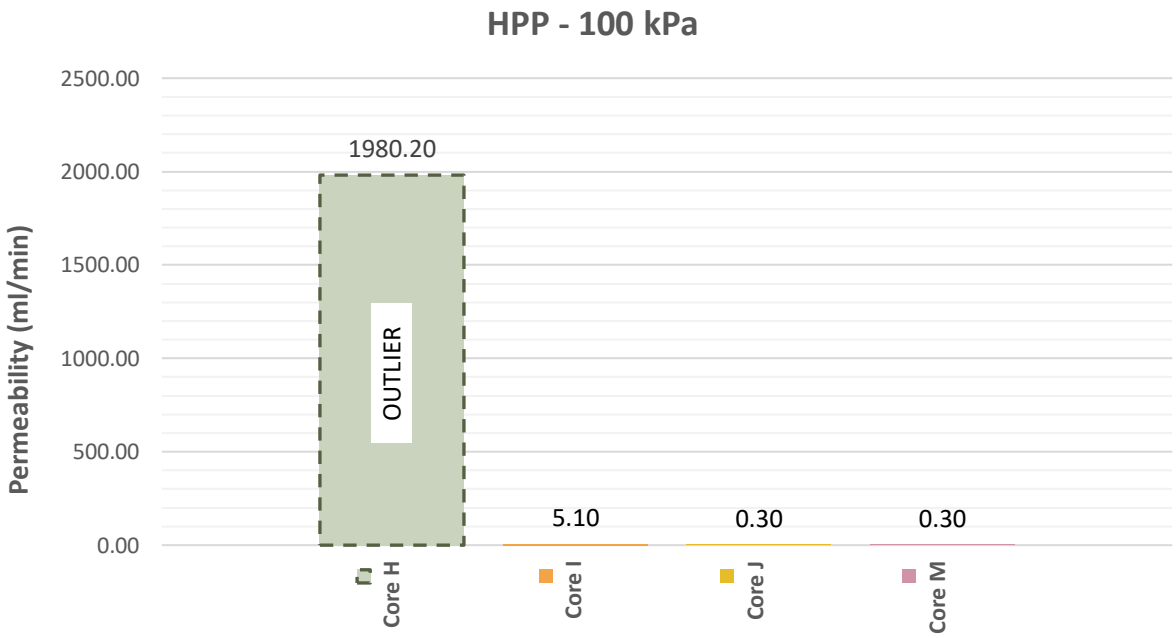

Figure 8.20: HPP permeability at 100 kPa

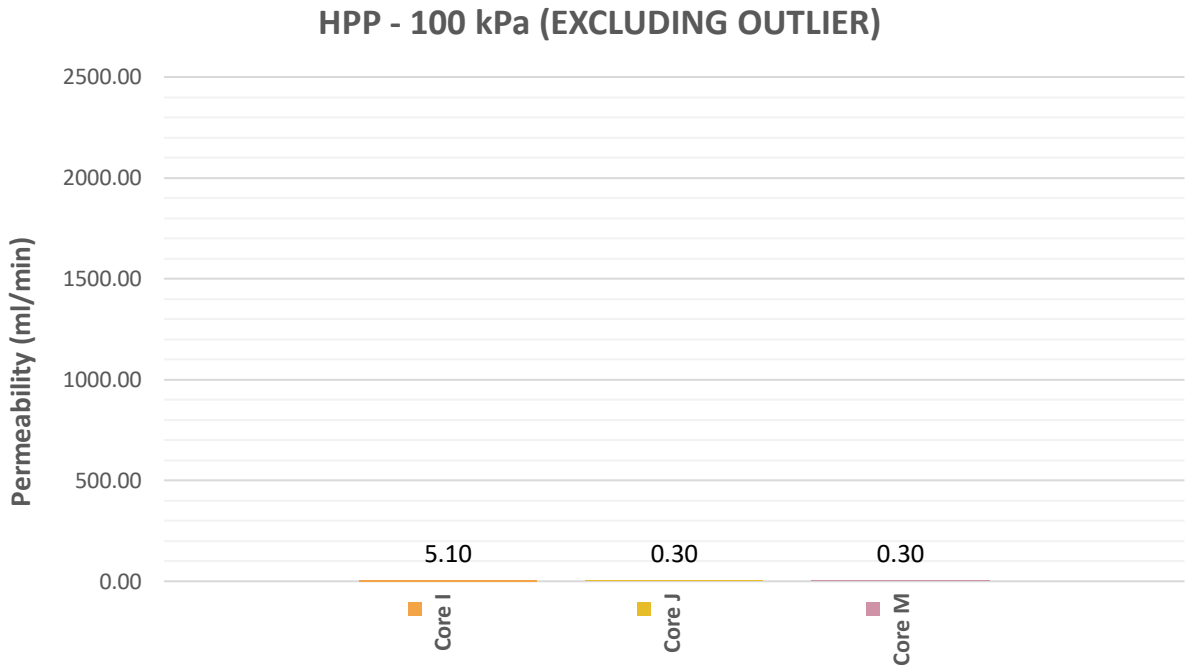

Figure 8.21: HPP permeability at 100 kPa (excluding outlier)

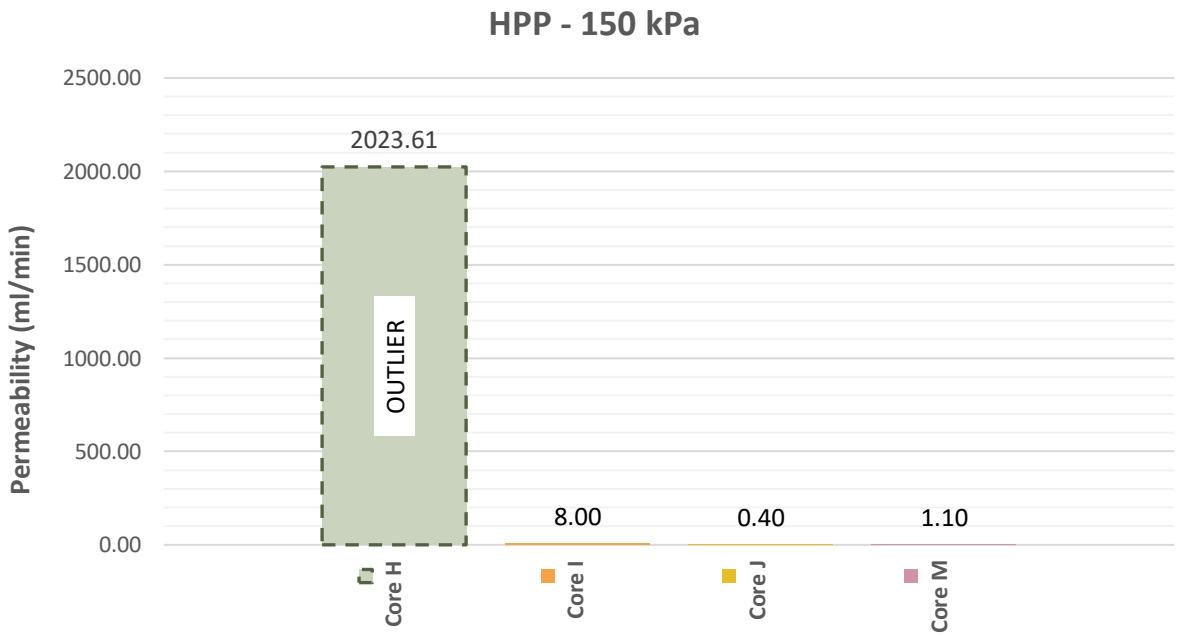

Figure 8.22: HPP permeability at 150 kPa

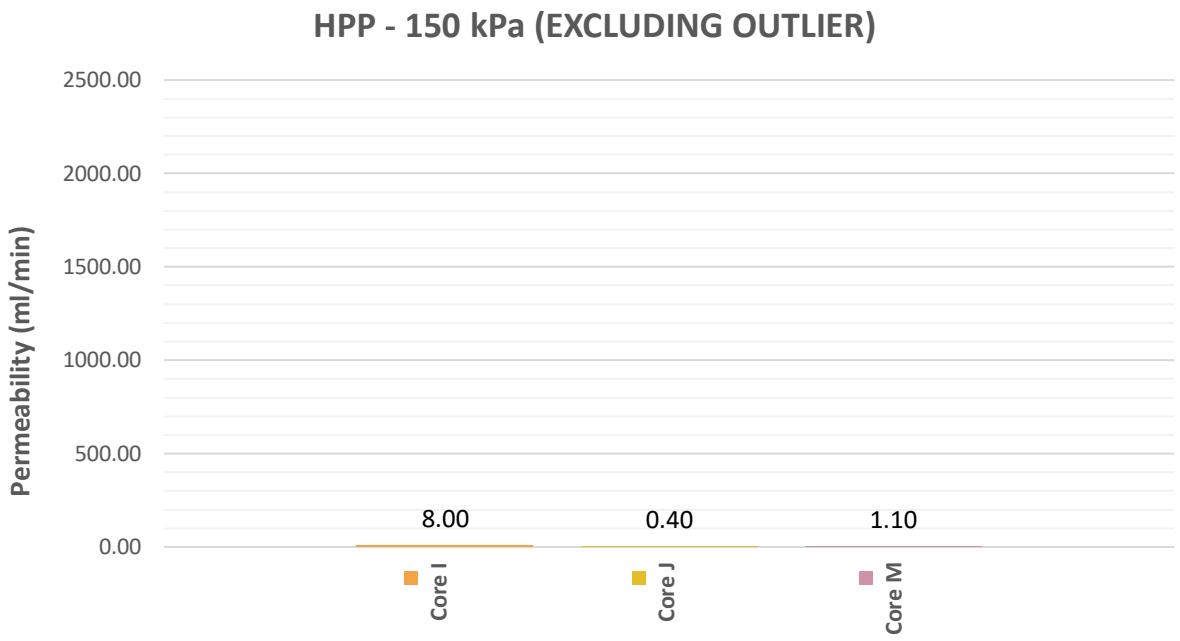

Figure 8.23: HPP permeability at 150 kPa (excluding outlier)

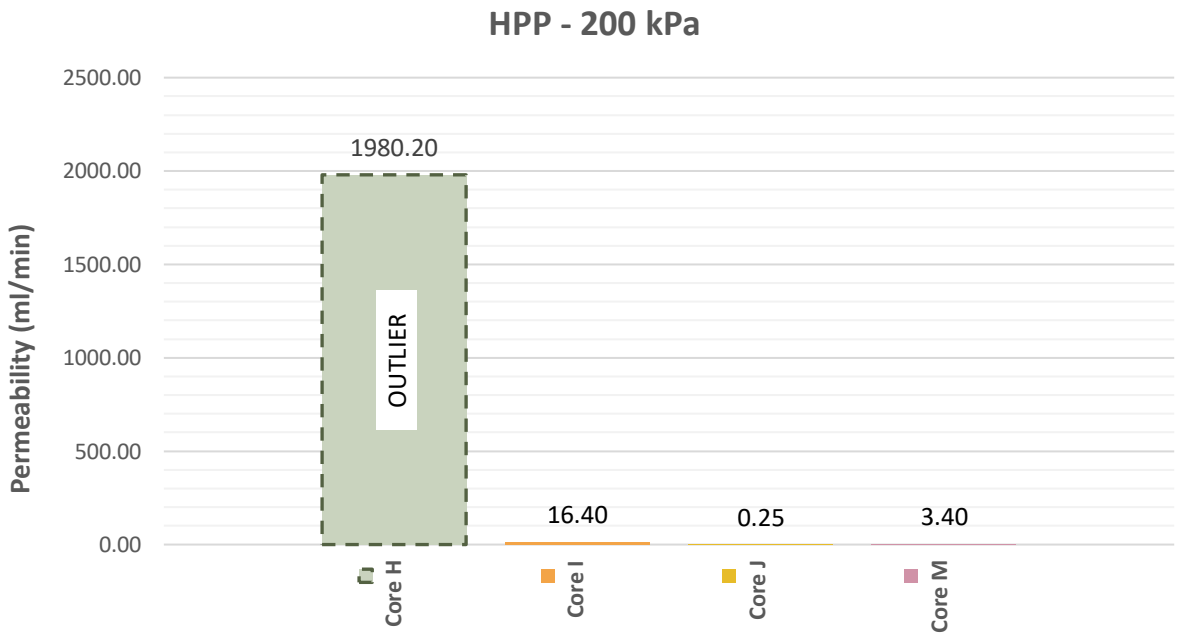

Figure 8.24: HPP permeability at 200 kPa

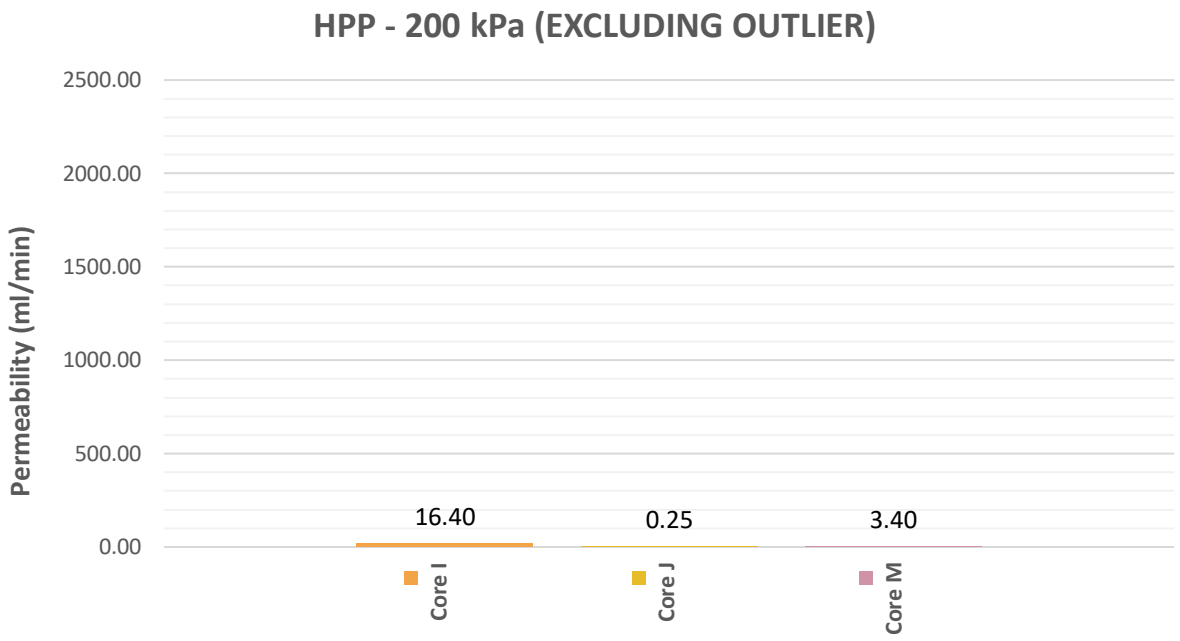

Figure 8.25: HPP permeability at 200 kPa (excluding outlier)

F.3 RAUBEX – SECTION 3

Table 8.3: HPP permeability results for Section 3

Core	Permeability *(mℓ/min)*		
	100 kPa	**150 kPa**	**200 kPa**
N	14,40	21,40	37,97
O	12,60	16,00	19,70
P	1035,38	1282,05	1470,59
Q	15,40	19,20	40,40

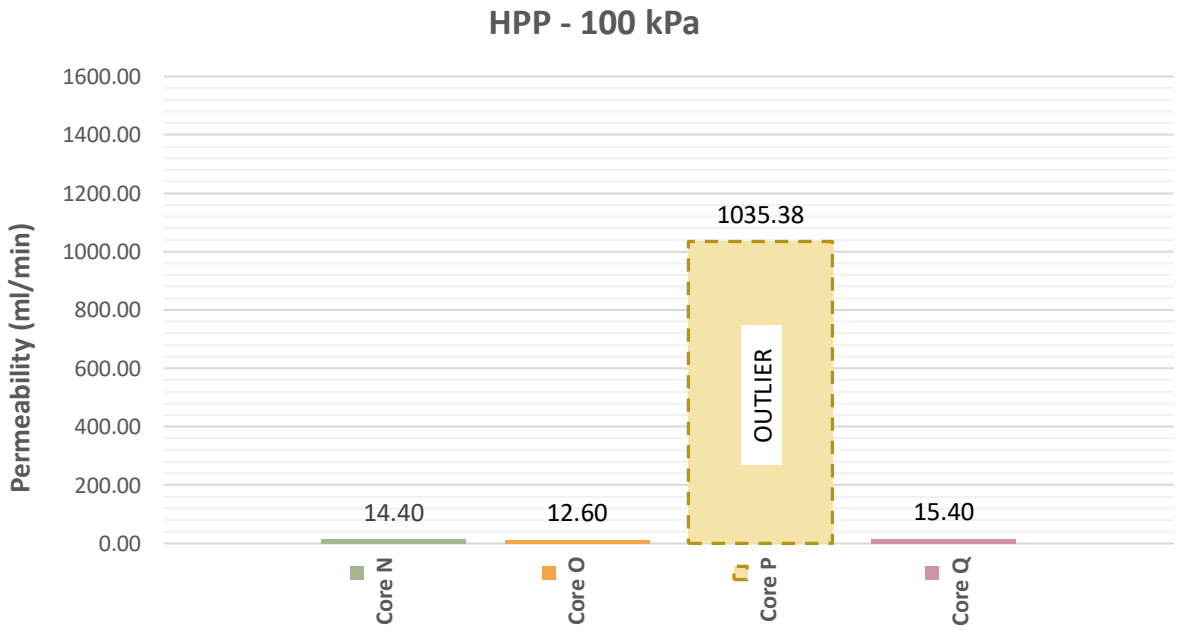

Figure 8.26: HPP permeability at 100 kPa

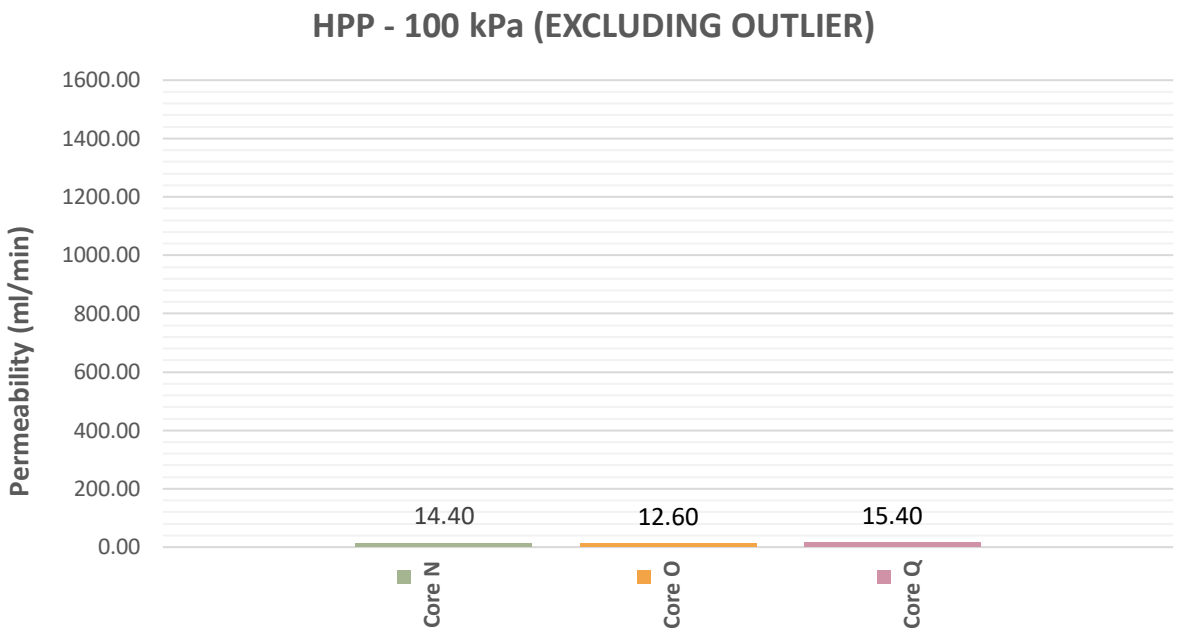

Figure 8.27: HPP permeability at 100 kPa (excluding outlier)

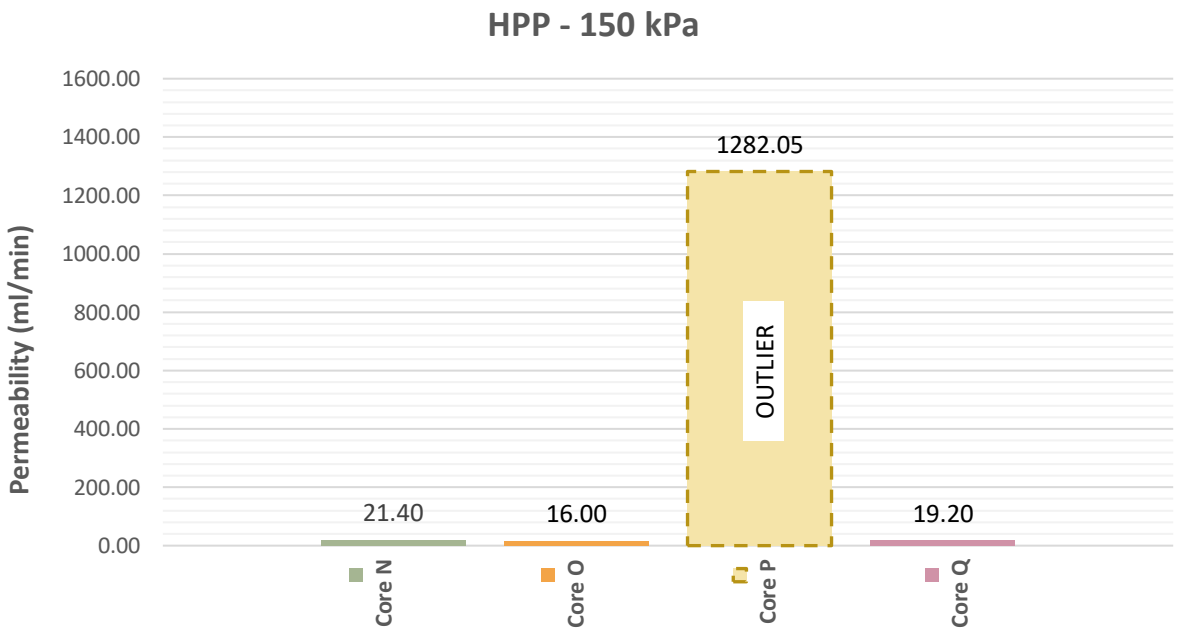

Figure 8.28: HPP permeability at 150 kPa

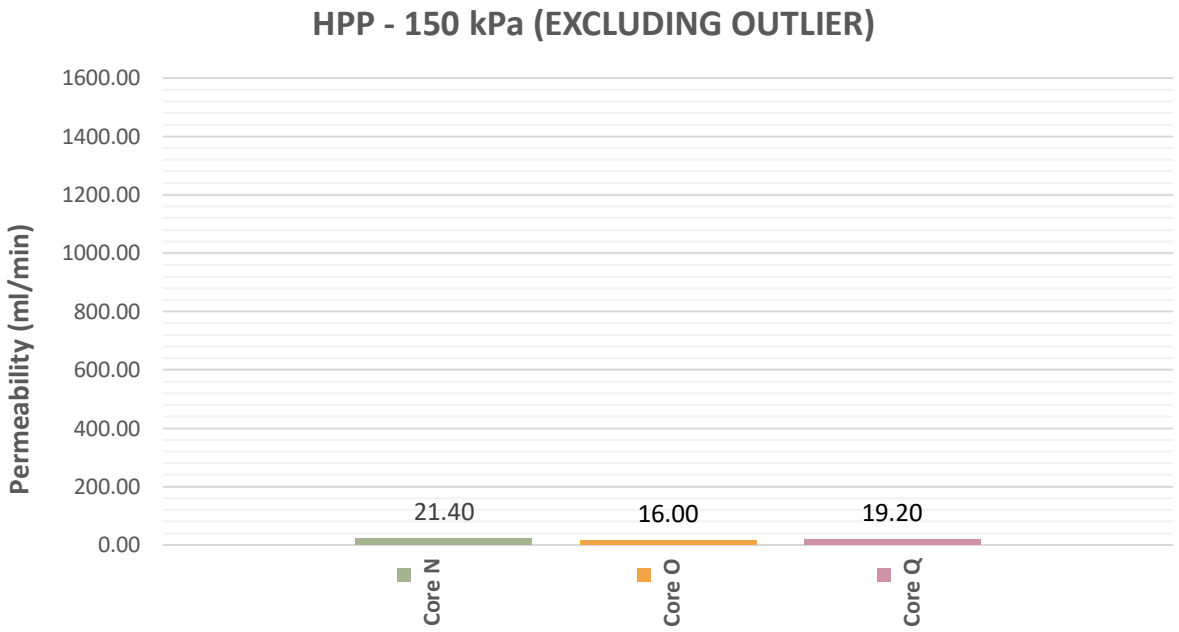

Figure 8.29: HPP permeability at 150 kPa (excluding outlier)

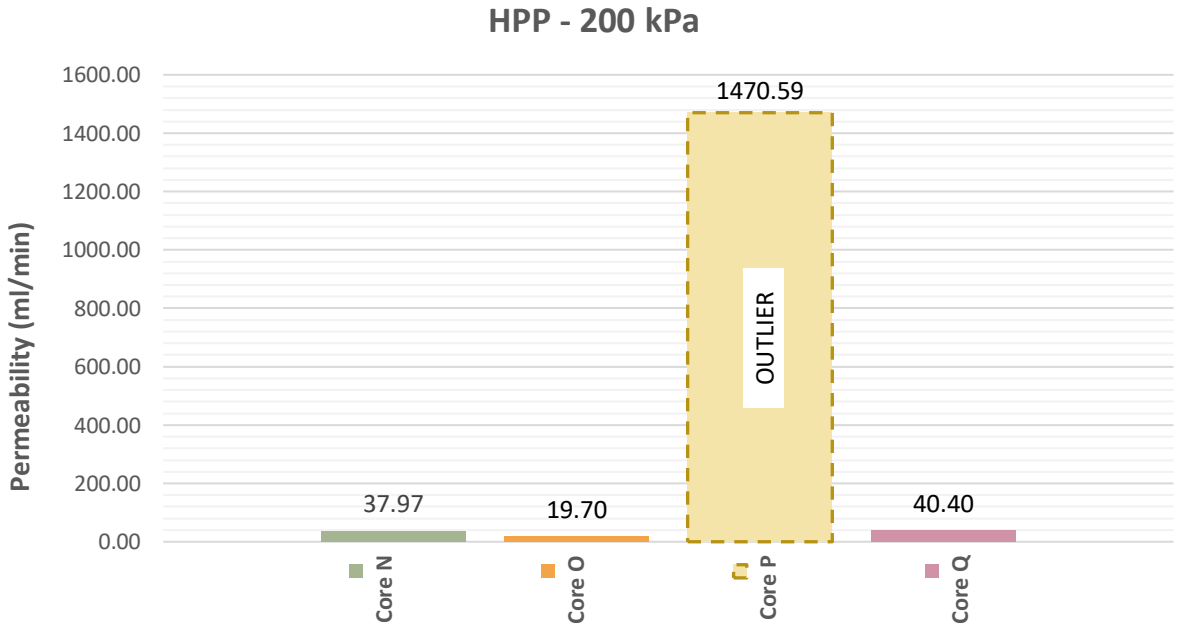

Figure 8.30: HPP permeability at 200 kPa

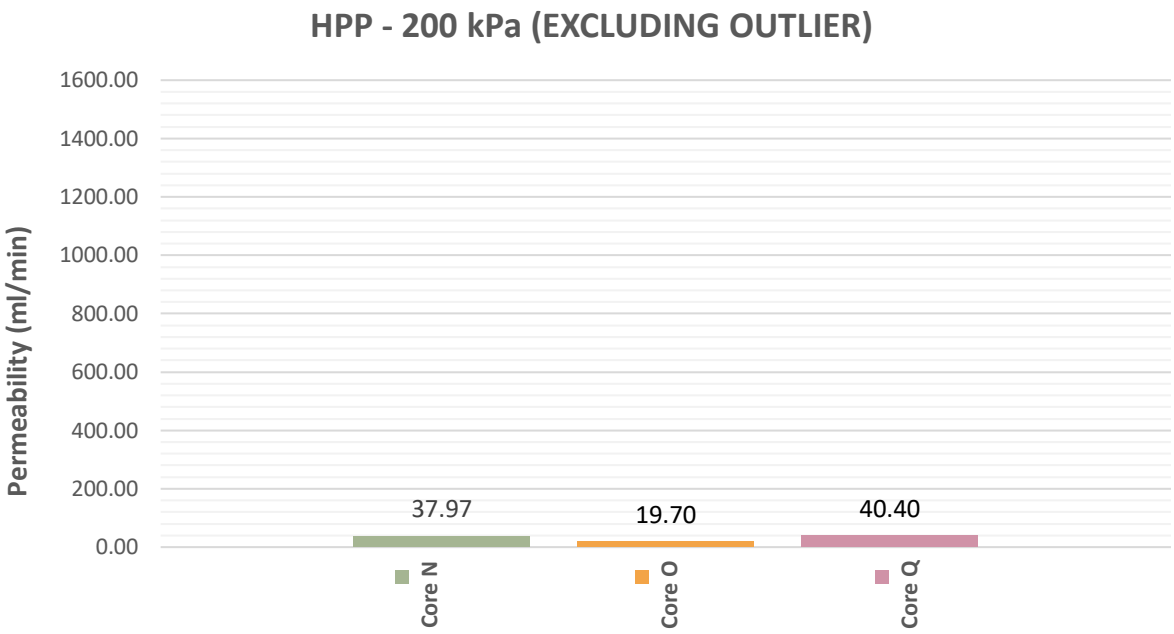

Figure 8.31: HPP permeability at 200 kPa (excluding outlier)

F.4 N3TC – MIX CD

Table 8.4: HPP permeability results for Mix Cd

Core	Permeability *(mℓ/min)*		
	100 kPa	**150 kPa**	**200 kPa**
1	90,36	137,99	178,47
2	158,88	184,28	299,63
3	0,00	0,00	4,50
4	103,61	136,71	137,69
5	40,29	100,85	212,58
6	26,31	50,24	227,49

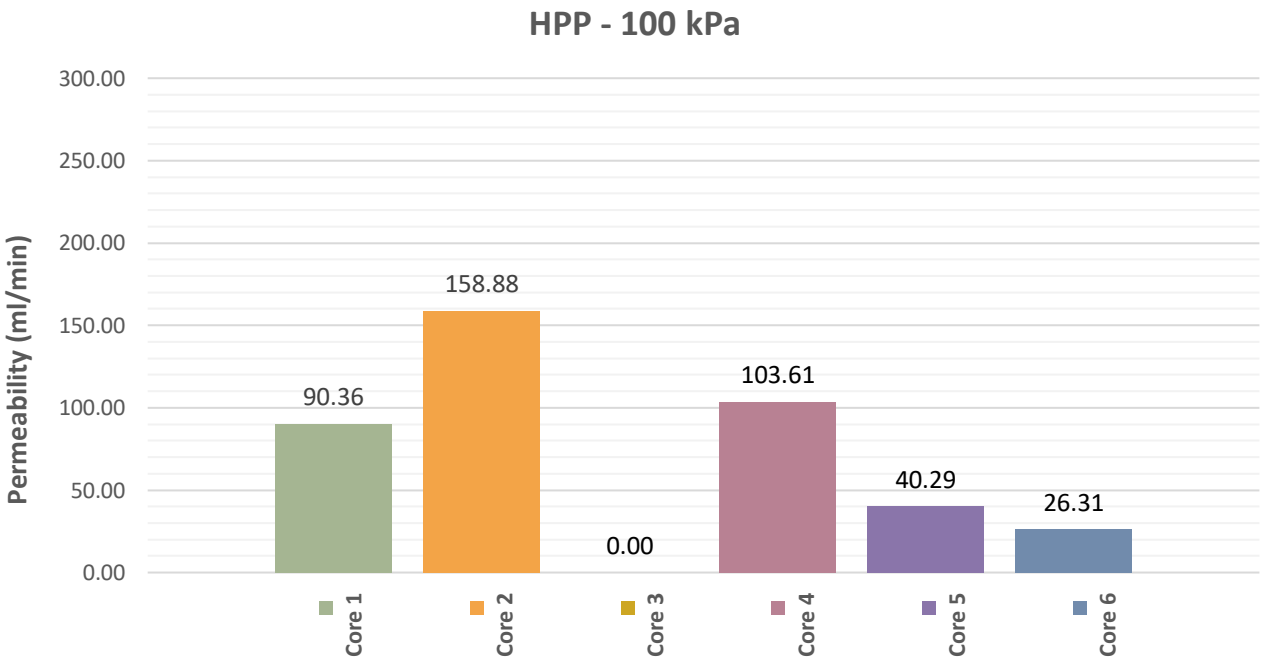

Figure 8.32: HPP permeability at 100 kPa

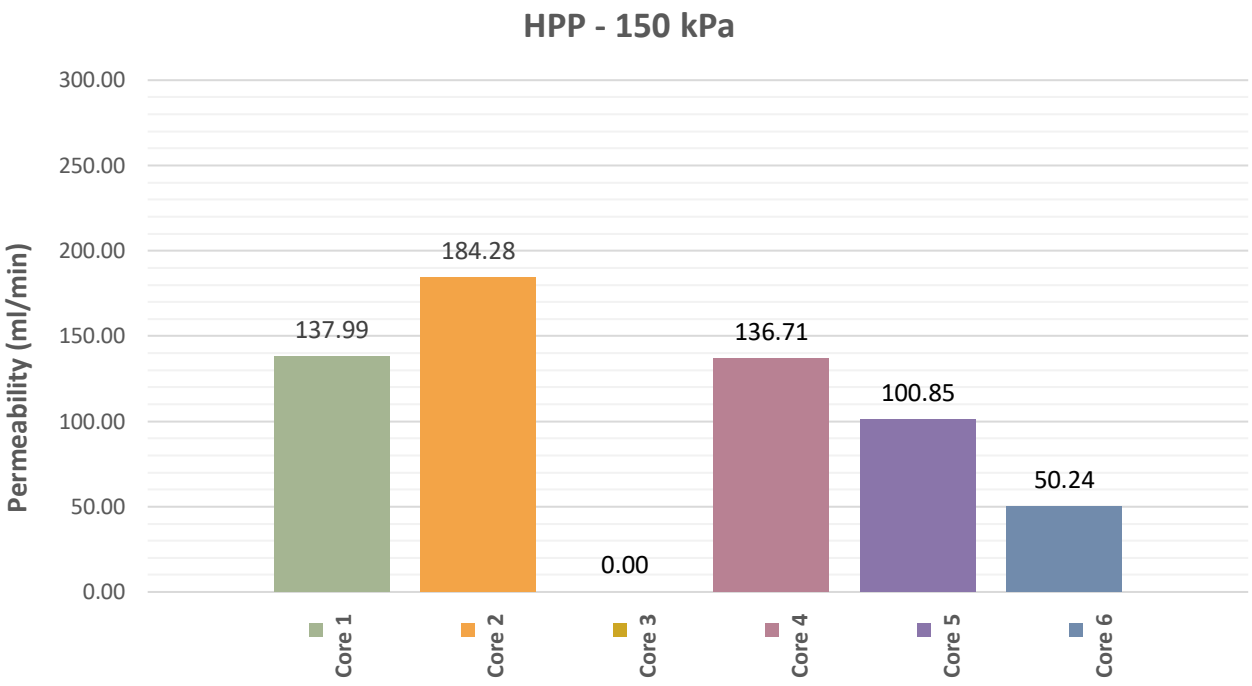

Figure 8.33: HPP permeability at 150 kPa

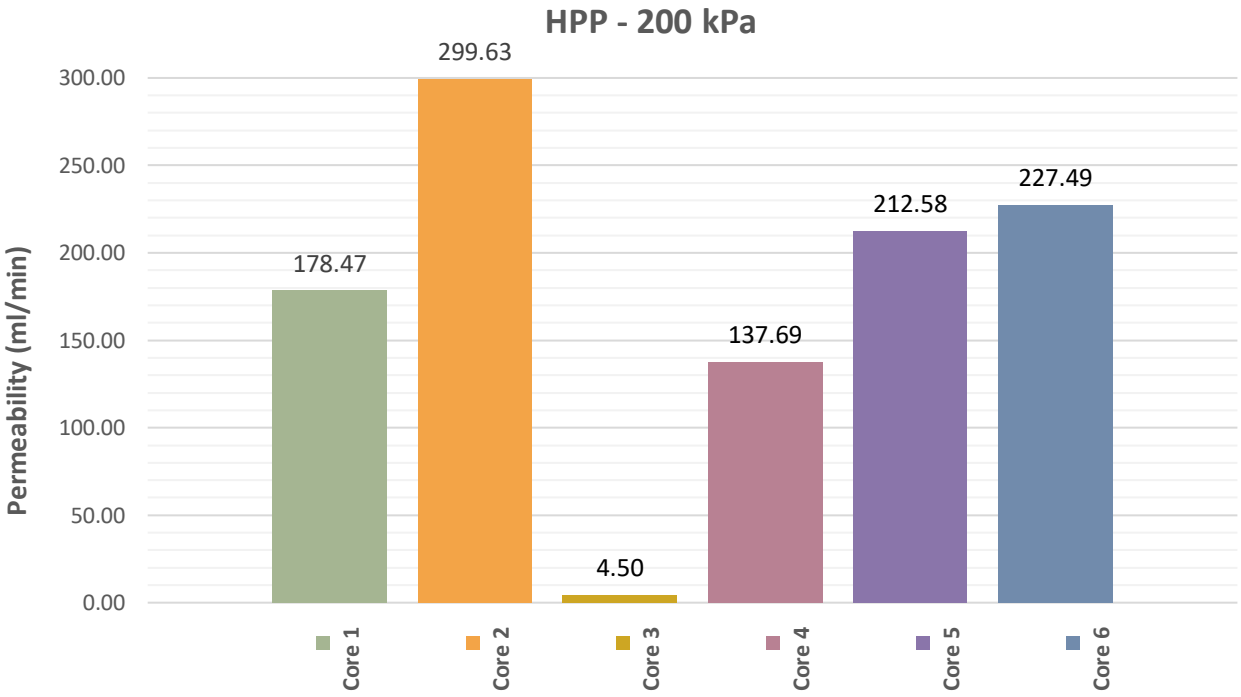

Figure 8.34: HPP permeability at 200 kPa

F.5 N3TC – MIX CP

Table 8.5: HPP permeability results for Mix Cp

Core	Permeability *(mℓ/min)*		
	100 kPa	**150 kPa**	**200 kPa**
7	0,00	7,50	75,00
8	1,00	2,00	3,50
9	2,25	5,75	9,00
10	109,87	200,20	265,37
11	1,25	7,50	56,80
12	0,00	0,00	7,25

It is important to note that Core 10 was cored down to a 95 *mm* diameter, but due to an operating error, the drill damaged the core and a slight deformation occurred which deemed the specimen useless (see Figure 8.35). This led to Core 10 being an outlier and was not used in any final result calculations.

Figure 8.35: Core 10 deformation

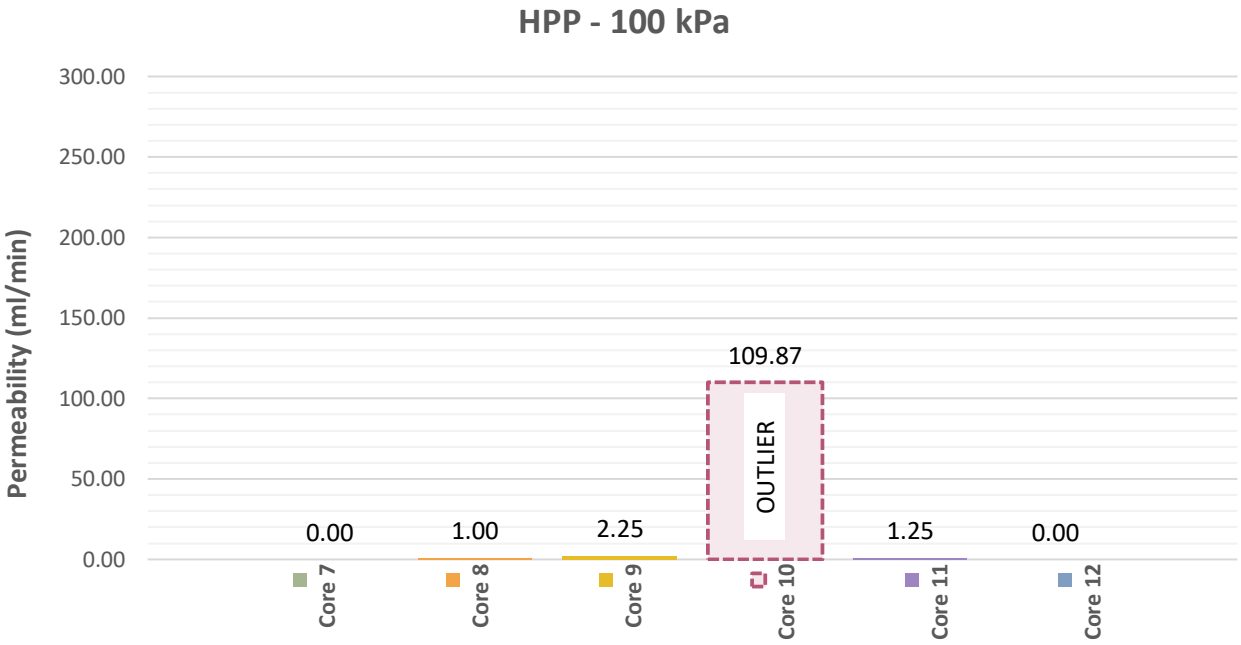

Figure 8.36: HPP permeability at 100 kPa

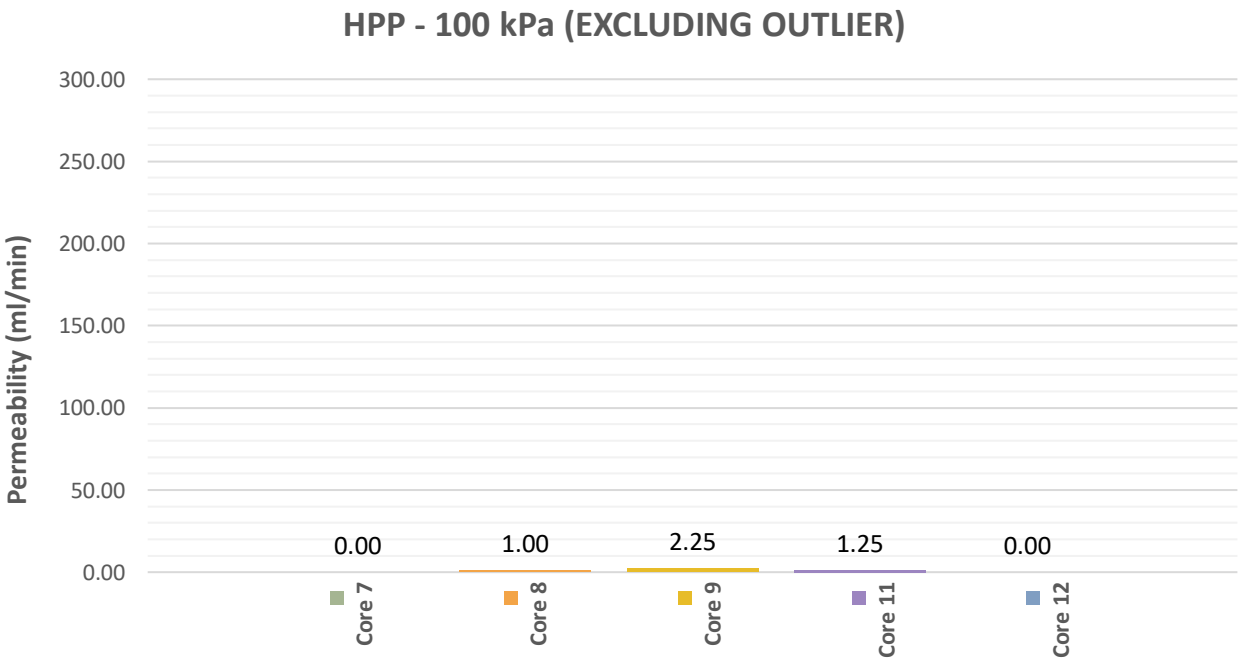

Figure 8.37: HPP permeability at 100 kPa (excluding outlier)

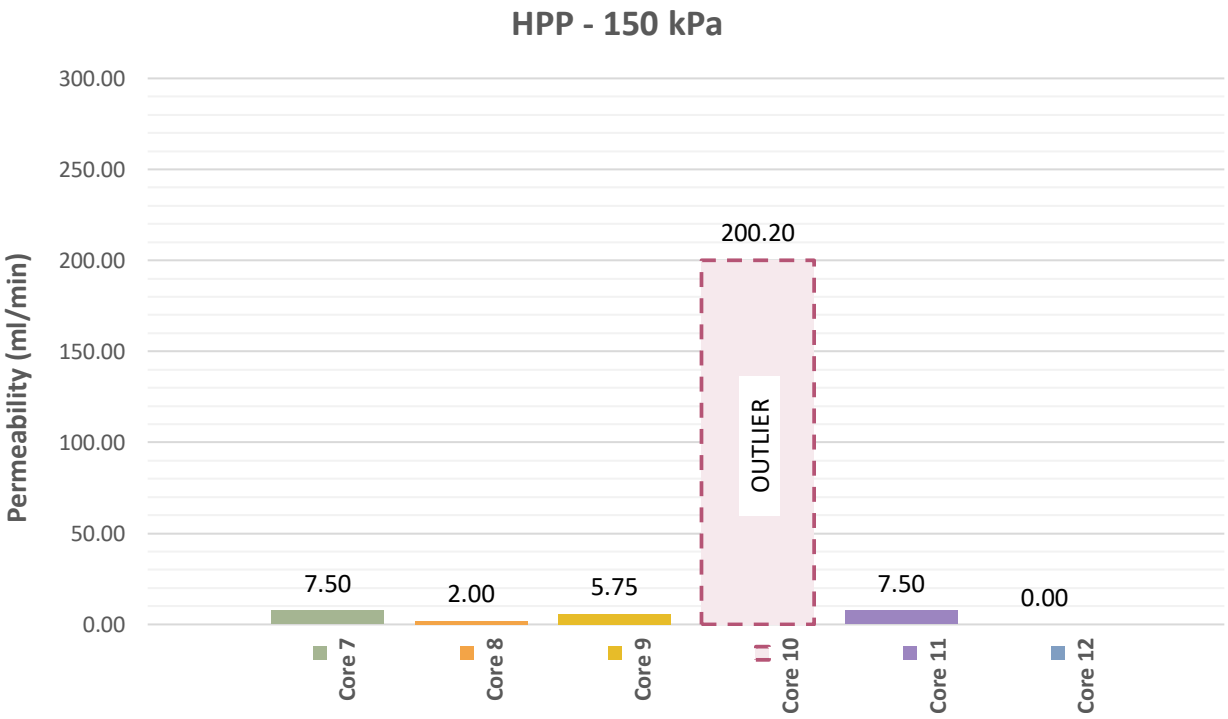

Figure 8.38: HPP permeability at 150 kPa

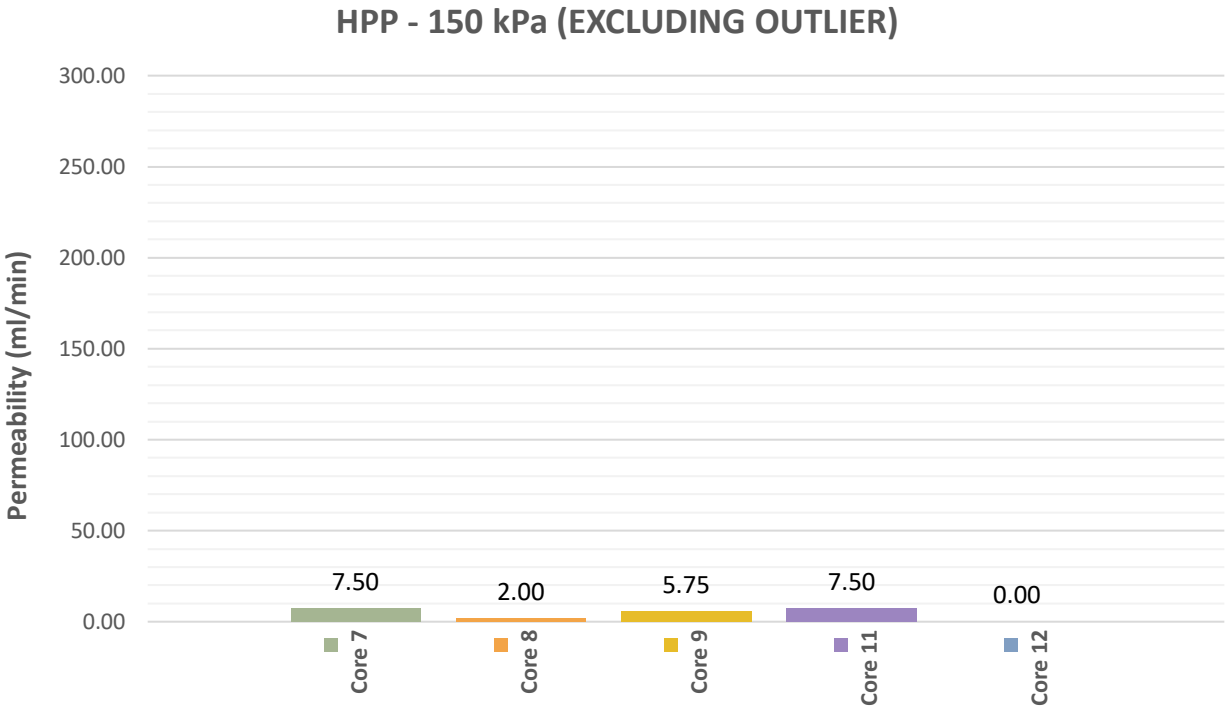

Figure 8.39: HPP permeability at 150 kPa (excluding outlier)

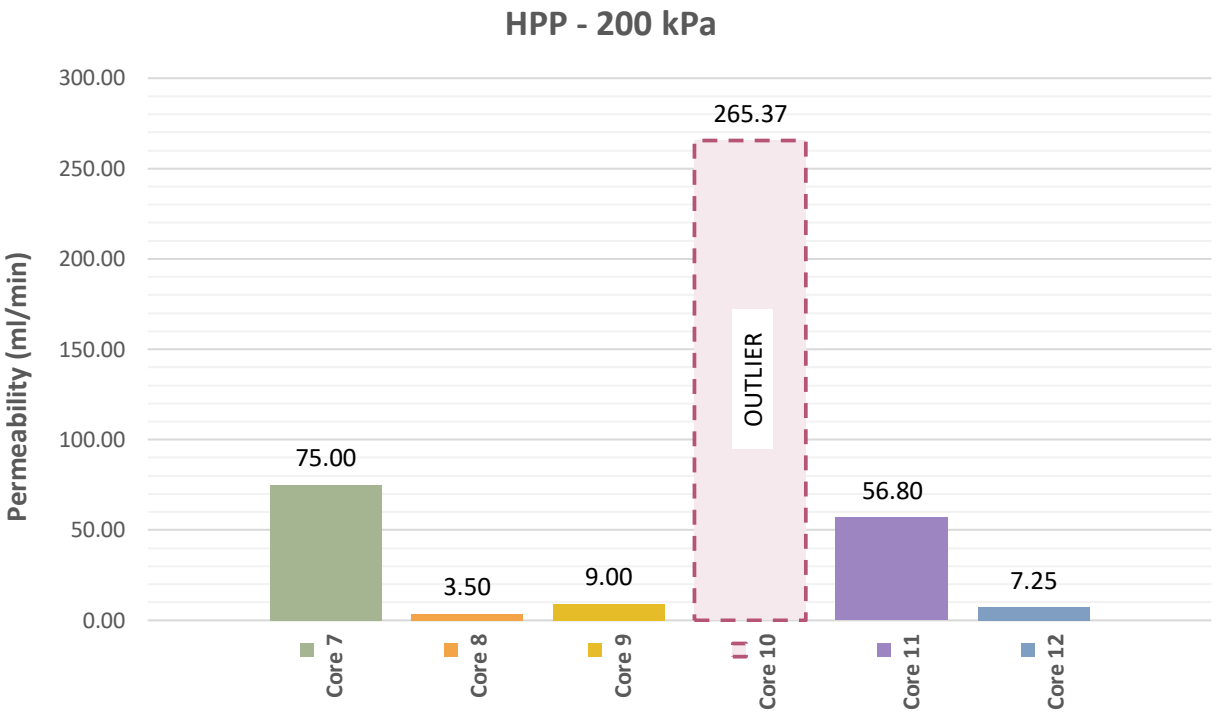

Figure 8.40: HPP permeability at 200 kPa

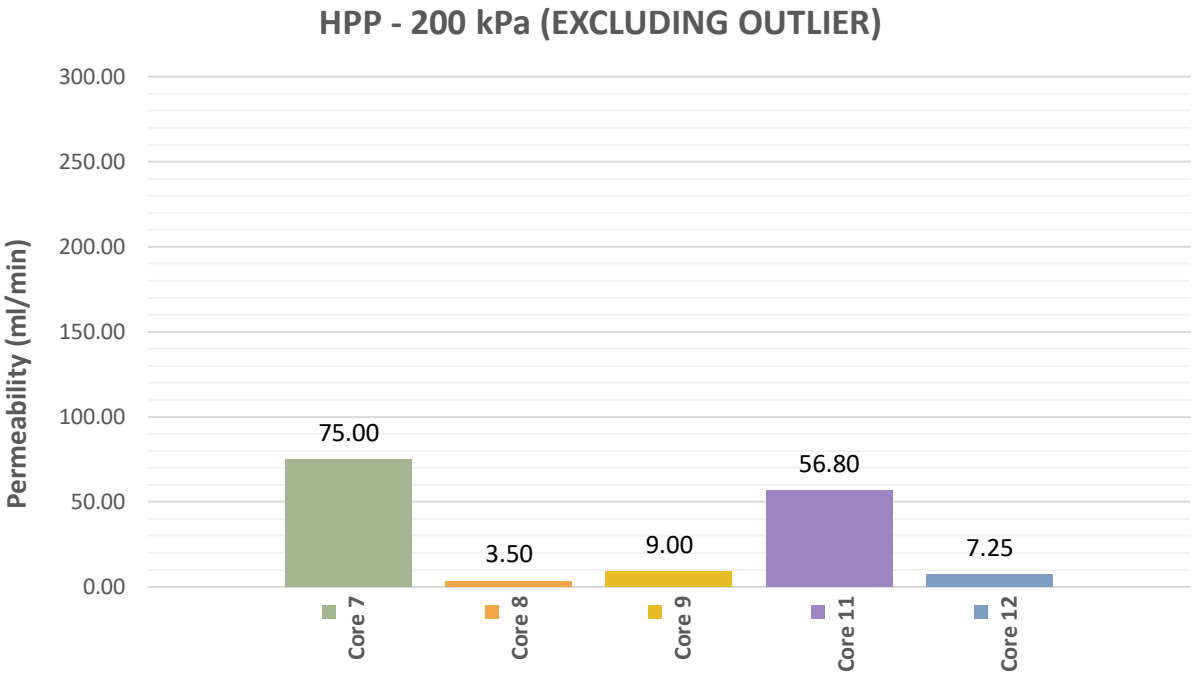

Figure 8.41: HPP permeability at 200 kPa (excluding outlier)

F.6 N3TC – MIX EV

Table 8.6: HPP permeability results for Mix Ev

Core	Permeability *(mℓ/min)*		
	100 kPa	150 kPa	200 kPa
23/01/2017 - 1	637,96	769,72	930,23
23/01/2017 - 2	430,42	623,05	768,25
23/01/2017 - 3	279,46	358,53	485,04
24/01/2017 - 1	276,31	400,00	489,60
24/01/2017 - 2	314,14	423,73	501,25

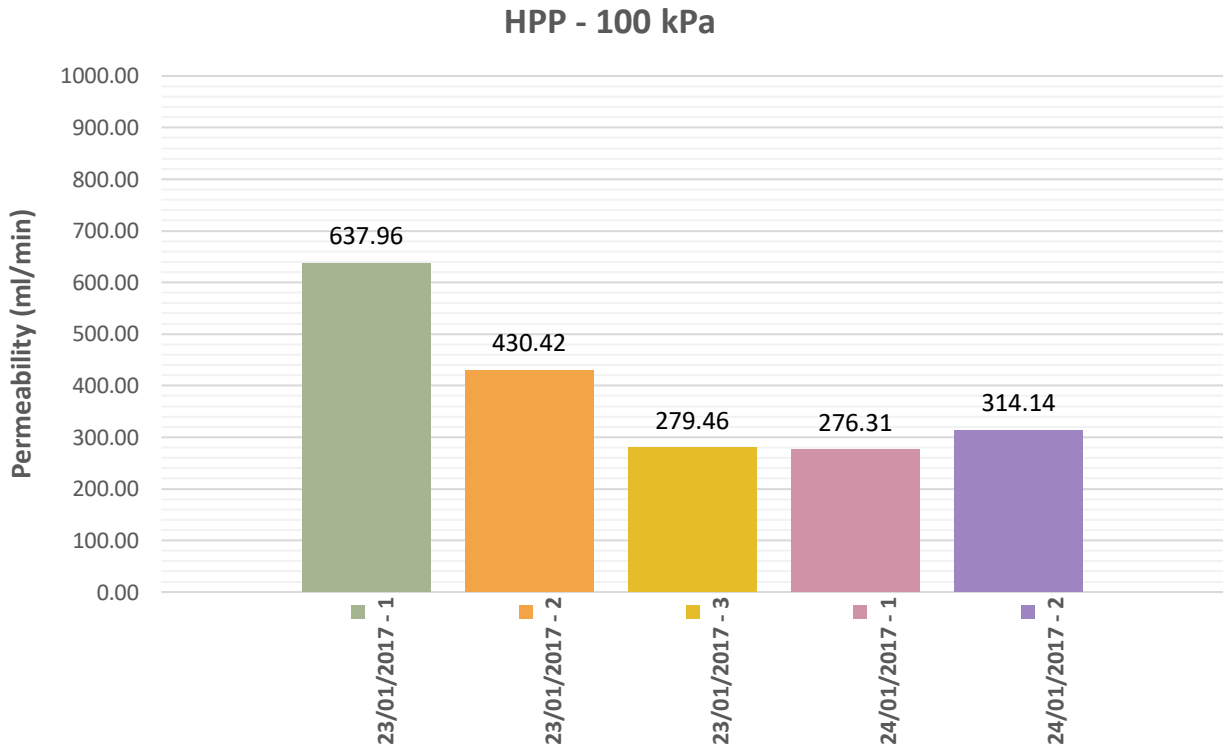

Figure 8.42: HPP permeability at 100 kPa

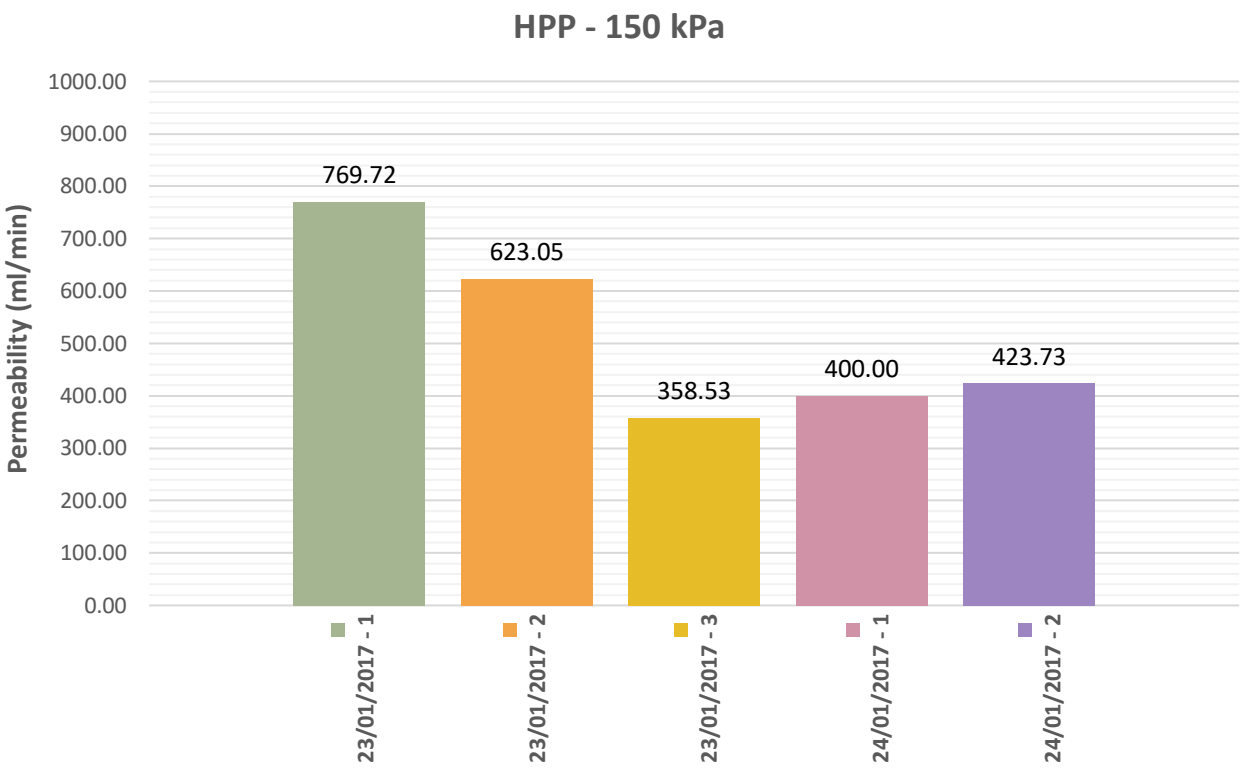

Figure 8.43: HPP permeability at 150 kPa

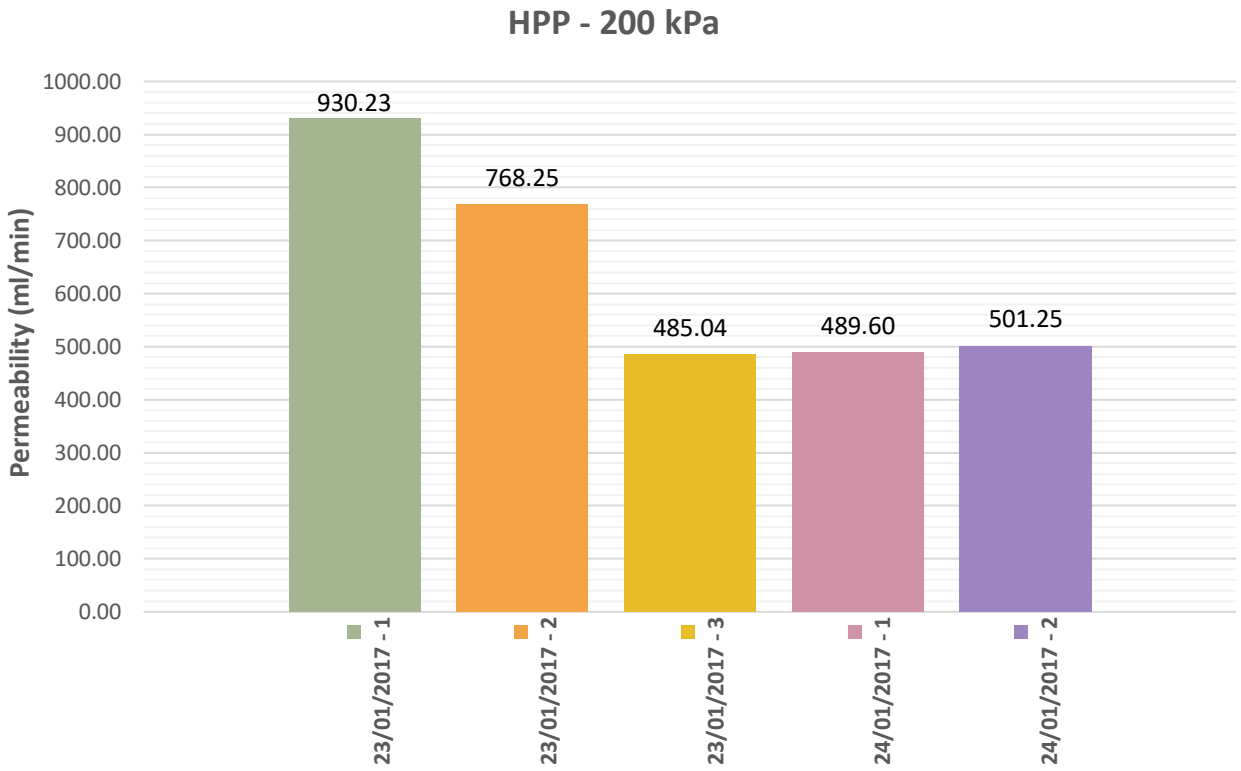

Figure 8.44: HPP permeability at 200 kPa

F.7 N7

Table 8.7: HPP permeability results for N7

Core	Permeability *(mℓ/min)*		
	100 kPa	150 kPa	200 kPa
Core V	0,04	0,04	0,03
Core W	0,04	0,00	0,00
Core X	0,05	0,04	0,03
Core Y	0,02	0,01	0,01
Core Z	0,03	0,02	0,01

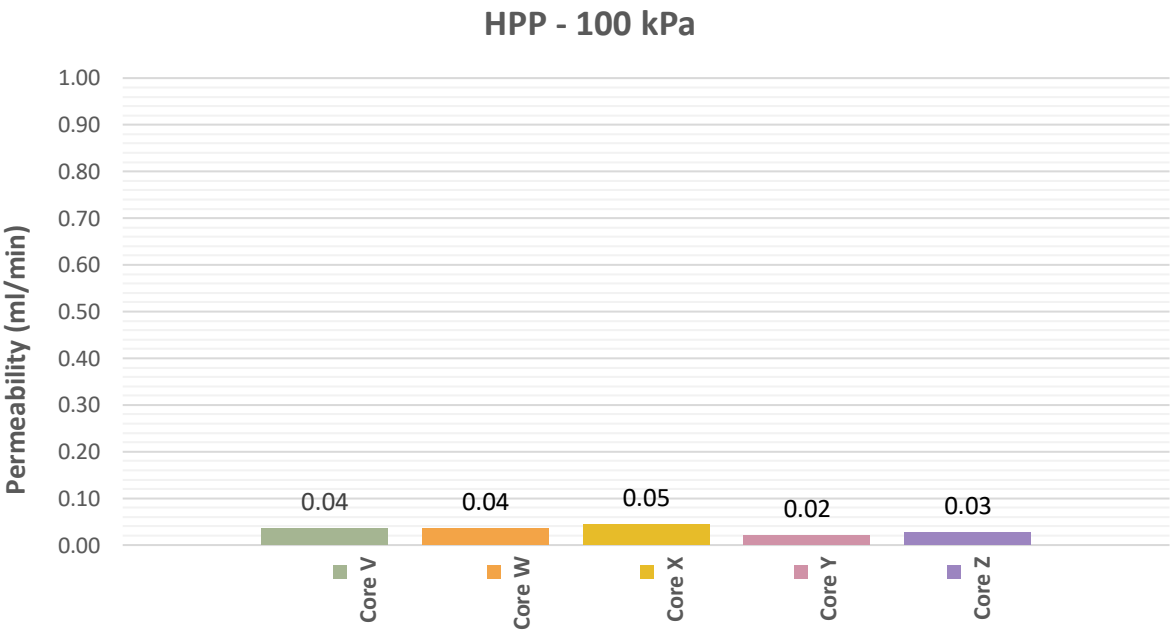

Figure 8.45: HPP permeability at 100 kPa

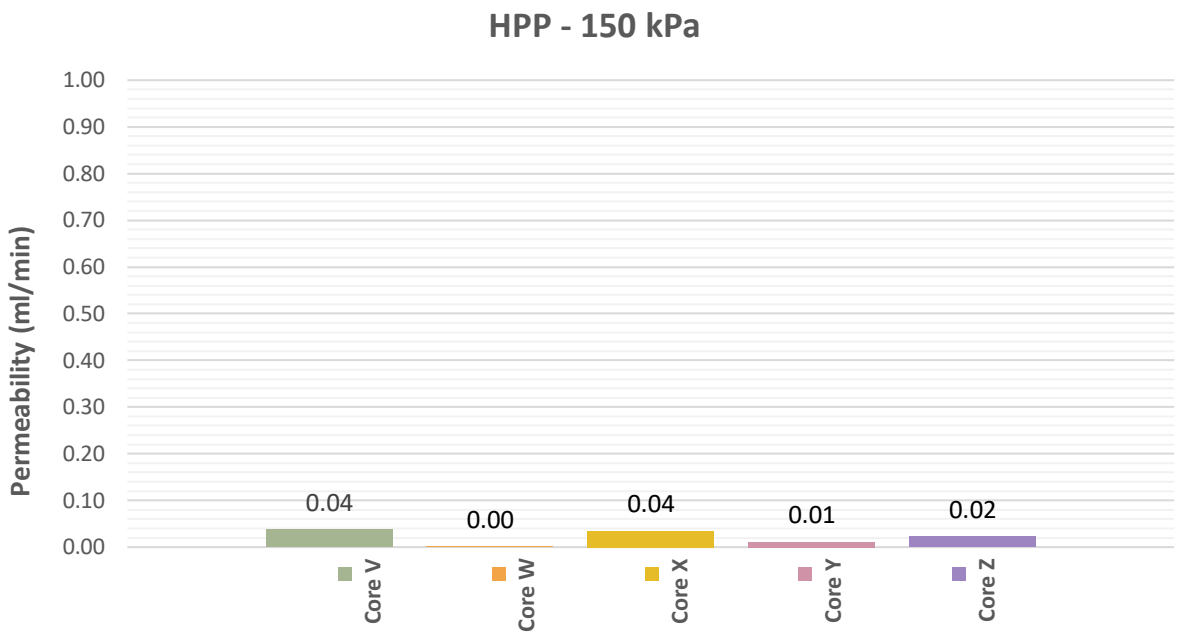

Figure 8.46: HPP permeability at 150 kPa

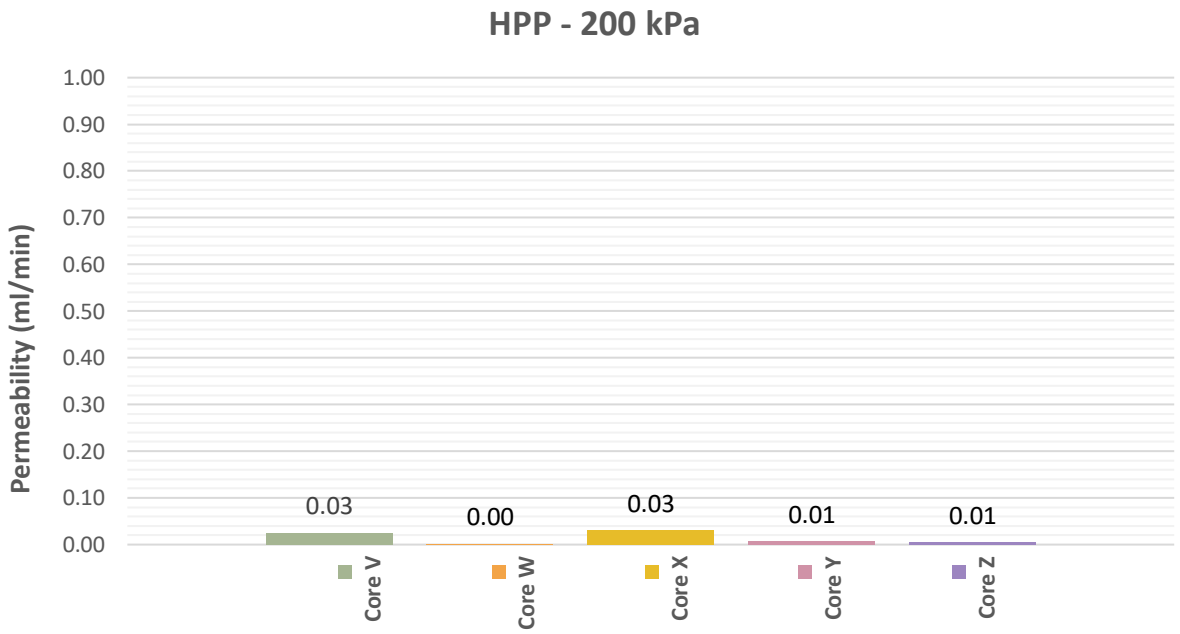

Figure 8.47: HPP permeability at 200 kPa

F.8 MUCH ASPHALT – SEMI-GAP GRADED

Table 8.8: HPP permeability results for semi-gap graded

Core	Permeability *(mℓ/min)*		
	100 kPa	150 kPa	200 kPa
1	0,00	0,00	0,00
2	0,00	0,00	0,00

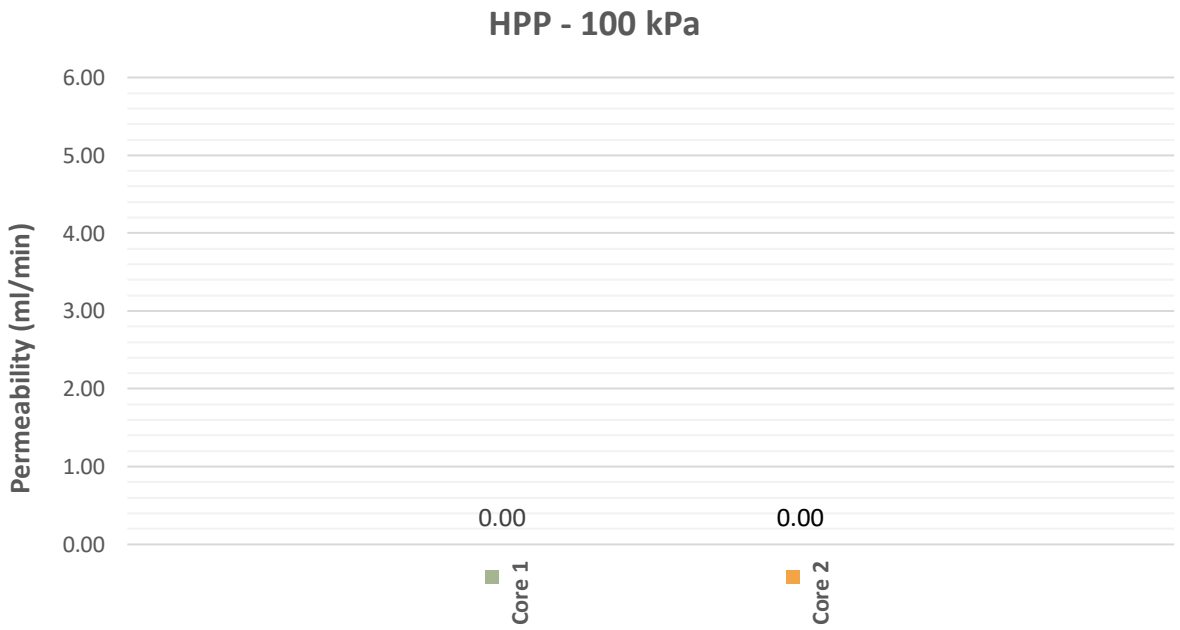

Figure 8.48: HPP permeability at 100 kPa

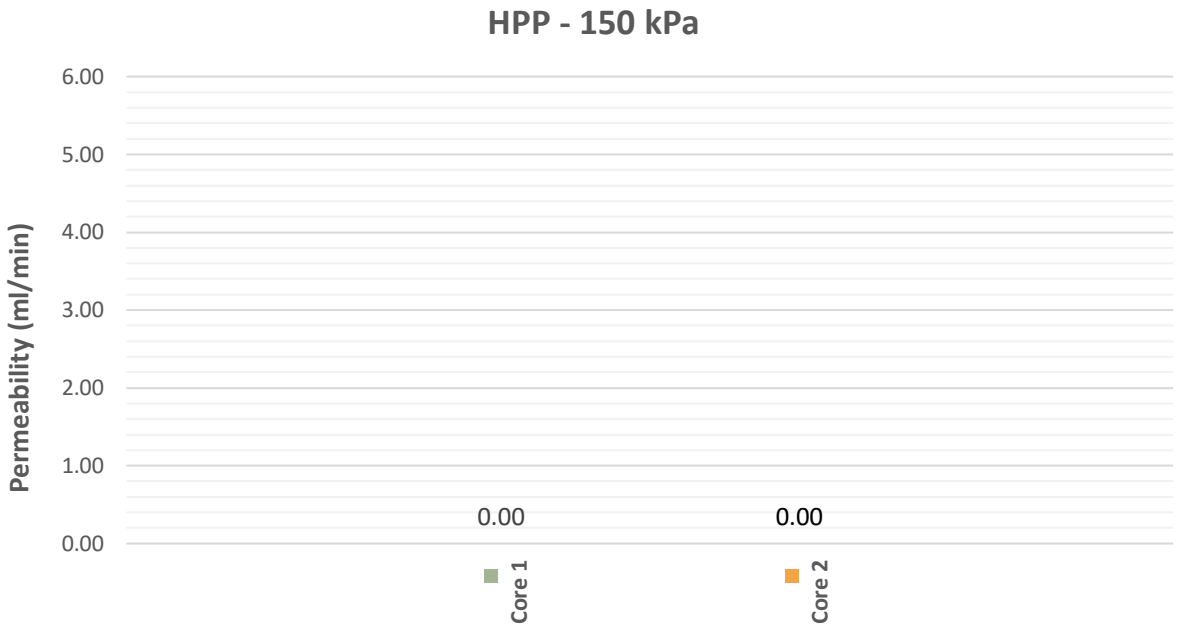

Figure 8.49: HPP permeability at 150 kPa

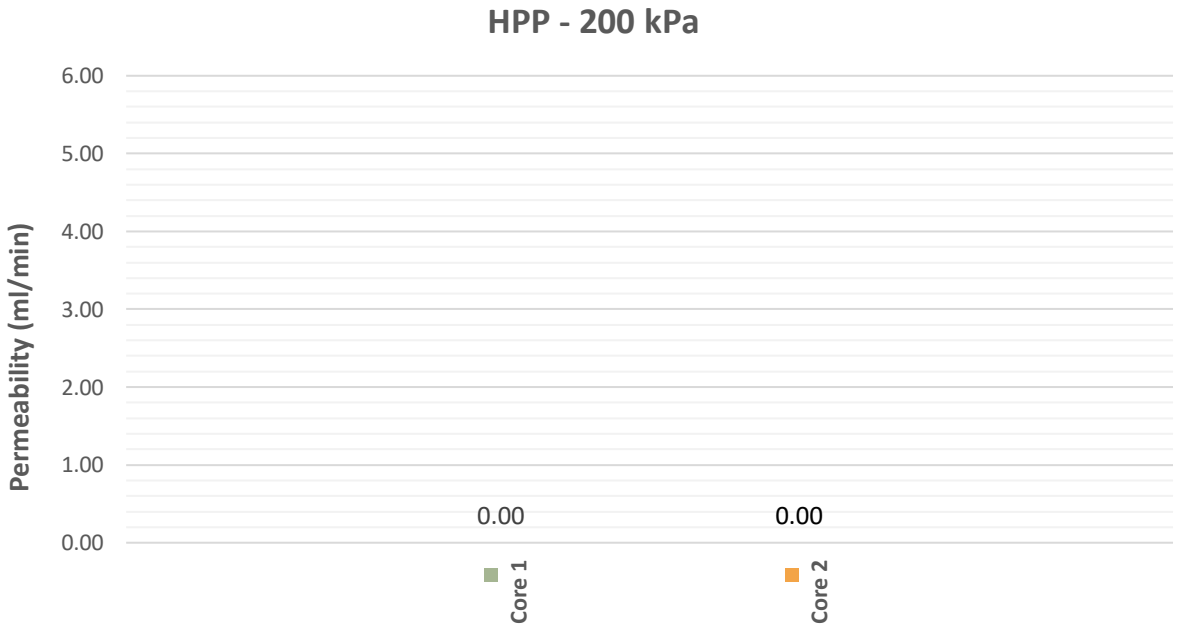

Figure 8.50: HPP permeability at 200 kPa

F.9 MUCH ASPHALT – COLTO MEDIUM

Table 8.9: HPP permeability results for COLTO medium

Core	Permeability *(mℓ/min)*		
	100 kPa	150 kPa	200 kPa
5	0,00	0,00	0,00
6	0,00	0,00	0,00

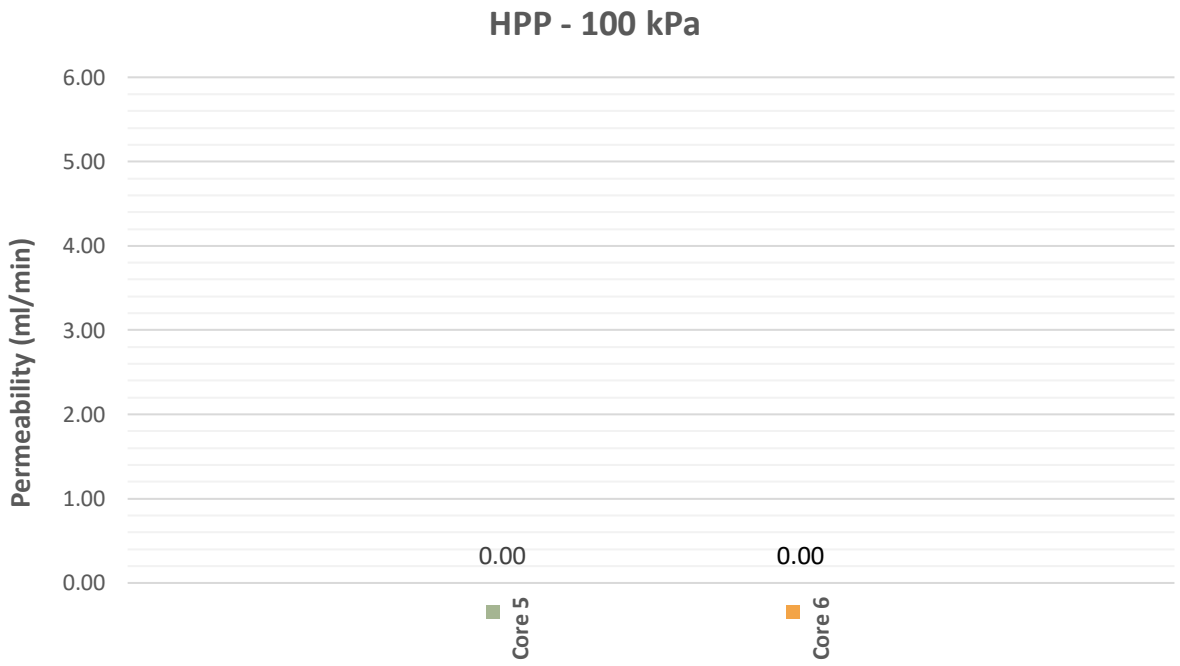

Figure 8.51: HPP permeability at 100 kPa

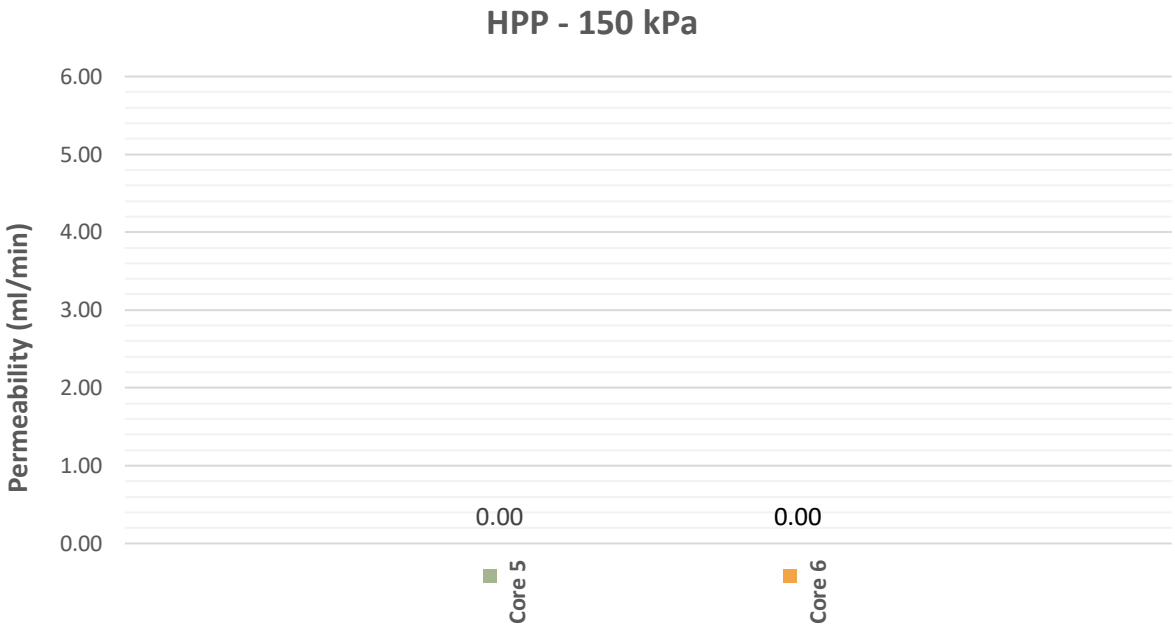

Figure 8.52: HPP permeability at 150 kPa

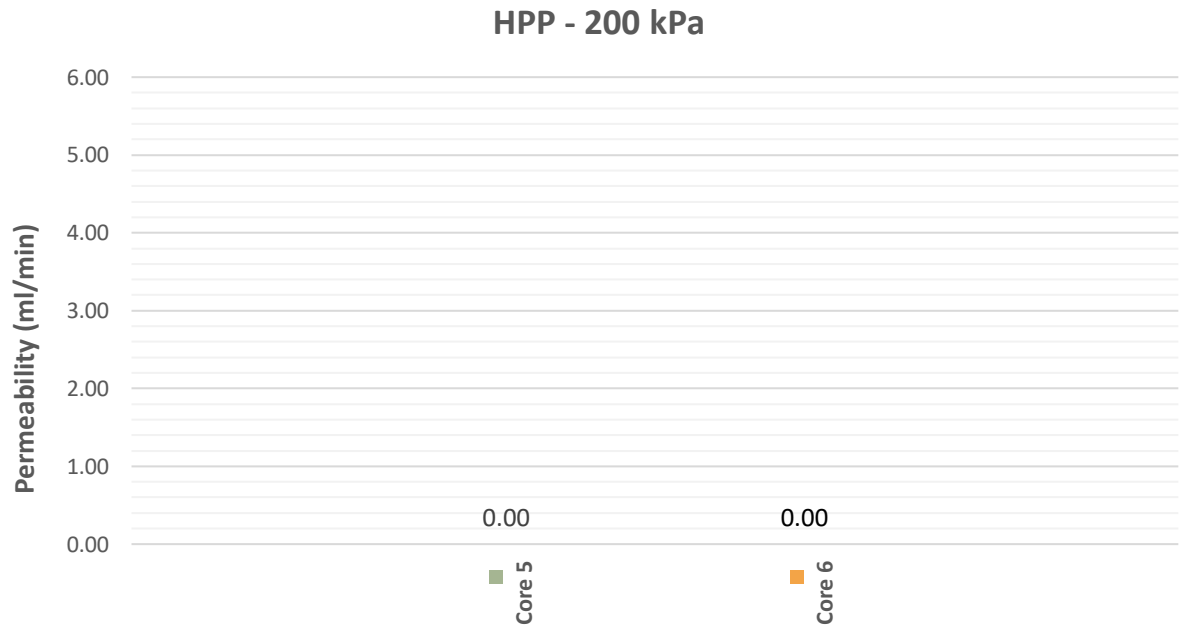

Figure 8.53: HPP permeability at 200 kPa

APPENDIX G RESULTS – HPP POST MIST

G.1 RAUBEX – SECTION 1

Table 8.10: HPP (MIST) permeability results for Section 1

Core	Permeability *(mℓ/min)*		
	100 kPa	150 kPa	200 kPa
B	19,90	35,43	35,43
F	14,20	17,20	24,67

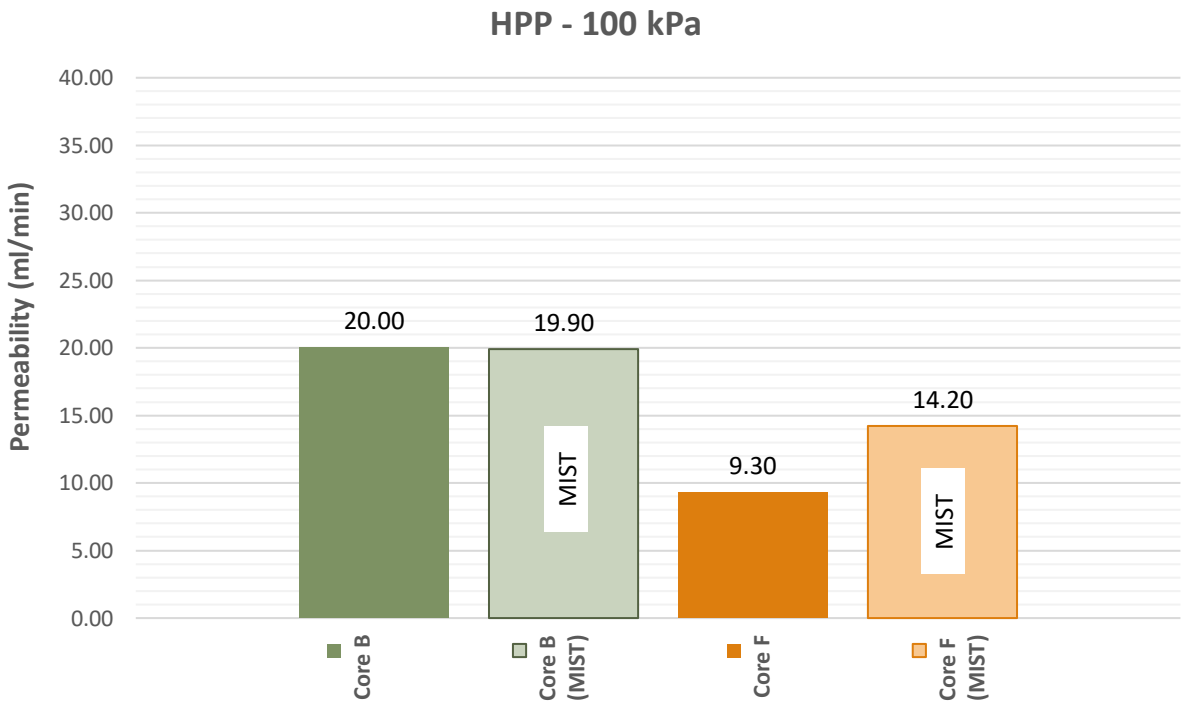

Figure 8.54: HPP (MIST) permeability at 100 kPa

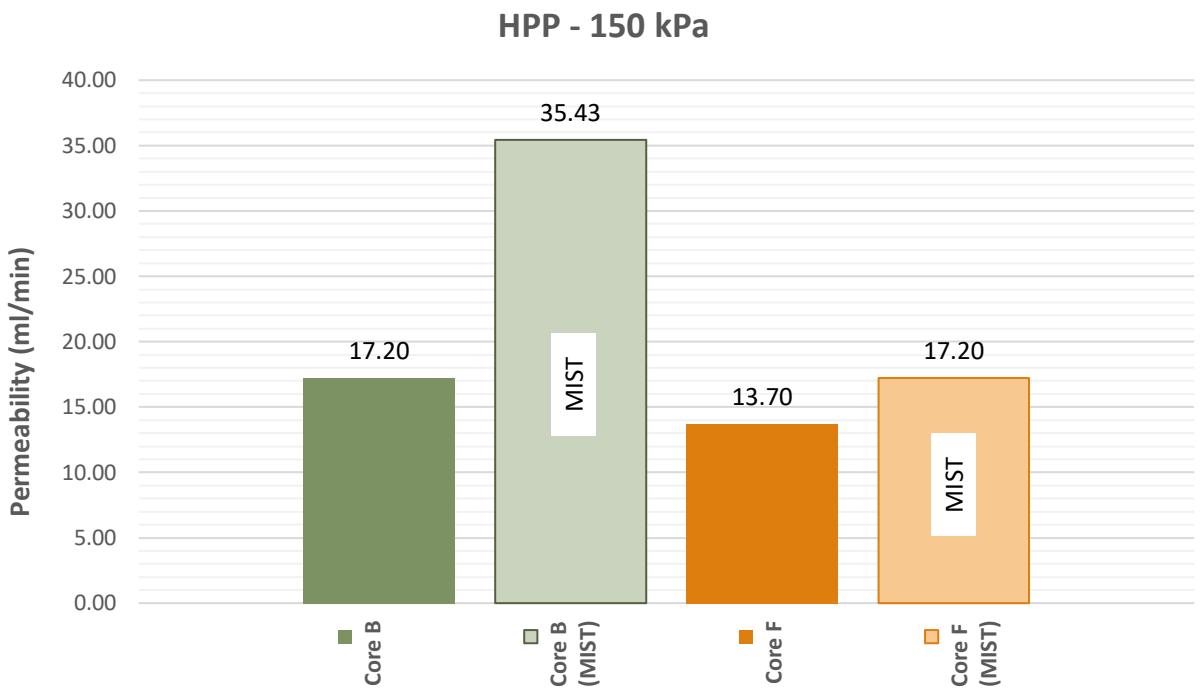

Figure 8.55: HPP (MIST) permeability at 150 kPa

Figure 8.56: HPP (MIST) permeability at 200 kPa

G.2 RAUBEX – SECTION 2

Table 8.11: HPP (MIST) permeability results for Section 2

Core	Permeability *(mℓ/min)*		
	100 kPa	**150 kPa**	**200 kPa**
I	264,78	433,37	526,32
M	1,50	2,70	3,40

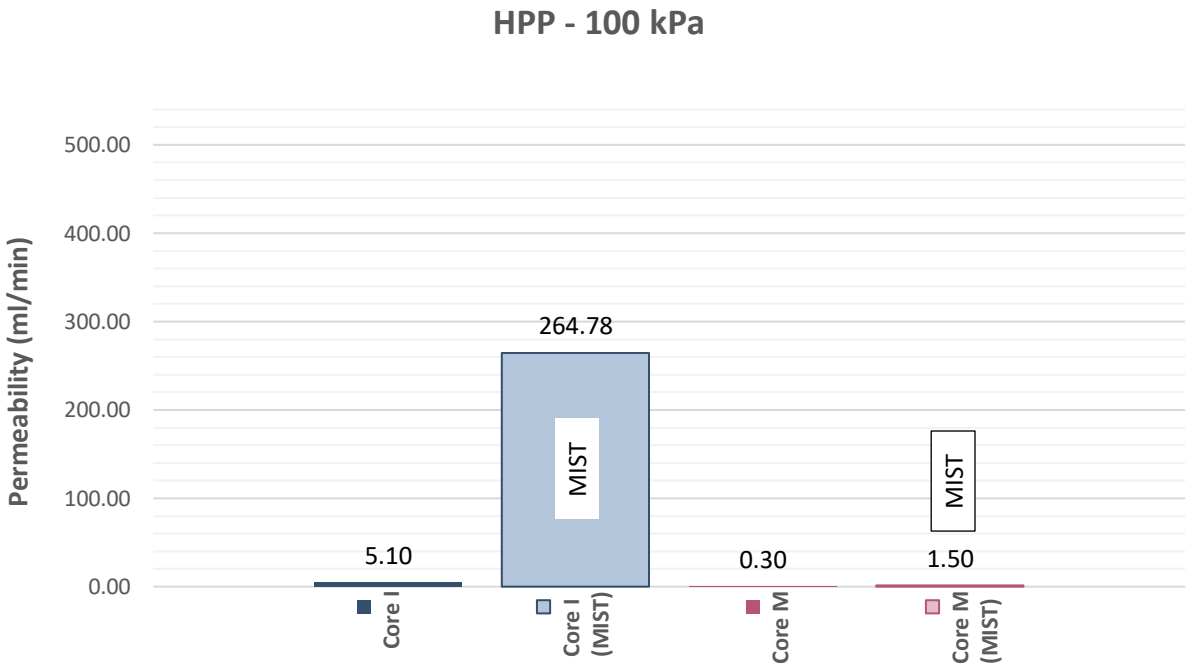

Figure 8.57: HPP (MIST) permeability at 100 kPa

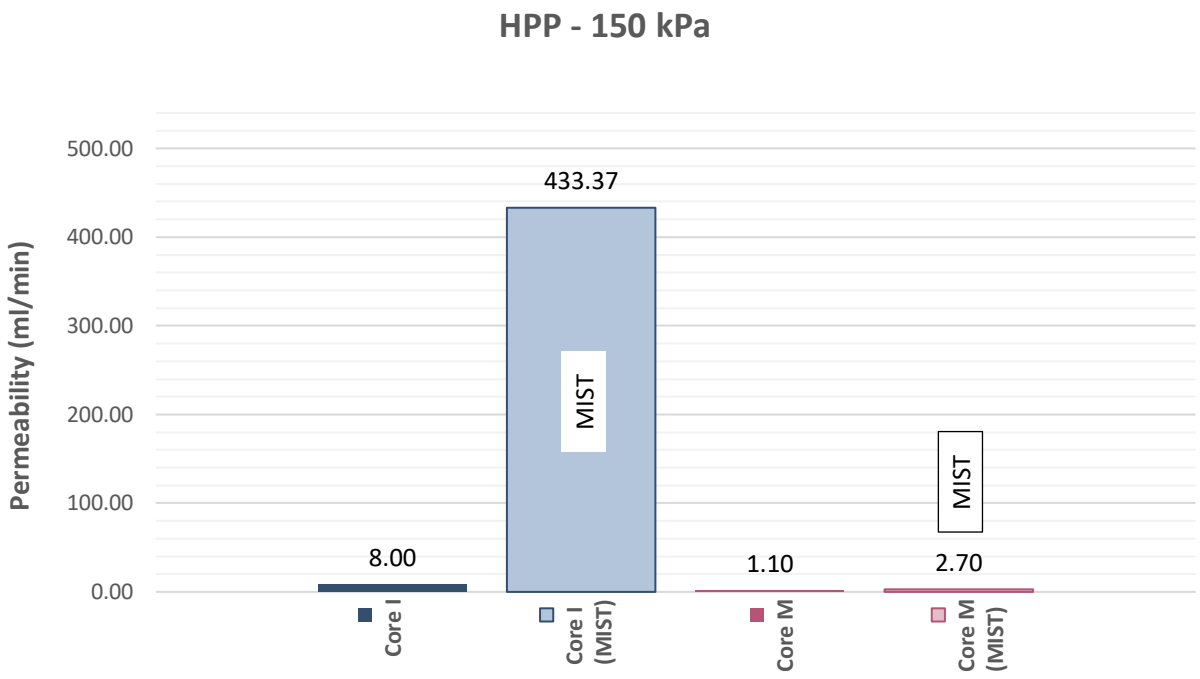

Figure 8.58: HPP (MIST) permeability at 150 kPa

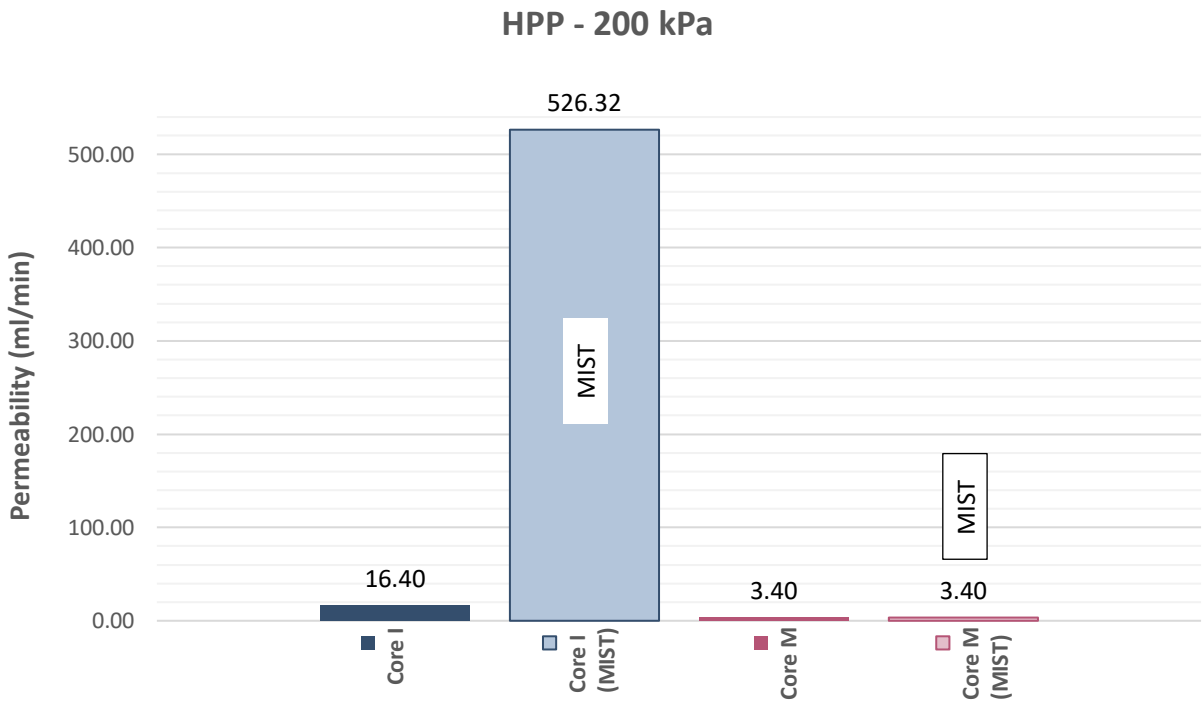

Figure 8.59: HPP (MIST) permeability at 200 kPa

G.3 RAUBEX – SECTION 3

Table 8.12: HPP (MIST) permeability results for Section 3

Core	Permeability *(mℓ/min)*		
	100 kPa	**150 kPa**	**200 kPa**
O	20,40	32,00	50,70
P	1880,88	2054,79	2065,40

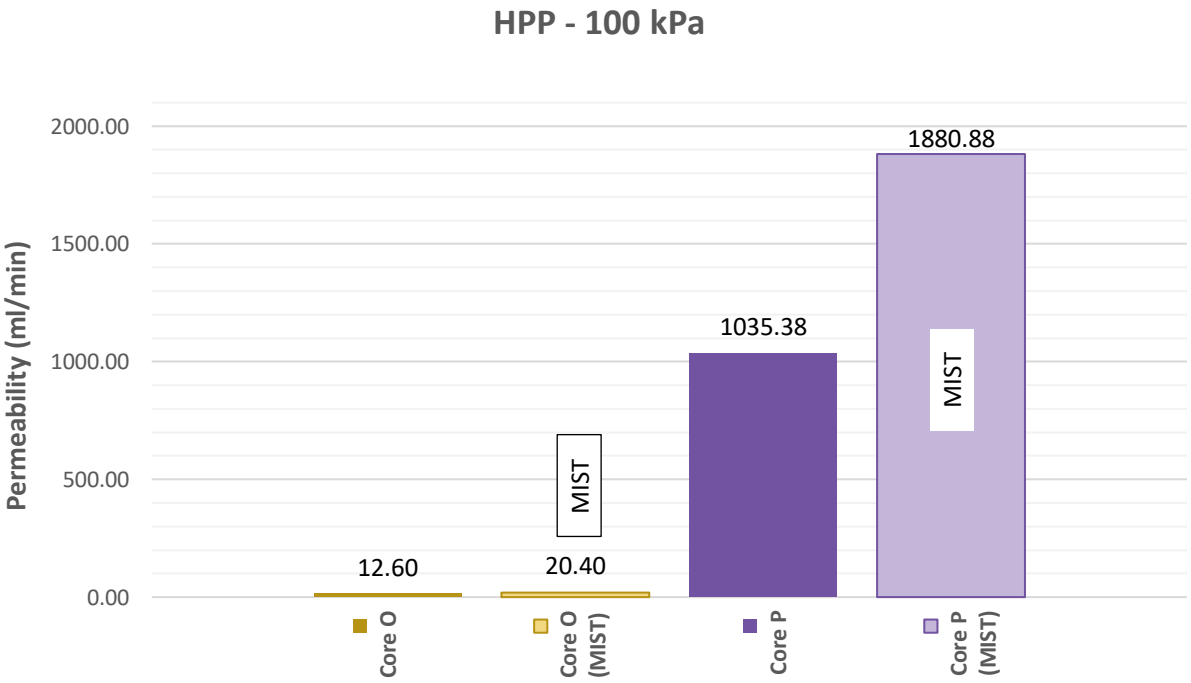

Figure 8.60: HPP (MIST) permeability at 100 kPa

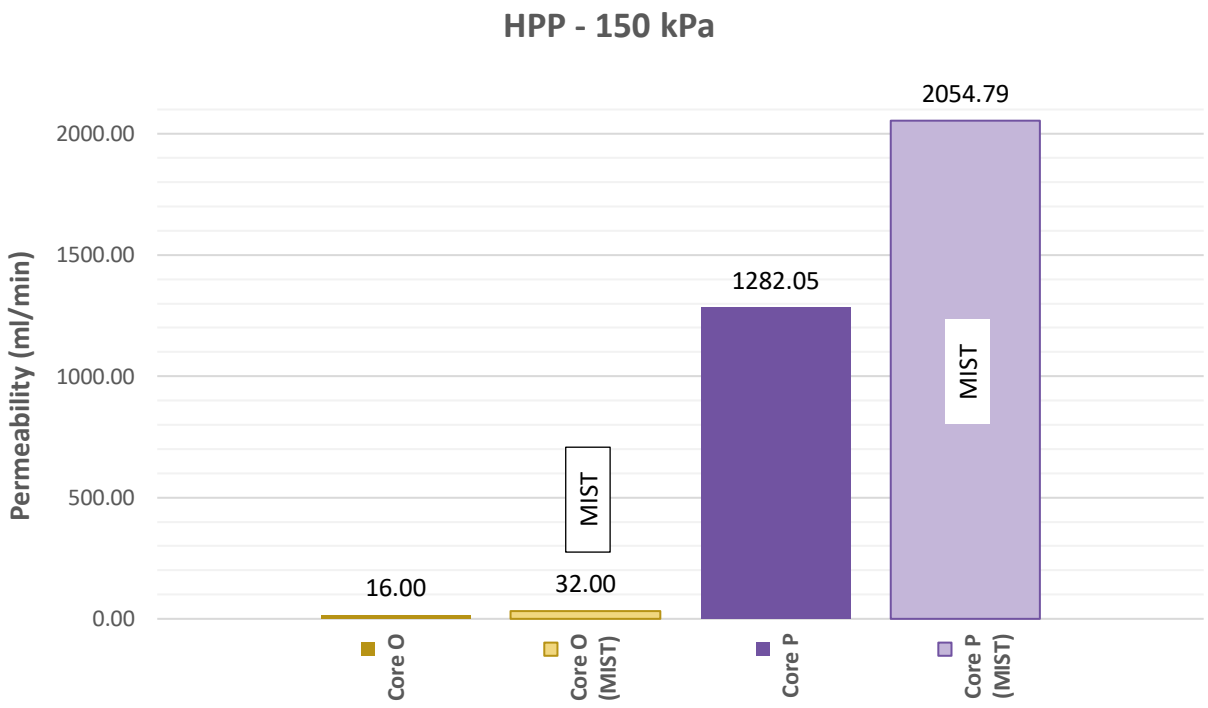

Figure 8.61: HPP (MIST) permeability at 150 kPa

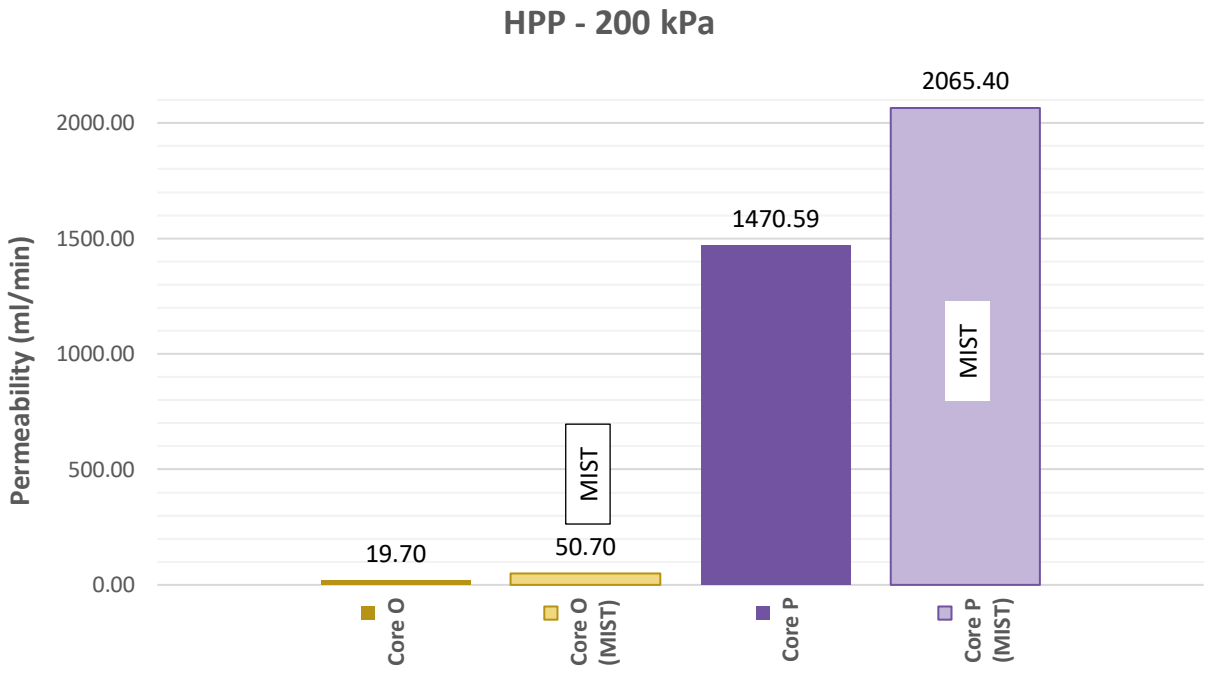

Figure 8.62: HPP (MIST) permeability at 200 kPa

G.4 N3TC – MIX CD

Table 8.13: HPP (MIST) permeability results for Mix Cd

Core	Permeability *(mℓ/min)*		
	100 kPa	**150 kPa**	**200 kPa**
1	179,32	210,86	261,72
2	113,65	153,67	168,87
5	73,99	90,00	160,69

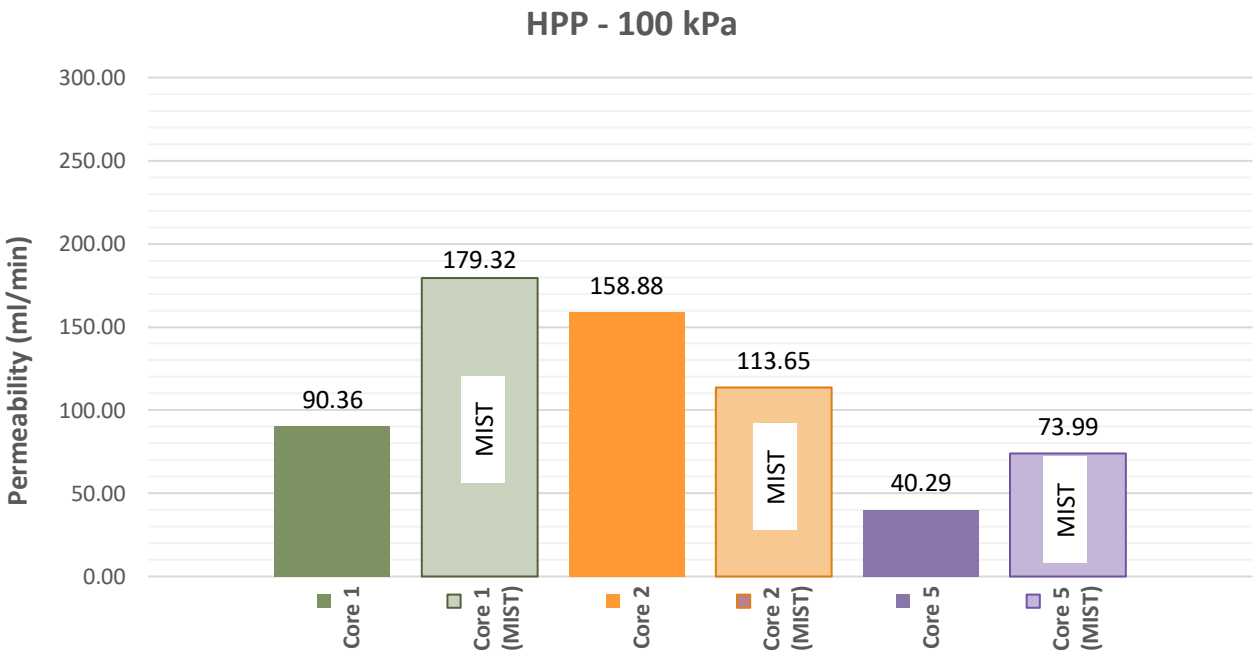

Figure 8.63: HPP (MIST) permeability at 100 kPa

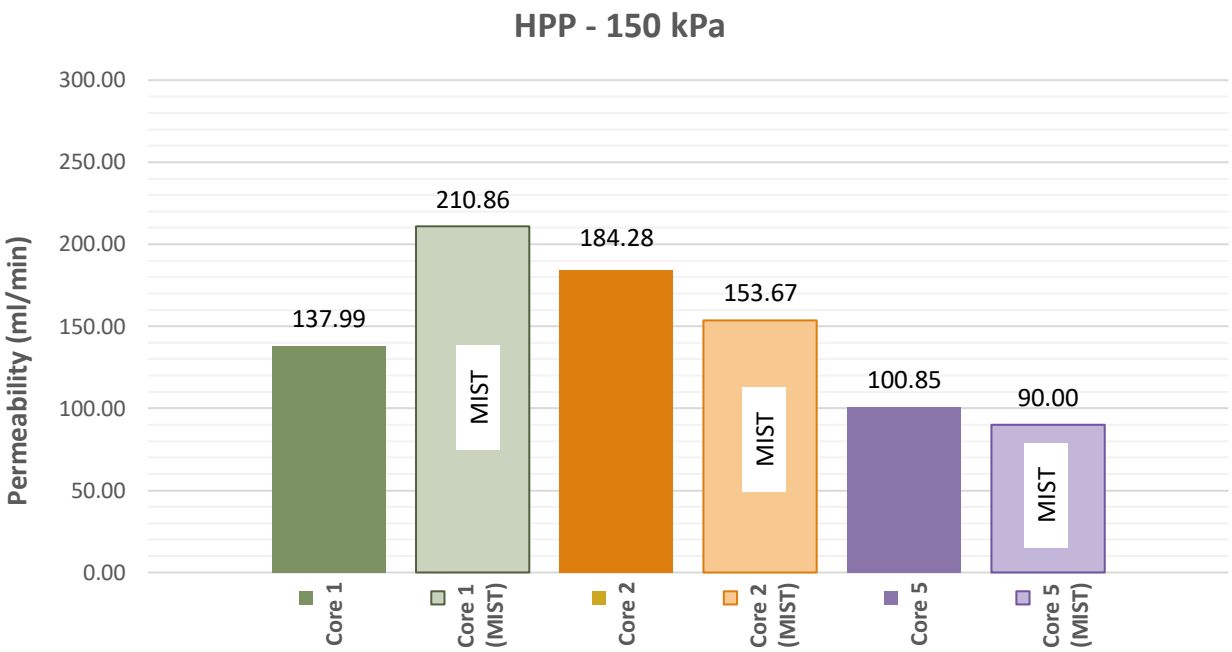

Figure 8.64: HPP (MIST) permeability at 150 kPa

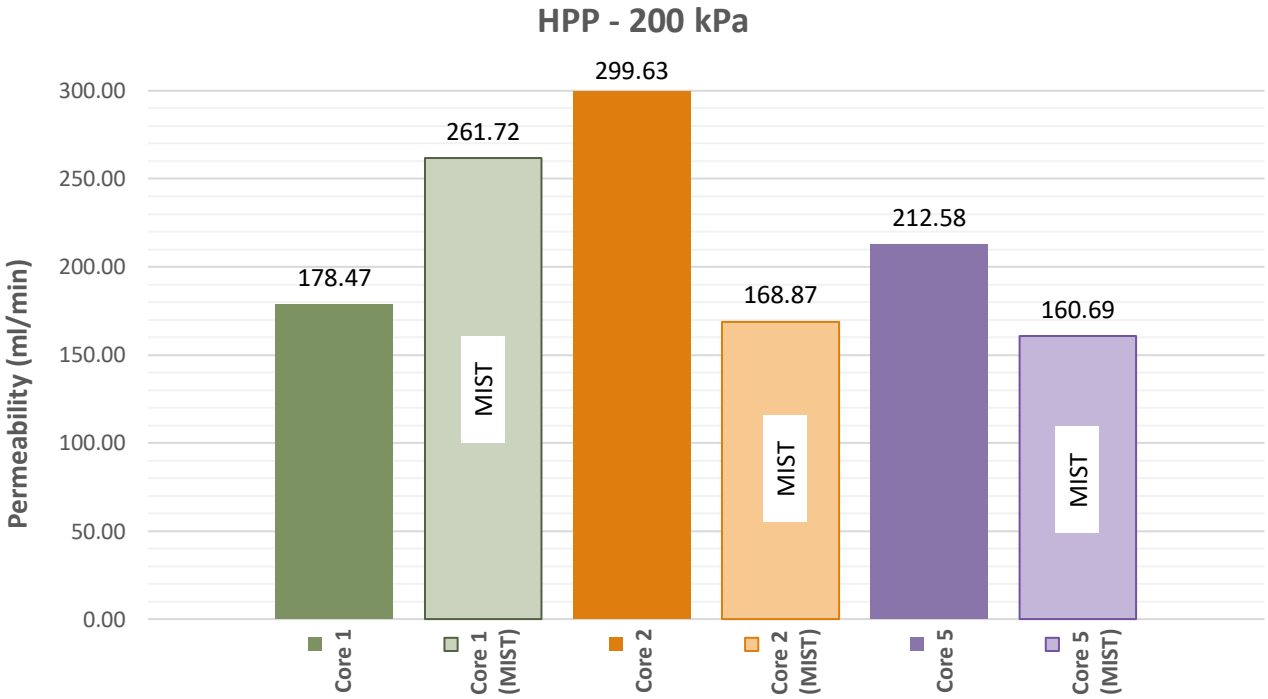

Figure 8.65: HPP (MIST) permeability at 200 kPa

G.5 N3TC – MIX CP

Table 8.14: HPP (MIST) permeability results for Mix Cp

Core	Permeability *(mℓ/min)*		
	100 kPa	150 kPa	200 kPa
7	0,00	3,25	95,22
9	0,00	2,25	4,00
12	0,00	0,00	0,50

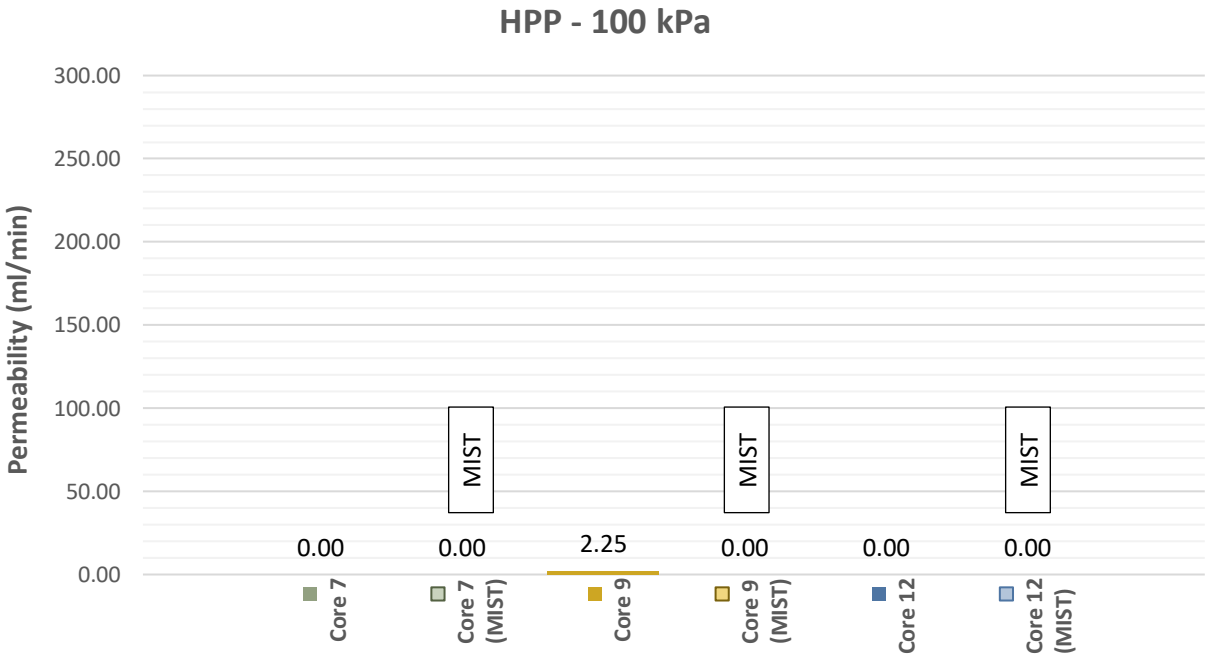

Figure 8.66: HPP (MIST) permeability at 100 kPa

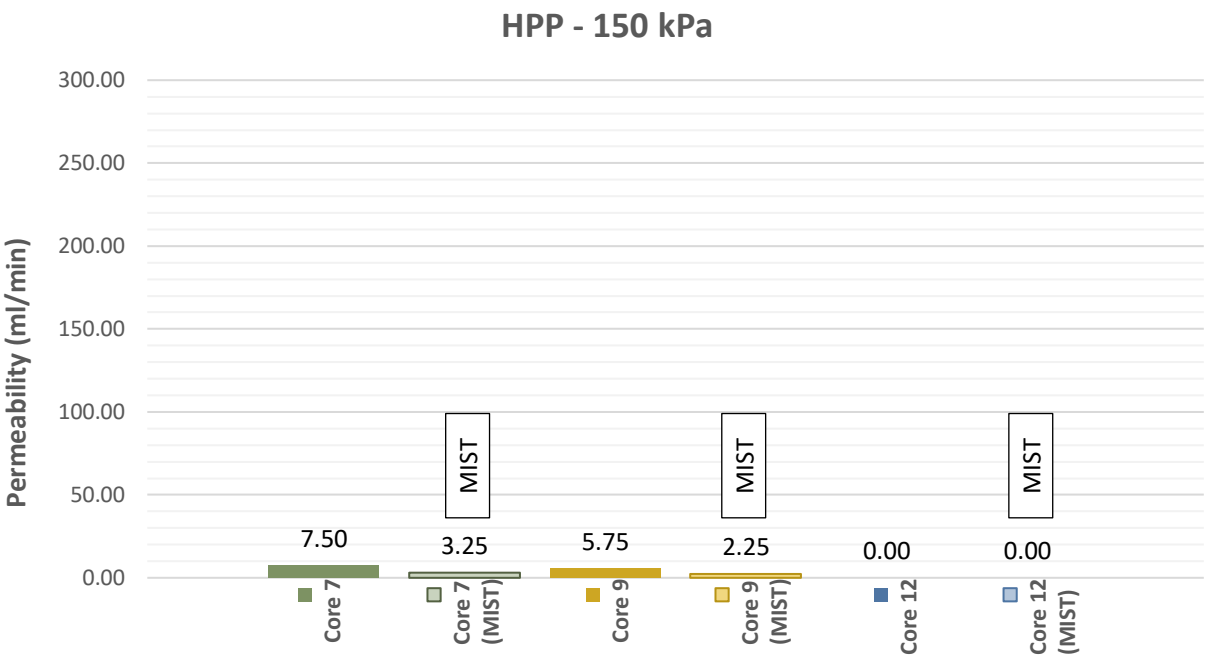

Figure 8.67: HPP (MIST) permeability at 150 kPa

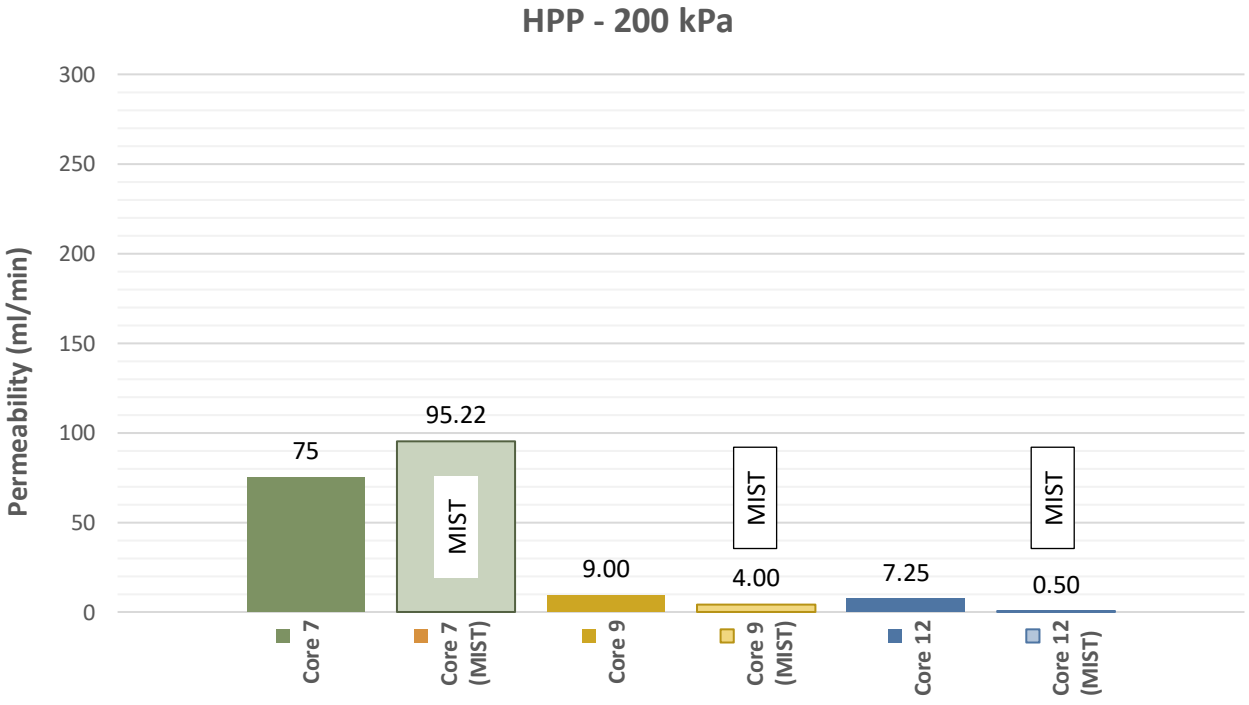

Figure 8.68: HPP (MIST) permeability at 200 kPa

G.6 N3TC – MIX EV

Table 8.15: HPP (MIST) permeability results for Mix Ev

Core	Permeability *(mℓ/min)*		
	100 kPa	150 kPa	200 kPa
23/01/2017 - 1	384,49	455,93	476,76
23/01/2017 - 3	201,38	239,43	311,12
24/01/2017 - 2	184,36	216,22	245,25

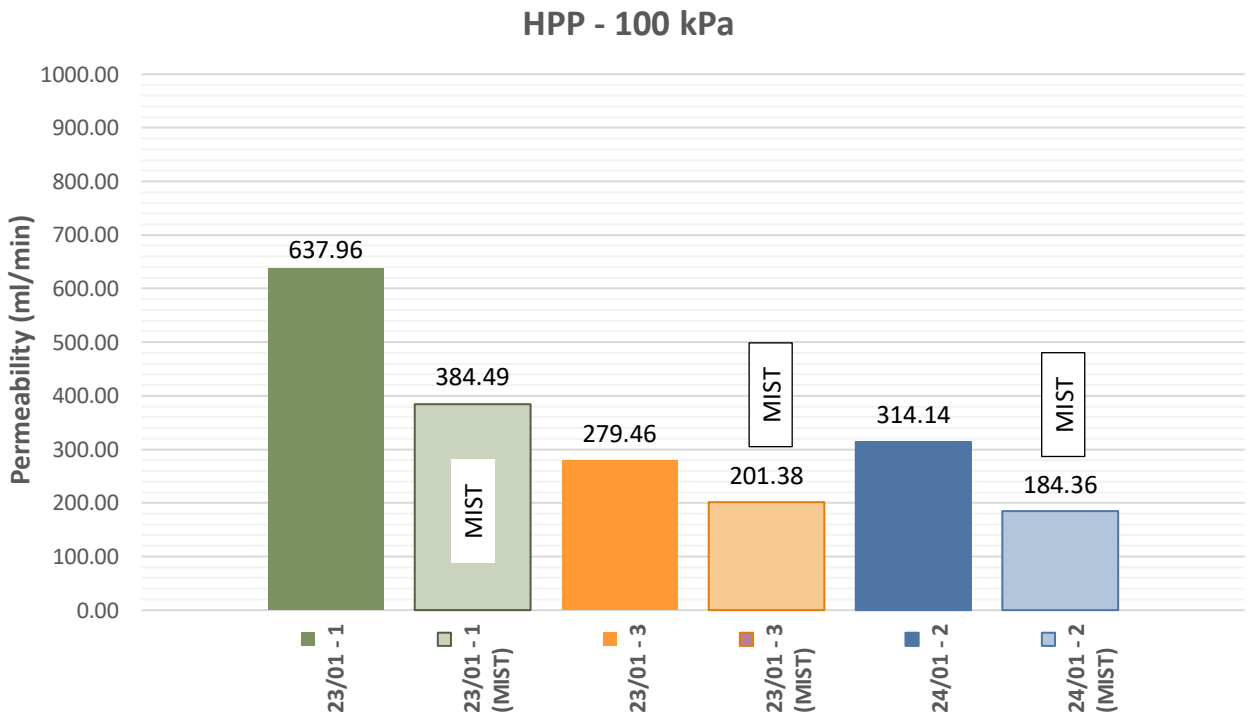

Figure 8.69: HPP (MIST) permeability at 100 kPa

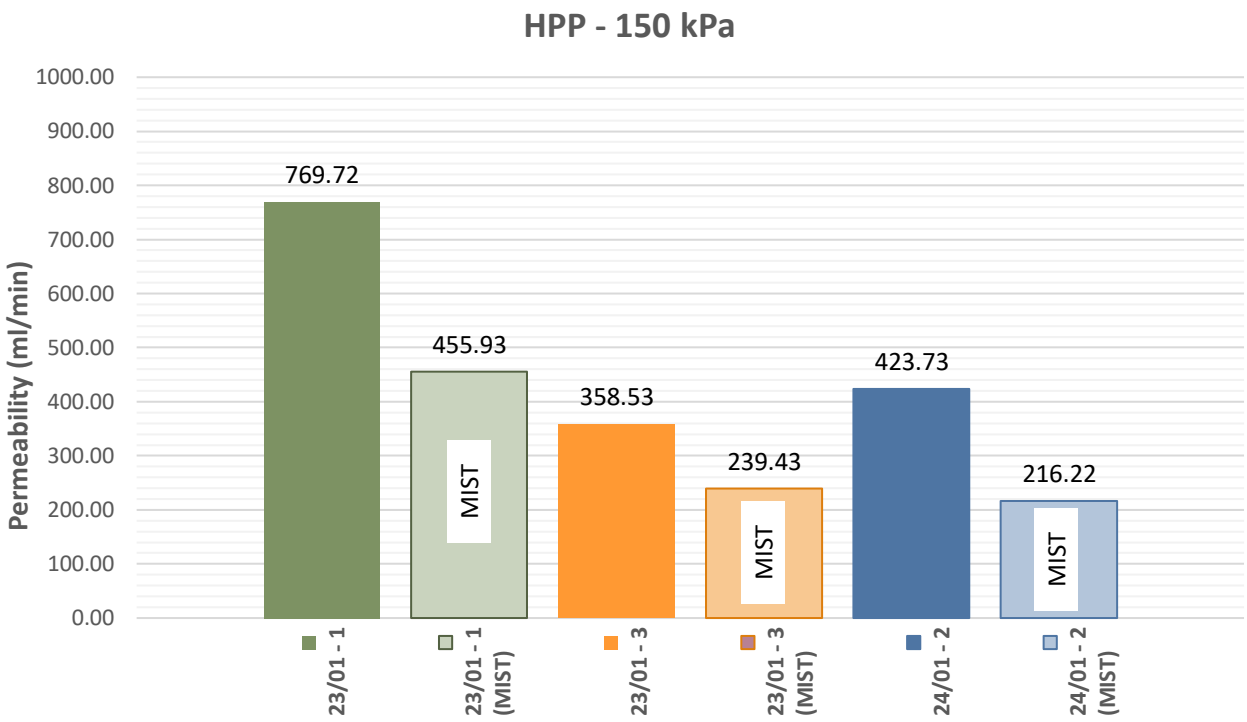

Figure 8.70: HPP (MIST) permeability at 150 kPa

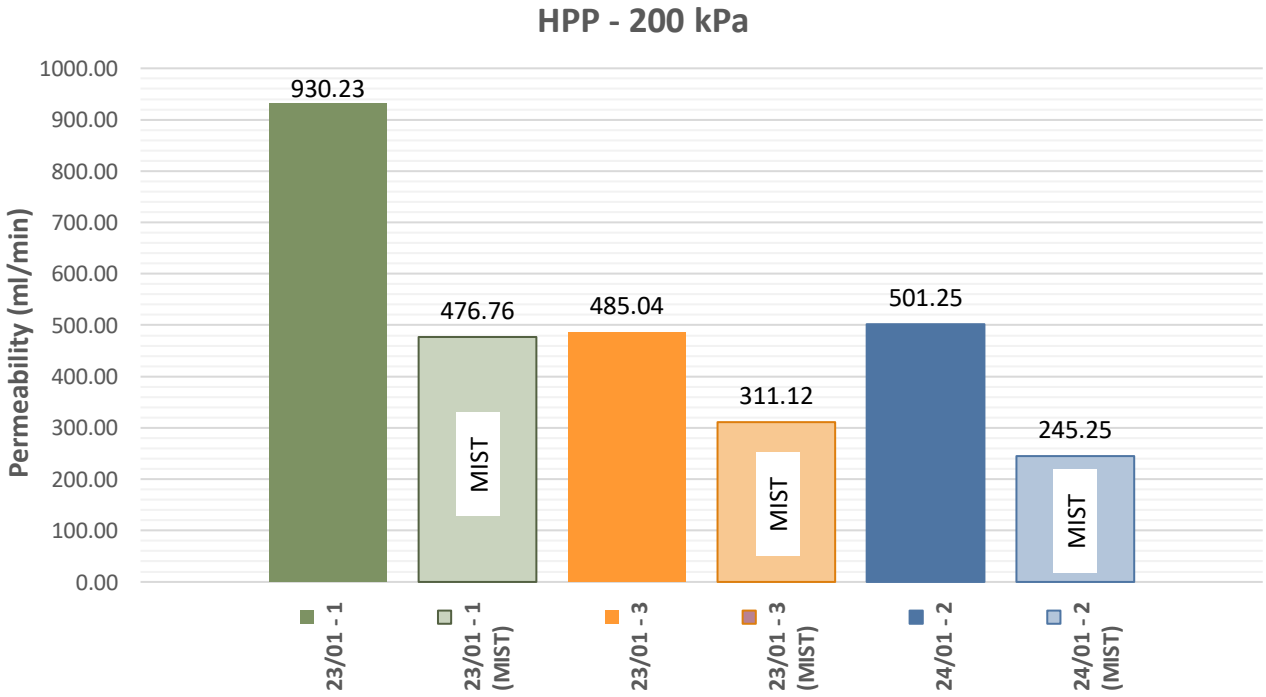

Figure 8.71: HPP (MIST) permeability at 200 kPa

APPENDIX H RESULTS – CT SCANS

H.1 N3TC - MIX CD

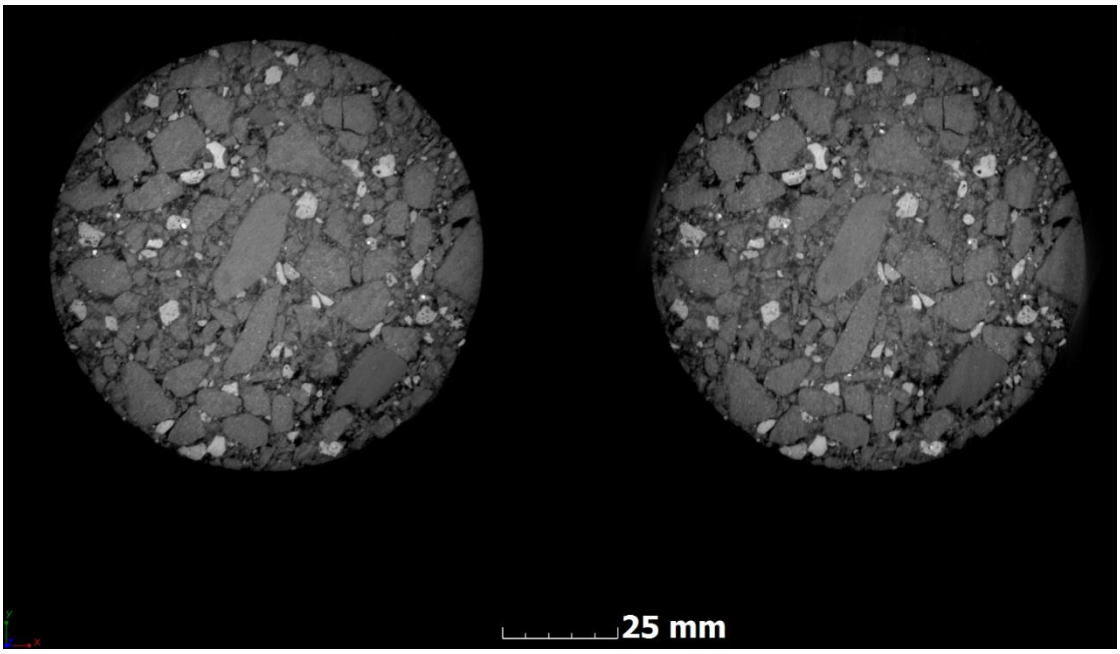

Figure 8.72: Core 1 CT-scan before MIST (left) and after MIST (right)

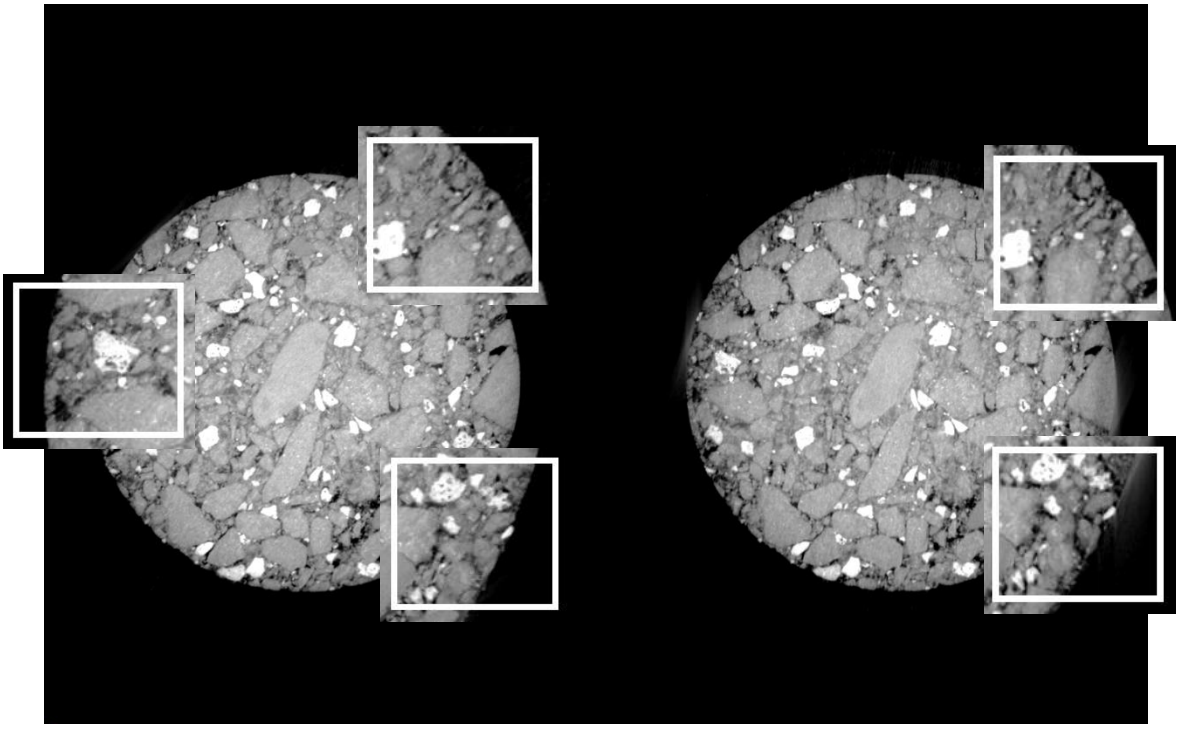

Figure 8.73: Core 1 inter-connected voids before MIST (left) and after MIST (right)

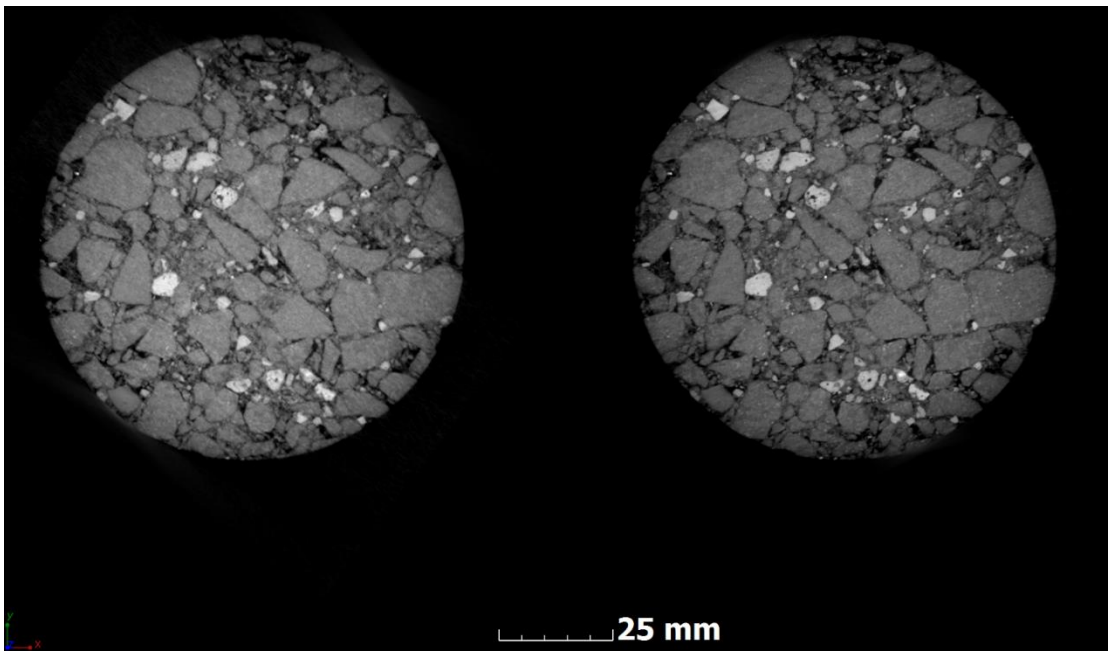

Figure 8.74: Core 2 CT-scan before MIST (left) and after MIST (right)

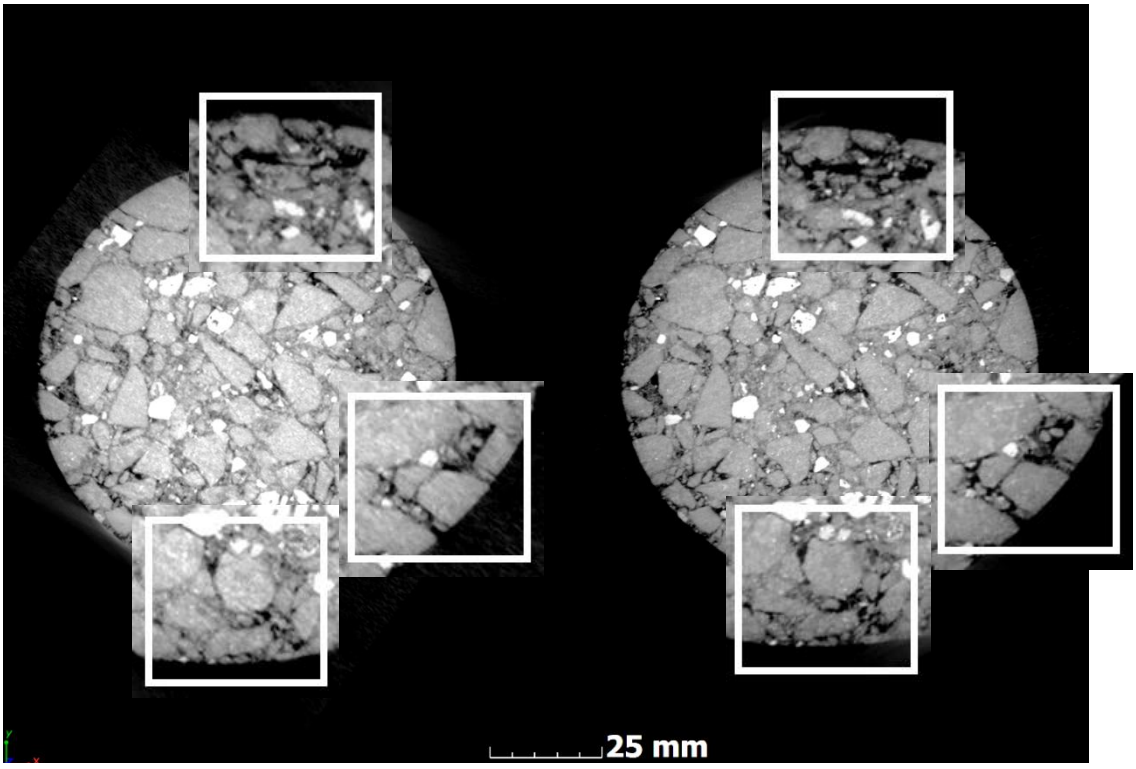

Figure 8.75: Core 2 inter-connected voids before MIST (left) and after MIST (right)

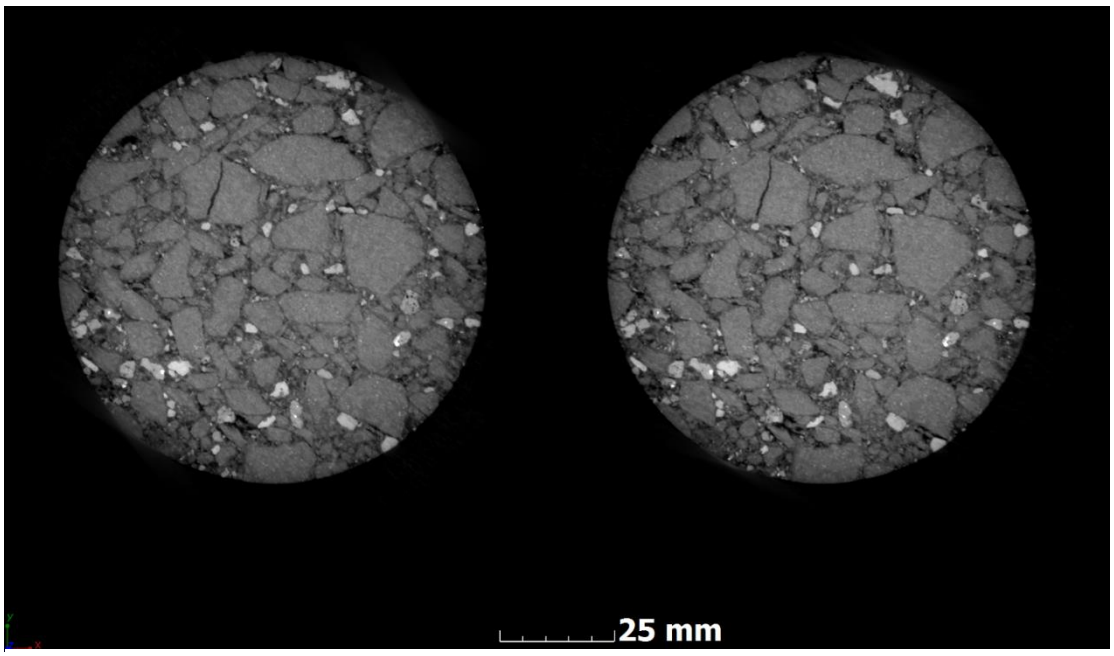

Figure 8.76: Core 5 CT-scan before MIST (left) and after MIST (right)

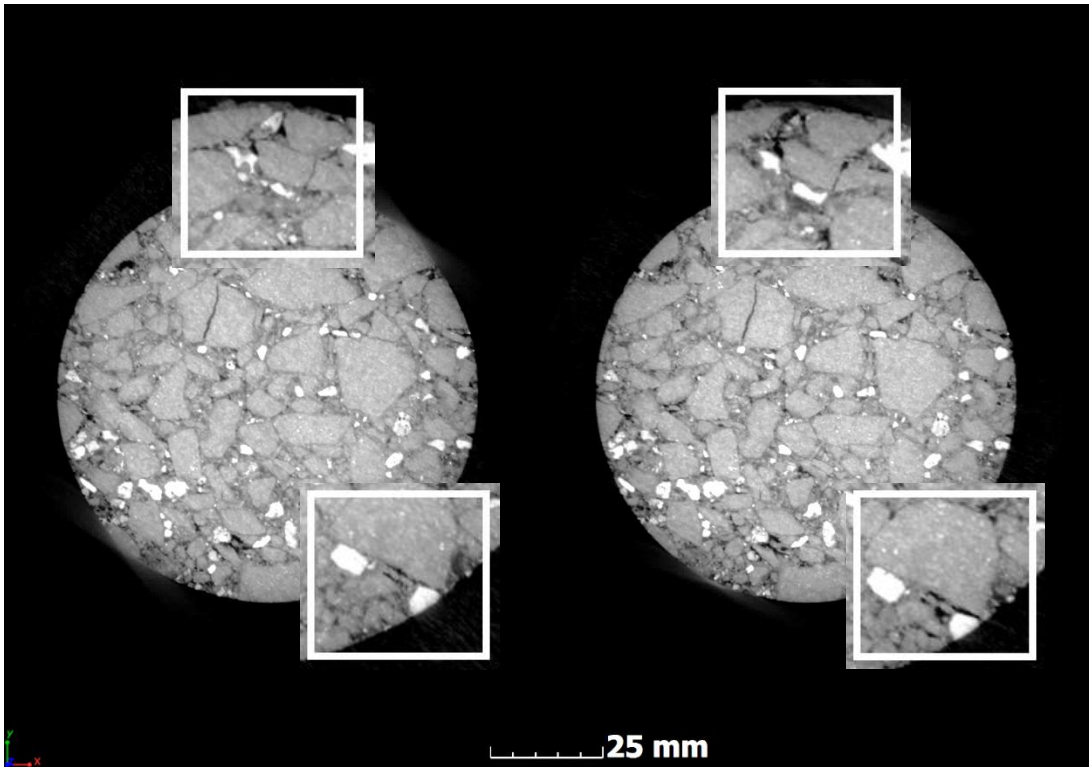

Figure 8.77: Core 5 inter-connected voids before MIST (left) and after MIST (right)

H.2 N3TC - MIX CP

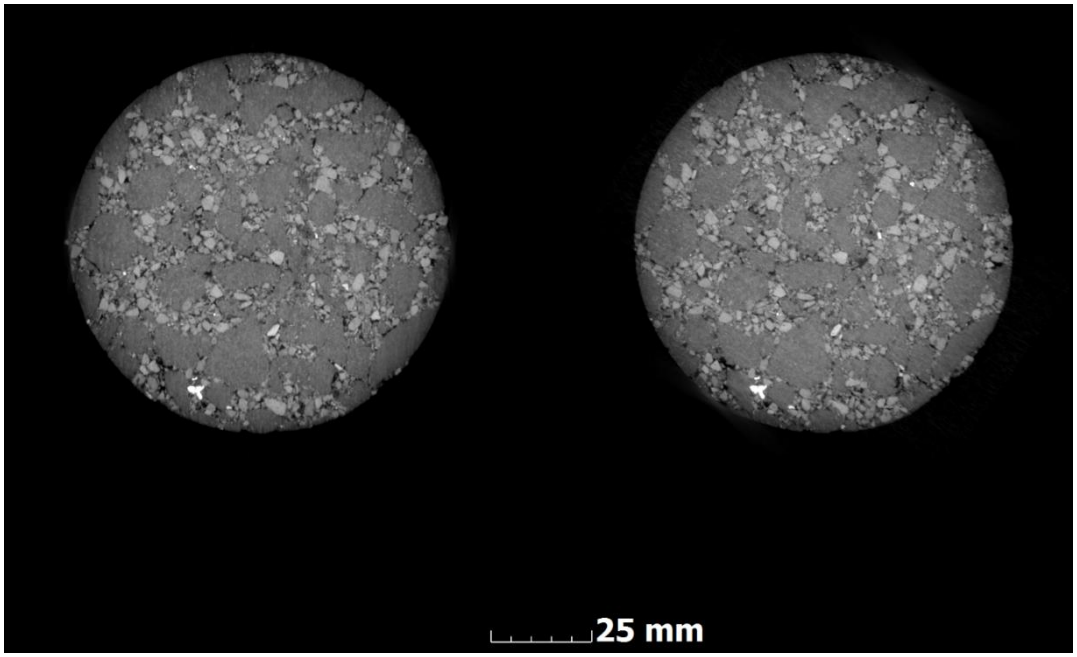

Figure 8.78: Core 7 CT-scan before MIST (left) and after MIST (right)

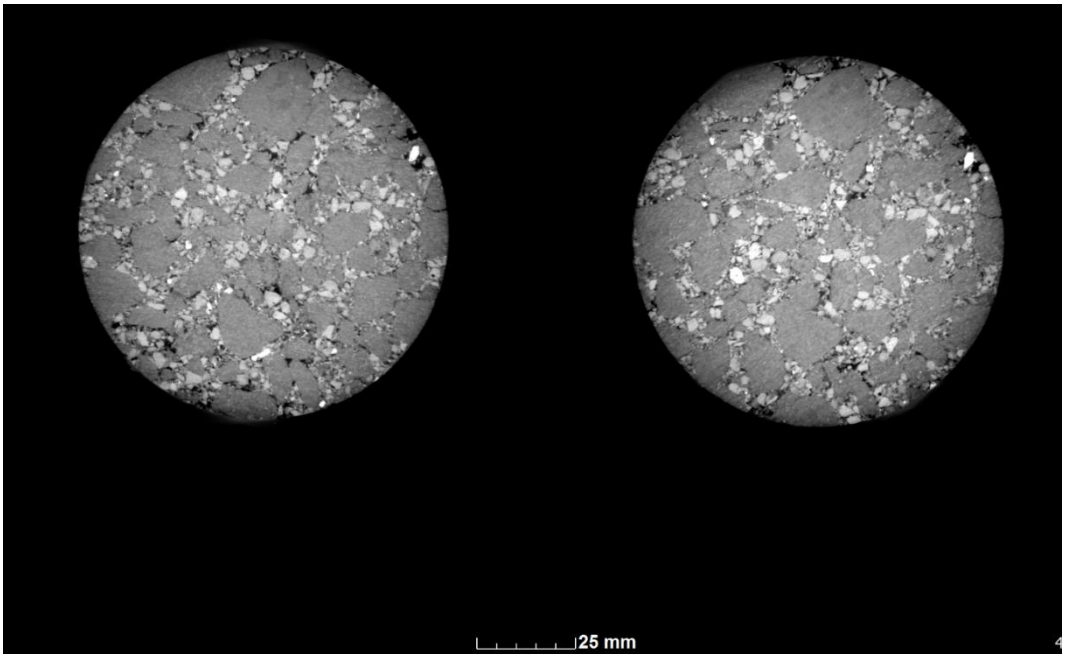

Figure 8.79: Core 9 CT-scan before MIST (left) and after MIST (right)

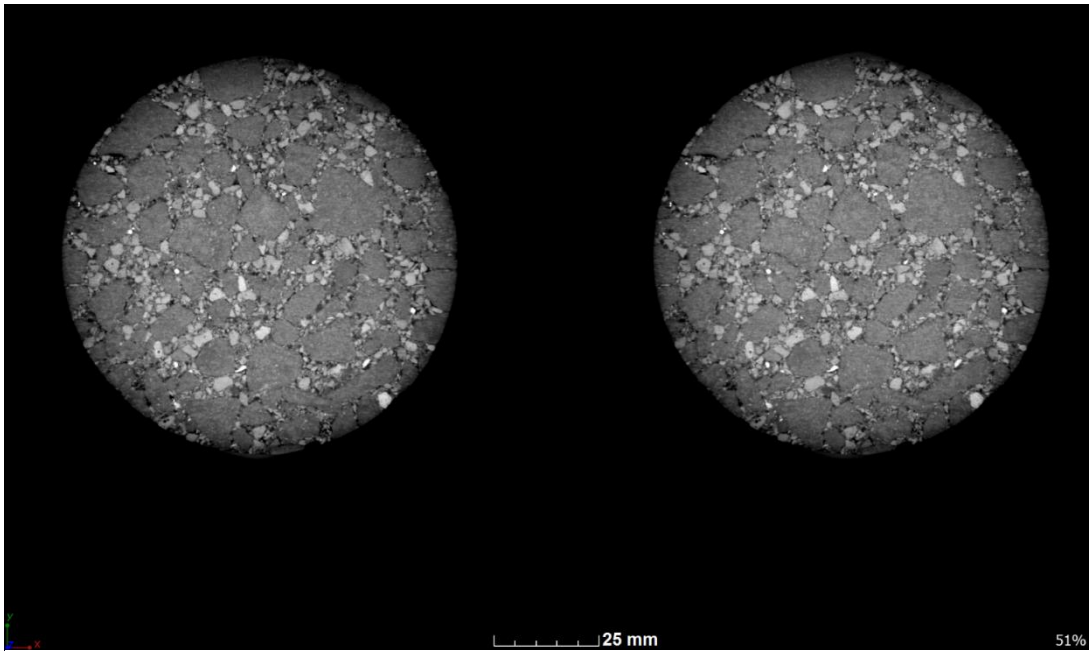

Figure 8.80: Core 12 CT-scan before MIST (left) and after MIST (right)

APPENDIX I RESULTS – ITS TEST

I.1 RAUBEX

Table 8.16: ITS input parameters and test results

	Core No.	Core Diameter (mm)	Average Core Thickness (mm)	Max Applied Load (kN)	ITS (kPa)	Average ITS (kPa)
Section 1	Core A	102	44,88	4,20	584,01	523,66
	Core B	102	41,63	3,19	477,87	
	Core F	102	45,60	2,98	407,47	
	Core L	102	41,03	4,11	625,28	
Section 2	Core H	102	31,75	1,59	312,56	476,32
	Core I	102	32,06	1,43	278,37	
	Core J	102	36,75	4,92	835,41	
	Core M	102	42,28	3,24	478,94	
Section 3	Core N	102	36,88	4,06	686,34	596,48
	Core O	102	39,18	2,81	448,01	
	Core P	102	37,81	2,22	365,78	
	Core Q	102	37,68	5,35	885,80	

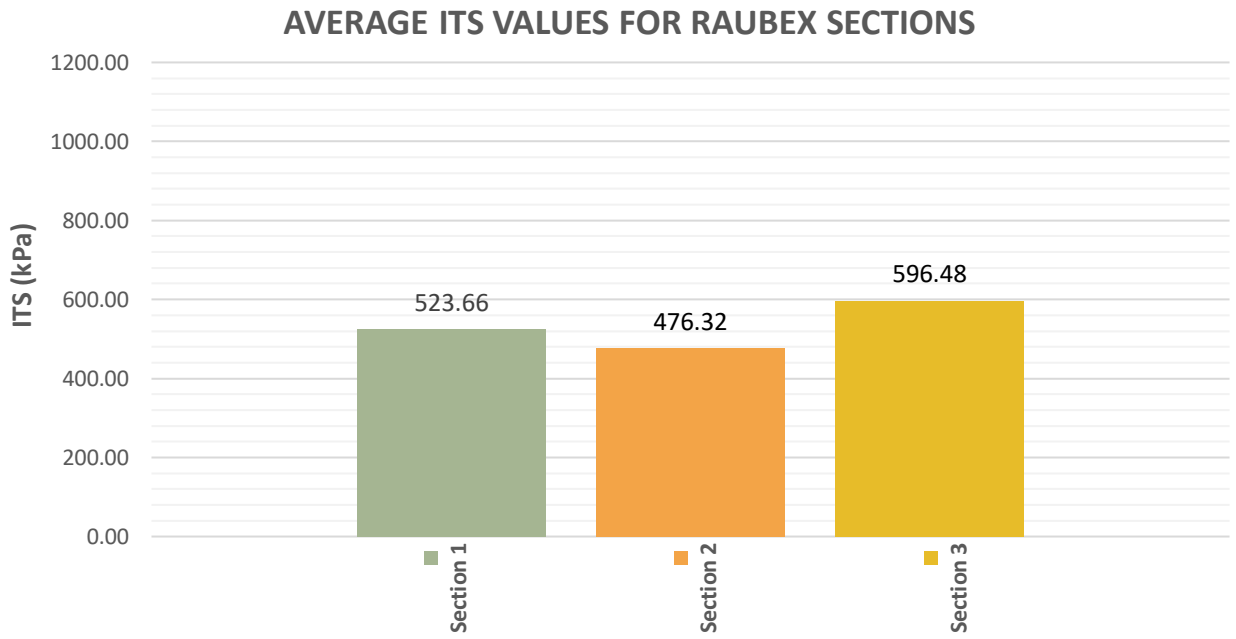

Figure 8.81: Average ITS values for Raubex cores

I.2 N3TC

Table 8.17: ITS input parameters and test results

	Core No.	Core Diameter (mm)	Average Core Thickness (mm)	Max Applied Load (kN)	ITS (kPa)	Average ITS (kPa)
Mix Cd	Core 1	95	41,38	2,78	450,10	677,93
	Core 2	95	45,00	3,14	468,05	
	Core 3	95	41,13	6,39	1041,08	
	Core 4	95	40,75	4,31	709,10	
	Core 5	95	41,75	3,98	638,83	
	Core 6	95	48,13	5,46	760,43	
Mix Cp	Core 7	95	38,13	4,16	731,56	797,61
	Core 8	95	36,88	4,97	903,19	
	Core 9	95	30,63	3,74	818,16	
	Core 11	95	36,38	4,00	736,17	
	Core 12	95	41,38	4,93	798,97	
Mix Ev	23/01 - 1	100	66,00	7,52	725,46	853,54
	23/01 - 2	100	72,38	11,62	1022,11	
	23/01 - 3	100	60,00	10,44	1107,51	
	24/01 - 1	100	98,75	9,66	622,50	
	24/01 - 2	100	63,00	7,82	790,12	

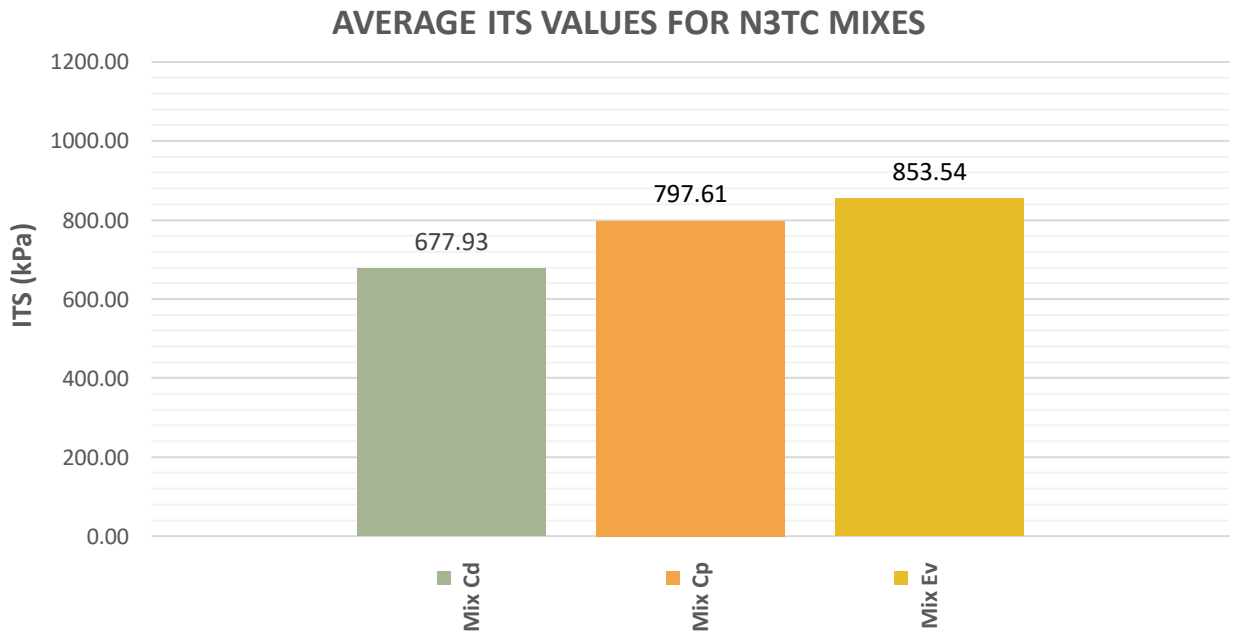

Figure 8.82: Average ITS values for N3TC cores

APPENDIX J MARVIL VS HPP

J.1 RAUBEX

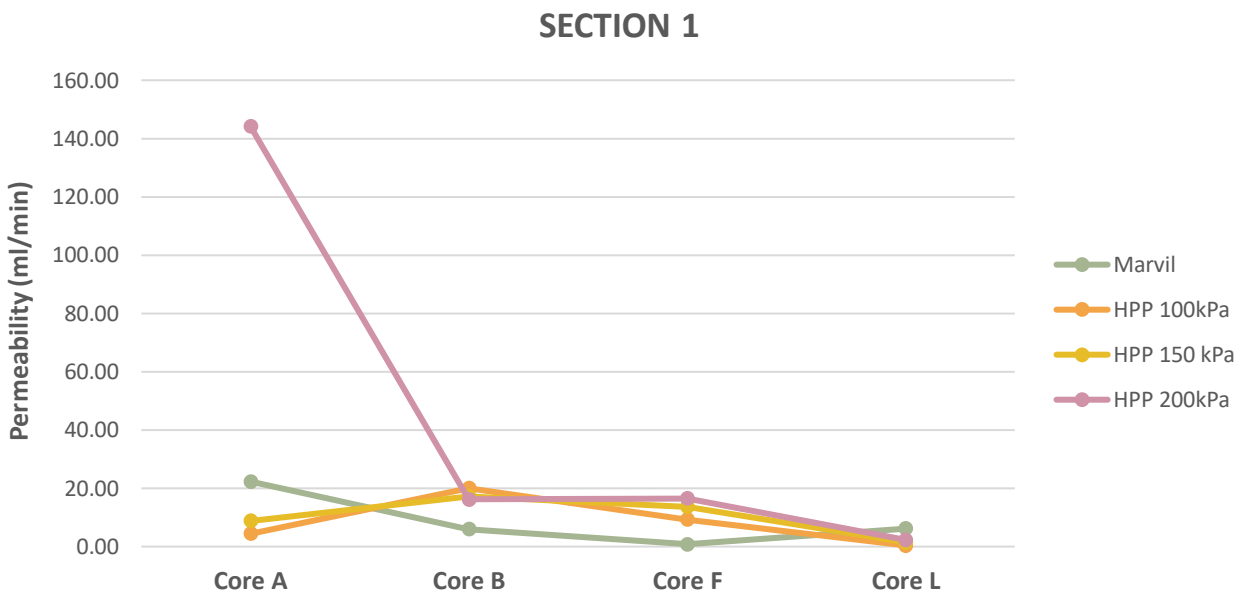

Figure 8.83: Section 1 - Marvil vs HPP

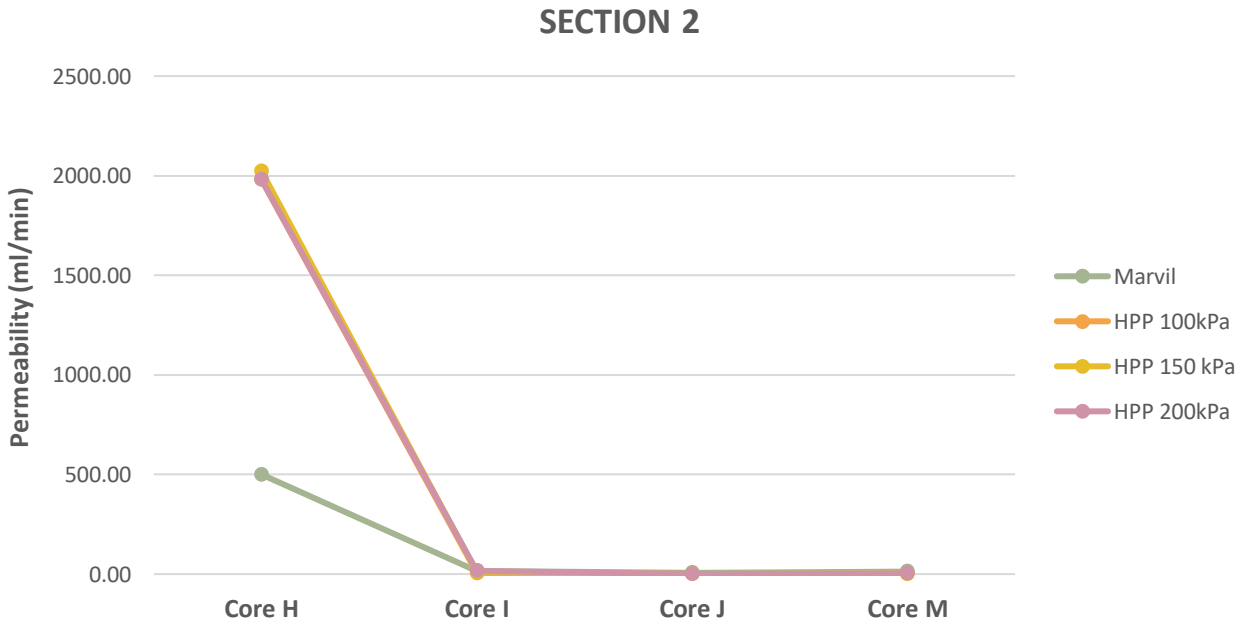

Figure 8.84: Section 2 - Marvil vs HPP

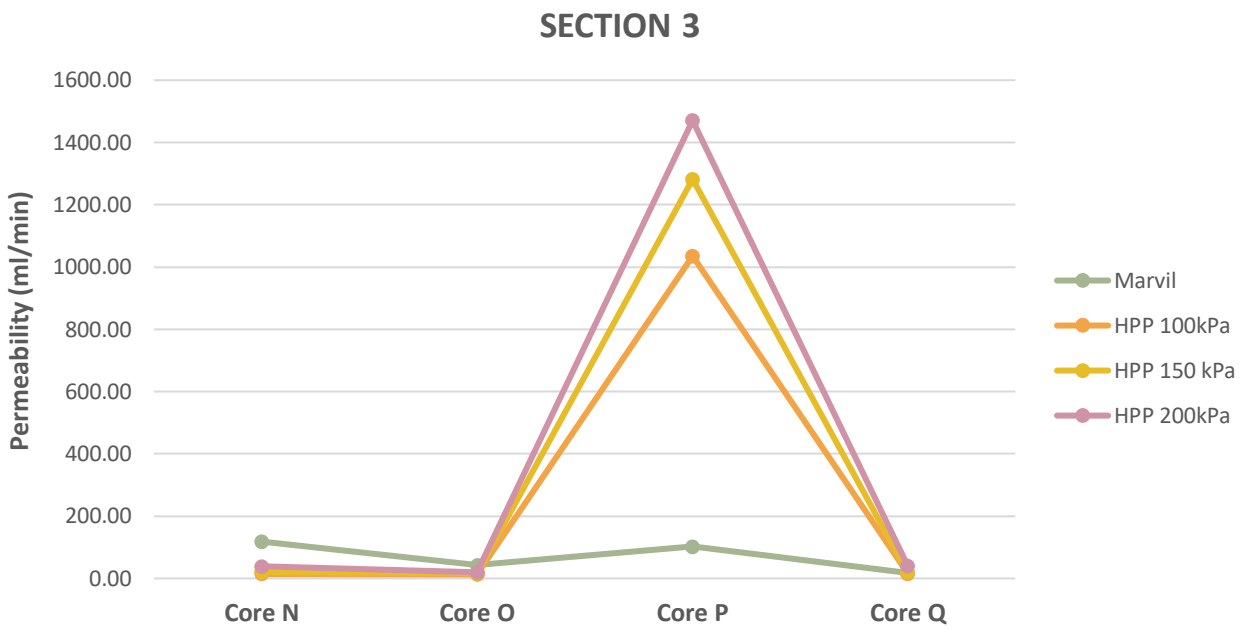

Figure 8.85: Section 3 - Marvil vs HPP

J.2 N3TC

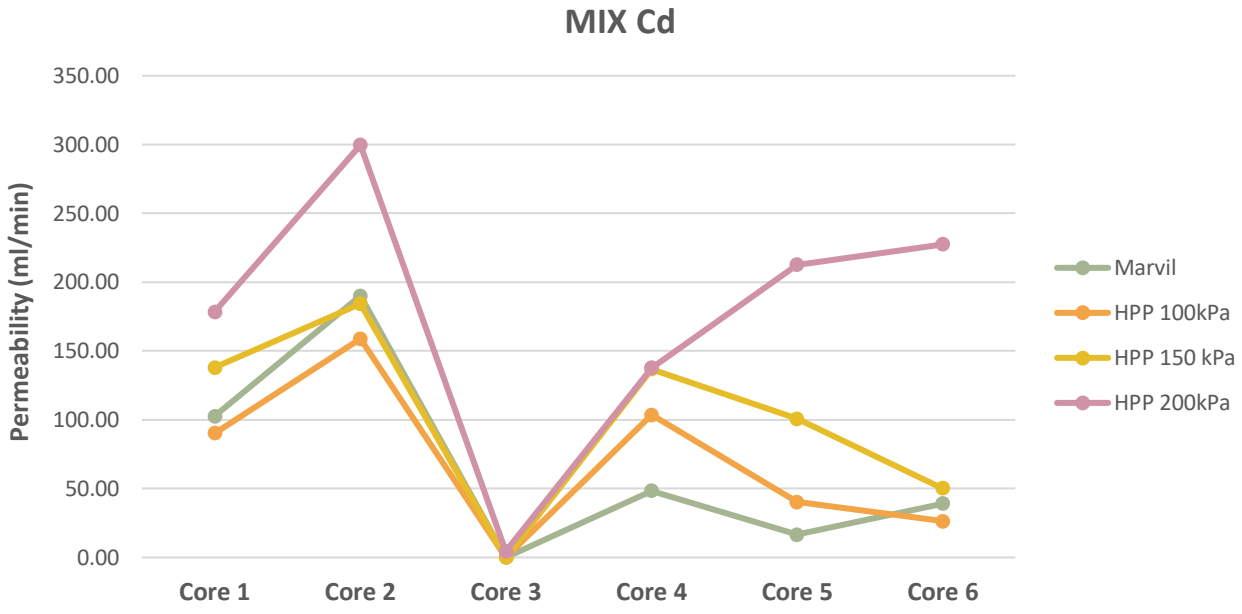

Figure 8.86: Mix Cd - Marvil vs HPP

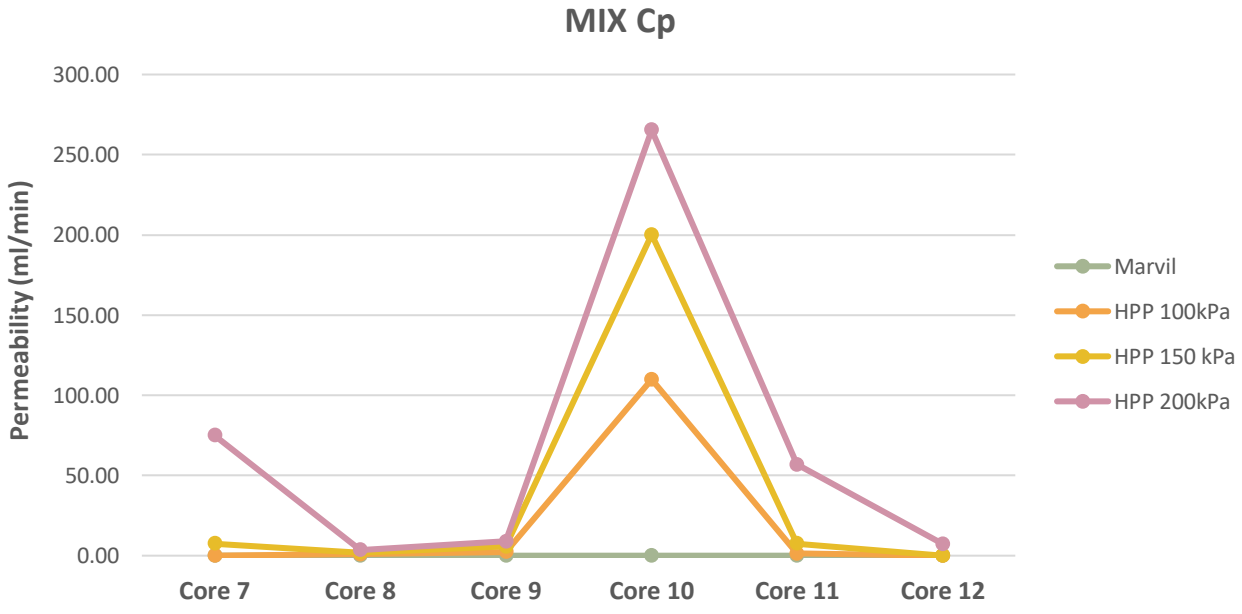

Figure 8.87: Mix Cp - Marvil vs HPP

J.3 N3TC BOTTOM ASPHALT CORES

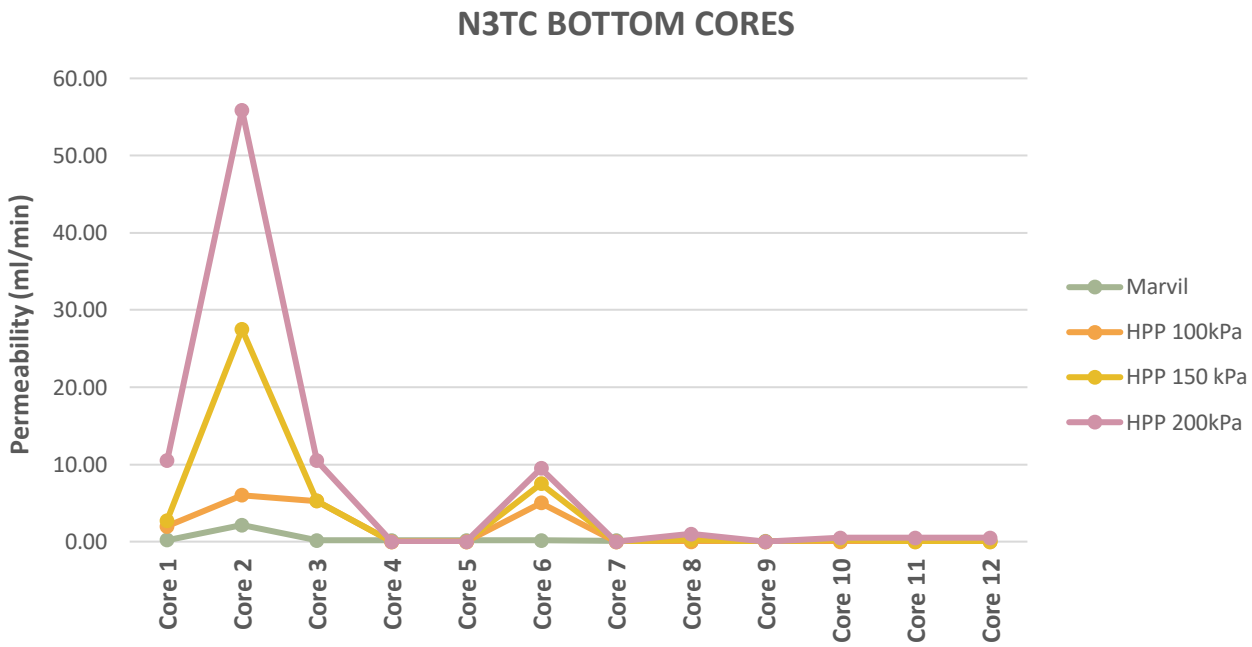

Figure 8.88: N3TC bottom asphalt cores - Marvil vs HPP

J.4 N7

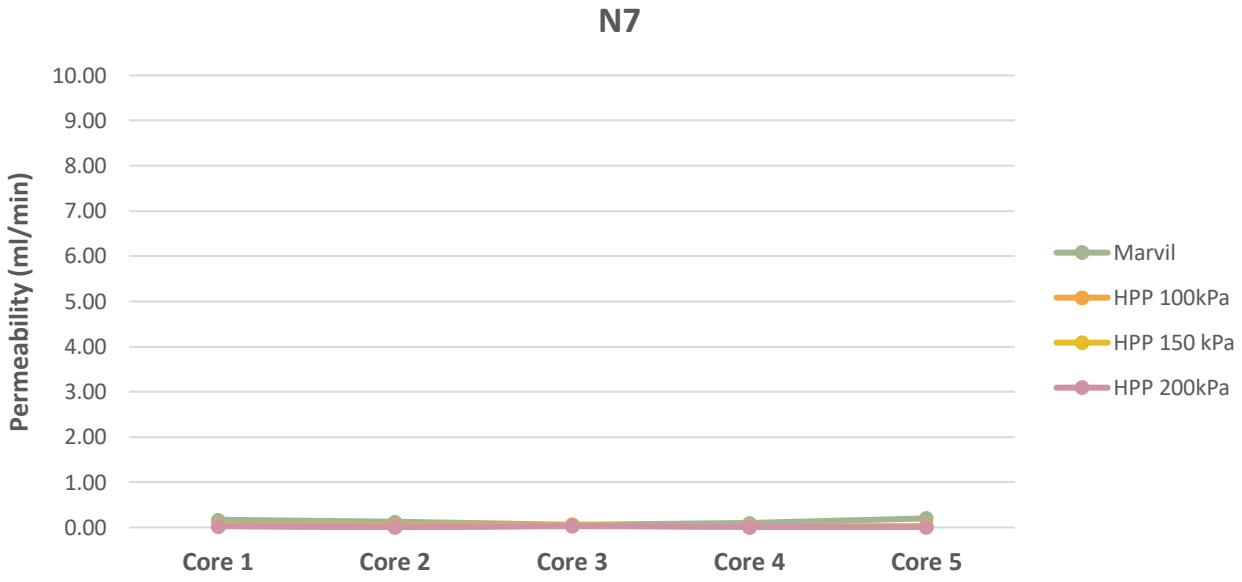

Figure 8.89: N7 - Marvil vs HPP

APPENDIX K MARVIL VS VOIDS

K.1 RAUBEX

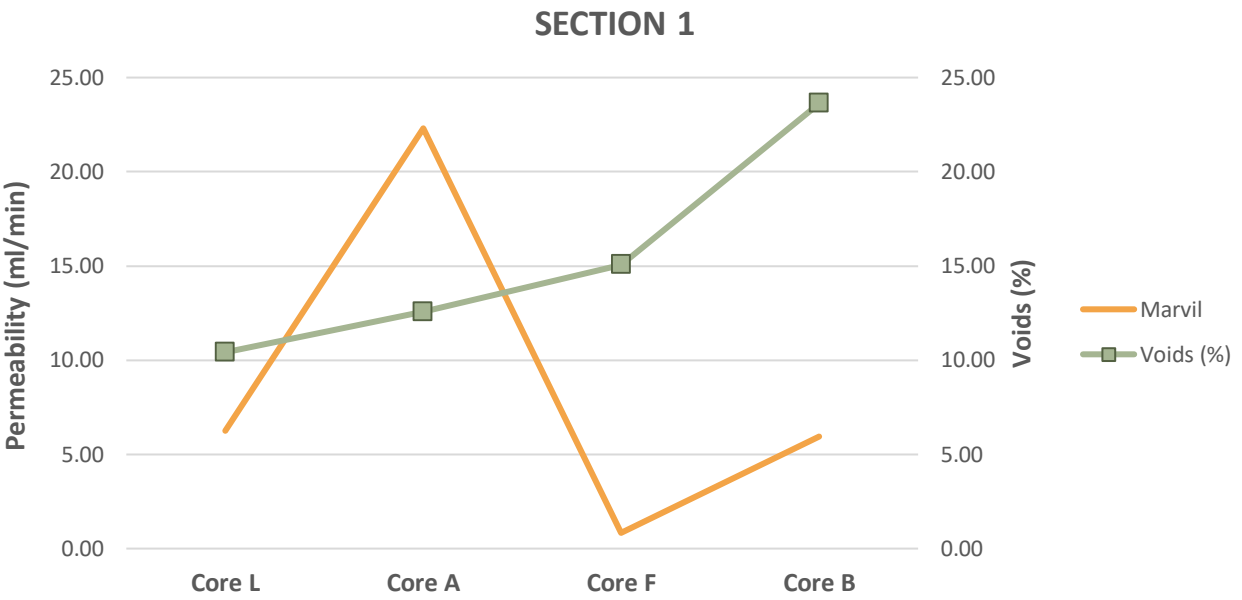

Figure 8.90: Section 1 - Marvil vs Voids

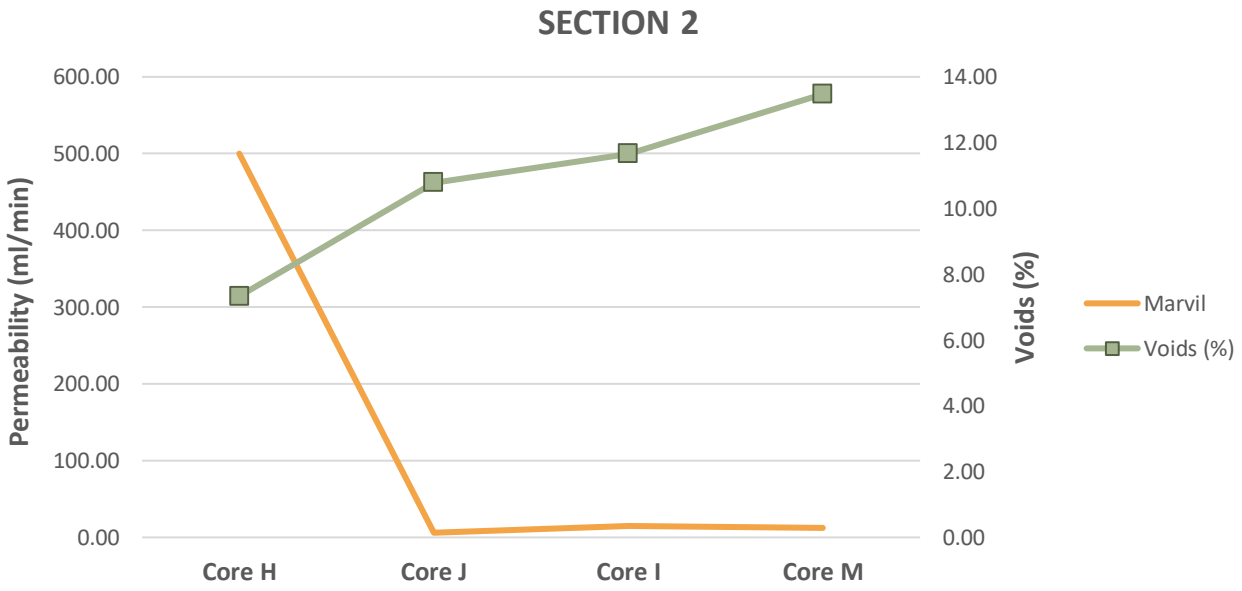

Figure 8.91: Section 2 - Marvil vs Voids

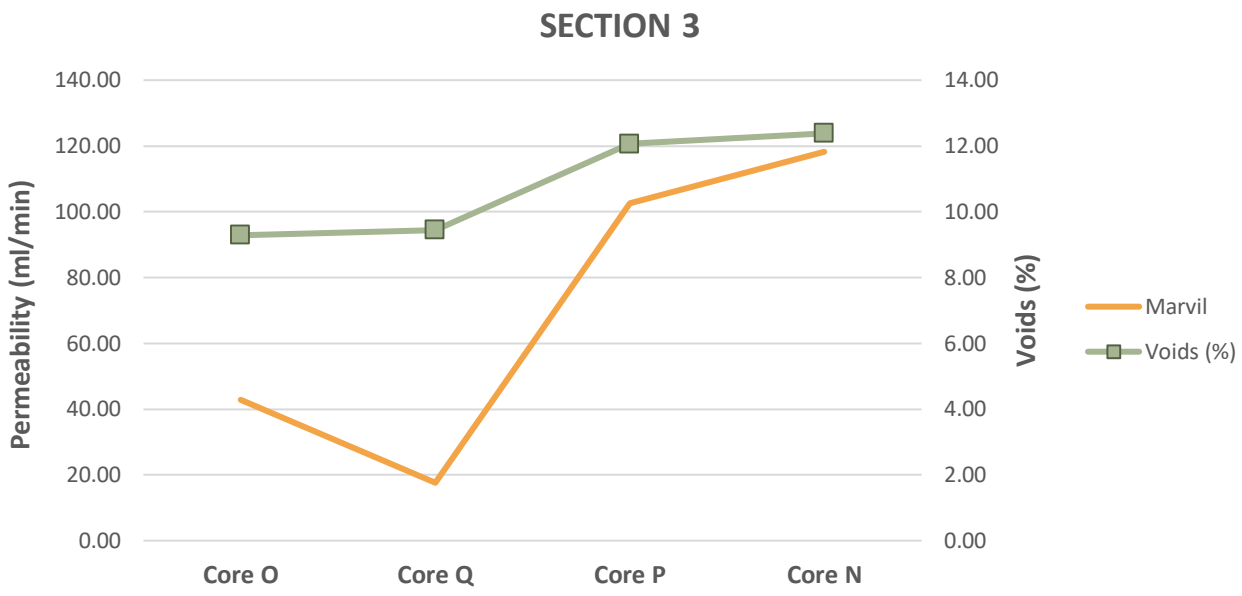

Figure 8.92: Section 3 - Marvil vs Voids

K.2 N3TC

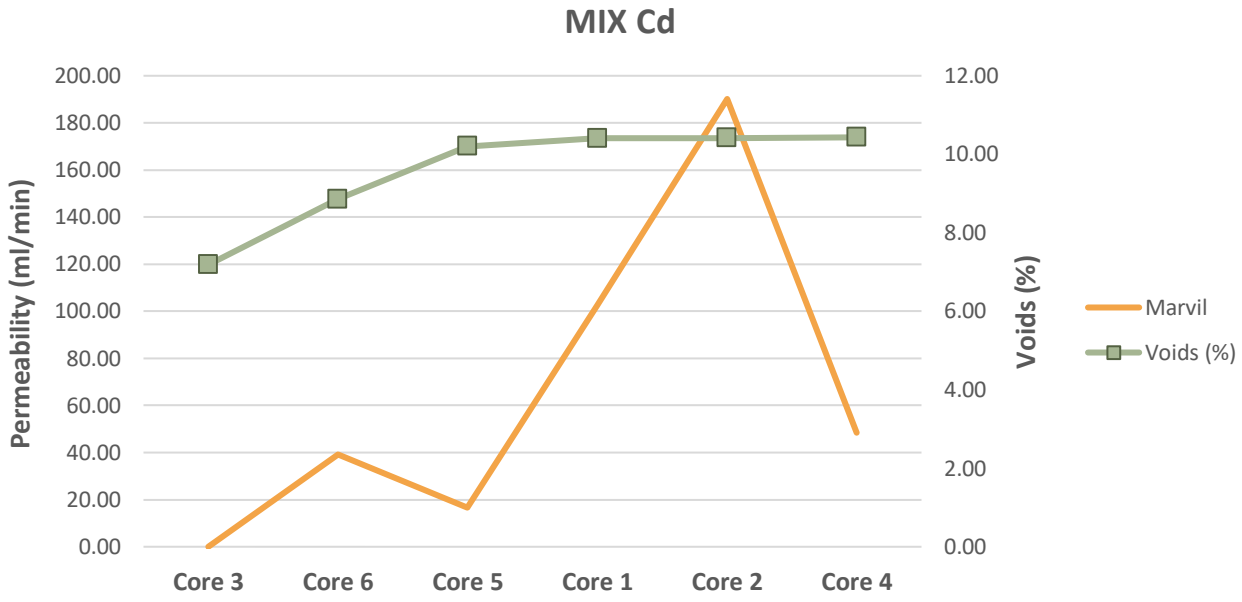

Figure 8.93: Mix Cd - Marvil vs Voids

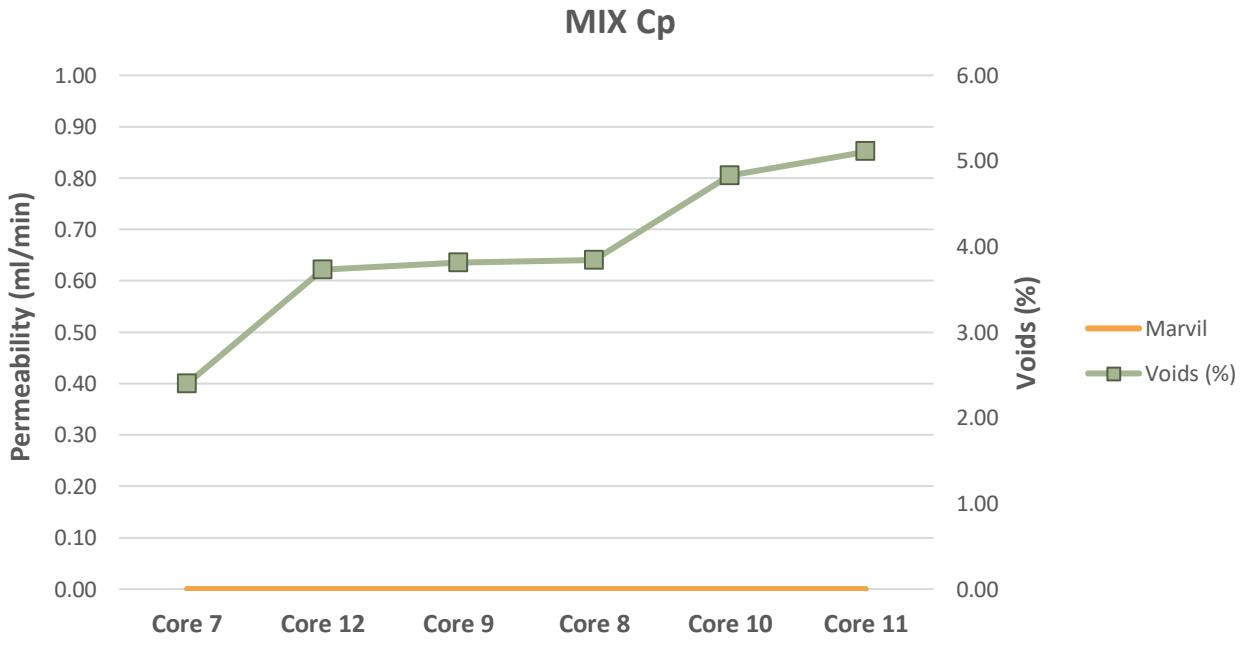

Figure 8.94: Mix Cp - Marvil vs Voids

K.3 N3TC BOTTOM ASPHALT CORES

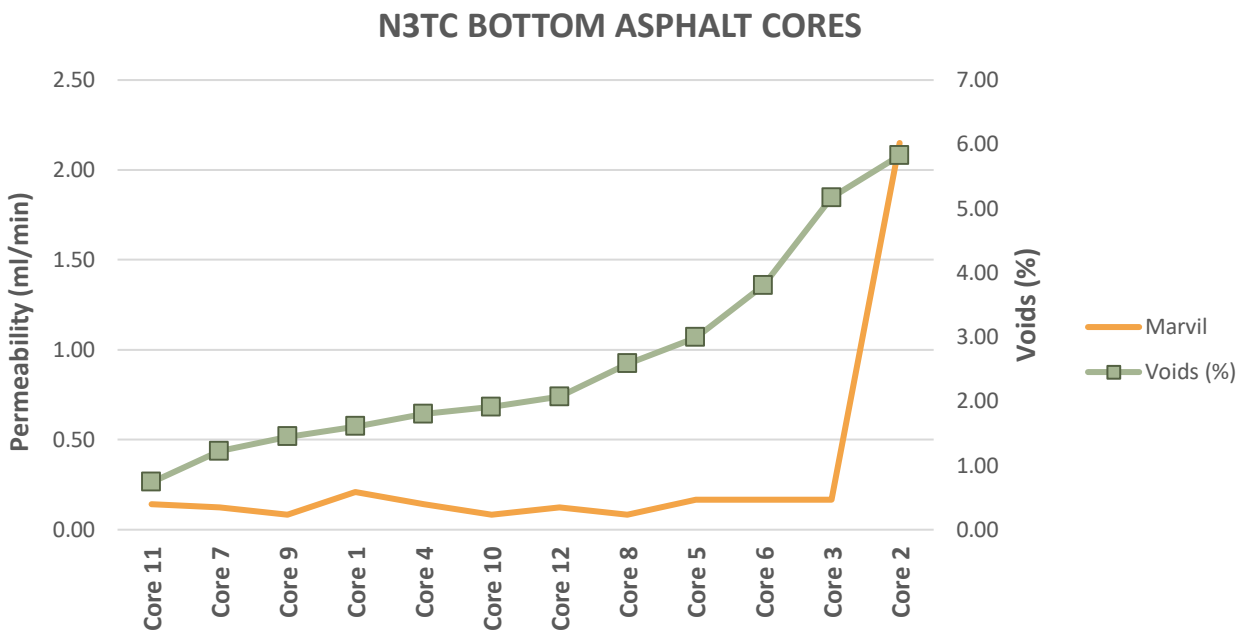

Figure 8.95: N3TC bottom asphalt cores - Marvil vs Voids

K.4 N7

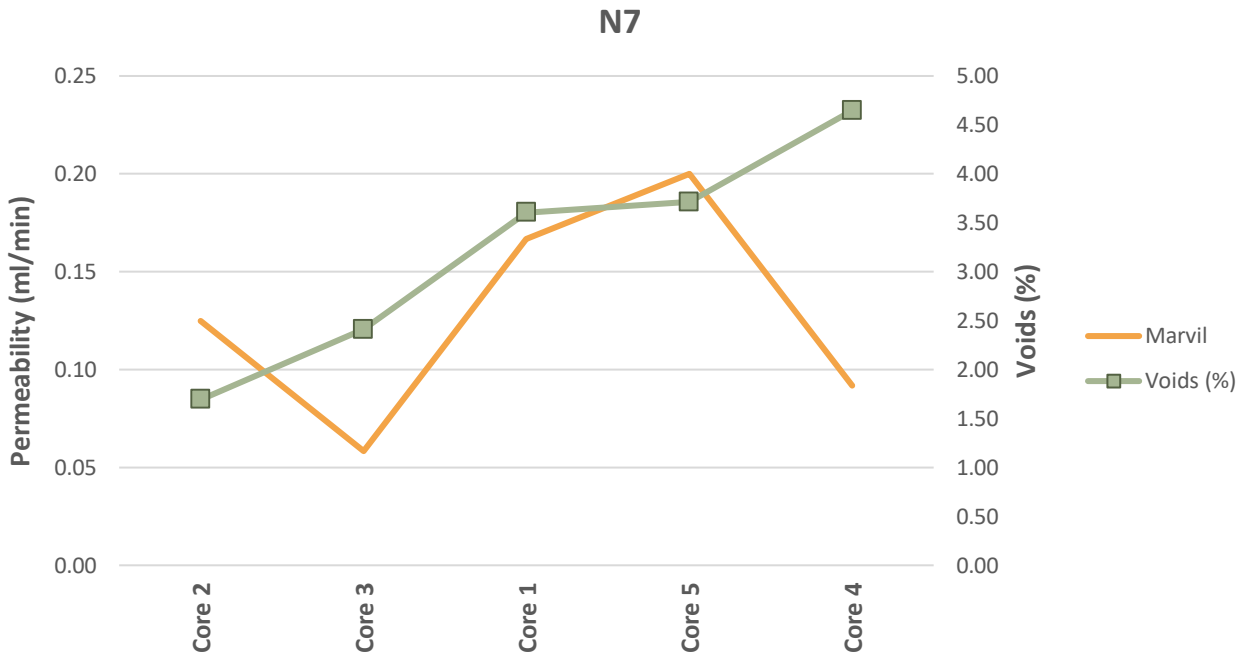

Figure 8.96: N7 - Marvil vs Voids

APPENDIX L HPP VS VOIDS

L.1 RAUBEX

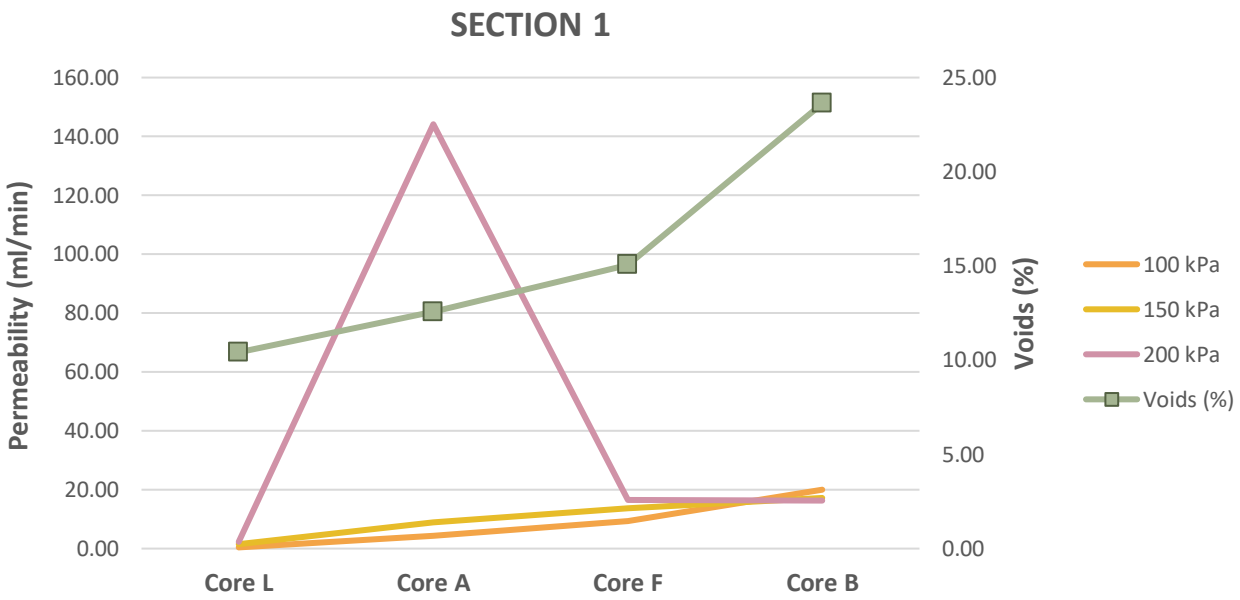

Figure 8.97: Section 1 - HPP vs Voids

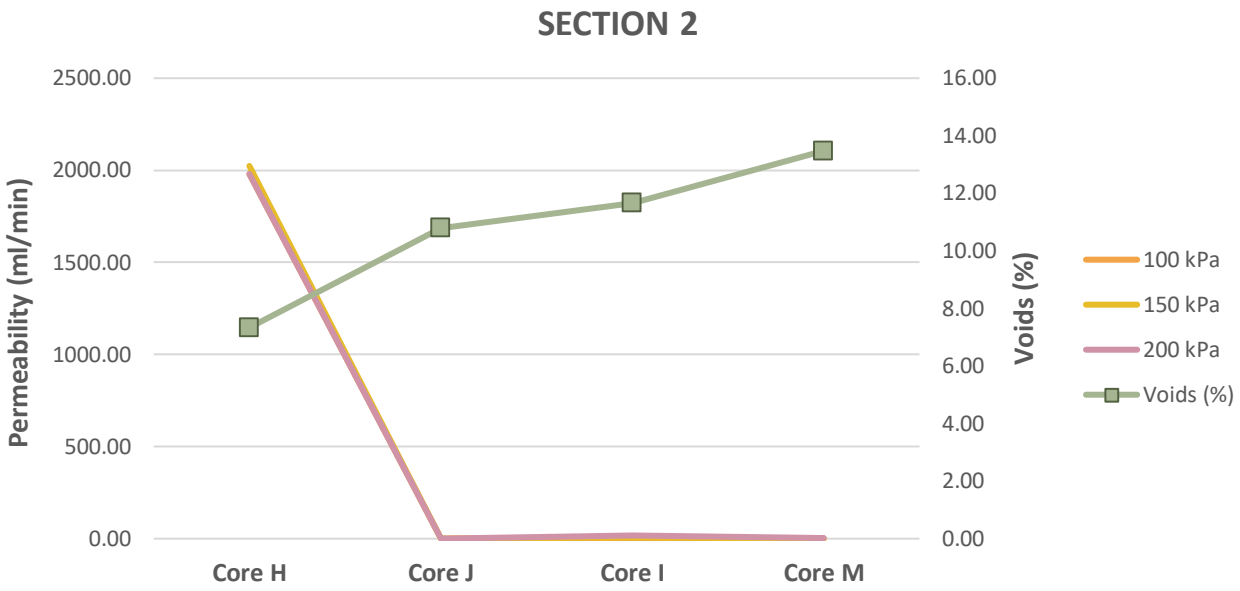

Figure 8.98: Section 2 - HPP vs Voids

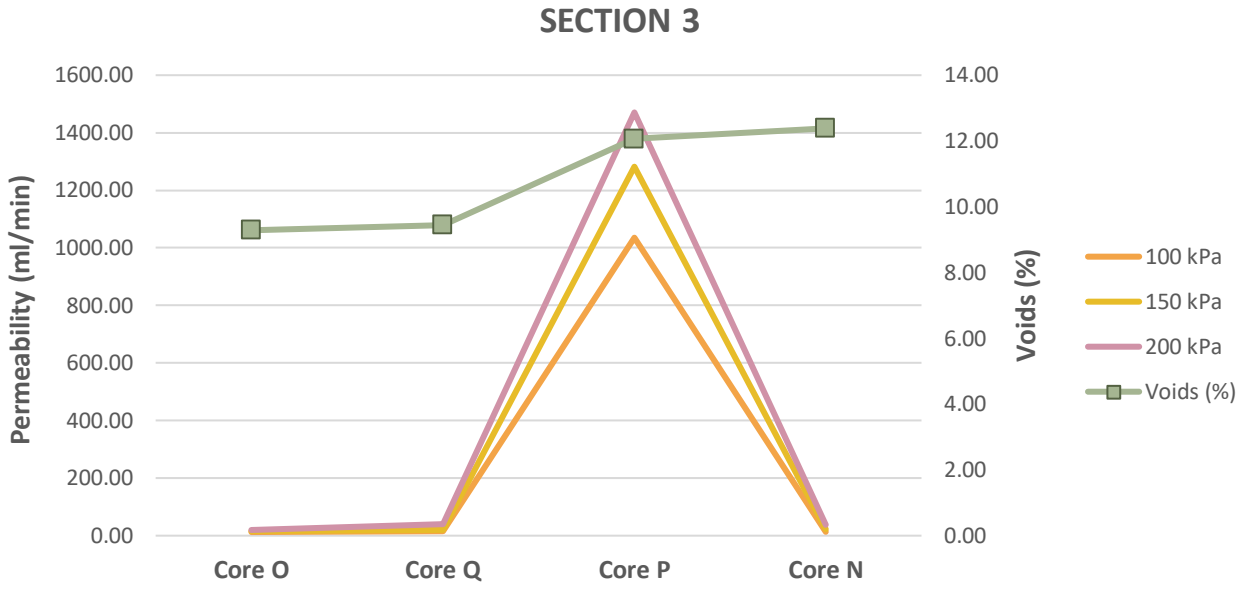

Figure 8.99: Section 3 - HPP vs Voids

L.2 N3TC

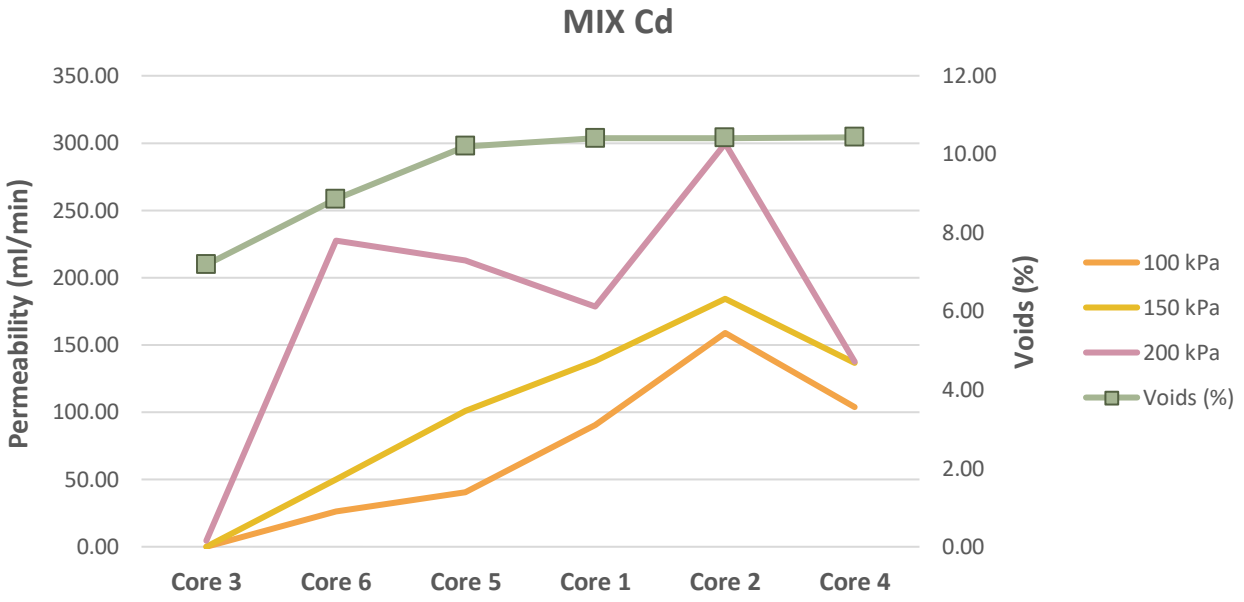

Figure 8.100: Mix Cd - HPP vs Voids

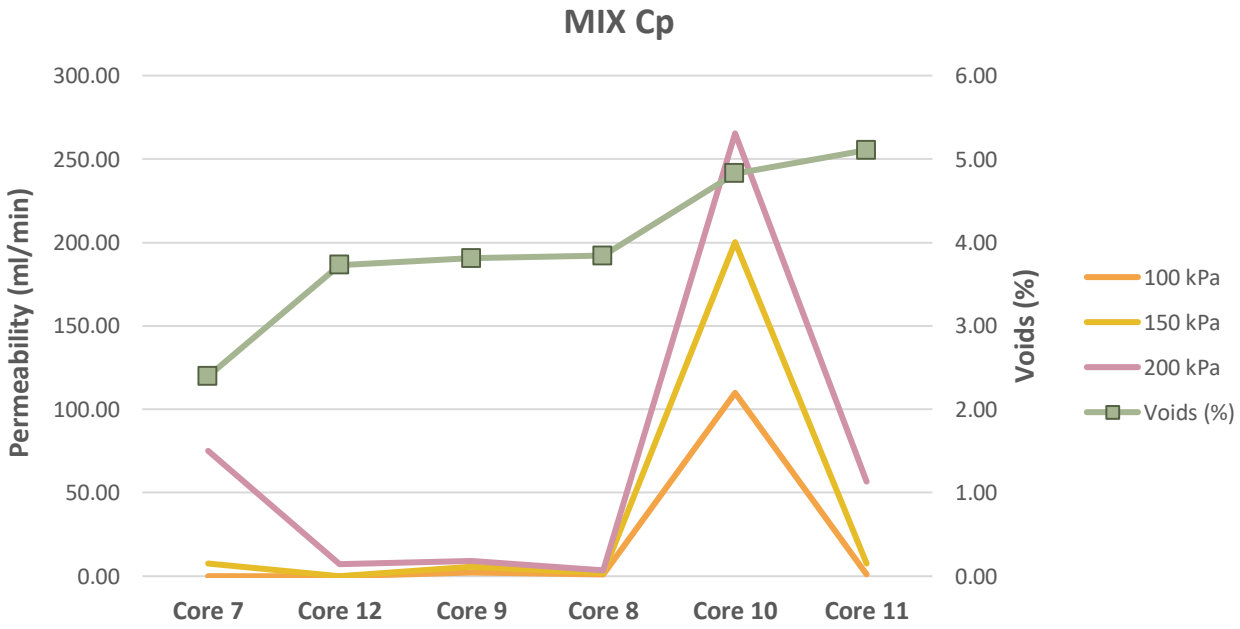

Figure 8.101: Mix Cp - HPP vs Voids

L.3 N3TC BOTTOM ASPHALT CORES

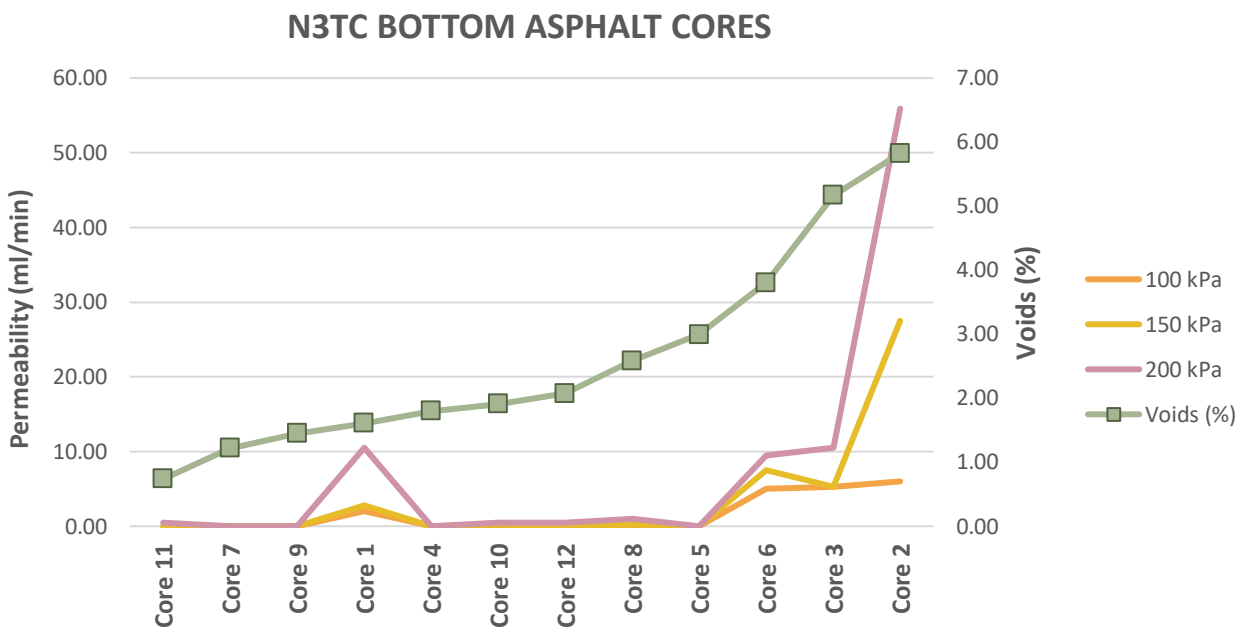

Figure 8.102: N3TC bottom asphalt cores - HPP vs Voids

L.4 N7

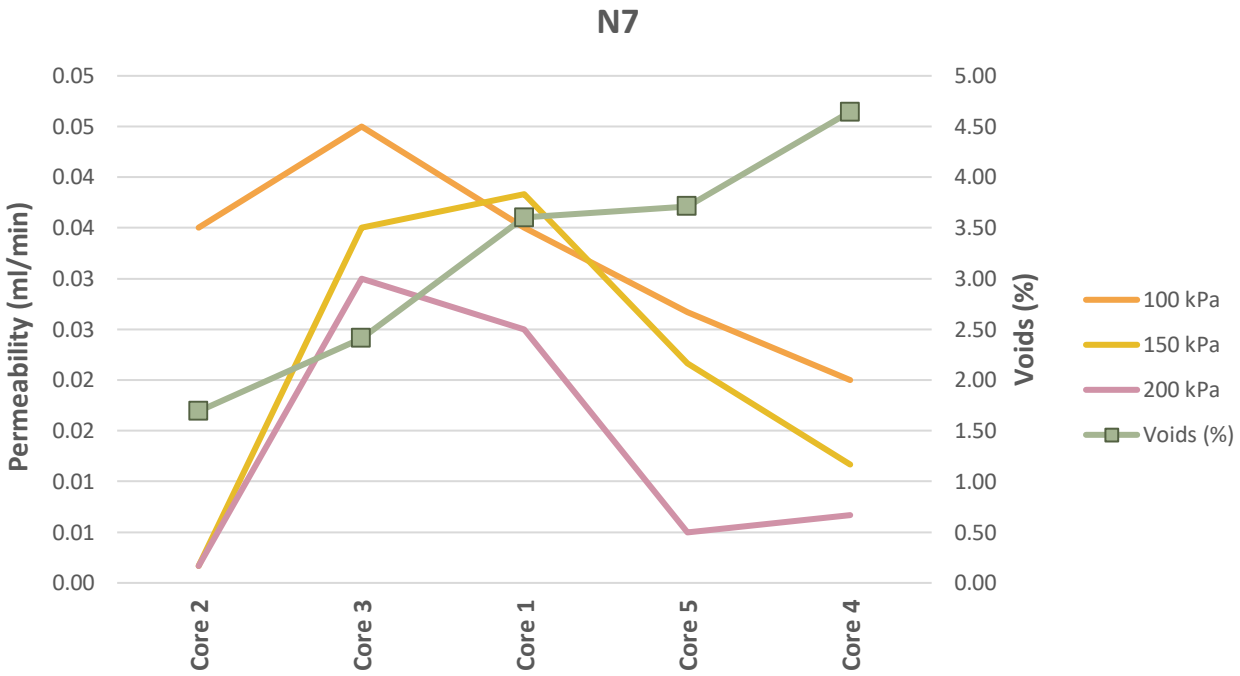

Figure 8.103: N7 - HPP vs Voids

APPENDIX M ANOVA: MARVIL VS HPP

M.1 Y = A + B(X1) + C(X2)

Where: Y = Marvil Permeability (*mℓ/min*)

X1 = HPP at 100 *kPa* (*mℓ/min*)

X2 = HPP at 150 *kPa* (*mℓ/min*)

Table 8.18: ANOVA analysis P-values for Y = A + B(X1) + C(X2)

	P-Value	Variable
Raubex	0,126	X1
	0,051	X2
N3TC	0,021	X1
	0,340	X2
N3TC Bottom	0,688	X1
	0,999	X2
N7	0,580	X1
	0,747	X2

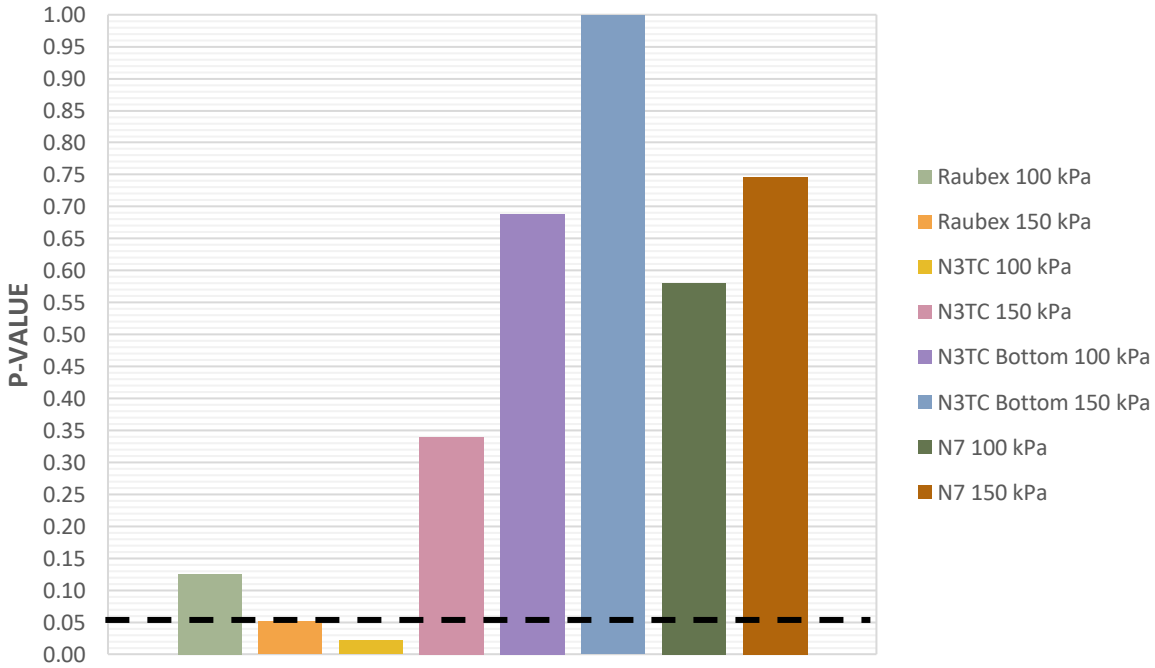

Figure 8.104: ANOVA analysis P-values for Y = A + B(X1) + C(X2)

M.2 $Y^2 = A + B(X1) + C(X2)$

Where: Y^2 = Marvil Permeability (*mℓ/min*) - squared

X1 = HPP at 100 *kPa* (*mℓ/min*)

X2 = HPP at 150 *kPa* (*mℓ/min*)

Table 8.19: ANOVA analysis P-values for $Y^2 = A + B(X1) + C(X2)$

	P-Value	Variable
Raubex	0,177	X1
	0,081	X2
N3TC	0,015	X1
	0,099	X2
N3TC Bottom	0,749	X1
	0,937	X2
N7	0,582	X1
	0,678	X2

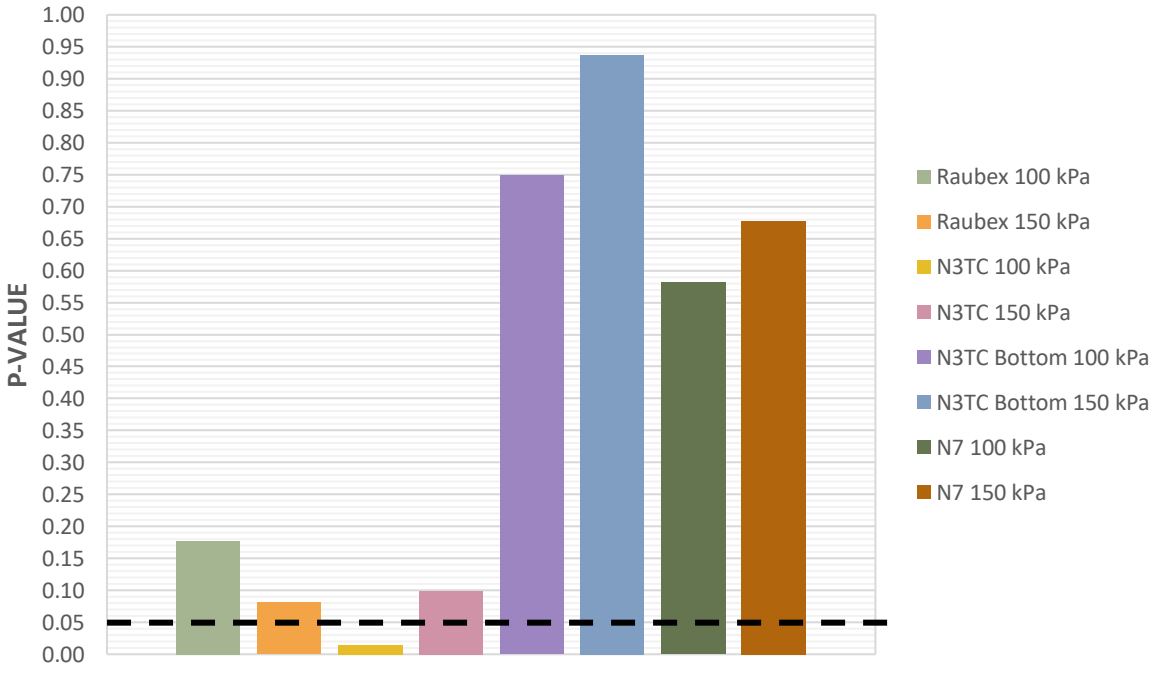

Figure 8.105: ANOVA analysis P-values for $Y^2 = A + B(X1) + C(X2)$

M.3 $Y^3 = A + B(X1) + C(X2)$

Where: Y^3 = Marvil Permeability (*mℓ/min*) - cubed

X1 = HPP at 100 *kPa* (*mℓ/min*)

X2 = HPP at 150 *kPa* (*mℓ/min*)

Table 8.20: ANOVA analysis P-values for $Y^3 = A + B(X1) + C(X2)$

	P-Value	Variable
Raubex	0,201	X1
	0,098	X2
N3TC	0,017	X1
	0,081	X2
N3TC Bottom	0,820	X1
	0,879	X2
N7	0,577	X1
	0,638	X2

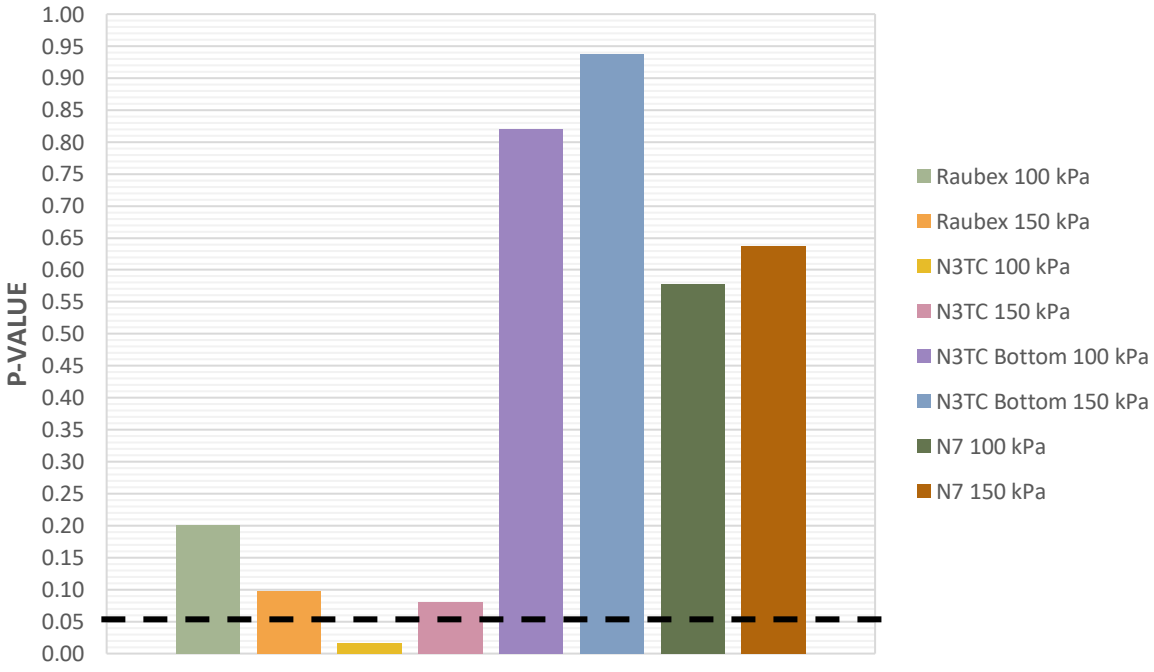

Figure 8.106: ANOVA analysis P-values for $Y^3 = A + B(X1) + C(X2)$

APPENDIX N ANOVA: MARVIL VS VOIDS

N.1 Y = A + B(X1)

Where: Y = Void Percentage

X1 = Marvil Permeability (*mℓ/min*)

Table 8.21: ANOVA analysis P-values for Y = A + B(X1)

	P-Value	Variable
Raubex	0,902	X1
N3TC	0,023	X1
N3TC Bottom	0,364	X1
N7	0,716	X1

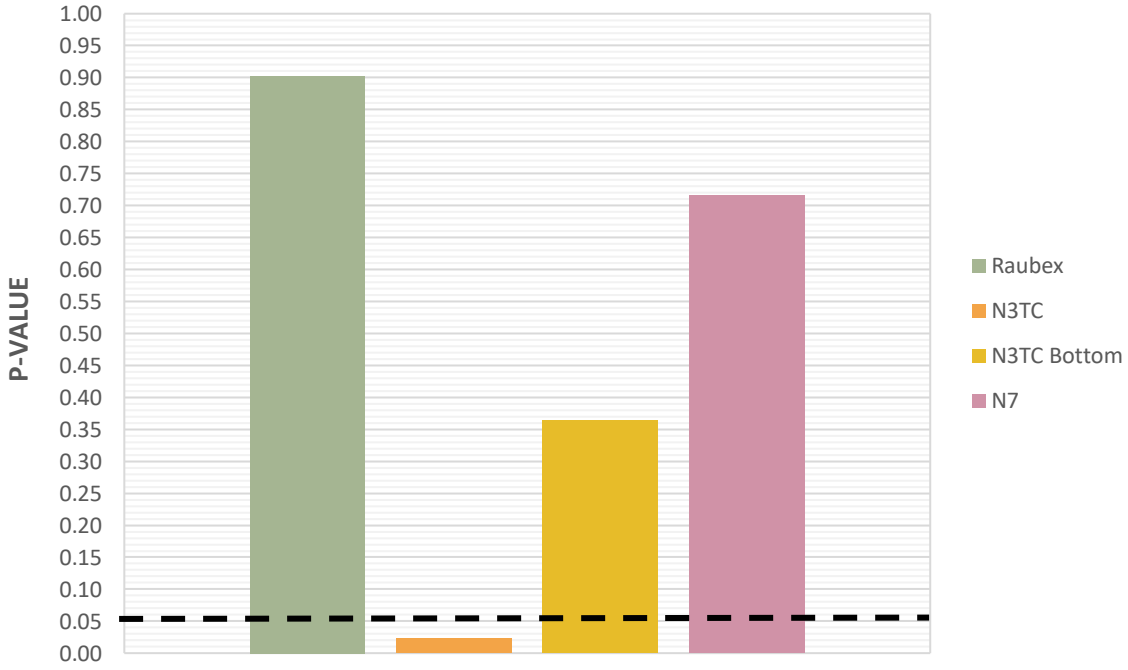

Figure 8.107: ANOVA analysis P-values for Y = A + B(X1)

N.2 $Y^2 = A + B(X1)$

Where: Y^2 = Void Percentage - squared

X1 = Marvil Permeability (*mℓ/min*)

Table 8.22: ANOVA analysis P-values for $Y^2 = A + B(X1)$

	P-Value	Variable
Raubex	0,859	X1
N3TC	0,015	X1
N3TC Bottom	0,314	X1
N7	0,789	X1

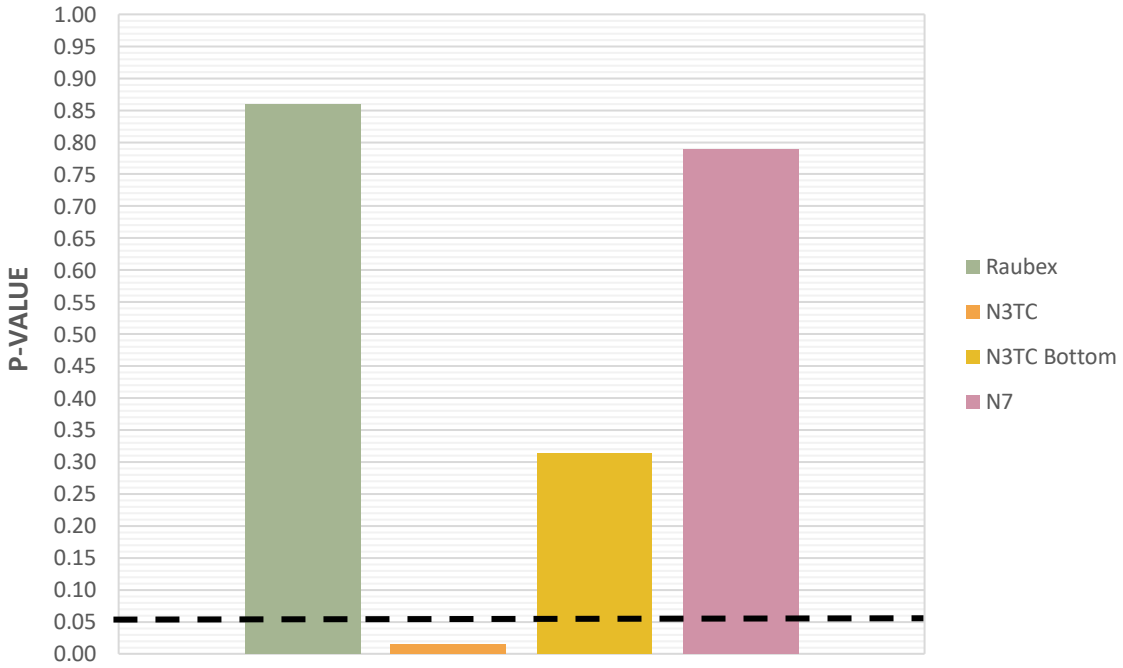

Figure 8.108: ANOVA analysis P-values for $Y^2 = A + B(X1)$

N.3 $Y^3 = A + B(X1)$

Where: Y^3 = Void Percentage - cubed

X1 = Marvil Permeability (*mℓ/min*)

Table 8.23: ANOVA analysis P-values for $Y^3 = A + B(X1)$

	P-Value	Variable
Raubex	0,813	X1
N3TC	0,012	X1
N3TC Bottom	0,311	X1
N7	0,883	X1

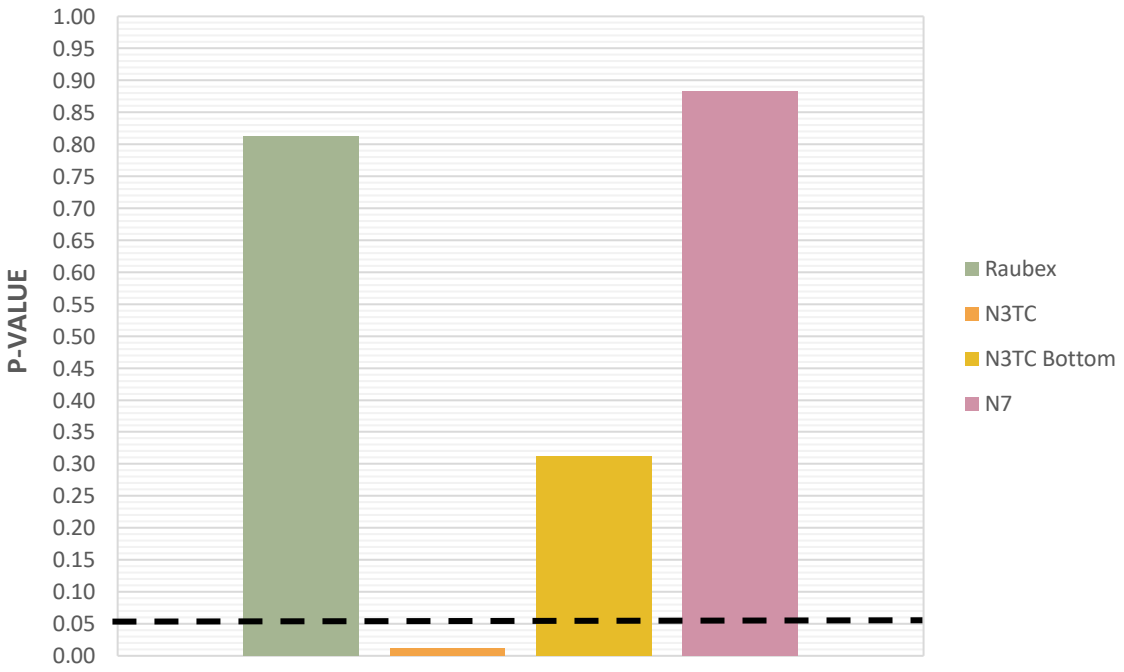

Figure 8.109: ANOVA analysis P-values for $Y^3 = A + B(X1)$

APPENDIX O ANOVA: HPP VS VOIDS

O.1 Y = A + B(X1) + C(X2)

Where: Y = Void Percentage

X1 = HPP at 100 *kPa* (*mℓ/min*)

X2 = HPP at 150 *kPa* (*mℓ/min*)

Table 8.24: ANOVA analysis P-values for Y = A + B(X1) + C(X2)

	P-Value	Variable
Raubex	0,081	X1
	0,091	X2
N3TC	0,178	X1
	0,023	X2
N3TC Bottom	0,082	X1
	0,297	X2
N7	0,022	X1
	0,052	X2

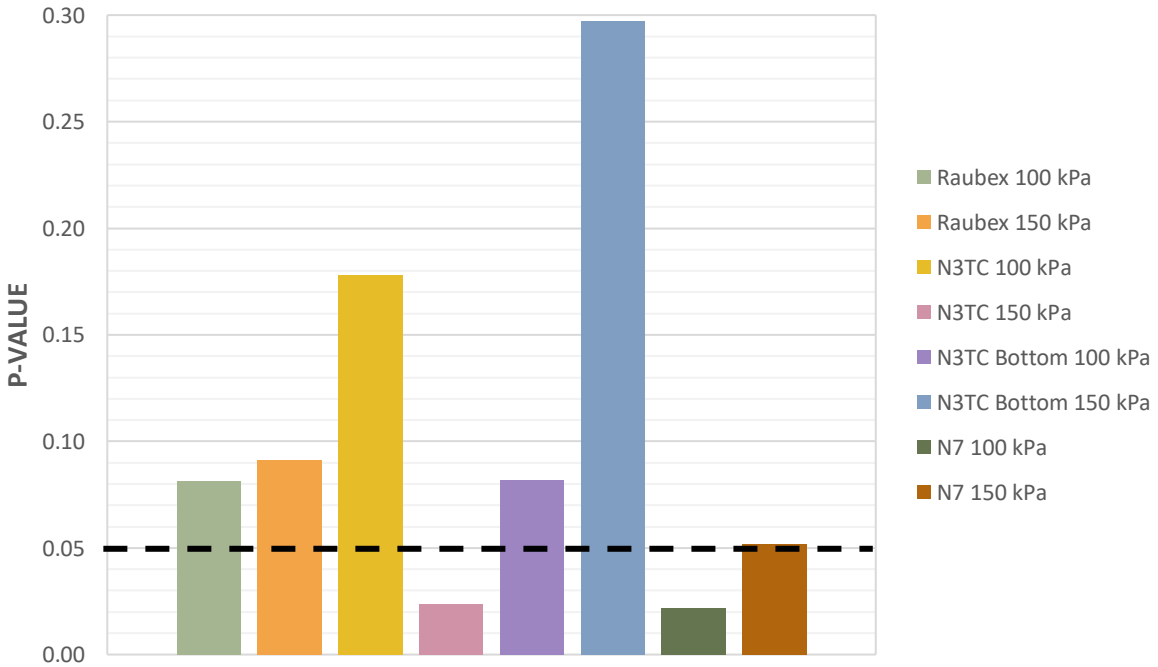

Figure 8.110: ANOVA analysis P-values for Y = A + B(X1) + C(X2)

O.2 $Y^2 = A + B(X1) + C(X2)$

Where: Y^2 = Void Percentage - squared

X1 = HPP at 100 *kPa* (*mℓ/min*)

X2 = HPP at 150 *kPa* (*mℓ/min*)

Table 8.25: ANOVA analysis P-values for $Y^2 = A + B(X1) + C(X2)$

	P-Value	Variable
Raubex	0,111	X1
	0,121	X2
N3TC	0,087	X1
	0,006	X2
N3TC Bottom	0,007	X1
	0,046	X2
N7	0,036	X1
	0,115	X2

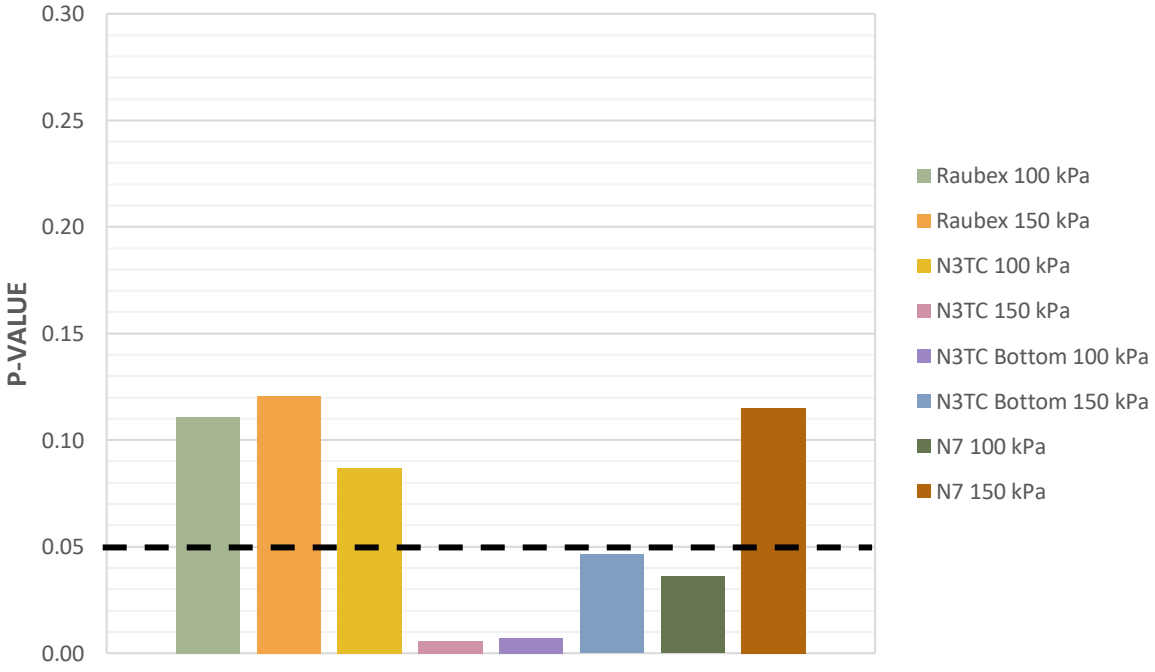

Figure 8.111: ANOVA analysis P-values for $Y^2 = A + B(X1) + C(X2)$

O.3 $Y^3 = A + B(X1) + C(X2)$

Where: Y^3 = Void Percentage - cubed

X1 = HPP at 100 *kPa* (*mℓ/min*)

X2 = HPP at 150 *kPa* (*mℓ/min*)

Table 8.26: ANOVA analysis P-values for $Y^3 = A + B(X1) + C(X2)$

	P-Value	Variable
Raubex	0,147	X1
	0,156	X2
N3TC	0,037	X1
	0,001	X2
N3TC Bottom	0,001	X1
	0,004	X2
N7	0,058	X1
	0,231	X2

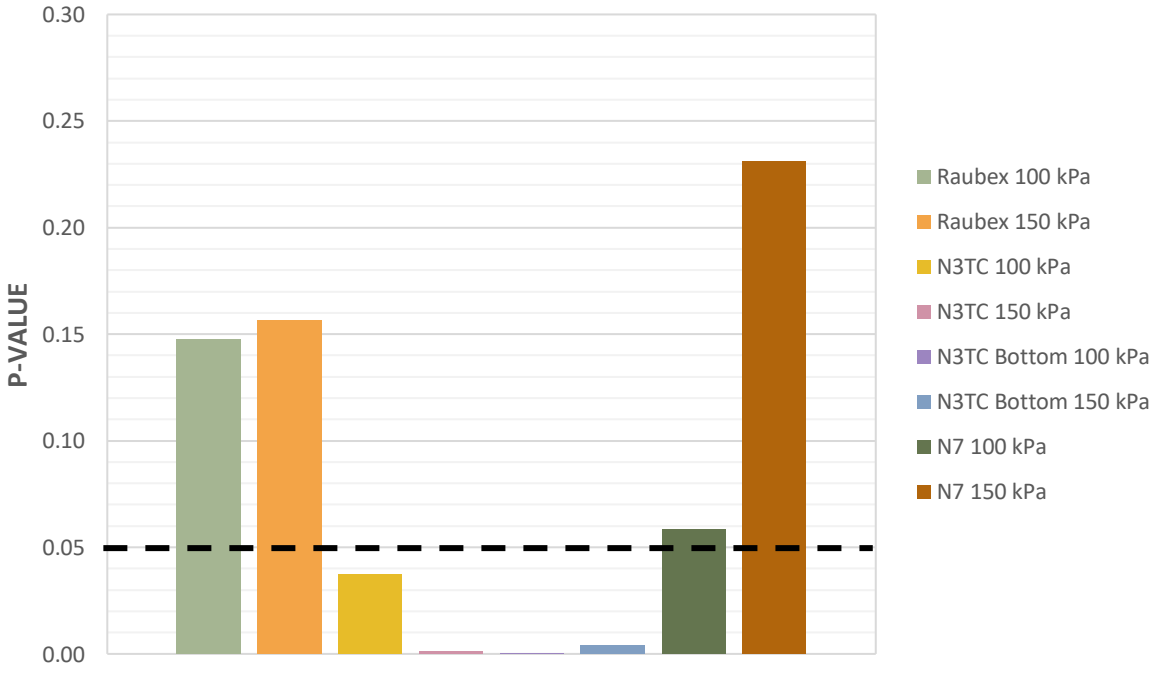

Figure 8.112: ANOVA analysis P-values for $Y^3 = A + B(X1) + C(X2)$